UNIVERSIDAD DE SEVILLA

CONSEJO SUPERIOR DE INVESTIGACIONES CIENTÍFICAS

Departamento de Química Inorgánica

Instituto de Investigaciones Químicas

Cooperative Bond Activation by Bimetallic Frustrated Lewis Pairs and Related Systems

Nereida Hidalgo Reinoso

Tesis Doctoral

Sevilla, 2021

Cooperative Bond Activation by Bimetallic Frustrated Lewis Pairs and Related Systems

Nereida Hidalgo Reinoso

Trabajo presentado para aspirar
al Título de Doctora en Química
Sevilla, 2021

Nereida Hidalgo Reinoso

Director:

Jesús Campos Manzano
(Científico Titular, CSIC)

Table of Contents

Consideraciones Generales

La química organometálica, química de las moléculas con enlaces metal-carbono (y normalmente extendida también a aquellas con enlace metal-hidruro), es una ciencia que se ha expandido enormemente desde sus comienzos como disciplina a mediados del siglo XX. Esta área está implicada en numerosos campos que poseen aplicaciones prácticas, entre las que destacan las relacionadas con diversos procesos de la vida, química bioinórganica, la ciencia de los materiales y el desarrollo de nuevas formas de obtención de energía. No obstante, la contribución de la química organometálica que ha sido posiblemente más transcendental es en la catálisis homogénea. Los catalizadores organometálicos facilitan la activación de sustratos orgánicos, promoviendo el desarrollo y la aplicación de estos en la producción industrial de polímeros, productos de la química fina o fármacos, entre otros muchos.

Los resultados que se presentan en esta Memoria se encuadran en una de las líneas de investigación que desarrolla el grupo de Química Organometálica y Catálisis Homogénea del Instituto de Investigaciones Químicas (Centro Mixto CSIC−Universidad de Sevilla), que tiene como objetivo el estudio de sistemas bimetálicos para la activación de moléculas pequeñas, así como la aplicación en diversas reacciones catalíticas.

Los experimentos que se describen en esta Tesis Doctoral incluyen la síntesis de compuestos organométalicos que contienen ligandos voluminosos, principalmente fosfinas, capaces de modular y controlar el diseño de sistemas cooperativos bimetálicos. Entre las aproximaciones investigadas se encuentran la creación de sistemas de pares de Lewis frustrados (FLPs, por sus siglas en inglés) basados en metales de transición,

así como sus correspondientes aductos de Lewis bimetálicos. Estas especies se han empleado en estudios de activación de moléculas pequeñas con enlaces polares y apolares, controlando la regioselectividad y haciendo hincapié en estudios de mecanismos de reacción.

El contenido de esta Tesis se organiza en tres capítulos, siendo redactada la mayor parte en inglés, exceptuando este resumen inicial y las conclusiones finales, que aparecen en ambos idiomas. El capítulo 1 es una introducción general a los sistemas de pares de Lewis frustrados, con especial énfasis en aquellos basados en metales de transición, y también a los compuestos bimetálicos de diversa índole, especialmente aquellos que guardan una estrecha relación con sistemas frustrados. Este capítulo se ha dividido en dos secciones. En la primera se ha expuesto el concepto de FLP y su aplicación en la activación de enlaces y en catálisis, convirtiéndose en los últimos años en un nuevo campo en la química de elementos que pertenecen al grupo principal. Tras esto, se amplía el concepto de FLPs introduciéndose metales de transición como uno de los componentes del sistema teniendo en cuenta las limitaciones que presentan los que contienen elementos del grupo principal. En esta parte se resumen los ejemplos más relevantes desde la definición del concepto en 2006 por el Prof. D. W. Stephan y como estos se aplican tanto en estudios estequiométricos como en catálisis. En la segunda parte, se realiza una breve introducción a los sistemas bimetálicos, homobimetálicos y heterobimetálicos con enlaces metal-metal polarizados y como estos están implicados en reacciones de activación de enlace por mecanismos cooperativos.

Los capítulos 2 y 3 tienen una estructura clásica basada en: Introducción, Resultados y Discusión, y Parte Experimental. La sección bibliográfica se ha incluido a pie de página al hacer mención a cada una de

las referencias citadas y, además, se recoge el listado global al final de cada capítulo. La numeración de las referencias es independiente para cada uno de los tres capítulos.

El capítulo 2 se centra en la síntesis de pares de Lewis frustrados en los que tanto el componente básico como el ácido están basados en metales de transición. El primer sistema de este tipo fue publicado por el grupo de investigación y está basado en una especie de Au(I) que se comporta como ácido y otra de Pt(0) con comportamiento básico. En este capítulo se describen las investigaciones llevadas a cabo tanto con este sistema original como con otros preparados por primera vez como parte de esta Tesis Doctoral. Estos estudios se han centrado en estudiar el mecanismo por el cual operan estos FLPs bimetálicos así como en identificar su capacidad para activar hidrógeno, alquinos y tetrilenos.

En el capítulo 3 se estudia la síntesis y la caracterización de pares de Lewis con metales de transición (MOLPs, por sus siglas en inglés) y la reactividad que presentan con pequeñas moléculas que poseen enlaces polares y apolares. Concretamente se han investigado pares de Lewis basados en sistemas de tipo P(0)/Ag(I) y otros derivados de la reactividad entre una especie de Pt(0) y precursores de zinc en estados de oxidación I y II.

Las conclusiones generales obtenidas de este trabajo se encuentran resumidas al final de la Tesis. Los compuestos presentados tienen una numeración independiente en cada capítulo y se encuentran resumidos en la sección “Summary of Compounds”. Los estudios computacionales que se exponen en esta Tesis han sido realizados independientemente por los colaboradores mencionados en cada caso.

Publications

Chapter II

Section II.2.1. and II.2.2. N. Hidalgo, J. J. Moreno, M. Pérez-Jiménez, C. Maya, J. López-Serrano, J. Campos. *Chem. Eur. J.* **2020**, *26*, 5982–5993.

Section II.2.3. N. Hidalgo, J. J. Moreno, M. Pérez-Jiménez, C. Maya, J. López-Serrano, J. Campos. *Organometallics* **2020**, *39*, 2534–2544.

Section II.2.4. N. Hidalgo, S. Bajo, J. J. Moreno, C. Navarro-Gilabert, B. Q. Mercado, J. Campos. Dalton Trans. **2019**, *48*, 9127–9138.

Chapter III

Section III.1. N. Hidalgo, C. Maya, J. Campos. *Chem. Commun.* **2019**, *55*, 8812–8815.

Section III.2. N. Hidalgo, C. Romero-Pérez, C. Maya, I. Fernández, J. Campos. *Organometallics* **2021**, *40*, 1113–1119.

Others:

M. G. Alférez, J. J. Moreno, N. Hidalgo, J. Campos. *Angew. Chem. Int. Ed.* **2020**, *59*, 20863–20867.

N. Hidalgo, M. G. Alférez, J. Campos. Frustrated Lewis Pairs based on Transition Metals, in the book Frustrated Lewis Pairs **2021**. Editors C. Slootweg and A. Jupp. Springer.

Acknowledgements

Dr. Joaquín López-Serrano and Dr. Juan José Moreno (Instituto de Investigaciones Químicas, CSIC-Universidad de Sevilla) for the computational studies presented in Chapter II.

Dr. Israel Fernández (Universidad Computense de Madrid) for the computational studies presented in Chapter III.

Dr. Celia Maya (Universidad de Sevilla) for her assistance with the X-ray structural determination.

Abbreviations

[D_n]	Number of deuterium atoms in a molecule
Å	Amstrong
Anal. Calc.	Analysis Calculated
Ar	Aryl
Ar’	*m*-terphenyl group
Ar^{Dipp2}	2,6-bis(2,6-diisopropylphenyl)phenyl, $–C_6H_3$-2,6-$Dipp_2$
Ar^{Dtbp2}	2,6-bis(3,5-di-*tert*-butylphenyl)phenyl, $–C_6H_3$-2,6-$Dtbp_2$
Ar^{Xyl2}	2,6-bis(2,6-dimethylphenyl)phenyl, $–C_6H_3$-2,6-Xyl_2
atm	Atmosphere
BCP	Bond Critical Point
BP	Bond Path
C	Celsius
CCDC	Cambridge Crystallographic Data Centre
cm	Centimeter
Cp	Cyclopentadienyl, C_5H_5
Cp*	Pentamethylcyclopentadienyl, C_5Me_5
Cy	Cyclohexyl, $–C_6H_{11}$
Cyp	Cyclopentyl, $–C_5H_9$

Dipp	2,6-diisopropylphenyl, –C_6H_3-2,6-$^{i}Pr_2$
Dtbp	3,5-di-*tert*-butylphenyl, –C_6H_3-3,5-$^{t}Bu_2$
e^-	Electron
EDA	Energy Decomposition Analysis
ee	Enantiomeric excess
EF	Electric Field
EIE	Equilibrium Isotope Effect
equiv.	Equivalents
Et	Ethyl, -CH_2CH_3
ET	Electron transfer
Et_2O	Diethyl ether, $CH_3CH_2OCH_2CH_3$
Exp.	Experimental
FLP	Frustrated Lewis Pair
FRP	Frustrated Radical Pair
g	Gram
h	Hour
HOMO	Highest Occupied Molecular Orbital
IMes	1,3-Dimesitylimidazol-2-ylidene
^{i}Pr	Isopropyl, -$CH(CH_3)_2$
IR	Infrared

I^{t}Bu	1,3-di-*tert*-butylimidazolin-2-ylidene
K	Kelvin
*K*eq	Equilibrium constant
KIE	Kinetic Isotopic Effect
LUMO	Lowest Unoccupied Molecular Orbitals
m	*meta*
M	Metal
Me	Methyl, -CH_3
Mes	Mesityl, (2,4,6-trimethylphenyl), –C_6H_2-2,4,6-$(CH_3)_3$
mg	Miligram
min	Minutes
mL	Milliliter
MMA	Methyl methacrylate
mmol	Millimol
MOLP	Metal-Only Lewis Pair
MS-ESI	Mass Spectrometry-ElectroSpray Ionization
nb	Norbornene
NBO	Natural Bond Orbital
NDI	Naphthyridine-diimine pincer ligand
NHC	N-Heterocyclic Carbene

NTf_2	Bis(trifluoromethane)sulfonimide, $–N(S(O)_2CF_3$
^{o}	Degree
o	*ortho*
ORTEP	Crystallographic representation (Oak Ridge Thermal Ellipsoid Program)
OTf	Trifluoromethylsulfonate, triflate, $–OS(O)_2CF_3$
o-tolyl	2-methylphenyl, $–C_6H_5$-2-CH_3
p	*para*
Ph	Phenyl, $-C_6H_5$
QTAIM	Quantum Theory of Atoms In Molecules
R, R’	Alkyl group
RE	Rare-Earth element
ref.	Reference
rt	room temperature
^{t}Bu	*tert*-butyl, CMe_3
THF	Tetrahydrofuran, C_4H_8O
THT	Tetrahydrothiophene, C_4H_8S
TM	Transition Metal
TMFLP	Transition Metal Frustrated Lewis Pair
TMOFLP	Transition Metal-Only Frustrated Lewis Pair

Tol	Toluene
TON	Turn Over Number
TS	Transition State
vol	Volume
Xyl	Xylyl, 2,6-$Me_2C_6H_3$
ZPE	Zero-Point Energy
η	Number of atoms of a ligand directly bound to a metal center
κ	Ligand hapticity
ν	Infrared vibrational frequency (cm^{-1})

NMR ABBREVIATIONS

br.	Broad
COSY	^1H-^1H Correlation Spectroscopy
d	Doublet
DOSY	Diffusion Ordered Spectroscopy
EXSY	Exchange Spectroscopy
HMBC	^1H-^{13}C correlation spectroscopy (Heteronuclear Multiple Bond Correlation)
HSQC	^1H-^{13}C correlation spectroscopy (Heteronuclear Single Quantum Coherence)

Hz	Hertz
m	Multiplet
$^{n}J_{AB}$	Coupling constant (Hz) between A and B nuclei separated by n bonds
NMR	Nuclear Magnetic Resonance
NOESY	Nuclear Overhauser Enhancement Spectroscopy
ppm	Parts per million
q	Quartet
s	Singlet
sept	Septet
t	Triplet
δ	Chemical shift in ppm

Summary of Compounds

Chapter II

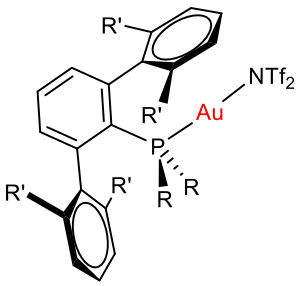

1a: R = Me; R' = Me
1b: R = Me; R' = ^{i}Pr
1c: R = Cyp; R' = Me

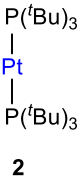

2

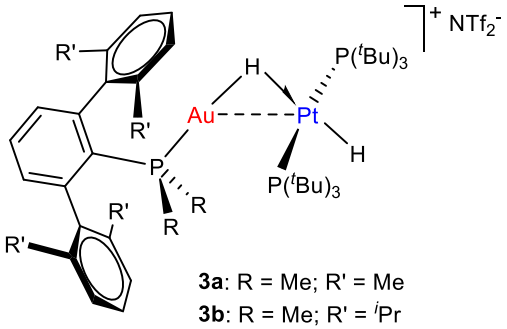

3a: R = Me; R' = Me
3b: R = Me; R' = ^{i}Pr

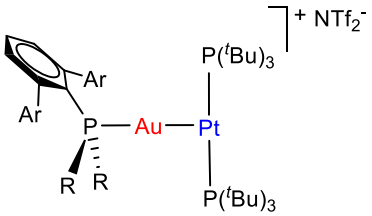

4a: R = Me; Ar = Xyl
4b: R = Me; Ar = Dipp

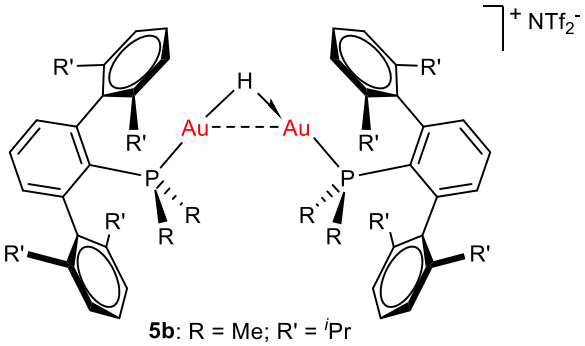

5b: R = Me; R' = ^{i}Pr
5c: R = Cyp; R' = Me

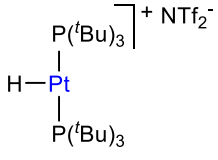

6

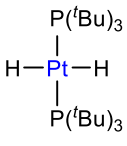

7

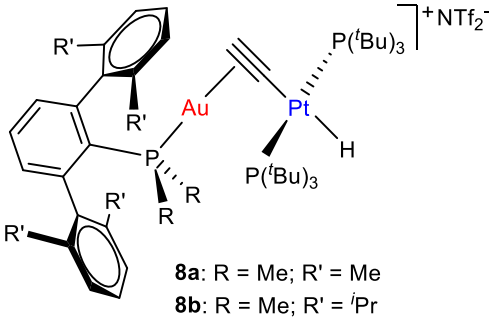

8a: R = Me; R' = Me
8b: R = Me; R' = ^{i}Pr
8c: R = Cyp; R' = Me

Chapter II

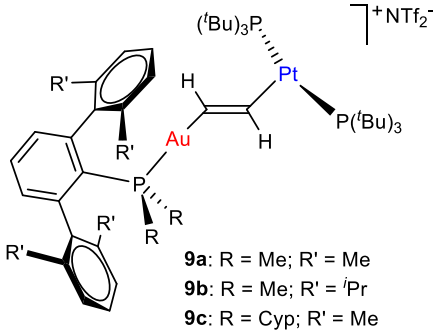

9a: R = Me; R' = Me
9b: R = Me; R' = ^{i}Pr
9c: R = Cyp; R' = Me

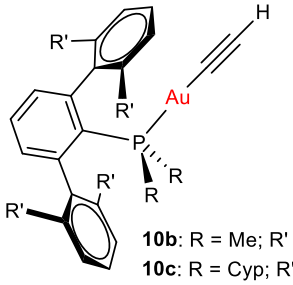

10b: R = Me; R' = ^{i}Pr
10c: R = Cyp; R' = Me

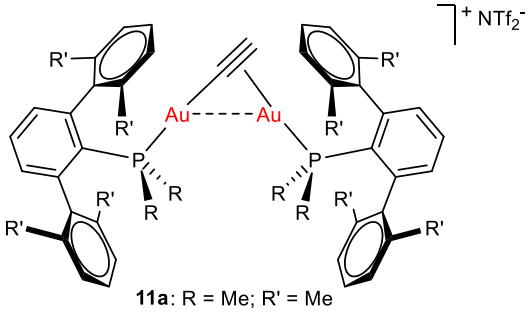

11a: R = Me; R' = Me
11b: R = Me; R' = ^{i}Pr
11c: R = Cyp; R' = Me

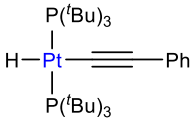

13

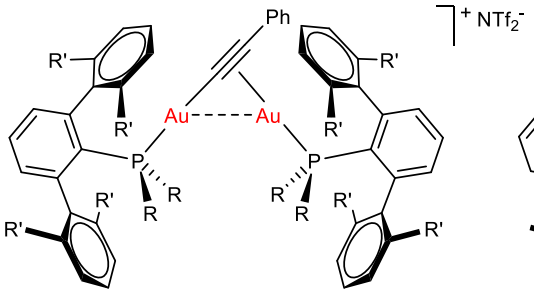

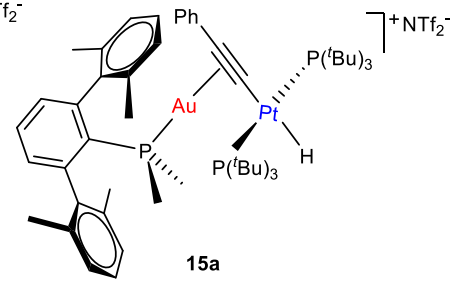

15a

14b: R = Me; R' = ^{i}Pr
14c: R = Cyp; R' = Me

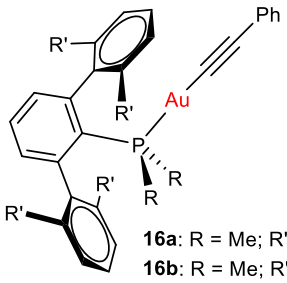

16a: R = Me; R' = Me
16b: R = Me; R' = ^{i}Pr
16c: R = Cyp; R' = Me

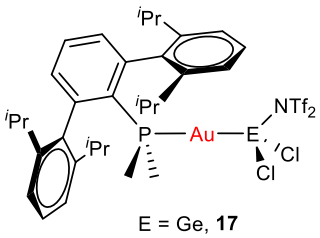

E = Ge, **17**
E = Sn, **18**

Chapter II

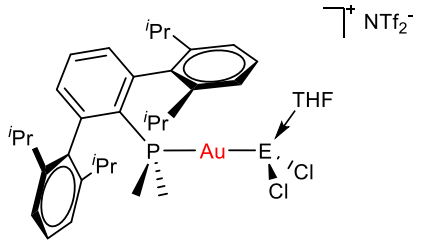

E = Ge, **17·THF**
E = Sn, **18·THF**

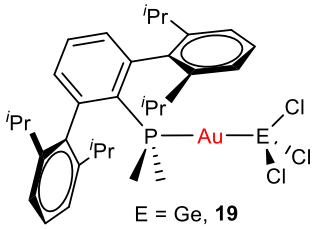

E = Ge, **19**
E = Sn, **20**

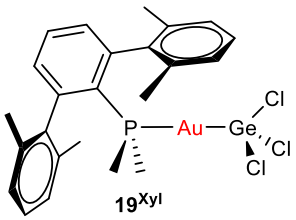

19^{Xyl}

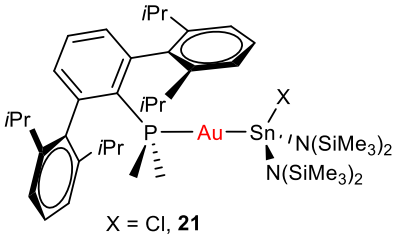

X = Cl, **21**
X = NTf_2, **22**

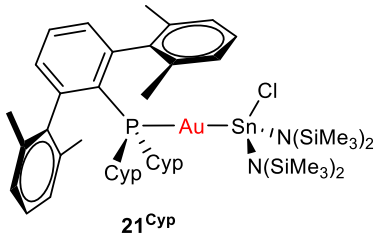

21^{Cyp}

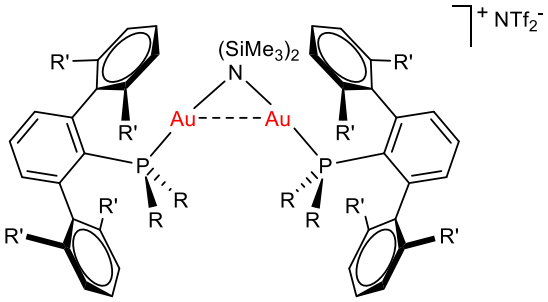

[Au_2(μ-N($SiMe_3$)$_2$)(PMe_2Ar^{Dipp2})$_2$]: R = Me; R' = ^{i}Pr
[Au_2(μ-N($SiMe_3$)$_2$)(PMe_2Ar^{Xyl2})$_2$]: R = Me; R' = Me

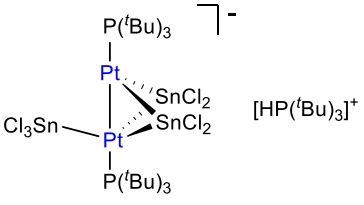

23

24

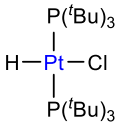

25

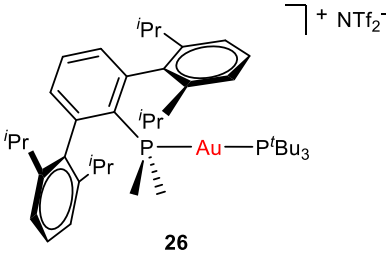

26

Chapter II

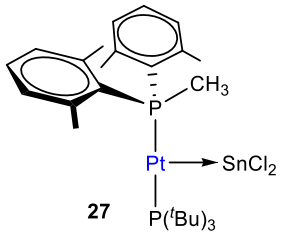

27

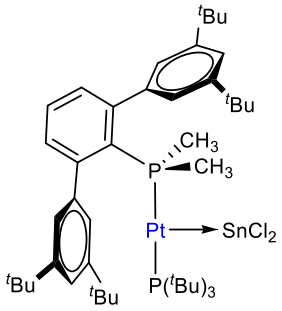

28

Chapter III

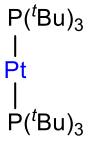

1

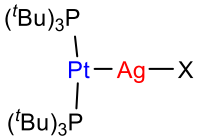

2, X = NTf_2
3, X = OTf

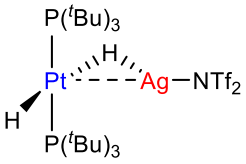

4

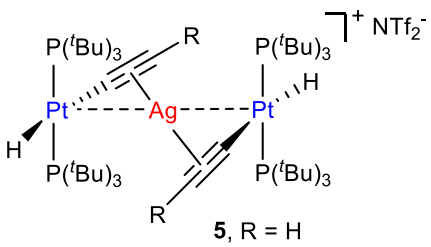

5, R = H
6, R = Ph

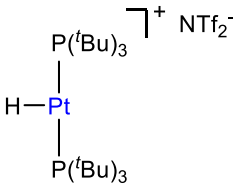

7

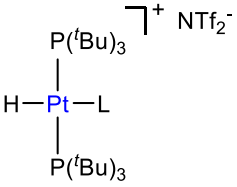

8a, L = OH_2
8b, L = NH_3
8c, L = CH_3CN

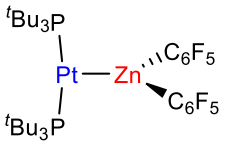

9

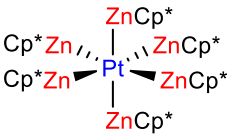

10

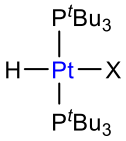

11a, X=Cl
11b, X = Br
11c, X = I

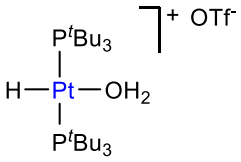

12

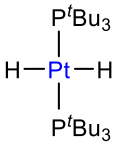

13

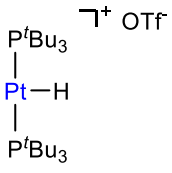

14

CHAPTER I. Introduction:

Frustrated Lewis Pairs and Transition Metals

I.1. The Chemistry of Frustrated Lewis pairs (FLPs)

I.1.1. The Concept of Frustrated Lewis Pair (FLP)

In 1923, Lewis defined electron-donating and electron-accepting molecules as bases and acids, respectively. Lewis bases have one electron-pair in high lying 'highest occupied molecular orbitals' (HOMOs) which can interact with low-lying 'lowest unoccupied molecular orbitals' of Lewis acids (LUMOs).[1] Thus, when they are combined a new dative bond is formed in what has been termed a Lewis adduct. A classic example of this concept is the formation of a dative B−N bond by the reaction of trifluoroborane and ammonia (Scheme 1).[2] The vacant orbital on boron makes it an acid and the lone pair of electrons on nitrogen makes ammonia the base. When the two of them are mixed together the formation of the Lewis adduct takes place immediately and the chemistry exhibited by the adduct is distinct form the original components.

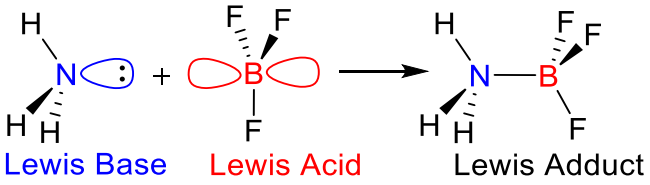

Scheme 1. Formation of a Lewis acid-base adduct.

The concept of Lewis acids and bases is fundamental in inorganic chemistry. This theory is central for the understanding of much of main group and transition metal chemistry and a guiding tool to understand bonding interactions and reactivity. However, there have been exceptions

[1] a) G. N. Lewis. *Valence and the Structure of Atoms and Molecules.* Chemical Catalogue Company. New York, **1923**.
[2] S. G. Shore, R. W. Parry. *J. Am. Chem. Soc.* **1955**, *77*, 6084–6085.

to traditional Lewis acid-base behaviour. The following Figure represents some of the early examples in which the anticipated Lewis adducts were not form, setting the foundations for what later became the area of Frustrated Lewis Pairs (FLPs). This brief historical perspective will be presented along the next paragraphs.

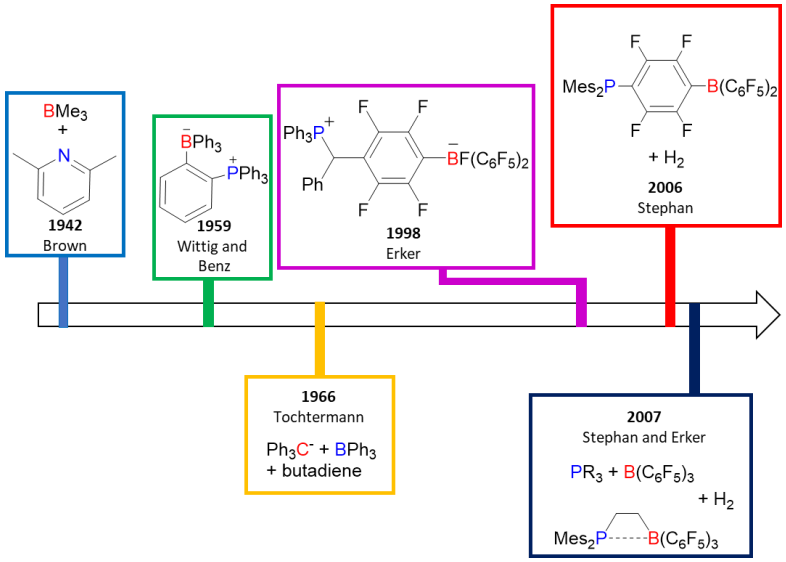

Figure 1. Historical timeline leading to the development of FLP chemistry through some selected representative examples.

In 1942, Brown and co-workers described the interaction of pyridines with boranes.[3] They observed that most combinations of Lewis bases and acids led to dative B−N bonds, forming the corresponding Lewis adducts. For example, Lutidine (**1**) formed a stable adduct with BF_3 (**2**), however, with trimethylborane (BMe_3), this Lewis base did not react (Scheme 2A). The authors attributed this result to the steric hindrance of the methyl groups of the borane with the *ortho*-methyl group of lutidine.

[3] a) H. C. Brown, H. I. Schlesinger, S. Z. Cardon. *J. Am. Chem. Soc.* **1942**, *64*, 325–329. b) H. C. Brown, B. Kanner. *J. Am. Chem. Soc.* **1966**, *88*, 986–992.

A few years later, Wittig and Benz reported the reaction of 1,2-didehydrobenzene, generated in situ from *o*-fluorobromobenzene **3**, with triphenylborane as Lewis acid and triphenylphosphine as Lewis base. Rather than being inert, the P–B adduct reacts with a transient benzyne **4** to yield the *o*-phenylenebridged phosphonium-borate **5** (Scheme 2B).[4]

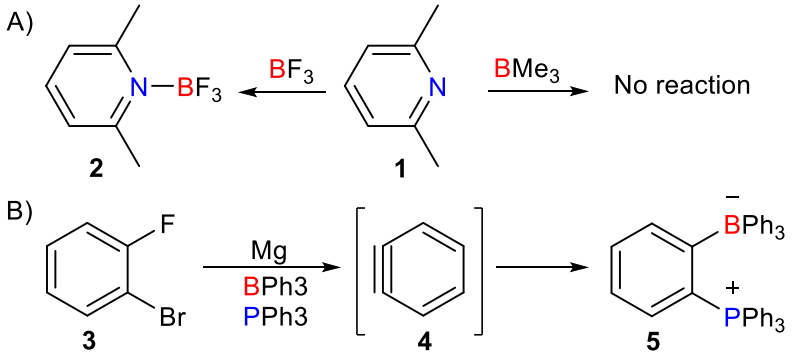

Scheme 2. Early developments towards the concept of frustrated Lewis pairs. A) Interaction of lutidine with boranes reported by Brown and co-workers. B) Wittig and Benz's reaction for the formation of *o*-phenylene bridged phosphonium-borate **5**.

In the 1960's, Tochtermann described a similar addition reaction of trityl anion and BPh_3 to butadiene to give 1,2- and 1,4-addition products **6** and **7** (Scheme 3A).[5] Two other examples based on the related trytil cation and where the formation of the expected Lewis adduct was ruled out are the following. Damico and Broadus reported that the trityl cation abstract an α-proton from amines to produce an iminium cation **8** (Scheme 3B).[6] In the case of pyridine as the base, reactions of trityl cation give rise to nucleophilic attack at the *para*-position of a phenyl ring instead of N–C

[4] G. Wittig, E. Benz. *Chem. Ber.* **1959**, *92*, 1999–2013.
[5] W. Tochtermann. *Angew. Chem. Int. Ed.* **1966**, *5*, 351–371.
[6] R. Damico, C. D. Broadus. *J. Org. Chem.* **1966**, *31*, 1607–1612.

interaction with the more electrophilic carbocation as may have been anticipated (scheme 3C).[7]

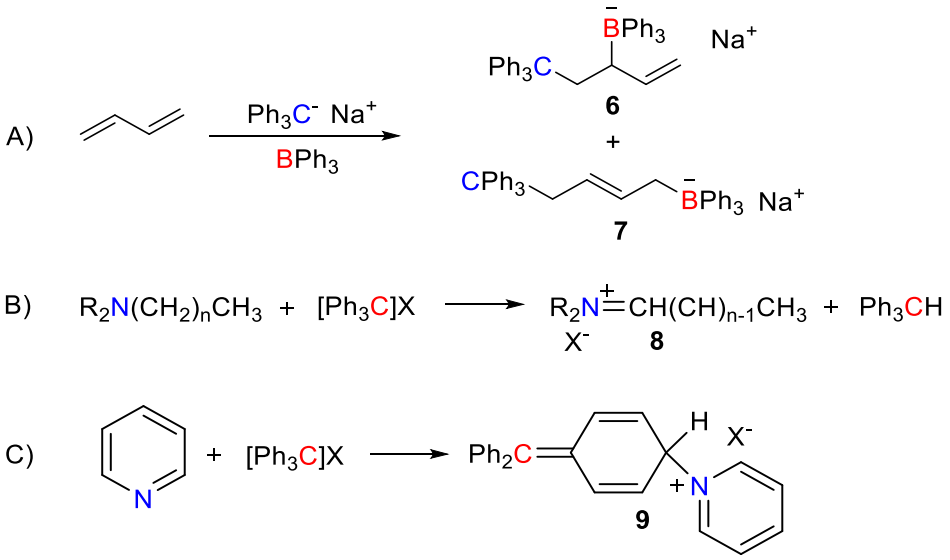

Scheme 3. A) Addition of trityl anion and BPh_3 to butadiene. B) Proton abstraction to produce an iminium cation. C) Reaction of trityl cation with pyridine.

Moreover, in 1998, Erker described an example involving the combination of ylide, Ph_3PCHPh, and the Lewis acid $B(C_6F_5)_3$. While the simple ylide/borane adduct **10** was shown to form at room temperature, this species exhibited thermal rearrangement resulting in the formation of compound **11** (Scheme 4). There is one important implication of these results, namely the need for reversibility in the formation of adduct **10**. Both ylide and borane needs to be set free to effect the attack by ylide at

[7] H. Lankamp, W. T. Nauta, C. MacLean. *Tetrahedron Lett.* **1968**, *9*, 249–254.

the *para*-position of the one of the fluorinated arene rings to give the specie **11** after subsequent C−F bond cleavage.[8]

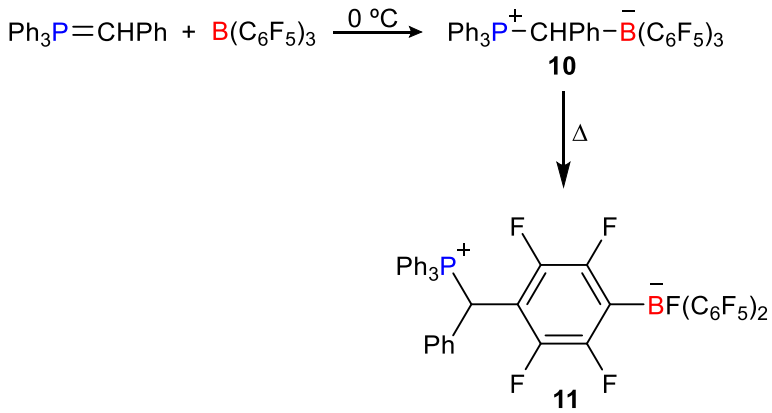

Scheme 4. Erker's example of the combination of Ph_3PCHPh and $B(C_6F_5)_3$.

The examples described above represent early cases in which the traditional Lewis acid-base adduct formation principles were not fulfilled. These and other related studies set the foundations for what we know today as frustrated Lewis pairs. Nevertheless, in most of the cases, the authors attribute the reactivity of the studied chemistry to steric reasons, which albeit being important do not tell the whole story about the chemical transformations taking place. Besides, these early studies do not discuss in depth the reactivity presented in terms of reaction mechanisms and the implications that they could have to exploit further reactivity.

It was not until 2006 when Stephan and co-workers discovered that the intramolecular Lewis base/Lewis acid **12** is capable of activating dihydrogen under ambient conditions. Moreover, the reaction was proved

[8] S. Doering, G. Erker, R. Fröhlich, O. Meyer, K. Bergander. *Organometallics* **1998**, *17*, 2183–2187.

to be reversible when complex **13** was exposed to high temperatures (Scheme 5A).[9] This fact remarked a major development in cooperative Lewis base/acid chemistry and constituted a revolution in the area of main group chemistry because of being the first example of main group elements effecting the heterolytic cleavage of dihydrogen, a transformation so far believed to be exclusive of transition metals. Then, in 2007, the same group proved that combinations of $B(C_6F_5)_3$ with bulky phosphines lead to intermolecular systems that also cleaved hydrogen to produce the respective phosphonium/hydridoborate salts **14** (Scheme 5B)[10] and the term 'Frustrated Lewis Pair' (FLP) was coined.[11] In the same year, Erker's group published the intramolecular ethylene-bridged borane/phosphine Lewis pair **15** which is also a highly active non-metallic system that activates hydrogen to form **16** (Scheme 5C).[12]

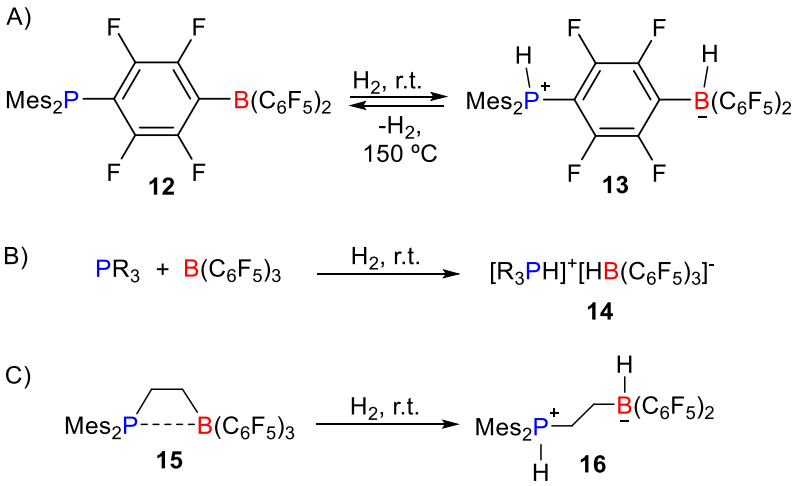

Scheme 5. First examples of frustrated Lewis pairs.

[9] G. C. Welch, R. R. S. Juan, J. D. Masuda, D. W. Stephan. *Science* **2006**, *314*, 1124–1126.
[10] G. C. Welch, D. W. Stephan. *J. Am. Chem. Soc.* **2007**, *129*, 1880–1881.
[11] J. S. J. McCahill, G. C. Welch, D. W. Stephan. *Angew. Chem. Int. Ed.* **2007**, *46*, 4968–4971.
[12] P. Spies, G. Erker, G. Kehr, K. Bergander, R. Fröhlich, S. Grimme, D. W. Stephan. *Chem. Commun.* **2007**, 5072–5074.

These three publications marked the beginning of a remarkably rapid development of new chemistry arising from the combination of bulky Lewis acids with bulky Lewis bases. The field of frustrated Lewis pairs was established and today it is hard to find any issue of an organic or inorganic chemistry journal that does not contain some examples of FLP systems. One of the driving forces of this development is without no doubt the possibility to accomplish metal-free catalysis. As such, hydrogen activation rapidly led to the development of metal-free FLP-catalyzed hydrogenations. In fact, this hypothesis was first demonstrated very early for nitrogen-based unsaturated molecules, in the same year in which the concept FLP was indeed termed.[13] Initial protonation of the imine and hydride transfer from the hydridoborate **12** to the iminium carbon are the first steps of the mechanism for metal free imine reductions (scheme 6). This net transfer of proton and hydride from the phosphonium-borate **13** to the imine regenerates the Lewis acid-base pair, which is then available for subsequent activation of H_2 regenerating the phosphonium-borate. This mechanism is consistent with the observed reactivity trends in which the electron-rich imine, ^{t}BuN=CPh(H), is reduced significantly faster than the electron poor imine, $PhSO_2N$=CPh(H). This foremost study on the catalytic implications of FLP systems constituted another landmark in the field that has been followed by many other catalytic applications, some of which will be briefly discussed along this section.

[13] P. A. Chase, G. C. Welch, T. Jurca, D. W. Stephan. *Angew. Chem. Int. Ed.* **2007**, *46*, 8050–8053.

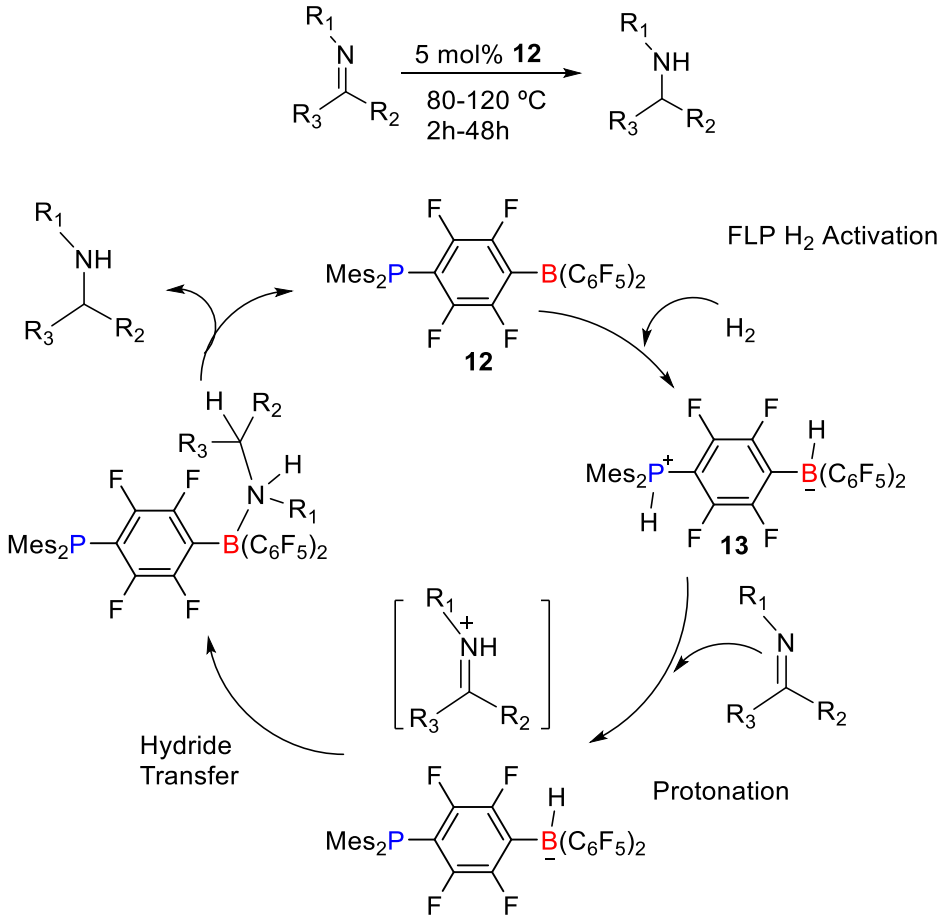

Scheme 6. Mechanism of imines hydrogenation catalysed by FLP **12**.

The rapid expansion of FLP chemistry was also due to the great variability of the cooperative reactions of FLPs with a range of other substrates, leading to small molecule binding and activation. This kind of chemistry is often experimentally rather simple to perform and it affords the possibility of discovering new reactions as a result of the cooperative action by Lewis acid and Lewis base sites. Most relevant examples will also be discussed along this Chapter.

Finally, one of the most attractive aspects of frustrated Lewis pairs, and one that has seduced the curiosity of researchers across very different areas, is the mechanism by which these systems mediate bond cleavage processes. Within these considerations there is one realization that was soon recognized, namely the existence of Lewis adducts that exhibit FLP behaviour. In this systems, although the resting state contains a dative bond between the acid and basic sites, there is an equilibrium that allows the two components to participate in cooperative activation. These systems were named 'thermally induced FLPs' and represent an important addition to the field that highly widen the design principles of frustrated systems (Scheme 7).[14]

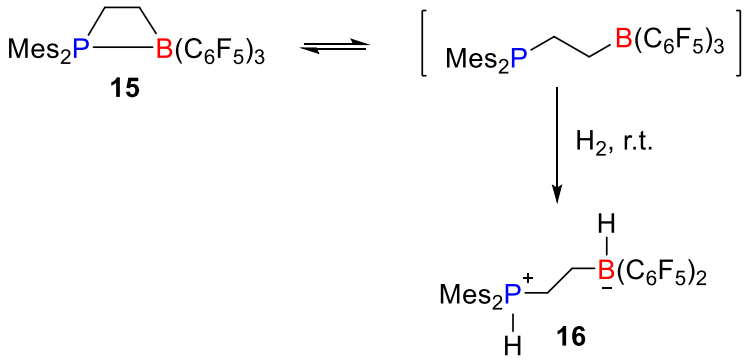

Scheme 7. Selected example for the activation of H_2 by the thermally induced FLP **15**.[12]

Beyond the aforementioned equilibrium and the concept of thermally induced adduct dissociation, there is the question of how FLPs mediate the cleavage of strong bonds such as that in dihydrogen. Despite

[14] T. A. Rokob, A. Hamza, A. Stirling, I. Pápai. *J. Am. Chem. Soc.* **2009**, *131*, 2029–2036.

apparently simple it remains a matter of intense debate[15] and although more details will be presented during the discussion of our own results on the field, it is pertinent to make a brief mention here. For simplicity the activation of dihydrogen may be considered. The cleavage of the H−H bond proceeds in an heterolytic manner and two alternative visions, the electron transfer (ET) and the electric field (EF) models, were originally proposed (Figure 2A). The ET model is somehow analogous to the oxidative addition of dihydrogen over a transition metal, since the bonding pair of electrons on H_2 is donated to the empty p orbital of the acid, while the lone pair of the base is donated to the σ* antibonding orbital of H_2 in a cooperative push-pull interaction. On the contrary, the EF model suggests that the dihydrogen molecule becomes polarized in the pocket created by the encounter acid-base complex to the point that H_2 splitting is almost barrierless.

Moreover, in recent times an alternative mechanism has been proposed by the action of a frustrated radical pair (FRP), in which an electron is transferred from the Lewis base to the acid (Figure 2B).[16] In this new discover, FLPs formed by $E(C_6F_5)_3$ (E = B, Al) and $PMes_3$ react with Ph_3SnH via a radical pathway (homolytic), whereas those from $P(^tBu)_3$ and $E(C_6F_5)_3$ proceeded by a heterolytic mechanism. To explore this FRP mechanism a series of chalcogens and chalcogenides derivatives was studied to produce exotic chalcogenide-based B or Al anion salts.[17] Overall, these findings suggest that either heterolytic or homolytic

[15] a) G. Skara, F. De Vleeschouwer, P. Geerlings, F. De Proft, B. Pinter. *Sci. Rep.* **2017**, *7*, 16024. b) D. Yepes, P. Jaque, I. Fernández. *Chem. Eur. J.* **2016**, *22*, 18801–18809. c) J. Paradies. *Eur. J. Org. Chem.* **2019**, 283–294.
[16] L. L. Liu, L. L. Cao, Y. Shao, G. Ménard, D. W. Stephan. *Chem* **2017**, *3*, 259–267.
[17] L. L. Liu, L. L. Cao, Y. Shao, D. W. Stephan. *J. Am. Chem. Soc*. **2017**, *139*, 10062–10071.

mechanisms could be operative for the cleavage of H_2 and other small molecules depending on the nature of the FLPs.

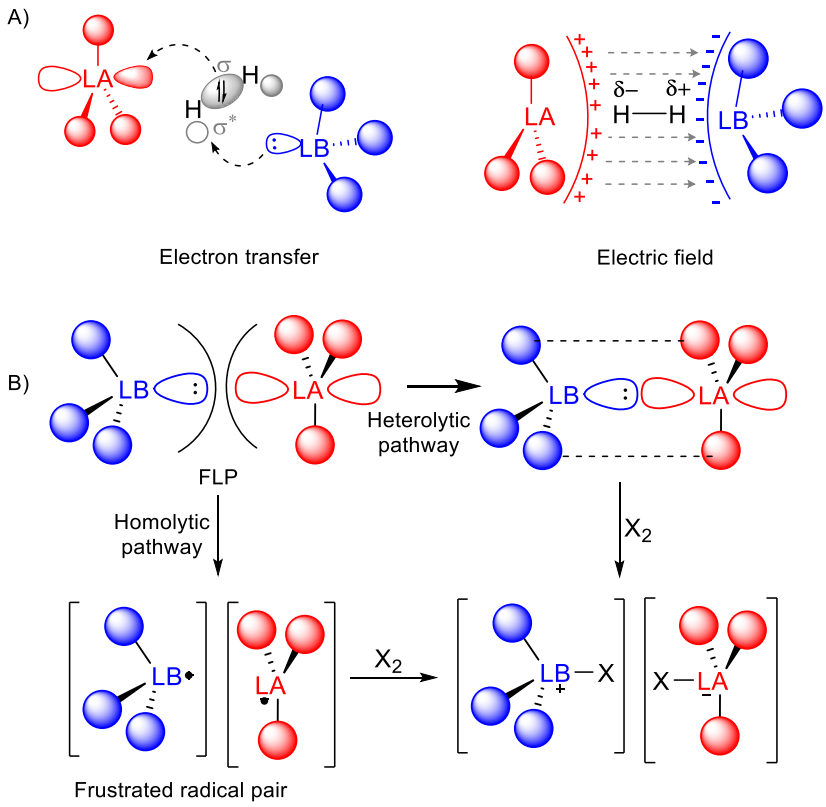

Figure 2. A) Electron transfer (ET) and electric field (EF) models for the heterolytic activation of dihydrogen by FLPs. B) Homolytic vs heterolytic pathways for FLP reactivity.

Overall, the principles established by Lewis and the recent developments of FLP chemistry have now spread to understand areas of organic, organometallic, solid state chemistry and surface science, among

other fields. Definitely, the influence of this simple rationale for bonding involving filled and vacant molecular orbitals put forward by Lewis some 100 years ago has a strong impact across diverse disciplines. In fact, it continues to be one of the most powerful tools for both understanding and predicting a broad spectrum of chemical reactivity. The more recent concept of frustration provides fresh air into the broad field of cooperativity and holds great interest from many different views. In the following two sections somewhat more traditional FLP systems based on main group elements will be firstly discussed, followed by those constructed around transition metals. The latter have been developed more recently and serve as the central core of this Thesis.

I.1.2. Metal-Free FLP Systems

The emergence of the FLP concept has provided new strategies for chemists to develop metal-free routes for the activation of small molecules and even for catalysis. In the last fifteen years a wide range of small molecules have been activated by FLPs and the implications in catalysis continuously spanned. Numerous reviews have been published that detail specific aspects of FLP chemistry.[18] This section provides a brief overview of homogeneous metal-free FLPs without the aim of being comprehensive, but rather discussing some selected examples to offer a general overview of the field. Stoichiometric reactions with small molecules will be firstly described. In particular, we have selected three substrates that arguably represent the paradigm of FLP-reactivity. This discussion will be followed by the use of FLPs in combination with these substrates for catalytic applications. Other sound catalytic applications of FLPs that are less directly related to this Thesis, such as the borylation of C−H bonds,[19] defluorination reactions[20] or polymerazation processes[21] will not be covered.

[18] Some examples: a) A. R. Jupp, D. W. Stephan. *Trends in Chemistry* **2019**, *1*, 35–48. b) D. W. Stephan, G. Erker. *Angew Chem. Int. Ed.* **2015**, *54*, 6400–6441. c) D. W. Stephan, G. Erker. *Chem. Sci.* **2014**, *5*, 2625–2641. d) D. W. Stephan, G. Erker. *Top. Curr. Chem.* **2013**, *332*, 1–311. e) D. W. Stephan, G. Erker. *Top. Curr. Chem.* **2013**, *334*, 1–345. f) J. C. Slootweg, A. R. Jupp. *Molecular Catalysis* **2021**, *2*, 1–408.

[19] Some examples: a) M. A. Legare, M. A. Courtemanche, E. Rochette, F. G. Fontaine. *Science* **2015**, *349*, 513–516. b) M. A. Legare, E. Rochette, J. L. Lavergne, N. Bouchard, F. G. Fontaine. *Chem. Commun.* **2016**, *52*, 5387–5390. c) K. Chernichenko, M. Lindqvist, B. Kotai, M. Nieger, K. Sorochkina, I. Pápai, T. Repo. *J. Am. Chem. Soc.* **2016**, *138*, 4860–4868.

[20] Some examples: a) C. B. Caputo, D. W. Stephan. *Organometallics* **2012**, *31*, 27–30. b) J. T. Zhu, M. Pérez, D. W. Stephan. *Angew. Chem. Int. Ed.* **2016**, *55*, 8448–8451. c) J. Zhu, M. Pérez, C. B. Caputo, D. W. Stephan. *Angew. Chem. Int. Ed.* **2016**, *55*, 1417–1421.

[21] Some examples: a) M. Hong, J. Chen, E. Y.-X. Chen. *Chem. Rev.* **2018**, *118*, 10551–10616. b) L. Chen, R. Liu, Q. Yan. *Angew. Chem. Int. Ed.* **2018**, *57*, 9336–9340. c) T.

I.1.2.1. Stoichiometric Reactions with FLP Systems

Hydrogen activation

The activation of dihydrogen is the most paradigmatic example of bond activation in the context of FLPs, since it established the landmark achievement that main group elements were also capable of mediating this bond cleavage. After the seminal studies of Stephan and Erker,[9,10,12] other combinations of Lewis acids and bases were reported for the same purpose. In fact, the activation of dihydrogen remains as the most exploited strategy to gauge FLP behaviour. Some relevant examples will be discussed along the following lines.

For example, to study the difference in hydrogen activation according to the Lewis acidity of the borane, B(*p*-$C_6F_4H)_3$ was used, which has a reduced acidity compared to B($C_6F_5)_3$.[22] A mixture of the former acid with P(*o*-$C_6H_4Me)_3$ produces, [(*o*-$C_6H_4Me)_3$PH][HB(*p*-$C_6F_4H)_3$] upon exposure to hydrogen (4 atm) at 25 ºC. The reduced acidity of the borane employed facilitate reversibility, with the release of hydrogen taking place under vacuum even at 25 ºC (c.f. 60 ºC with B($C_6F_5)_3$ in the only other known system).[23]

Although weaker than phosphines, bulky pyridines are also effective bases as demonstrated by Brown in 1942. As shown in the previous section, this group was the first to report data on the reactivity of pyridines with different boranes.[3] Inspired by these results, Stephan's group reported in 2009 the activation of hydrogen with lutidine/B($C_6F_5)_3$ as

Wang, C. G. Daniliuc, C. Mück-Lichtenfeld, G. Kehr, G. Erker. *J. Am. Chem. Soc.* **2018**, *140*, 3635–3643.

[22] a) M. Ullrich, A. J. Lough, D. W. Stephan. *J. Am. Chem. Soc.* **2009**, *131*, 52−53. b) M. Ullrich, A. J. Lough, D. W. Stephan. *Organometallics* **2010**, *29*, 3647−3654.

[23] H. Wang, R. Fröhlich, G. Kehr, G. Erker. *Chem. Commun.* **2008**, 5966−5968.

an FLP,[24] taking advantage from the fact that an equilibrium exists between free Lewis acid and base and the corresponding adduct, **17**. This equilibrium facilitated FLP activation. Thus a solution of lutidine/$B(C_6F_5)_3$ under dihydrogen lead to **18**, [2,6-$Me_2C_5H_3NH$][$HB(C_6F_5)_3$] (Scheme 8A).

However, Lewis bases that do not belong to group 15 are also suitable. For instance, a year before, with the same Lewis acid, $B(C_6F_5)_3$, hydrogen activation by a FLP in which an N-heterocyclic carbene (NHC) was used as a C-centred base, led to the corresponding zwitterion **19** at low temperature (Scheme 8B).[25]

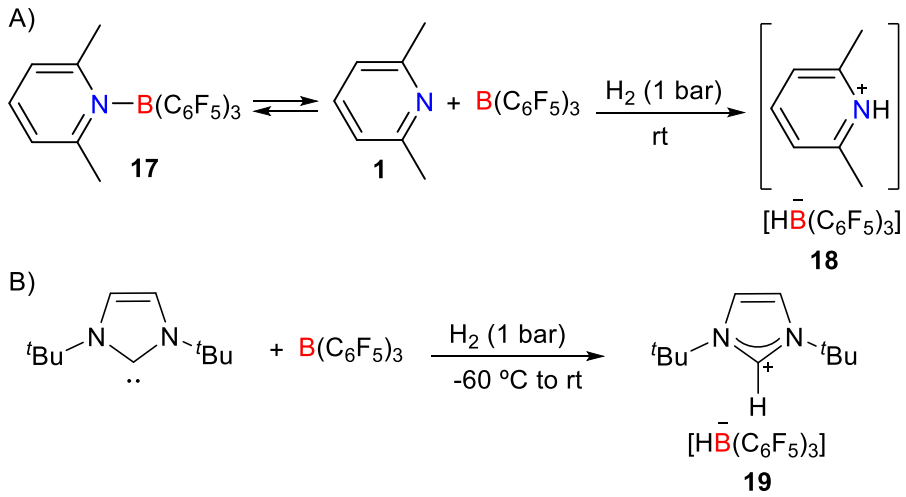

Scheme 8. A) Activation of hydrogen with lutidine/$B(C_6F_5)_3$ FLP. B) FLP with a N-heterocyclic carbene as Lewis base.

[24] a) S. J. Geier, A. L. Gille, T. M. Gilbert, D. W. Stephan. *Inorg. Chem.* **2009**, *48*, 10466−10474. b) S. J. Geier, D. W. Stephan. *J. Am. Chem. Soc.* **2009**, *131*, 3476−3477.
[25] a) P. A. Chase, D. W. Stephan. *Angew. Chem. Int. Ed.* **2008**, *47*, 7433−7437. b) S. J. Geier, P. A. Chase, D. W. Stephan. *Chem. Commun.* **2010**, *46*, 4884−4886. c) D. Holschumacher, T. Bannenberg, C. G. Hrib, P. G. Jones, M. Tamm. *Angew. Chem. Int. Ed.* **2008**, *47*, 7428−7432.

The heterolytic cleavage of H_2 by FLPs has subsequently been generalized to a wide variety of acid/base combinations derived from boranes, alanes, Lewis acidic transition metals (which will be discussed in next sections), and even C- and Si-based acids in combination with a range of sterically hindered donors.[26] In this context, it was obvious that the application to catalytic hydrogenations would find success, as it will be discussed later.

Alkynes activation

Depending on the nature of the Lewis base, metal-free FLPs react with terminal alkynes via two pathways, namely 1,2-addition and deprotonation.[27] Thus, highly basic phosphines, such P^tBu_3 lead to deprotonation products (**20**) while other exhibiting reduced basicity (i.e. $PMes_3$, $P(o\text{-tolyl})_3$, PPh_3; Mes = 2,4,6-trimethylphenyl, *o*-tolyl = 2-methylphenyl) tend to react through 1,2-addition routes (**21**, Scheme 9A). Interestingly, the latter reactivity has been exploited using intramolecular FLPs[28] or FLP reactions with less basic polyphosphines as bases[29] to produce macrocyclic and chain-like species **22**[29a] and **23**,[29b] respectively (Scheme 9B and 9C).

[26] a) D. W. Stephan. *Org. Biomol. Chem.* **2012**, *10*, 5740−5746. b) D. W. Stephan, G. Erker. *Angew. Chem. Int. Ed.* **2010**, *49*, 46−76.
[27] M. A. Dureen, D. W. Stephan. *J. Am. Chem. Soc.* **2009**, *131*, 8396−8397. b) J. Paradies. *Angew. Chem. Int. Ed.* **2014**, *53*, 3552−3557.
[28] M. A. Dureen, C. C. Brown, D. W. Stephan. *Organometallics* **2010**, *29*, 6594−6607.
[29] a) S. J. Geier, M. A. Dureen, E. Y. Ouyang, D. W. Stephan. *Chem. Eur. J.* **2010**, *16*, 988−993. b) C. F. Jiang, O. Blacque, H. Berke. *Organometallics* **2010**, *29*, 125−133.

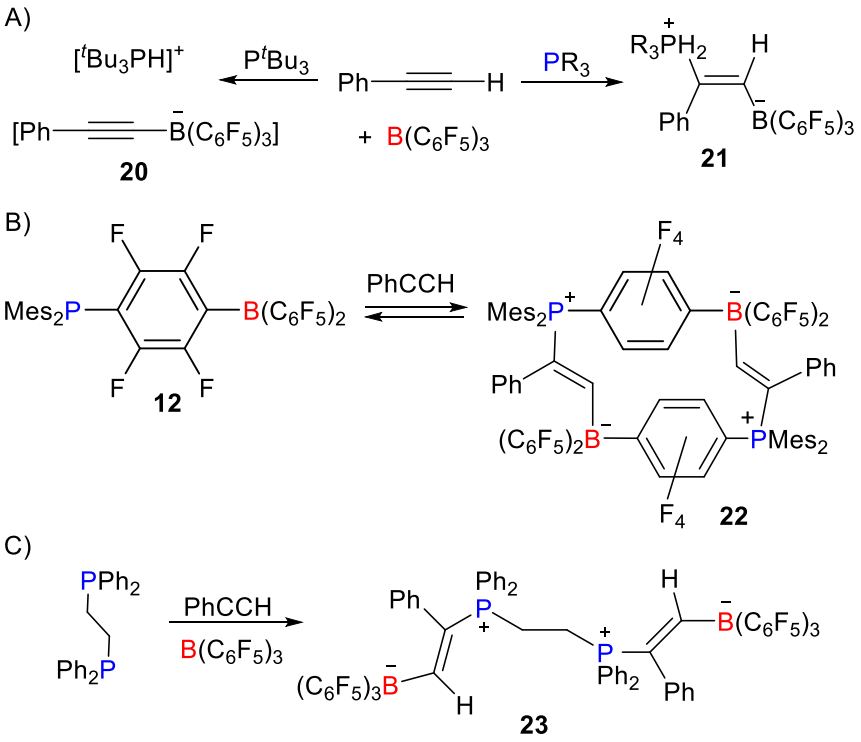

Scheme 9. Metal-free FLP reactivity with phenylacetylene.

In another interesting study, pyrrole derivatives were shown to act as C-based nucleophiles for the FLP activation of phenylacetylene in combination with $B(C_6F_5)_3$, providing a strategy for C−C bond formation. A 3:2 mixture of addition products derived from the 2- and 3-substituted pyrroles was observed with the less hindered N-methylpyrrole.[30] Nevertheless, the bulky N-tertbutylpyrrole gave exclusively the 3-substituted product **24** (Scheme 10). Next, with thermally induced proton migrations the reaction evolved to a new series of vinyl pyrroles, **25**, and in the case of adding a phosphine deprotonation resulted in the salt **26**, $[^tBu_3PH][^tBuNC_4H_3(PhC{=}C(H)B(C_6F_5)_3)]$.

[30] M. A. Dureen, C. C. Brown, D. W. Stephan. *Organometallics* **2010**, *29*, 6422−6432.

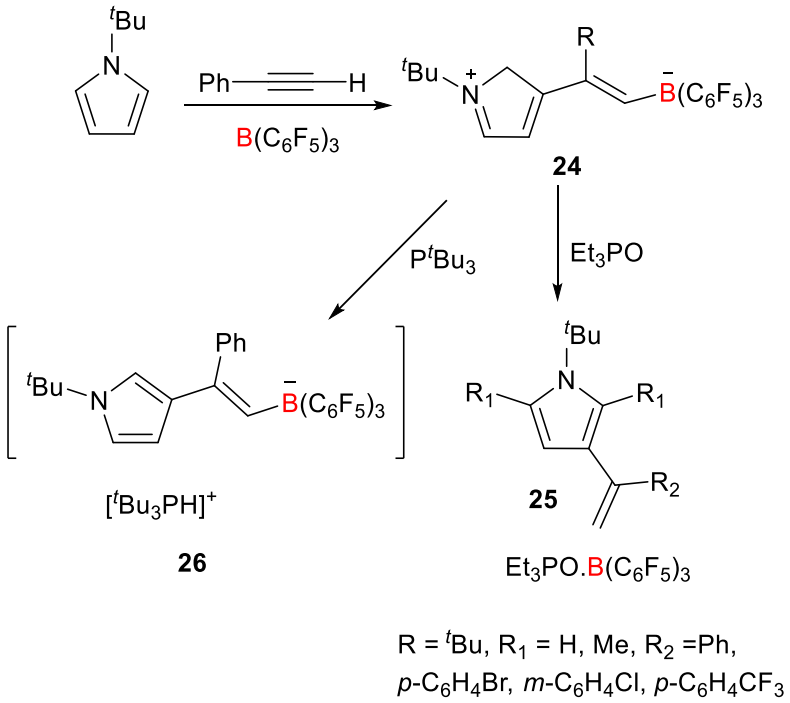

Scheme 10. FLP-type reactions of pyrroles and $B(C_6F_5)_3$ with phenylacetylene.

Carbon dioxide activation

Inter- and intramolecular FLPs are capable to activate a wide range of unsaturated molecules and heterocumulenes.[18] Among those, the capture CO_2 has attracted considerable attention due to its inert nature and environmental implications.[31] Stephan's group demonstrated that a solution of a Lewis base, P^tBu_3, and a Lewis acid, $B(C_6F_5)_3$, in bromobenzene is capable to effect the reversible binding of carbon dioxide under mild conditions (25 ºC, 1 bar). This system produces **27** which was isolated as a white powder in 87% yield (Scheme 11). In a similar way, the

[31] C. M. Mömming, E. Otten, G. Kehr, R. Fröhlich, S. Grimme, D. W. Stephan, G. Erker. *Angew. Chem. Int. Ed.* **2009**, *48*, 6643−6646.

intramolecular Lewis pair **15**, upon exposure to carbon dioxide (25 ºC, 2 bar), results in formation of $Mes_2P(CH_2)_2B(C_6F_5)_2(CO_2)$, **28**, in a very good yield. Complex **27** led to the starting materials after heat at 80 ºC under vacuum, instead, compound **28** in polar solvents as CH_2Cl_2 return to **15** even a low temperature (-20 ºC).

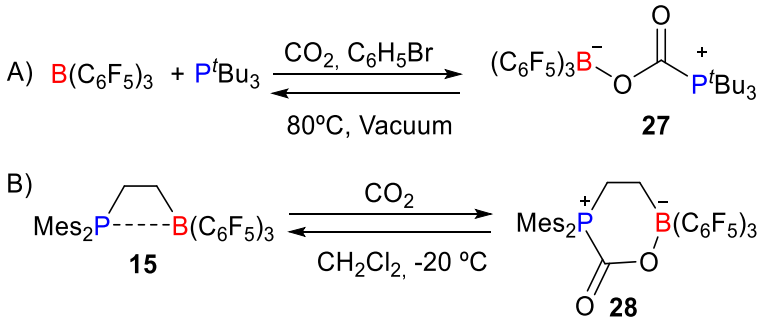

Scheme 11. First examples of carbon dioxide with inter- and intramolecular FLPs.

After these results, bis(boranes) **29** and **30** were used to isolate $Me_2C{=}C\text{-}(BCl_2)_2O_2CP^tBu_3$ and $Me_2C{=}C(B(C_6F_5)_2)_2O_2CP^tBu_3$,[32] **31** and **32**, respectively (Scheme 12), which exhibit bidentate binding of CO_2. The cyclic nature of the activated product is not maintained when using the pair $C_6H_4(BCl_2)_2/^tBu_3P$, which traps CO_2 forming a single boron-oxygen bond and a bridging chloride between the two boron centres.[33]

[32] X. Zhao, D. W. Stephan. *Chem. Commun.* **2011**, *47*, 1833−1835.
[33] M. J. Sgro, J. Domer, D. W. Stephan. *Chem. Commun.* **2012**, *48*, 7253−7255.

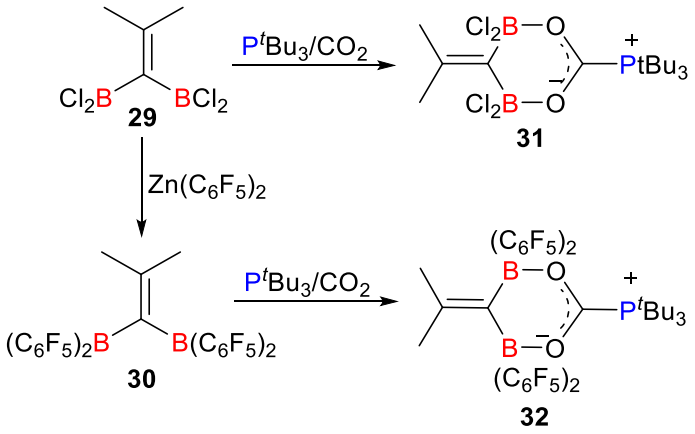

Scheme 12. Reactions of bis(boranes) with CO_2.

The activation of CO_2 has also been documented with N-centred bases. Two representative examples of intramolecular CO_2 activation are collected in Scheme 13. The four-membered ring containing a Lewis acidic P(V) centre in **33** inserts CO_2 in an FLP manner, yielding $C_6H_4(NMe)(CO_2)PFPh_2$, **34**. In turn, the four membered boron amidinate **35** reacts with CO_2 to give $HC(^iPrN)_2(CO_2)B(C_6F_5)_2$, **36**. Mechanistic investigations revealed that this reaction proceed via an equilibrium involving an open B/N FLP (Scheme 13). These are just some systems that exemplify the vast body of work on carbon dioxide activation by CO_2. However, many other different systems have already been investigated, exploring B[34] and Si[35] compounds as acids or NHC,[36] amine,[37] phosphinimine and pyrazol as Lewis bases.

[34] a) I. Peuser, R. C. Neu, X. Zhao, M. Ulrich, B. Schirmer, J. A. Tannert, G. Kehr, R. Fröhlich, S. Grimme, G. Erker, D. W. Stephan. *Chem. Eur. J.* **2011**, *17*, 9640−9650. b) M. Harhausen, R. Fröhlich, G. Kehr, G. Erker. *Organometallics* **2012**, *31*, 2801−2809. c) R. C. Neu, G. Ménard, D. W. Stephan. *Dalton Trans.* **2012**, *41*, 9016−9018. d) F. Bertini, V. Lyaskoyskyy, B. J. J. Timmer, F. J. J. de Kanter, M. Lutz, A. W. Ehlers, J. C. Slootweg, K. Lammertsma. *J. Am. Chem. Soc*. **2012**, *134*, 201−204.

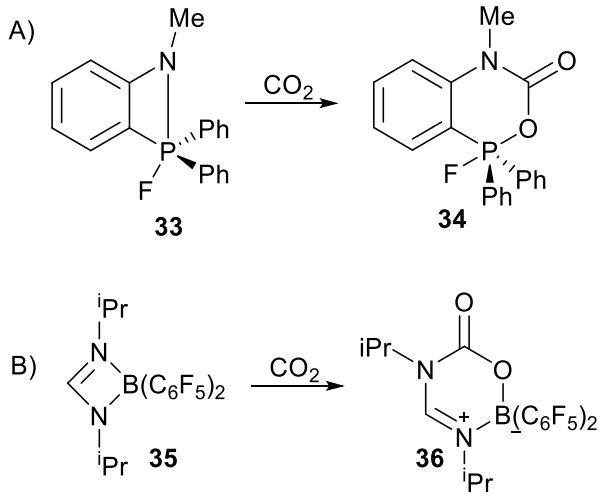

Scheme 13. Reactions of four-membered rings with CO_2.

[35] M. Reißmann, A. Schäfer, S. Jung, T. Müller. *Organometallics* **2013**, *32*, 6736−6744.
[36] a) M. Feroci, I. Chiarotto, S. V. Ciprioti, A. Inesi. *Electrochim. Acta* **2013**, *109*, 95−101. b) J. D. Holbrey, W. M. Reichert, I. Tkatchenko, E. Bouajila, O. Walter, I. Tommasi, R. D. Rogers. *Chem. Commun.* **2003**, 28−29. c) E. L. Kolychev, T. Bannenberg, M. Freytag, C. G. Daniliuc, P. G. Jones, M. Tamm. *Chem. Eur. J.* **2012**, *18*, 16938−16946. d) E. Theuergarten, T. Bannenberg, M. D. Walter, D. Holschumacher, M. Freytag, C. G. Daniliuc, P. G. Jones, M. Tamm. *Dalton Trans.* **2014**, *43*, 1651−1662.
[37] a) Y. Liu, G. P. Jessop, M. Cunningham, C. A. Eckert, C. L. Liotta, *Science* **2006**, *313*, 958−960. b) P. G. Jessop, D. H. Heldebrant, X. Li, C. A. Eckert, C. L. Liotta. *Nature* **2005**, *436*, 1102. c) D. A. Dickie, M. V. Parkes, R. A. Kemp. *Angew. Chem. Int. Ed.* **2008**, *47*, 9955−9957. d) T. Voss, T. Mahdi, E. Otten, R. Fröhlich, G. Kehr, D. W. Stephan, G. Erker. *Organometallics* **2012**, *31*, 2367−2378.

I.1.2.2. Metal-Free FLPs in Catalysis

Hydrogen catalysis

Hydrogenation of unsaturated substrates is undoubtedly the most investigated catalytic transformation in the context of FLPs.[26] For instance, sterically demanding aldimines, protected nitriles, and an aziridine were effectively hydrogenated in the presence of 5 mol% of $(R_2PH)(C_6F_4)BH(C_6F_5)_2$ (R = ^{t}Bu, Mes, **13**) at 80−120 °C under hydrogen atmosphere (1−5 atm), with reaction times ranging from 1 to 48 h (Scheme 14).[13] Hydrogenation was extended to imines, which under H_2 atmosphere and in the presence of $B(C_6F_5)_3$ can be readily hydrogenated owing to the intrinsic basic nature of the nitrogen that form an FLP with the borane.[38] Catalyst design and screening of conditions have allowed to reach excellent catalytic performance with catalysts loadings as low as 0.1 mol%. This strategy has been expanded to reduce diimines, pyridyldiimines and imine precursors for antidepressants, herbicides and anticancer drugs (Scheme 14).[39] One of the limitations of these FLP catalysts is their reduced tolerance to polar, sterically unencumbered donors, such as water.[39] Apart from the design of water stable FLPs,[40] which has typically proved synthetically challenging, the use of ^{i}Bu$_3$Al or Et$_3$SiH has also proved useful to eliminate traces of adventitious water.[41]

[38] P. A. Chase, T. Jurca, D. W. Stephan. *Chem. Commun.* **2008**, 1701−1703.
[39] D. W. Stephan, S. Greenberg, T. W. Graham, P. A. Chase, J. J. Hastie, S. J. Geier, J. M. Farrell, C. C. Brown, Z. M. Heiden, G. C. Welch, M. Ullrich. *Inorg. Chem.* **2011**, *50*, 12338−12348.
[40] V. Fasano, M. J. Ingleson. *Synthesis* **2018**, *50*, 1783−1795.
[41] J. W. Thomson, J. A. Hatnean, J. J. Hastie, A. Pasternak, D. W. Stephan, P. A. Chase. *Org. Process Res. Dev.* **2013**, *17*, 1287−1292.

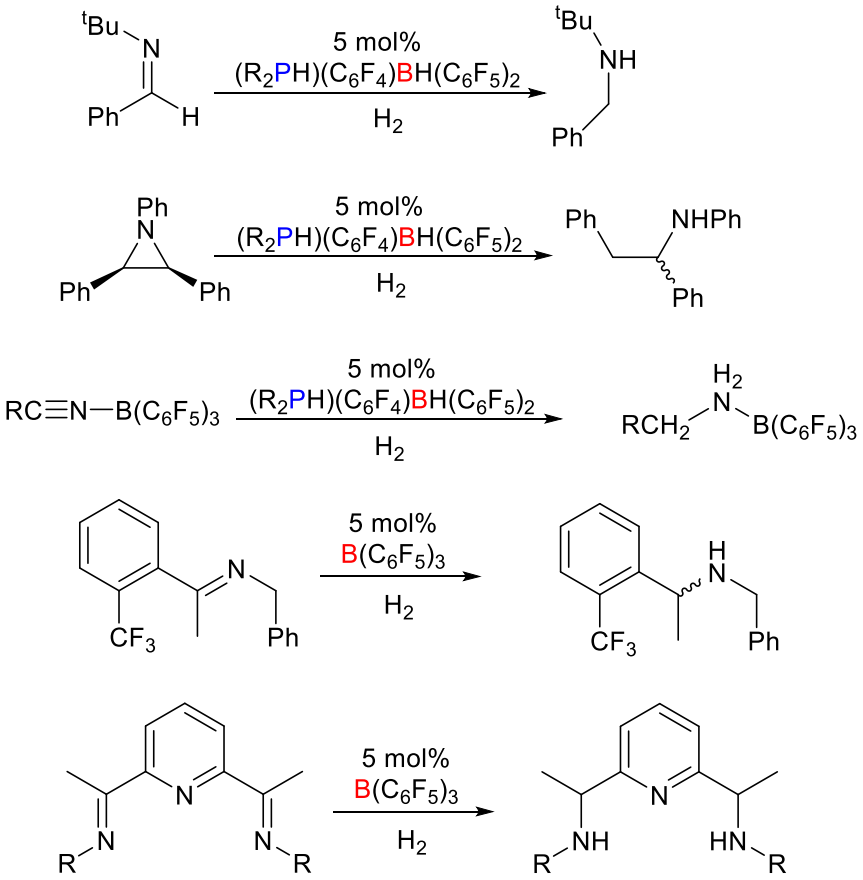

Scheme 14. Selected examples of catalytic FLP hydrogenation.

This rapid development on metal-free hydrogenation was later extended to enantioselective versions. In 2008, Klankermayer and co-workers reported the first FLP-catalyzed asymmetric hydrogenation of an imine using α-pinene-derived chiral borane **37** to furnish the desired chiral amine with 13% ee (Scheme 15). Moreover, the same group published the first example of highly enantioselective hydrogenation with chiral FLP salts, more precisely with **38**. Then, Repo's group reported the use of chiral *ansa*-ammonium borate **39** for the asymmetric hydrogenation of imines and 2-phenylquinoline with up to 37% ee (Scheme 15).

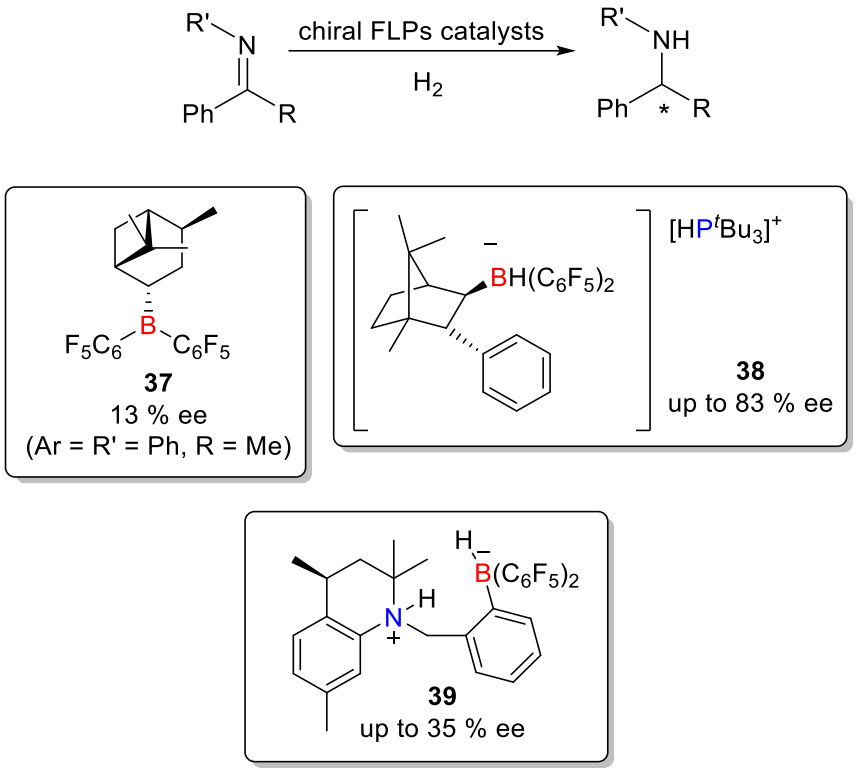

Scheme 15. Examples of FLP-catalyzed asymmetric hydrogenation of imines.

The hydrogenation of unsaturated C−C bonds was proved to be more challenging, although it did not escape the catalytic ability of FLPs. The pair $B(C_6F_5)_3/P(C_6F_5)Ph_2$ does not react with hydrogen at room temperature; however, at -80 ºC the phosphonium species $[(C_6F_5)Ph_2PH]^+$ was observed. This fact is due to the low barrier to reversible activation of H_2 that results from the generation of a highly acidic cation.[42] Nonetheless, this high acidity was exploited for the protonation of 1,1-disubstituted olefins. Under catalytic conditions, this forms a carbocation capable of

[42] L. Greb, P. Oña-Burgos, B. Schirmer, S. Grimme, D. W. Stephan, J. Paradies. *Angew. Chem. Int. Ed.* **2012**, *51*, 10164−10168.

hydride capture from the borate regenerating the active FLP. Initially, 20 mol% of the P/B FLP catalyst was used, although these species can be reduced to 5 mol% introducing a base as *p*-Tol_2NMe.[42] Interestingly, the potential of heterolytic H_2 cleavage by an ether-borane adduct was also analysed, revealing that this pair is also effective for the hydrogenation of 1,1-disubstituted olefins (Scheme 16).[43]

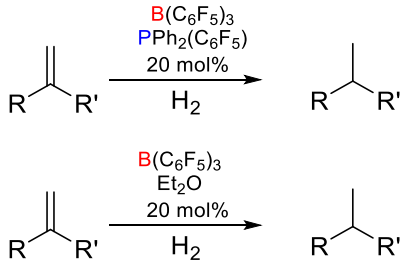

Scheme 16. Examples of catalytic hydrogenations of olefins.

Paradies broadened the substrate scope by studying the hydrogenation of β-Nitrostyrenes. This group used the combination of $B(2,6\text{-}C_6H_3F_2)_3$ and 2,6-lutidine to hydrogenate the double bond at 40 °C (Figure 17A).[44] Also, allenic esters can catalytically be hydrogenated with $B(C_6F_5)_3$ and 2,6-lutidine or (1,4)-diazabicyclo[2.2.2]octane (DABCO) (10−15 mol%) (Figure 17B).[45]

[43] L. J. Hounjet, C. Bannwarth, C. N. Garon, C. B. Caputo, S. Grimme, D. W. Stephan. *Angew. Chem. Int. Ed.* **2013**, *52*, 7492−7495.
[44] L. Greb, C. G. Daniliuc, K. Bergander, J. Paradies. *Angew. Chem. Int. Ed.* **2013**, *52*, 5876−5879.
[45] B. Inés, D. Palomas, S. Holle, S. Steinberg, J. A. Nicasio, M. Alcarazo. *Angew. Chem. Int. Ed.* **2012**, *51*, 12367−12369.

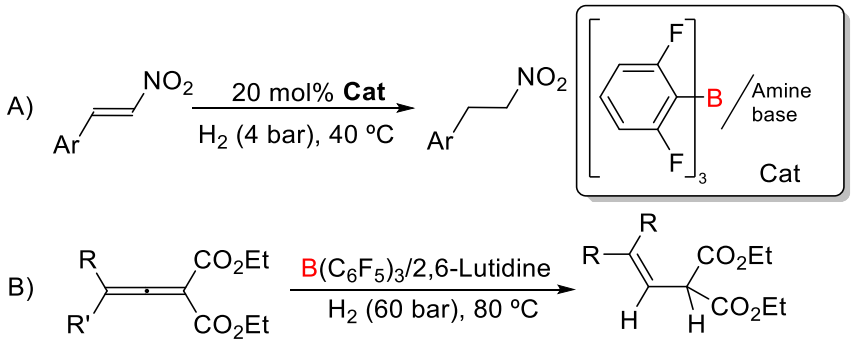

Scheme 17. Catalytic olefin and allene-ester hydrogenation.

Besides, Repo and co-workers[46] extended catalytic hydrogenation to internal alkynes using the intramolecular FLP, **40**, $C_6H_4(NMe_2)B(C_6F_5)_2$. Reaction with H_2 formed free C_6F_5H and produced **41** (Scheme 18), which is capable of hydroborate the alkyne. Then another H_2 molecule induces protonolysis to afford the *cis*-alkene and regenerate the catalyst.

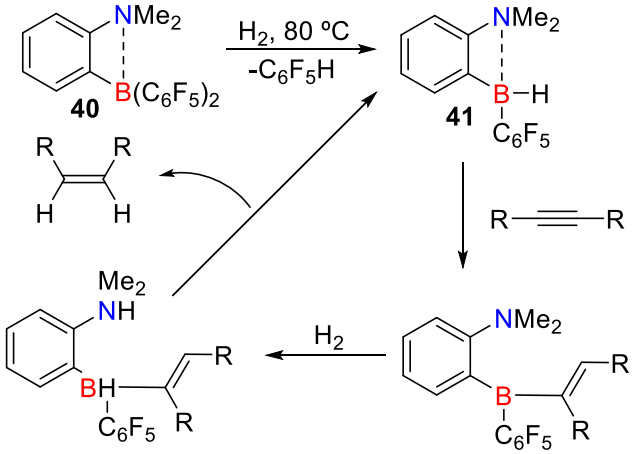

Scheme 18. Catalytic hydrogenation of alkynes.

[46] K. Chernichenko, A. Madarász, I. Pápai, M. Nieger, M. Leskelä, T. A. Repo. *Nat. Chem.* **2013**, *5*, 718−723.

Alkynes functionalization

The reaction between 2 equivalents of PhC≡CH with $B(C_6F_5)_3$, in the presence of N-alkylanilines or diarylamines, results in the stoichiometric C−N bond formation that yields compounds **42** and **43**, respectively (Scheme 19A).[47] These initial results set the basis to study the potential for metal-free catalytic hydroamination of alkynes. In fact, following the same strategy a series of aryl enamines was produced in yields between 62 and 84%. Moreover, a one-pot route to amines was developed by the combination of hydroamination/hydrogenation processes (Scheme 19B).

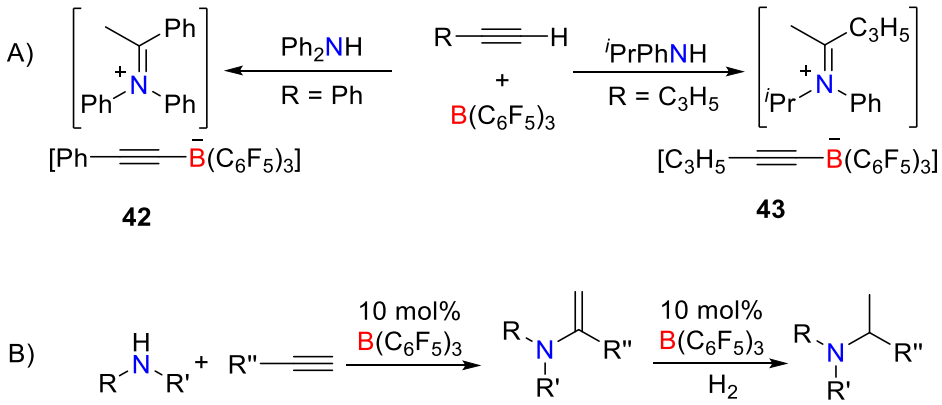

Scheme 19. A) Stoichiometric reactions of arylamine, borane and alkyne. B) Catalytic hydroaminations of alkynes.

[47] T. Mahdi, D. W. Stephan. *Angew. Chem. Int. Ed.* **2013**, *52*, 12418−12421.

Carbon dioxide functionalization

In 2009, Ashley and O'Hare[48] demonstrated the selective hydrogenation of CO_2 to CH_3OH by using an FLP consisting of the combination of tetramethylpiperidine (TMP) and $B(C_6F_5)_3$. CO_2 reduction took place at low pressures (1−2 atm) after 6 days at 160 ºC. In a related study, Piers and co-workers used Et_3SiH to effect catalytic reduction of CO_2, yielding CH_4 and $(Et_3Si)_2O$.[49] Mechanistic investigations permitted to disclose a stepwise process. Thus, in the presence of excess $B(C_6F_5)_3$ and triethylsilane, a formatoborate is produced and hydrosilated, leading to a formatosilane and $[TMPH]^+[HB(C_6F_5)_3]^-$. The formatosilane in turn is rapidly hydrosilated by the $B(C_6F_5)_3/Et_3SiH$ system to CH_4, with $(Et_3Si)_2O$ as the byproduct.

The hydroboration of CO_2 has also been amply investigated. For instance, Fontaine's group prepared the main-group FLP **44** (Scheme 20) which proved active for this transformation.[50] With 1 mol% of **44**, the yields can be as high as 99% with exclusive formation of CH_3OBR_2 or $(CH_3OBO)_3$ with TON between 86 and 2950. One year after Stephan published the use of **45** to catalyse the hydroboration of CO_2 to methoxyboranes and BOB species.[51] In this case catalyst loadings were as low as 3 mol% with TON values between 100−240.

[48] A. E. Ashley, A. L. Thompson, D. O'Hare. *Angew. Chem. Int. Ed.* **2009**, *48*, 9839−9843.
[49] A. Berkefeld, W. E. Piers, M. Parvez. *J. Am. Chem. Soc.* **2010**, *132*, 10660−10661.
[50] M. A. Courtemanche, M. A. Legare, L. Maron, F. G. Fontaine. *J. Am. Chem. Soc.* **2013**, *135*, 9326−9329.
[51] T. Wang, D. W. Stephan. *Chem. Eur. J.* **2014**, *20*, 3035−3039.

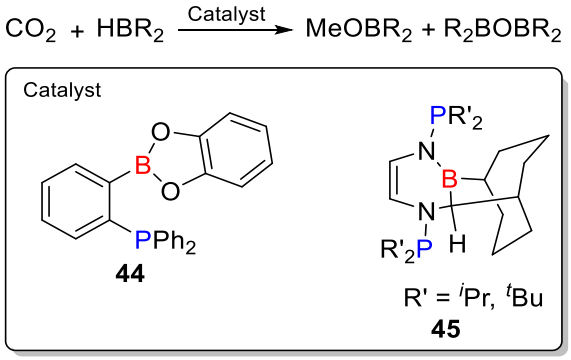

Scheme 20. Catalytic hydroboration of CO_2 with P/B FLPs.

I.1.3. TMFLPs with One Transition Metal Centre

It has already been stated that, in the field of main group chemistry, the concept of frustration and its application to bond activation and catalysis has represented a revolutionary advance over the last fifteen years. Although first developed to rationalize and predict the reactivity of combinations of bulky main group Lewis acids and Lewis bases, these systems also offer a valuable paradigm for transition metal complexes. In fact, the introduction of transition metals as integrating components of frustrated designs has emerged as a promising approach to overcome the main limitations of main group FLPs in the area of catalysis. This incorporation might seem a disadvantage due to the capacity of main group systems to mediate catalytic transformations in the absence of transition metals. Nevertheless, extending the concept to include transition metals as the Lewis basic or acidic components provides an enormous usefulness that justify this research area.

First, there is a wide variety of possibilities and combinations derived from introducing three series of transition metals (even more if lanthanides and actinides are to be considered). Moreover, the presence of partly occupied *d* orbitals with accessible energies in FLP systems gives access to a set of elementary reactions such as oxidative addition, reductive elimination or migratory insertion that are usually unavailable for traditional main group FLPs. The reluctance of main group elements to mediate these types of transformations has probably precluded their broader implementation into catalytic cycles more exotic that the ones previously discussed.

Transition metal organometallic and coordination complexes present an enormous structural and electronic diversity. Coordination numbers typically range from two to six for the d-block, though they can reach up to nine (e.g. $[ReH_9]^{2-}$).[52] This leads to a wide variety of structures and geometries around the metal centre that finds no parallel in the main group.

As an additional advantage, the synthetic methods to prepare transition metal compounds have been published over the last decades in many synthetic protocols with relatively simple and expeditious routes. Similarly, phosphines, the most common basic partners in traditional FLPs, are readily prepared and their commercial catalogue is extensive. However, accessing the type of fluorinated boranes that are typically used as the Lewis acid in FLPs is challenging,[53] contrasting with the synthetic amenability of transition metal Lewis acids.

In addition, a transition metal element (particularly mid-TMs) can behave as a base or an acid depending on its oxidation state and ligand environment, which also contrasts with the main group series, where the same behavior, though being well-known, is less versatile. Besides, transition metals exhibit a large diversity of affinities towards specific elements. Specifically, while main group elements are highly oxophilic, the degree of oxophilicity found in the transition metal series is wider, from the high tendency of early transition metals such as titanium or hafnium to bind oxygen, to the oxophobic character of gold or palladium.[54]

[52] C. Li, J. Agarwal, H. T. Schaefer. *J. Phys. Chem. B* **2014**, *118*, 6482−6490.
[53] Z. Lu, H. Ye, H. Wang. *New organoboranes in "frustrated Lewis pair" chemistry.* In: G. Erker, D. Stephan (eds) Frustrated Lewis Pairs II. Topics in Current Chemistry. **2012**. Springer, Berlin, Heidelberg, p 59−80.
[54] K. P. Keep. *Inorg. Chem.* **2016**, *55*, 9461−9470.

Controlling the degree of affinity may thus be key for enhancing catalytic efficiency.

Overall, all these advantages imply a high potential for catalysis derived from the introduction of transition metal elements into FLP designs. In fact, the use of transition metals either as the acid or basic site (or both) in the design of TM-based FLPs has attracted continuous attention since the pioneering work of the groups of Wass[55] and Erker[56] on zirconium/phosphine pairs. However, prior to these works, Stephan mentioned this possibility in the development of FLP chemistry using complexes of the type $[CpTi(NPR_3)Me(PR_3)][MeB(C_6F_5)_3]$ ($Cp = \eta^5\text{-}C_5H_5$), which did not lead to adduct formation with bulky phosphines, for example, P^tBu_3.[57]

This section will mainly concentrate on representative examples where the transition metal functions as one of the active sites of the cooperative moiety, while those in which it merely acts as a structural pillar will not be covered.[58] Homogeneous chemistry that seem to operate though FLP-like mechanisms will also be discussed. These designs will be classified into those constructed around early transition metals and those incorporating mid and late counterparts. In addition, recent systems based on rare-earth elements will be briefly revisited. The logical continuation of

[55] a) A. M. Chapman, M. F. Haddow, D. F. Wass. *J. Am. Chem. Soc.* **2011**, *133*, 8826–8829. b) A. M. Chapman, M. F. Haddow, D. F. Wass. *J. Am. Chem. Soc.* **2011**, *133*, 18463−18478. c) A. M. Chapman, M. F. Haddow, D. F. Wass. *Eur. J. Inorg. Chem.* **2012**, 1546−1554.

[56] a) X. Xu, R. Fröhlich, C. G. Daniliuc, G. Kehr, G. Erker. *Chem. Commun.* **2012**, *48*, 6109−6111. b) X. Xu, G. Kehr, C. G. Daniliuc, G. Kehr, G. Erker. *J. Am. Chem. Soc.* **2013**, *135*, 6465−6476.

[57] D. W. Stephan. *Org. Biomol. Chem.* **2008**, *6*, 1535−1539.

[58] a) N. S. Lambic, R. D. Sommer, E. A. Ison. *J. Am. Chem. Soc.* **2016**, *138*, 4832−4842. b) N. Zwettler, S. P. Walg, F. Belaj, N. C. Mösch-Zanetti. *Chem. Eur. J.* **2018**, *24*, 7149–7160. c) G. Erker. *Dalton Trans.* **2011**, *40*, 7475–7483.

these cooperative designs are those in which the two components of the FLP are based on transition metals. However, that particular discussion, which constitute the crux of this Thesis, will be specifically presented in the next section of this introductory Chapter.

I.1.3.1. Early and Mid-Transition Metals

Electron deficient early transition metal compounds have been extensively used as Lewis acid catalysts for several transformations,[59] specifically complexes with metals in high oxidation states. In 2011, Wass's group synthesized the first well-characterized transition metal FLP system (**46**, Scheme 21).[55a] They introduced zirconium as the acidic component, with an aryloxide phosphine ligand with bulky *tert*-butyl groups preventing the existence of a Zr−P bond. This system activates a wide range of small molecules such as CO_2, H_2, C_2H_4 and formaldehyde, as well as C–X bonds (X = Cl, F, O) (Scheme 20).[55a] It is worth highlighting the importance of steric effects: While the Zr/P pair that contain pentamethylcyclopentadienyl ligand (Cp* = η^5-C_5Me_5) activates dihydrogen at ambient temperature, the analogous complex with an unsubstituted cyclopentadienyl ligand (η^5-C_5H_5) is unreactive under identical conditions due the existence of a Zr−P bond that quenches FLP reactivity.

[59] H. Yamamoto (Ed). *Lewis acids in organic synthesis.* **2000**. Wiley-VCH, Weinheim.

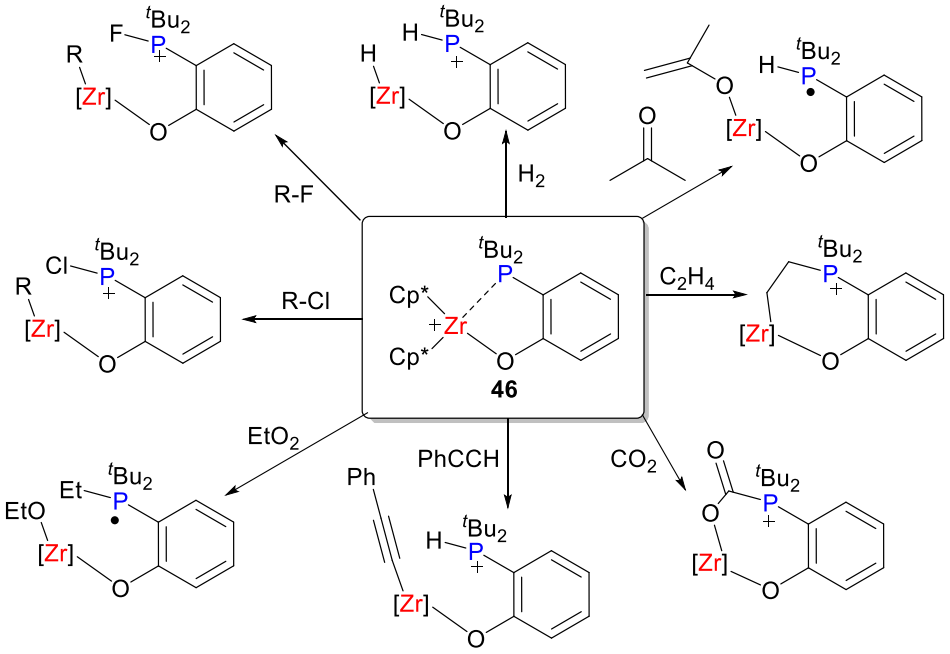

Scheme 21. Reactivity of the first comprehensively studied example of a transition metal FLP reported by Wass.

Cationic zirconocenes are likely the most investigated fragments in the area of metallic FLPs (Figure 3). In fact, Erker reported a geminal Zr^+/P pair **47** by the simple insertion of diphenylacetylene into the Zr–C σ-bond of cation $[Cp^*_2Zn(CH_3)]^+$.[56] Interestingly, a related vicinal Zr-based TMFLP **48**, as well as its hafnium version, were also prepared. Those derived from the reaction of the same cationic zirconocene with diphenylphosphino(trimethylsilyl)acetylene ($Me_3SiCCPPh_2$), which followed an alternative and unusual 1,1-carbozirconation reaction.[60] These earliest systems exhibit FLP-like reactivity towards common small molecules such as dihydrogen, carbon dioxide or a range of

[60] X. Xu, G. Kehr, C. G. Daniliuc, G. Erker. *Angew. Chem. Int. Ed.* **2013**, *52*, 13629–13632.

heterocumulenes. To compare the behavior of the electrophilic Zr centre with respect to the widely used borane moiety, an elegant competition study was carried out.[61]

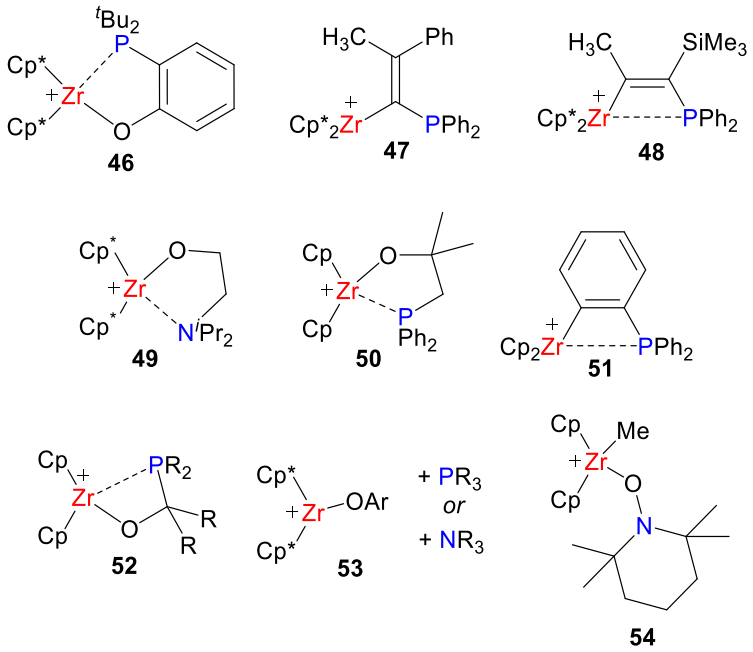

Figure 3. Representative examples of zirconocene-based FLPs. Counteranions have been omitted for clarity.

As aforesaid, the potential for catalysis is likely the most appealing benefit of extending the concept of frustration to transition metals. This became obvious since the publication of the aforementioned original works. For instance, while compound **48** promotes the catalytic dimerization of alkynes, zirconocene **46** mediates the dehydrogenation of amine boranes, the latter being the first example of such transformation in

[61] X. Xu, G. Kehr, C. G. Daniliuc, G. Erker. *Organometallics* **2013**, *32*, 7306–7311.

the FLP arena.[62] This has been lately explored in deeper detail by testing several intramolecular Zr^+/P complexes constructed around a variety of cyclopentadienyl and phosphinoaryloxide ligands.[63] These compounds are active in dimethylamine-borane ($Me_2NH{\cdot}BH_3$) dehydrogenation towards cyclic diborazane $[Me_2N–BH_2]_2$. Moreover, compound **46-Ind**, containing two indenyl ligands instead of the cyclopentadienyl fragments common to all other attempted catalysts, revealed the highest activity (TOF > 600 h^{-1}; Scheme 22). Although the more donating character of indenyl compared to cyclopentadienyl ligands[64] seems to indicate that the superior activity could be rationalized in terms of electronics, the authors highlight that steric factors and the more facile η^3 ring slippage of indenyl ligands[65] may also play a role. Mechanistic investigations using intermolecular Zr^+/P models evinced the existence of two concurrent pathways, the first involving the previously proposed FLP-like dehydrogenation,[55a] while the complementary route implies a phosphine-independent process that facilitates formation of the cyclic diborazane.

[62] a) Z. Mo, A. Rit, J. Campos, E. L. Kolychev, S. Aldridge. *J. Am. Chem. Soc.* **2016**, *138*, 3306–3309. b) Z. Mo, E. L. Kolychev, A. Rit, J. Campos, S. Aldridge. *J. Am. Chem. Soc.* **2015**, *137*, 12227–12230. c) G. Ma, G. Song, Z. H. Li. *Chem. Eur. J.* **2018**, *24*, 13238–13245. d) M. Boudjelel, E. D. Sosa Carrizo, S. Mallet-Ladeira, S. Massou, K. Miqueu, G. Bouhadir, D. Bourissou. *ACS Catal.* **2018**, *8*, 4459–4464.
[63] O. J. Metters, S. R. Flynn, C. K. Dowds, H. A. Sparkes, I. Manners, D. F. Wass. *ACS Catal.* **2016**, *6*, 6601–6611.
[64] P. M. Treichel, J. W. Johnson, K. P. Wagner. *J. Organomet. Chem.* **1975**, *88*, 227–230.
[65] A. Habib, R. S. Tanke, E. M. Holt, R. H. Crabtree. *Organometallics* **1989**, *8*, 1225–1231.

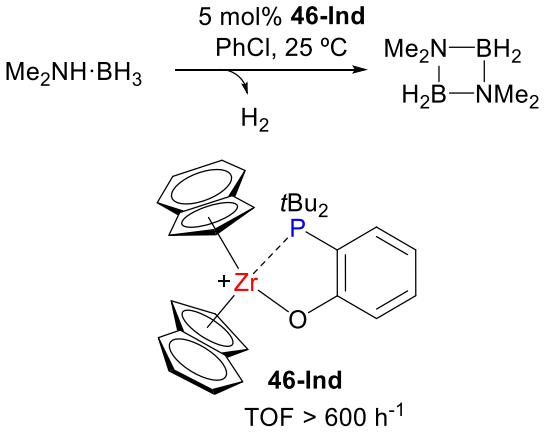

Scheme 22. Catalytic dehydrocoupling of dimethylamine-borane by a Zr^{+}/P intramolecular frustrated Lewis pair.

Introducing a pendant amine as the basic partner in this type of Zr-based FLPs allowed Erker to disclose a highly reactive frustrated system that was active not only in the activation of small molecules (H_2, CH_2Cl_2, terminal alkynes), but also in the catalytic hydrogenation of alkenes and internal alkynes under mild conditions (25 ºC, 1.5 bar H_2, 1−4 mol % Zr^{+}/N cat.). The authors propose a mechanism (Scheme 23) involving the FLP-like cleavage of H_2 to produce a zirconium hydride and a pendant ammonium group, followed by hydrozirconation of the olefin (or alkyne) substrate and subsequent protonolysis of the Zr−C σ-bond to release the hydrogenated product and regenerate the catalyst. Interestingly, the use of the persistent radical TEMPO permitted the isolation of compound **54** where the nitrogen centre behaves as an internal base for the FLP-like activation of phenylacetylene.[66] In a more recent report, Rocchigiani and Budzelaar explored the mechanism of related

[66] Y. Liu, G. Kehr, C. G. Daniliuc, G. Erker. *Organometallics* **2017**, *36*, 3407–3414.

zirconaziridinium compounds of formula $[Cp_2Zr(\eta^2\text{-}CH_2NR_2]^+$, which could potentially behave as TMFLPs for H_2 splitting.[67] However, a σ-bond metathesis mechanism seems to prevail in that case. Nevertheless, this reactivity generates cation $[Cp_2ZrH]^+$, whose subsequent combination with a released amine facilitates FLP-type H_2 cleavage.

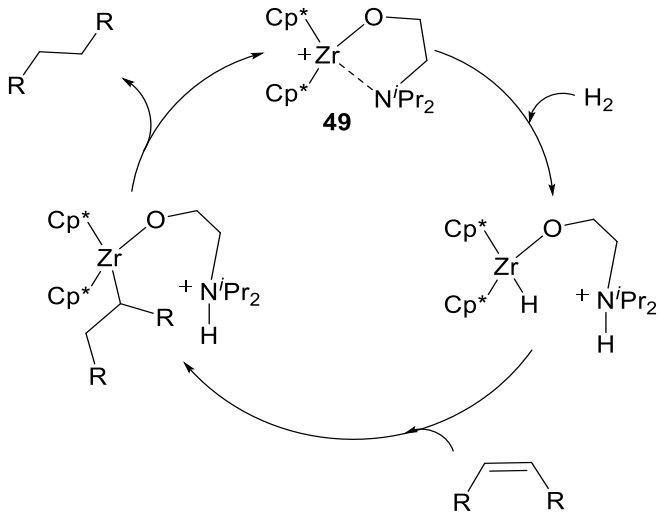

Scheme 23. Catalytic hydrogenation of alkenes by Zr^+/N FLP **49**.

The same group explored other related intramolecular Zr^+/P architectures, some of which are collected in Figure 3. Those include a P-based version of **49** in which the pendant amine is substituted by a PPh_2 terminus.[68] The corresponding zirconium cation dimerizes to yield an oxygen bridged dicationic product, despite which it undergoes the 1,4-addition of chalcone in an FLP-like manner. A richer reactivity was

[67] P. H. M. Budzelaar, D. L. Hughes, M. Bochmann, A. Macchionic, L. Rocchigiani. *Chem. Commun.* **2020**, *56*, 2542–2545.
[68] X. Xu, G. Kehr, C. G. Daniliuc, G. Erker. *Organometallics* **2015**, *34*, 2655–2661.

reported for compound **50**, whose bulkier steric profile prevented dimerization.[68] The latter compound exhibits FLP reactivity with benzaldehyde, nitrosobenzene and an ynone (Scheme 24). The similar Zr^+/P compound **51** was described shortly after and its FLP reactivity towards ketones, aldehydes, α,β-unsatutated carbonyl compounds and heterocumulenes was demonstrated.[69]

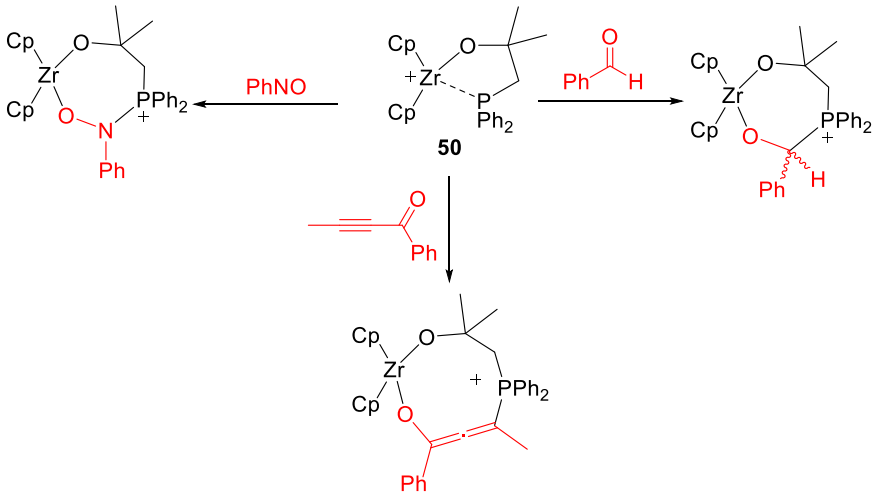

Scheme 24. FLP reactivity of Zr^+/P compound **50** towards benzaldehyde, nitrosobenzene and an ynone. Counteranions have been omitted for clarity.

Fine control of stereoelectronic properties in this type of systems remains a challenge from a synthetic point of view. To overcome this limitation, a more convenient route towards Zr^+-based pairs was reported by means of facile insertion of non-enolisable carbonyl compounds (including CO_2) into the Zr–E (E = P, N) bond of phosphido- and amidozirconocene complexes of type $[Cp_2Zr(ER_2)Me]$ (E = P, N) and

[69] Z. Jian, C. G. Daniliuc, G. Kehr, G. Erker. *Organometallics* **2017**, *36*, 424–434.

subsequent (or former) methyl abstraction by $B(C_6F_5)_3$.[66,70] Compounds **52** were prepared by this approach and their coordinating ability as ambiphilic ligands examined.[70]

Drawing on the same theme, Wass explored intermolecular Zr^+/P FLPs by combining zirconocene aryloxide compounds with a range of phosphines.[71] This approach offers even greater versatility considering the extensive amount of phosphines commercially available. The reactivity of these pairs towards H_2, CO_2, THF and phenylacetylene was investigated providing evidence for significant differences derived from subtle modification of the stereoelectronic properties of the phosphine base. For instance, while the weakly basic $P(C_6F_5)_3$ did not exhibit any FLP reactivity, the use of PPh_3 and $PMes_3$ led to opposite selectivity during phenylacetylene activation (**53**, Scheme 25). Besides, DOSY NMR spectroscopic studies were applied for the first time to a TMFLP system[72] and uncovered some degree of preorganization between the cationic zirconocene and the phosphine fragments. The same intermolecular approximation was subsequently employed by the group for the hydrogenation of imines using a range of zirconocenes bearing mesityl aryloxide and where the imine substrate served as the base as well.[73]

[70] A. T. Normand, C. G. Daniliuc, B. Wibbeling, G. Kehr, P. Le Gendre, G. Erker. *Chem. Eur. J.* **2016**, *22*, 4285–4293.
[71] O. J. Metters, S. J. K. Forrest, H. A. Sparkes, I. Manners, D. F. Wass. *J. Am. Chem. Soc.* **2016**, *138*, 1994–2003.
[72] L. Rocchigiani, G. Ciancaleoni, C. Zuccaccia, A. Macchioni. *J. Am. Chem. Soc.* **2014**, *136*, 112–115.
[73] S. R. Flynn, O. J. Metters, I. Manners, D. F. Wass. *Organometallics* **2016**, *35*, 847–850.

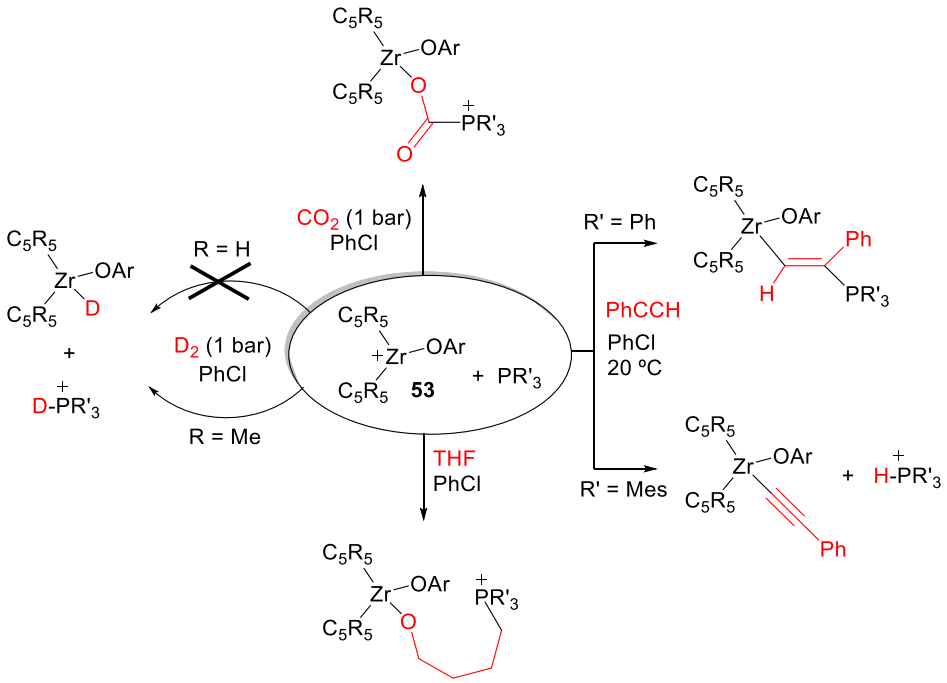

Scheme 25. FLP activation of small molecules by intermolecular Zr^{+}/P pairs based on zirconocene **53** and commercial phosphines. Counteranions have been omitted for clarity.

In an early example, prior to coining the term 'Frustrated Lewis Pair',[11] Stephan demonstrated that combining the acidic titanium compound [CpTi(N=P^{t}Bu$_3$)][B(C$_6$F$_5$)$_4$], with the sterically demanding P(*o*-MeC$_6$H$_4$)$_3$ phosphine, did not lead to ligand coordination due to steric clash providing instead cooperative cleavage of a C−Cl bond of a dichloromethane solvent molecule. In a later study, the group of Wass investigated an intramolecular titanocene-phosphinoaryloxy complex capable of heterolytically activating dihydrogen.[74] This system is

[74] A. M. Chapman, D. F. Wass. *Dalton Trans.* **2012**, *41*, 9067–9072.

analogous to a zirconium-based counterpart that the same group explored in detail in previous years.[55a,b]

Other intramolecular Ti-based TMFLPs were later reported by Erker. In their first strategy, the synthesis of a functionalized cyclopentadienyl ligand allowed access to a series of cationic titanium complexes with a pendant phosphine of general formula [$CpCp^PTiOAr$][BPh_4], **55**, (Cp=η^5-C_5H_5; Cp^P= η^5-$C_5H_4(CMe_2)PCy_2$) (Scheme 26A).[75] Although this species was completely unreactive towards gaseous substrates as H_2, CO_2, CO or C_2H_2, it readily reacted with benzaldehyde to yield the corresponding addition product **56**. Interestingly, compound **55** slowly reacts (9 days) with *trans*-chalcone to produce a 10-membered titanium macrocyle **57**. More recently, the same group described an intramolecular phosphidotitanocene cation **58** that revealed FLP reactivity with ferrocene carboxaldehyde to yield the expected addition product **59** (Scheme 26B).[76]

[75] A. T. Normand, P. Richard, C. Balan, C. G. Daniliuc, G. Kehr, G. Erker, P. L. Gendre. *Organometallics* **2015**, *34*, 2000–2011.
[76] A. T. Normand, Q. Bonnin, S. Brandès, P. Richard, P. Fleurat-Lessard, C. H. Devillers, C. Balan, P. L. Gendre, G. Kehr, G. Erker. *Chem. Eur. J.* **2019**, *25*, 2803–2815.

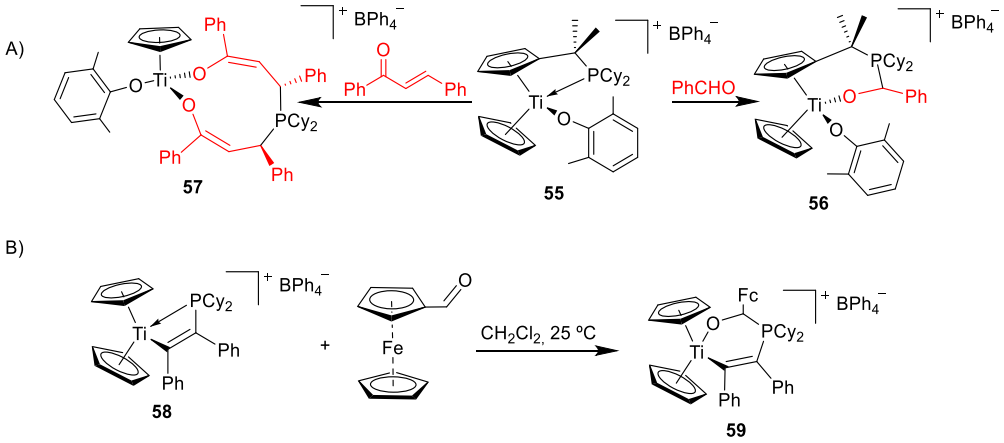

Scheme 26. Titanium based frustrated Lewis pairs reported by the group of Erker.

Beckhaus described a series of electrophilic cationic d^0 titanium complexes with a single ligand framework, more precisely a novel tridentate *Cp,N,P* system (**60**, Scheme 27A).[77] This design allowed the authors to explore the competence between the nitrogen termini and the phosphine ligand to cooperate with the acidic titanium centre to activate the C−H bonds in phenylacetylene and acetone (towards **61** and **62**, respectively). Although the overall reaction takes place at the Ti−N bond, as expected for the higher basicity of the nitrogen, a related compound missing the phosphine group **63** revealed no activity even under harsher conditions, which evinced the phosphorus centre playing a key role that remains under investigation. The same group reported a year later a similar d^0 titanium complex stabilized by a *Cp,O,N* ligand (**64**, Scheme 27B).[78] The pendant amine enabled the activation of C-halogen bonds, including

[77] M. Fischer, D. Barbul, M. Schmidtmann, R. Beckhaus. *Organometallics* **2018**, *37*, 1979–1991.
[78] M. Fischer, K. Schwitalla, S. Baues, M. Schmidtmann, R. Beckhaus. *Dalton Trans.* **2019**, *48*, 1516–1523.

C(sp^3)−F bonds, of different substrates under mild conditions (**65**), while compounds of type **60** were inactive.

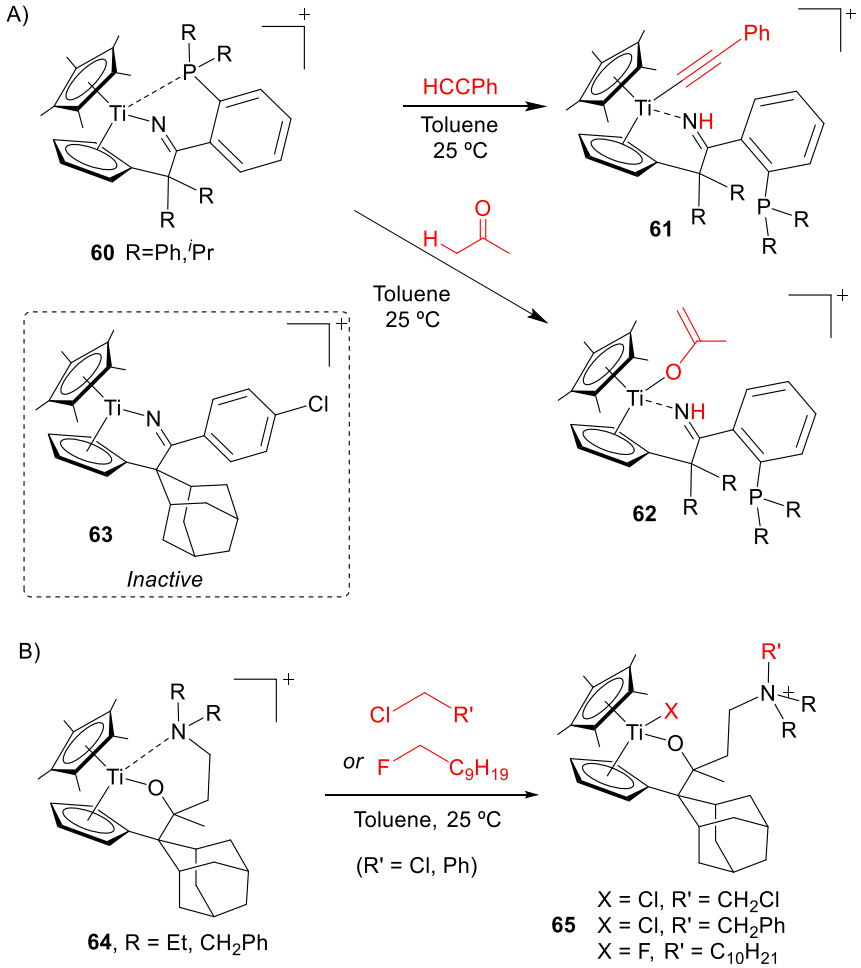

Scheme 27. C−H and C−halogen bond activation of electrophilic titanium complexes stabilized by Cp-based tridentate ligands with pendant basic functionalities. The $[BCH_3(C_6F_5)_3]^-$ counteranion has been omitted for clarity.

Moving forward to group 6 of the periodic table, Bullock explored the reversible and heterolytic cleavage of the H−H bond in a series of

molybdenum complexes containing a pendant amine (Scheme 28).[79] These studies built upon their previous expertise on related manganese[80] and iron[81] complexes with pendant amines as effective electrocatalysts for H_2 oxidation. The latter systems are particularly attractive since they serve as synthetic models of the [FeFe]-hydrogenase and [NiFe]-hydrogenases.[82] Back to molybdenum, it becomes clear that the strength of the interaction between the pendant amine and the acidic molybdenum centre is crucial to achieve H_2 splitting. Thus, while compounds **66** are unable to attain this activation,[83] introducing ring strain to destabilize the Mo−N interaction in **67** permits rapid cleavage of the H−H bond, **68**. The authors propose a mechanism involving initial coordination of H_2 to form a molybdenum dihydrogen or dihydride intermediate (not observed) followed by intramolecular deprotonation by the lateral amine, though a concerted FLP-like cleavage is not completely ruled out. The newly formed hydride and proton rapidly exchange even at low temperature, as evinced by NMR spectroscopy, while the rate of the process can be tuned by modifying the substituents of the phosphine and amine groups (Scheme 28). Introducing less basic amines and poorer P-donors increases acidity to the extent of recording a surprisingly high first-order kinetic constant of up to 10^7 s^{-1}. The relation between acidity and exchange rate was experimentally

[79] S. Zhang, A. M. Appel, R. M. Bullock. *J. Am. Chem. Soc.* **2017**, *139*, 7376–7387.
[80] a) E. B. Hulley, K. D. Welch, A. M. Appel, D. L. DuBois, R. M. Bullock. *J. Am. Chem. Soc.* **2013**, *135*, 11736–11739. b) E. B. Hulley, M. L. Helm, R. M. Bullock. *Chem. Sci.* **2014**, *5*, 4729–4741.
[81] a) T. Liu, D. L. DuBois, R. M. Bullock. *Nat. Chem.* **2013**, *5*, 228–233. b) T. Liu, X. Wang, C. Hoffmann, D. L. DuBois, R. M. Bullock. *Angew. Chem. Int. Ed.* **2014**, *53*, 5300–5304. c) T. Liu, Q. Liao, M. O. Hagan, E. B. Hulley, D. L. DuBois, R. M. Bullock. *Organometallics* **2015**, *34*, 2747–2764.
[82] a) J. C. Fontecilla-Camps, A. Volbeda, C. Cavazza, Y. Nicolet. *Chem. Rev.* **2007**, *107*, 4273–4303. b) W. Lubitz, H. Ogata, O. Rüdiger, E. Reijerse. *Chem. Rev.* **2014**, *114*, 4081–4148.
[83] S. Zhang, R. M. Bullock. *Inorg. Chem.* **2015**, *54*, 6397–6409.

investigated and provides important insights for future developments in TMFLPs and in the broader context of bifunctional catalysis.

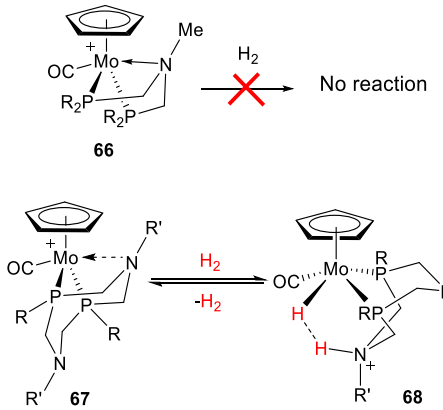

R	R'	k (s^{-1})	pK_a
Ph	Bn	3.9 x 10^5	13.8
Ph	Ph	4.0 x 10^7	9.3
^{t}Bu	Bn	6.9 x 10^4	15.3
^{t}Bu	Ph	4.1 x 10^6	10.7
^{t}Bu	^{t}Bu	2.1 x 10^3	17.7

Scheme 28. Reversible activation of dihydrogen by molybdenum complexes with a pendant amine base. Counteranions have been omitted for clarity.

I.1.3.2. Late Transition Metals

Late transition metals can act as either Lewis acids or bases depending on ligand environment and oxidation state. Traditionally, they have been used as Lewis acids and therefore their incorporation into FLP designs have followed the same role, particularly in many systems that parallel bifunctional catalysts with pendant bases. However, the use of late transition metals as Lewis bases[84] has also been contemplated. For example, Pt(0) species of the type [PtL_2] (L = N-heterocyclic carbene or bulky alkyl pohosphine) react with Lewis acids such as $AlCl_3$ to form the corresponding Pt→Al adduct. This type of metal-only Lewis pairs will be further discussed in section I.2.3.

The activation of the inert molecule dinitrogen remains a topic of intense research and its efficient catalytic functionalization one of the greatest challenges in contemporary chemistry. Metal-free FLP systems have some potential within this field, as discussed by Stephan in 2017.[85] During the same year Szymczak[86] and Simonneau[87] independently reported the activation of N_2 by a TMFLP approach based on iron **69** and molybdenum/tungsten **70** complexes, respectively (Scheme 29). On the basis of the similarities of the two systems, they will be jointly presented here rather than shifting the discussion on the molybdenum/tungsten pairs to the previous section. In both metallic systems the high barrier associated to the activation of the triple N≡N bond is overcome by a push-pull strategy in which the highly acidic $B(C_6F_5)_3$ borane releases electron

[84] J. Bauer, H. Braunschweig, R. D. Dewhurst. *Chem. Rev.* **2012**, *112*, 4320–4346.
[85] C. Tang, Q. Liang, A. R. Jupp, T. C. Johnstone, R. C. Neu, D. Song, S. Grimme, D. W. Stephan. *Angew. Chem. Int. Ed.* **2017**, *56*, 16588–16592.
[86] J. B. Geri, J. P. Shanahan, N. K. Szymczak. *J. Am. Chem. Soc.* **2017**, *139*, 5952–5956.
[87] A. Simonneau, R. Turrel, L. Vendier, M. Etienne. *Angew. Chem. Int. Ed.* **2017**, *56*, 12268–12272.

density from the coordinated dinitrogen. Computational analysis carried out on the iron system reveals that the trapped dinitrogen gets polarized, while its π^* orbital is stabilized, much like what is seen in traditional FLPs during H_2 activation.[15c,88] Similarly, this approach mimics the mechanism by which the active site of nitrogenase enzymes initially weakens the N≡N bond.[89] Moreover, while protonation of N_2 was achieved for the iron system by using $HBAr_F{\cdot}(OEt_2)_2$ (BAr_F^- = $[3,5\text{-}(CF_3)_2C_6H_3]_4B^-$), the molybdenum/borane and tungsten/borane pairs permit the stoichiometric borylation and silylation of N_2 under mild conditions (Scheme 29).

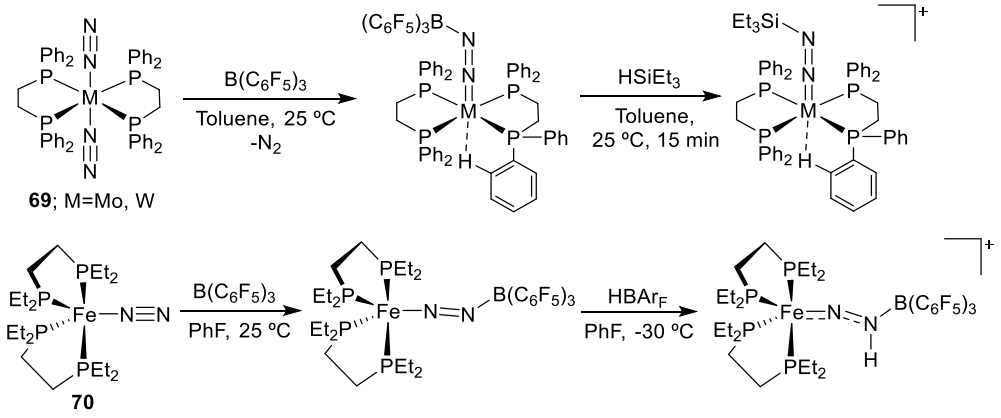

Scheme 29. Dinitrogen activation and functionalization by combining transition metal Lewis bases with $B(C_6F_5)_3$. Counteranions have been omitted for clarity.

[88] a) T. A. Rokob, I. Pápai. *Hydrogen activation by frustrated Lewis pairs: Insights from computational studies.* In: G. Erker, D. Stephan (eds) Frustrated Lewis Pairs I. Topics in Current Chemistry. **2013**. Springer, Berlin, Heidelberg, p 157–212. b) L. Rocchigiani. *Isr. J. Chem.* **2015**, *55*, 134–149. c) L. Liu, B. Lukose, P. Jaque, B. Ensing. *Green Energy & Environment* **2019**, *4*, 20–28.

[89] B. M. Hoffman, D. Lukoyanov, Z.-Y. Yang, D. R. Dean, L. C. Seefeldt. *Chem. Rev.* **2014**, *114*, 4041–4062.

Poater and Renaud also worked with iron complexes and they found inspiration in the FLP concept to exploit a family of iron carbonyl compounds stabilized by cyclopentadiene fragments (Scheme 30).[90] These complexes, highly reminiscent of the prominent Shvo catalyst,[91] efficiently promoted reductive amine alkylation[90a,c] and ketone alkylation.[90b] Carbon monoxide abstraction with Me_3NO provides a vacant site on the electrophilic iron centre where H_2 is coordinated. Computational studies revealed that substituting the cyclopentadienone in **71** by a cyclopentadienyl with a pendant amine group in **72** has an impact on the mechanism of H_2 splitting. While in the former case dihydrogen splitting is mediated by direct action of the oxygen centre, in compound **72** the lower energy pathway involves the action of an external amine. Although this may not be strictly considered a TMFLP, the authors highlighted the importance of applying the concepts derived from the field of frustrated systems to the area of cooperative catalysis with transition metals.

[90] a) T. T. Thai, D. S. Mérel, A. Poater, S. Gaillard, J. L. Renaud. *Chem. Eur. J.* **2015**, *21*, 7066–7070. b) C. Seck, M. D. Mbaye, S. Coufourier, A. Lator, J. F. Lohier, A. Poater, T. R. Ward, S. Gaillard, J. L. Renaud. *ChemCatChem* **2017**, *9*, 4410–4416. c) A. Lator, Q. G. Gaillard, D. S. Mérel, J. F. Lohier, S. Gaillard, A. Poater, J. L. Renaud. *J. Org. Chem.* **2019**, *84*, 6813–6829.

[91] B. L. Conley, M. K. Pennington-Boggio, E. Boz, T. J. Williams. *Chem. Rev.* **2010**, *110*, 2294–2312.

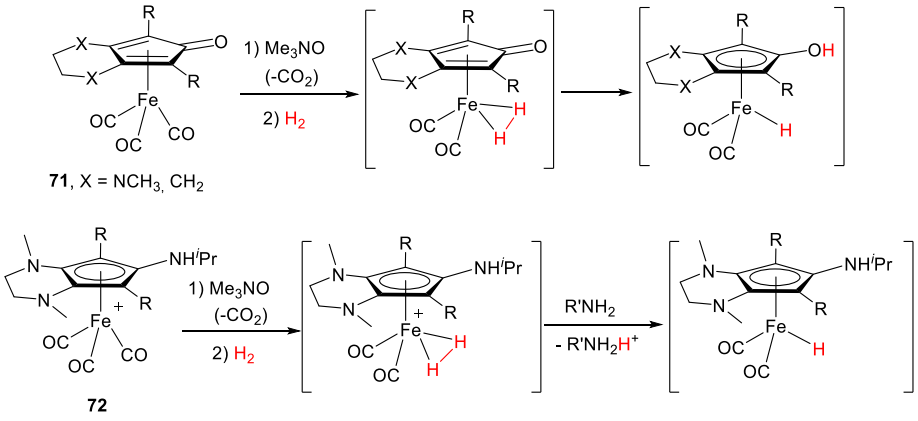

Scheme 30. Dihydrogen activation by intra- (**71**) and intermolecular (**72**) cooperative systems with mechanisms reminiscent of FLPs. Counteranions have been omitted for clarity.

In another cooperative example that resembles the chemistry of FLPs, the group of Oestreich and Tatsumi studied in detail the tethered ruthenium(II) thiolate complex **73**, whose Ru−S bond facilitates the cooperative activation of Si−H bonds to lead a terminal ruthenium hydride and an acidic silicon fragment that behaves as a silylium cation (**74**, Scheme 31). Mechanistic studies proposed a concerted σ-bond metathesis pathway across the Ru−S bond which, although differs from FLPs mode, shares some common features with the latter such as the polarized landscape between the two intervening nuclei and the heterolytic nature of the splitting. The electrophilic nature of the latter has been exploited for a number of catalytic applications,[92] including the enantioselective reduction

[92] a) H. F. T. Klare, M. Oestreich, J.-I. Ito, H. Nishiyama, Y. Ohki, K. Tatsumi. *J. Am. Chem. Soc.* **2011**, *133*, 3312–3315. b) C. D. F. Königs, H. F. T. Klare, Y. Ohki, K. Tatsumi, M. Oestreich. *Org. Lett.* **2012**, *14*, 2842–2845. c) J. Hermeke, H. F. T. Klare, M. Oestreich. *Chem. Eur. J.* **2014**, *20*, 9250–9254. d) C. D. F. Königs, M. F. Müller, N. Aiguabella, H. F. T. Klare, M. Oestreich. *Chem. Commun.* **2013**, *49*, 1506–1508. e) C. D. F. Königs, H. F. T. Klare, M. Oestreich. *Angew. Chem. Int. Ed.* **2013**, *52*, 10076–10079. f)

of imines after introducing axial chirality at the sulfur ligand.[93] At variance with other examples of cooperative activation across metal-ligand bonds, the Ru−S bond remains virtually intact after Si−H cleavage (**73**, d_{RuS} = 2.21; **74** d_{RuS} = 2.39 Å). A detailed mechanistic investigation into this activation event by a joint experimental/computational effort was also undertaken.[94] Related work by Tatsumi and Sakaki on a hydroxo-/sulfido-bridged ruthenium-germanium complex, capable to activate H_2, also draws the analogy with the heterolytic mode of activation of FLPs.[95]

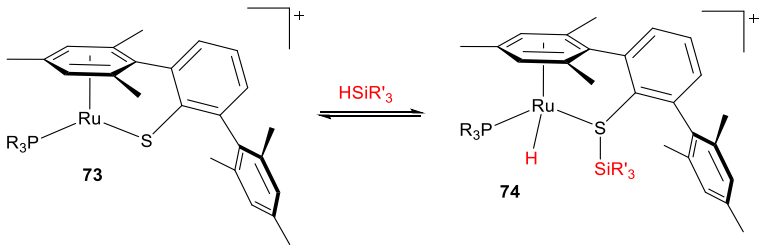

Scheme 31. Cooperative Si–H bond activation at a Ru−S bond. Counteranions have been omitted for clarity.

In the group 9 a very recent study by Carmona and Rodríguez[96] demonstrated that a thermally induced[14] rhodium FLP constructed around a tridentate guanidine-phosphine ligand (**75**) was effective for FLP-like

T. T. Metsänen, M. Oestreich. *Organometallics* **2015**, *34*, 543–546. g) T. Stahl, H. F. T. Klare, M. Oestreich. *J. Am. Chem. Soc.* **2013**, *135*, 1248–1251. h) S. Bähr, M. Oestreich. *Organometallics* **2017**, *36*, 935–943.

[93] S. Webbolt, M. S. Maji, E. Irran, M. Oestreich. *Chem. Eur. J.* **2017**, *23*, 6213–6219.

[94] T. Stahl, P. Hrobárik, C. D. F. Königs, Y. Ohki, K. Tatsumi, S. Kemper, M. Kaupp, H. F. T. Klare, M. Oestreich. *Chem. Sci.* **2015**, *6*, 4324–4334.

[95] a) N. Ochi, T. Matsumoto, T. Dei, Y. Nakao, H. Sato K. Tatsumi, S. Sakaki. *Inorg. Chem.* **2015**, *54*, 576–585. b) T. Matsumoto, Y. Nakaya, N. Itakura, K. Tatsumi. *J. Am. Chem. Soc.* **2008**, *130*, 2458–2459.

[96] M. Carmona, J. Ferrer, R. Rodríguez, V. Passarelli, F. J. Lahoz, P. García-Orduña, L. Cañadillas-Delgado, D. Carmona. *Chem. Eur. J.* **2019**, *25*, 13665–13670.

activation of dihydrogen and the O−H bond of water (Scheme 32). The lability of one of the Rh−N bond of **75** results from strong ring strain within the Rh−N−C−N moiety and gives access to a vacant coordination site at the acidic Rh(III) centre. This vacant is in close proximity to the basic imine and as such shows potential for FLP-like activation. Heterolytic dihydrogen splitting takes place under relatively mild conditions to yield a rhodium hydride fragment and a pendant iminium ion (**76**), as corroborated by X-ray diffraction studies. Partial reversibility was accomplished (*ca.* 30%) by heating the hydrogenated sample at 120 ºC for 30 min. More interesting is the reaction with deuterated water, which results in rapid H/D scrambling in all the methyl positions at the cyclopentadienyl fragment. Although the authors could not detect any intermediate for such a process, computational investigations support the notion of an initial FLP activation of the O−H bond by the cooperative action of the acidic Rh(III) centre and the basic role played by the pendant imine, followed by methyl deprotonation by the newly formed metal-hydroxide to produce a transient fulvene. Rapid equilibration among all proposed intermediates results in full deuteration of the cyclopentadienyl ring.

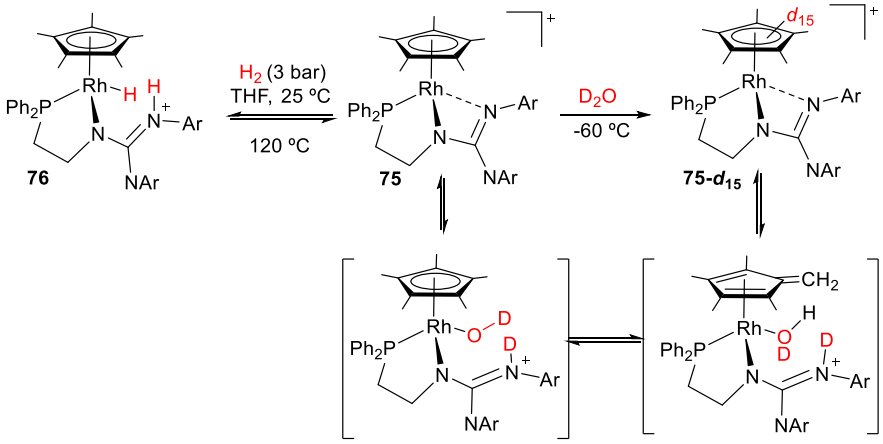

Scheme 32. Dihydrogen and D_2O heterolytic activation by an intramolecular rhodium/imine frustrated Lewis pair, including subsequent H/D scrambling at the cyclopentadienyl ring. Counteranions have been omitted for clarity.

The use of ligands with pendant boranes has been successful for designing efficient cooperative catalysts, particularly those involving hydrogen transfer between the metal centre and the boron atom.[97] The cooperative mechanism by which these complexes activate E−H (E = H, Si, C, O, N…) bonds is reminiscent of frustrated systems. This analogy was drawn by Peters regarding the study of a nickel metalloborane bearing a diphosphine-borane ligand which turned out to be an efficient hydrogenation catalyst.[98] The same group has made extensive use of diphosphine-borane ligands to impart cooperative reactivity to first-row transition metals.[99] In a recent study, the bond activation capacity of iron

[97] R. Gareth. *Chem. Soc. Rev.* **2012**, *41*, 3535−3546.
[98] W. H. Harman, J. C. Peters. *J. Am. Chem. Soc.* **2012**, *134*, 5080−5082.
[99] a) H. Fong, M.-E. Moret, Y. Lee, J. C. Peters. *Organometallics* **2013**, *32*, 3053−3062. b) S. N. MacMillan, W. H. Harman, J. C. Peters. *Chem. Sci.* **2014**, *5*, 590−597. c) W. H. Harman, T.-P. Lin, J. C. Peters. *Angew. Chem. Int. Ed.* **2014**, *53*, 1081–1086.

and cobalt metalloborane complexes was tested.[100] Compounds of type **77** permit rapid activation of a series of substrates containing E−H (E = O, S, N, C, Si) bonds (Scheme 33). Interestingly, the activation of a hydrosilane (Ph_2SiH_2) was found to be reversible for the cobalt system. This result prompted the authors to investigate the role of these compounds as hydrosilylation catalysts. In fact, cobalt compound **77** is remarkably efficient in the hydrosilylation of ketones and aldehydes.

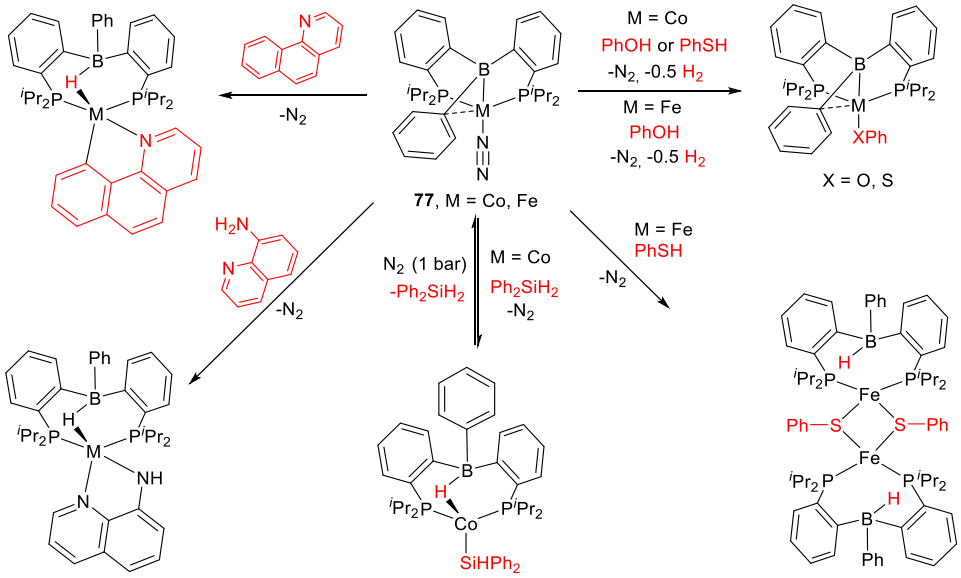

Scheme 33. Cooperative E−H bond activation using metalloborane iron and cobalt complexes.

The use of Pt(0) complex (**78**) as Lewis base in combination with a fluorinated borane as the acid allowed Wass to discover an apparently simple TMFLP. This compound perfectly emulates the behavior of main

[100] M. A. Nesbit. D. L. M. Suess, J. C. Peters. *Organometallics* **2015**, *34*, 4741−4752.

group frustrated systems and, in the case of ethylene activation, even revealed a novel and unexpected reactivity involving its coupling with carbon monoxide to yield a five-membered metallacycle (Scheme 34).[101] Mixing compound **78** with $B(C_6F_5)_3$ provided no spectroscopic hint of adduct formation. Beyond the intriguing formation of the metallacycle derived from ethylene/CO coupling, the reactivity with CO_2 is rather interesting since it involves CO displacement by a considerably poorer ligand such as CO_2. As expected, **78** does not react with CO_2 by itself, but in the presence of $B(C_6F_5)_3$ the corresponding CO_2 adduct is quantitatively formed after three days as a result of push-pull stabilization. These results were later extended to other related bisphosphine ligands and the products derived from the activation of small molecules analyzed with regards to ligand modification.[102]

[101] S. J. K. Forrest, J. Clifton, N. Fey, P. G. Pringle, H. A. Sparkes, D. F. Wass. *Angew. Chem. Int. Ed.* **2015**, *54*, 2223−2227.
[102] K. Mistry, P. G. Pringle, H. A. Sparkes, D. F. Wass. *Organometallics* **2020**, *39*, 468−477.

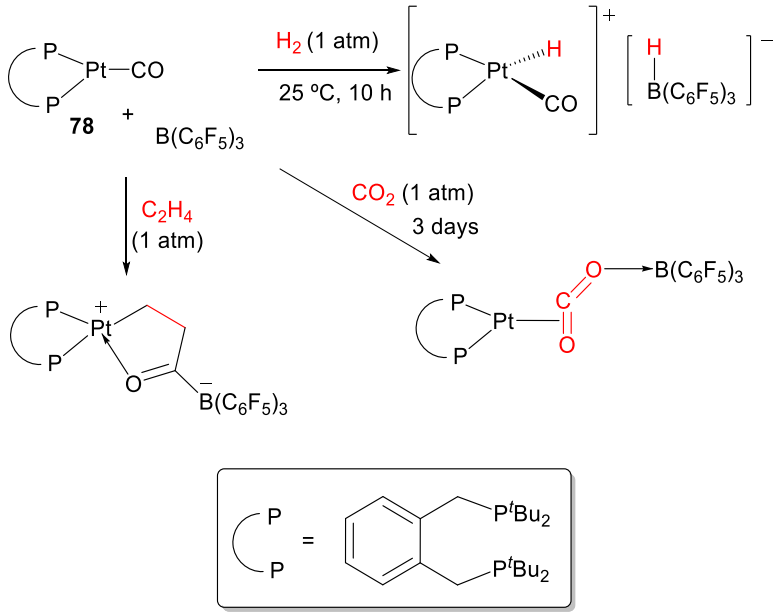

Scheme 34. Small molecule FLP activation by a Pt(0)/$B(C_6F_5)_3$ pair.

An intramolecular Pt(0)/borane pair (**79**) has also been studied by Figueroa after hydroboration of a *bis*-isonitrile Pt(0) compound that enables the formation of a chelating (boryl)iminomethane ligand.[103] The small bite angle of the latter framework seems to facilitate small molecule activation across the Pt→B bond in an FLP manner with a wide range of substrates (Scheme 35). For instance, compound **79** reacts with dihydrogen to produce the expected hydride/borohydride complex. Cleavage of polar E–H (O, N, C) bonds is also easily achieved for amines, alcohols and a terminal alkyne. Ketones and aldehydes react in the same fashion as main group FLPs, namely with the nucleophilic platinum centre coordinated to the carbon atom and the electrophilic boron to the carbonylic oxygen.

[103] a) B. R. Barnett, C. E. Moore, A. L. Rheingold, J. S. Figueroa. *J. Am. Chem. Soc.* **2014**, *136*, 10262−10265. b) B. R. Barnett, M. L. Neville, C. E. Moore A. L. Rheingold, J. S. Figueroa. *Angew. Chem. Int. Ed.* **2017**, *56*, 7195−7199.

Contrarily, reaction with CO_2 produces a metal-free boracarbamate with concomitant release of the parent *bis*-isonitrile Pt(0) from which compound **79** is prepared. The reaction with *tert*-butylisocyanate to generate a boraurea proceeds in a similar fashion. These two metal-free species are alternatively prepared by the free ambiphilic (boryl)iminomethane ligand whose FLP behavior was also explored. Other unsaturated substrates such as azides or acetonitrile also provided the corresponding FLP-like activation products, while addition of elemental sulfur (S_8) yielded the formal insertion of a sulfur atom into the Pt→B dative bond.

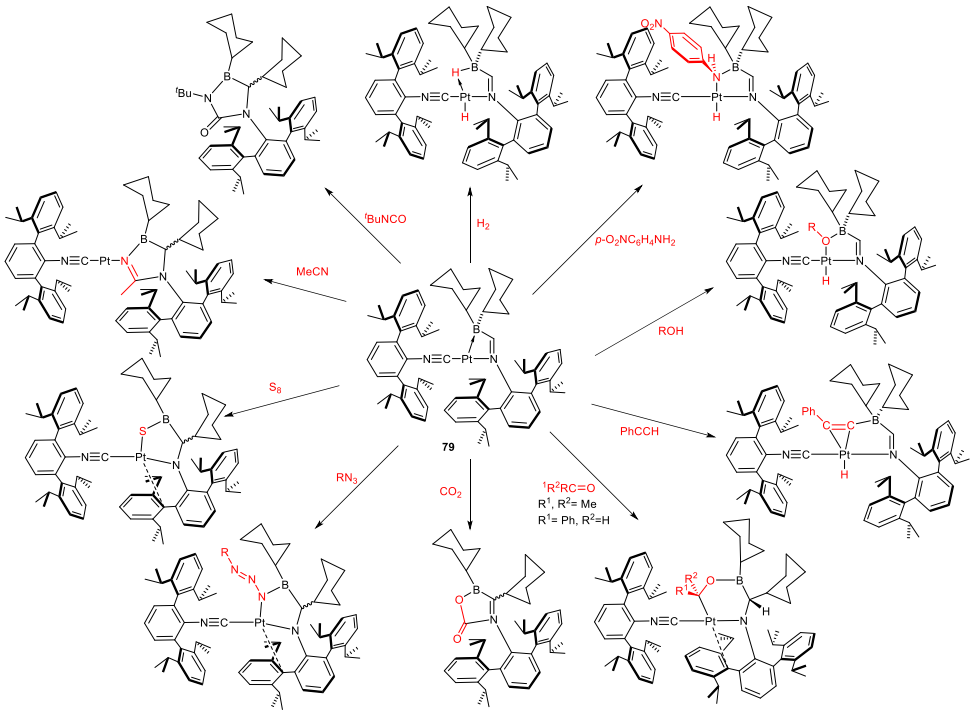

Scheme 35. Cooperative small molecule activation pinwheel for the geometrically constrained (boryl)iminomethane platinum compound **79**.

Gold chemistry became an obvious target to develop late transition metal FLPs considering the well-known electrophilicity of the $[LAu(I)]^+$ fragment, where L is a two electron donor ligand, typically a N-heterocyclic carbene or phosphine.[104] In a recent attempt to design a frustrated Au(I)/Phosphine pair Hashmi combined a cationic Au(I) fragment stabilized by an extremely bulky NHC ligand (IPr**)[105] with the sterically hindered phosphine $PMes_3$. Despite the bulkiness of the two ligands, the corresponding cationic complex $[(NHC)Au(PMes_3)]^+$ was easily formed,[106] which illustrates the complication of achieving metallic frustration with a linear compound (Scheme 36A).

Zhang explored the possibility of geometric frustration using a bifunctional phosphine ligand that integrate a pendant tertiary amine unavailable to intramolecular interaction with gold due to geometric constraints.[107] As a soft Lewis acid the Au(I) site in complex **80** (Scheme 36B) readily coordinates C≡C bonds with simultaneous weakening of the α-C–H bond, which is profited by the lateral amine to abstract the proton despite being a rather weak base ($pK_a \approx 4$; *c.f.* $R_2C(H)C{\equiv}CR'$: $pK_a > 30$). Conformational rigidity proved to be key for efficient isomerization, since substituting the adamantyl moieties bound to phosphorus considerably decreased the rate of catalysis. Based on this approach, a number of related studies were conducted to exploit the catalytic potential of gold compounds

[104] a) C. M. Friend, A. S. K. Hashmi. *Acc. Chem. Res.* **2014**, *47*, 729–730. b) I. Braun, A. M. Asiri, A. S. K. Hashmi. *ACS Catal.* **2013**, *3*, 1902–1907. c) M. Rudolph, A. S. Hashmi. *Chem. Soc. Rev.* **2012**, *41*, 2448–2462. d) N. Krause, C. Winter. *Chem. Rev.* **2011**, *111*, 1994–2009. e) A. Corma, A. Leyva-Pérez, M. J. Sabater. *Chem. Rev.* **2011**, *111*, 1657–1712. f) A. Fürstner. *Chem. Soc. Rev.* **2009**, *38*, 3208–3221. g) C. Obradors, A. M. Echavarren. *Chem. Commun.* **2014**, *50*, 16–28.
[105] S. G. Weber, C. Loos, F. Rominger, B. F. Straub. *ARKIVOC* **2012**, *23*, 226–242.
[106] S. Arndt, M. M. Hansmann, P. Motloch, M. Rudolph, F. Rominger, A. S. K. Hashmi. *Chem. Eur. J.* **2017**, *23*, 2542–2547.
[107] Z. Wang, Y. Wang, L. Zhang. *J. Am. Chem. Soc.* **2014**, *136*, 8887–8890.

bearing this type of bifunctional PN ligands.[108] The key feature in all cases is to maintain a geometry that avoids gold-amine adduct formation while forcing conformational constraints that facilitate activation of the organic substrate by the cooperative action of the two active sites.

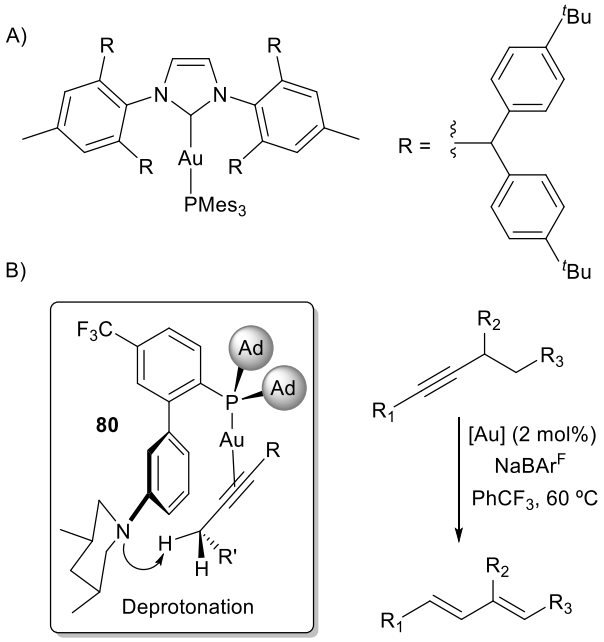

Scheme 36. A) Frustrated Au(I)/Phosphine pair designed by Hashmi. B) Catalytic isomerization of alkynes to 1,3-dienes by a bifunctional FLP-like Au(I)/NR_3 complex (**80**) that accelerates propargylic deprotonation.

[108] a) Z. Wang, A. Ying, Z. Fan, C. Hervieu, L. Zhang. *ACS Catal.* **2017**, *5*, 3676–3680. b) X. Li, X. Ma, Z. Wang, P.-N. Liu, L. Zhang. *Angew. Chem. Int. Ed.* **2019**, *58*, 17180–17184. c) X. Cheng, Z. Wang, C. D. Quintanilla, L. Zhang. *J. Am. Chem. Soc.* **2019**, *141*, 3787–3791.

I.1.3.3. Rare-Earth Elements

Due to their widespread use as Lewis acids in catalysis,[109] incorporating a rare-earth element increases the electron-accepting properties of the systems and affects the reactivity of the entire construct. The groups of Piers (Scheme 37A)[110] and Xu (Scheme 37B)[111] independently reported different scandium-based systems. Piers and Eisenstein were the first to study these systems and apply them in small molecule activation.[110] They published a electrophilic decamethylscandocinium cation $[Cp^*_2Sc]^+$ in combination with the hydrido-(perfluorophenyl)-borate anion $[HB(C_6F_5)_3]^-$ (**81**). This pair acts as an ionic FLP in which small molecules such as CO_2 or CO can be trapped in the polarized $Sc^+/^-HB$ pocket and subsequently activated by hydride transfer from the borate anion. This proved to be to an efficient cooperative method for the deoxygenative hydrosilylation of CO_2.

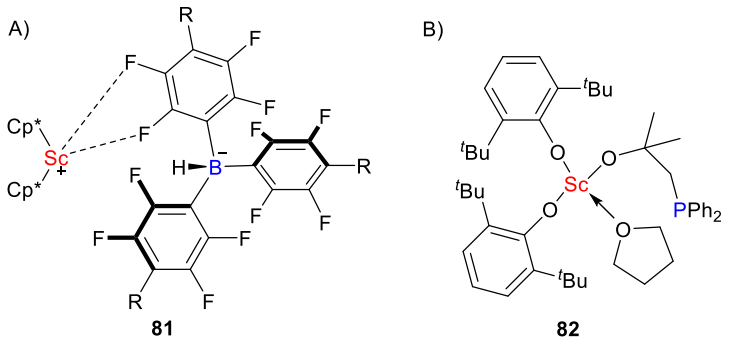

Scheme 37. Piers's and Xu's scandium-based FLPs systems.

[109] R. Anwander, S. Kobayashi, S. Kobayashi(Eds). *Lanthanides: chemistry and use in organic synthesis.* **1999**. Springer, Berlin, Heidelberg.
[110] a) A. Berkefeld, W. E. Piers, M. Parvez, L. Castro, L. Maron, O. Eisenstein. *J. Am. Chem. Soc.* **2012**, *134*, 10843–10851. b) A. Berkefeld, W. E. Piers, M. Parvez, L. Castro, L. Maron, O. Eisenstein. *Chem. Sci.* **2013**, *4*, 2152–2162.
[111] K. Chang, X. Xu. *Dalton Trans.* **2017**, *46*, 4514–4517.

With the same element, Xu reported a bisaryloxide complex (**82**) containing a bifunctional alkoxyde with a pendant phosphine.[111,112] This system highly resembles the related zirconium FLP **50** (see Figure 3). The scandium compound **82** presents a rich reactivity towards small molecules (Scheme 38) that compares well with related zirconium systems and with other metal-free FLPs. It should be noted that addition of an ynone or dimethyl acetylenedicarboxylate yielded a nine-membered metallacycle and an intriguing bimetallacyclic structure. It also reacts with unsaturated substrates such as an α-diketone, a cyclopropyl ketone and an epoxide. Other interesting reactivity are derived from benzaldehyde or chalcone to produce the corresponding 1,2- and 1,4-addition products, respectively. Carbon-halogen bond cleavage was achieved in the presence of benzyl bromide, while the addition of nitrogen containing species and elemental sulfur further confirmed the cooperative capacity of this intramolecular FLP to activate other small molecules.

[112] K. Chang, X. Wang, Z. Fan, X. Xu. *Inorg. Chem.* **2018**, *57*, 8568–8580.

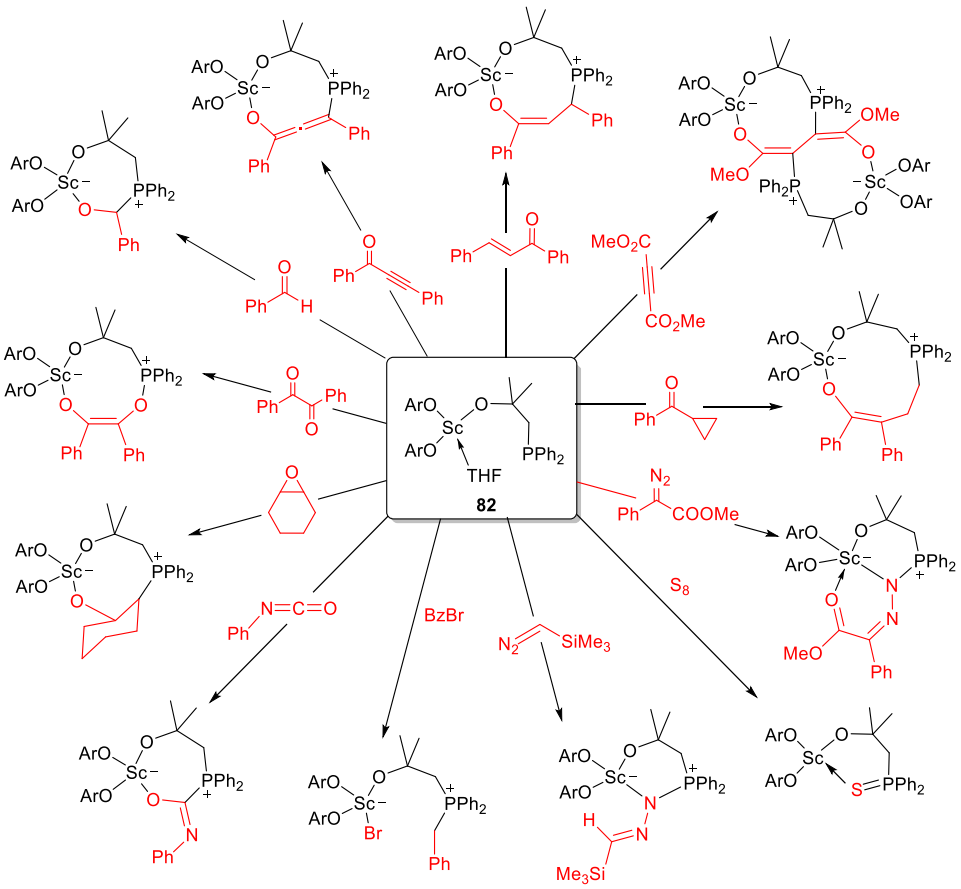

Scheme 38. Small molecule activation pinwheel of a bisaryloxide scandium complex containing a bifunctional alkoxide-phosphine ligand.

The same group reported the synthesis of other rare-earth metal complexes of scandium, yttrium and lutetium anchored by β-diketiminate ligands functionalized with a weakly coordinating phosphine.[113] These pairs also exhibit a FLP reactivity in polymerization catalysis and towards the activation of small molecules. To the first application, Xu used versions of their prior rare-earth-based FLPs to polymerization of polar

[113] a) P. Xu, Y. Yao, X. Xu. *Chem. Eur. J.* **2017**, *23*, 1263–1267. b) T. Yao, P. Xu, X. Xu. *Dalton Trans.* **2019**, *48*, 7743–7754.

alkenes because these elements have been employed as efficient catalysts in this reaction.[114]

Several RE complexes of type [RE(OAr)$_3$] (RE = Sc, Y, Sm, La; Ar = 2,6-^{t}Bu$_2$-C$_6$H$_3$) were combined with a range of phosphines as Lewis bases, more precisely PPh$_3$, PCy$_3$, PEt$_3$ and PMe$_3$.[115] Mechanistic investigations demonstrated that polymerization of polar alkenes is initiated by the FLP-like 1,4 addition of the substrate across the intermolecular Lewis pair. An example of this reactivity based on a trisalkoxide scandium compound **83** cooperating with PEt$_3$ is represented in Scheme 39.

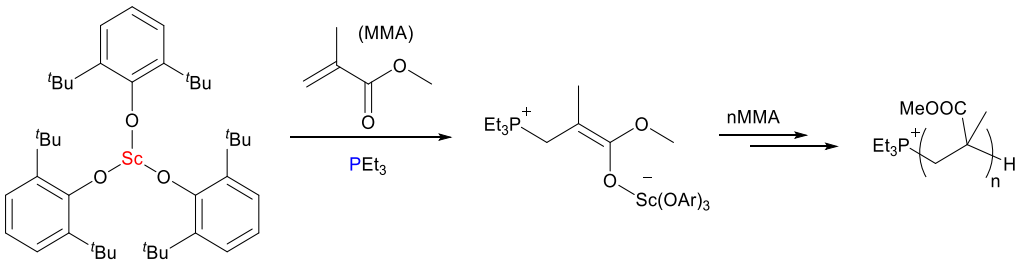

83

Scheme 39. 1,4-addition of methyl methacrylate (MMA) into the intermolecular FLP Sc/P pair formed by **83** and PEt$_3$ followed by MMA polymerization.

The use of carbon-based Lewis bases, more precisely two well-known NHC ligands such as I^{t}Bu and IMes (I^{t}Bu = 1,3-di-*tert*-

[114] a) H. Yasuda. *J. Organomet. Chem.* **2002**, *647*, 128−138. b) H. Yasuda. *J. Polym. Sci. Part A Polym. Chem.* **2001**, *39*, 1955−1959.
[115] a) P. Xu, X. Xu. *ACS Catal.* **2018**, *8*, 198–202. b) P. Xu, L. Wu, L. Dong, X. Xu. *Molecules* **2018**, *2*, 360–369.

butylimidazolin-2-ylidene; IMes = 1,3-Dimesitylimidazol-2-ylidene) was also interrogated during the polymerization of polar alkenes by Xu.[115a] In the same vein, the group demonstrated that a combination of rare-earth homoleptic aryloxides [RE(OAr)$_3$] (where RE = La, Sm or Y) with common N-heterocyclic carbenes effected dihydrogen activation.[116] Moreover, the rare-earth complexes were found to be active catalysts in the hydrogenation of NHCs towards aminals under mild conditions. These studies were connected to prior work from the group of Arnold based on the lability of RE−NHC[117] bonds, after which even a U−NHC bond was successfully examined.[118] In a more recent study, the same research group took advantage of a bidentate *ortho*-aryloxide–NHC motif to prepare a series of homoleptic lanthanide complexes **84** based on cerium, samarium and europium. Insertion of CO_2, RNCO (R = ^{t}Bu, Mes) and ^{t}BuNCS into the labile Ce–NHC bond was readily achieved under mild conditions.[119] Quantitative insertion of CO_2 into the three Ce–C bonds is instant under all attempted conditions (Scheme 40), while the number of isocyanate and isothiocyanate molecules inserted was controlled by solvent and steric tuning of the substrate, ranging from monoinserted to triply activated products. In terms of reversibility, only the more congested aryloxide–NHC ligand, namely the mesityl substituted one, liberates one molecule of CO_2 under dynamic vacuum (100 ºC, 10^{-3} mbar). This may be directly connected to the catalytic potential of these complexes, since only

[116] K. Chang, Y. Dong, X. Xu. *Chem. Commun.* **2019**, *55*, 12777–12780.
[117] a) P. L. Arnold, I. A. Marr, S. Zlatogorsky, R. Bellabarbac, R. P. Toozec. *Dalton Trans.* **2014**, *43*, 34–37. b) Z. R. Turner, R. Bellabarba, R. P. Tooze, P. L. Arnold. *J. Am. Chem. Soc.* **2010**, *132*, 4050–4051.
[118] P. L. Arnold, Z. R. Turner, A. I. Germeroth, I. J. Casely, G. S. Nichol, R. Bellabarba, R. P. Tooze. *Dalton Trans.* **2013**, *42*, 1333–1337.
[119] P. L. Arnold, R. W. F. Kerr, C. Weetman, S. R. Docherty, J. Rieb, F. L. Cruickshank, K. Wang, C. Jandl, M. W. McMullon, A. Pöthig, F. E. Kühn, A. D. Smith. *Chem. Sci.* **2018**, *9*, 8035–8045.

the latter promotes formation of propylene carbonate from propylene oxide and CO_2, while the compounds constructed around the less sterically demanding ligands provided no activity under the same conditions. Triple activation over a related cerium-based FLP stabilized by a heptadentate N_4P_3 ligand was also achieved recently. Capitalizing on the lability of Ce−P bonds, Zhu accomplished the triple activation of isocyanates, isothiocyanates, diazomethane and azides.[120]

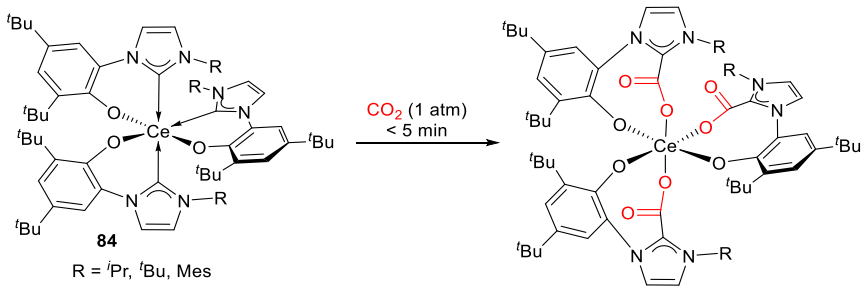

Scheme 40. Triple insertion of CO_2 across the Ce−NHC bonds in compounds **84**.

[120] X. Sun, W. Su, K. Shi, Z. Xie, C. Zhu. *Chem. Eur. J.* **2020**, *26*, 5354–5359.

I.2. Reactivity of Bimetallic Complexes.

I.2.1. General Considerations About Bimetallic Compounds

The notion of a single metal ion surrounded by a set of ligands was established by Alfred Werner in the 1900s.[121] From that time until the early 1960s the chemistry of transition metals was dominated by the investigation of the physicochemical properties of the individual metal ion, the interaction between the metal and its ligand set and the resulting geometrical and chemical properties of these compounds. These early studies produced remarkable advances in numerous fields, not only in inorganic and coordination chemistry, but also in other areas, permitting as well to acquire valuable fundamental knowledge, for example in the analysis of complex electronic structures or in bioinorganic systems. However, the existence of metal-metal bonding was not taken into consideration in these foremost studies.

After decades of debate, the existence of metal-metal bonding was confirmed in 1957 when the structures of complexes $Mn_2(CO)_{10}$ and $Re_2(CO)_{10}$ were reported.[122] These dimers are the first species with direct evidence of containing more than one metal centre to be held together exclusively by metal-metal bonds. A few years later, Cotton and co-workers synthesized for the first time a complex with a quadruple Re–Re bond. This compound, $[Re_2Cl_8]^{2-}$, supports the existence of transition metal complexes with bonds order higher than three, a feature so far unattainable at that time for main group systems. These discoveries marked the

[121] For general reviews: a) G. B. Kauffman. *Coord. Chem. Rev.* **1973**, *9*, 339–363. b) G. B. Kauffman. *Coord. Chem. Rev.* **1974**, *12*, 105–149. c) G. B. Kauffman. *Coord. Chem. Rev.* **1975**, *15*, 1–92.
[122] L. F. Dahl, E. Ishishi, R. E. Rundle. *J. Chem Phys.* **1957**, *26*, 1750–1751.

beginning of a new area of research in organometallic chemistry, specifically in binuclear and polynuclear chemistry.

In general, metal-metal bond formation depends on two factors: first, the valance orbitals involved must be sufficiently diffuse to afford substantial diatomic overlap, and second, competitive binding of additional ligands must be avoided. Actually, the design of sterically encumbered ligands that block access of other ligands to the metal coordination sphere holds part of the merit in the recent progress in the field of bimetallic compounds.

It is clear that bimetallic compounds hold a great fundamental interest on their own right. The study of the interactions between metal ions is crucial to gain a more profound understanding of the nature of chemical bonds. The last 20 years have been particularly productive in this regard. Among the most remarkable examples it is necessary to highlight the ultrashort Cr^{I}–Cr^{I} bond, the first example of a quintuple bond between two transition metals fully characterized in solution and in the solid state.[123] In the gas phase, even a bond of order six has been proposed for Mo_2 and W_2.[124] These high bond orders constitute very exotic examples that find no precedent in main group chemistry or monometallic transition metal systems. Other remarkable examples include Jones's Mg^{I}–Mg^{I} dimer[125] and Carmona's Zn^{I}–Zn^{I} compound in which Zn has oxidation state +1.[126] Heavier analogues of acetylene were also synthesized as

[123] T. Nguyen, A. D. Sutton, M. Brynda, J. C. Fettinger, G. J. Long, P. P. Power. *Science* **2005**, *310*, 844–847.
[124] G. Frenking, R. Tonner. *Nature* **2007**, *446*, 276–277.
[125] a) S. P. Green, C. Jones, A. Stasch. *Science* **2007**, *318*, 1754–1757. b) A. Stasch, C. Jones. *Dalton Trans.* **2011**, *40*, 5659–5672.
[126] I. Resa, E. Carmona, E. Gutierrez-Puebla, A. Monge. *Science* **2004**, *305*, 1136–1138.

distannynes[127] and diplumbynes[128] compounds, establishing the foundations for further developments in main group organometallic chemistry based on two metal or metalloid centres.

Nonetheless, it is in the field of catalysis where bimetallic compounds will likely meet their greatest potential. Despite remarkable progress in the organometallic chemistry of mononuclear complexes, particularly in the field of catalysis,[129] the incorporation of a second metal centre presents additional structural and electronic tunability (Figure 4) which may be exploited in reactivity studies and catalysis. Tunable parameters that are exclusive of bimetallic species include metal-metal bond order, distance and polarity or the intrinsic complementarity between two particular metals.[130] Overall, a common feature in many bimetallic systems is the fact that the active site is largely determined by the cooperative effects between the two metal centres and therefore it can be easily modified, providing a wide available space for reaction discovery.[131]

[127] a) M. Stender, A. D. Phillips, R. J. Wright, P. P. Power. *Angew. Chem. Int. Ed.* **2002**, *41*, 1785–1787. b) P. P. Power. *Organometallics* **2007**, *26*, 4362–4372.
[128] L. Pu, B. Twamley, P. P. Power. *J. Am. Chem. Soc.* **2000**, *122*, 3524–3525.
[129] B. Cornils, W. A. Herrmann, M. Beller, R. Paciello. *Applied homogeneous catalysis with organometallic compounds: a comprehensive handbook in four volumes.* 3rd ed. **2017**. New York, Wiley.
[130] J. Campos. *Nat. Rev. Chem*. **2020**, *4*, 696–702.
[131] a) P. Buchwalter, J. Rosé, P. Braunstein. *Chem. Rev.* **2015**, *115*, 28–126. b) N. P. Mankad. *Chem. Eur. J.* **2016**, *22*, 5822–5829. c) I. G. Powers, C. Uyeda. *ACS Catal.* **2017**, *7*, 936–958.

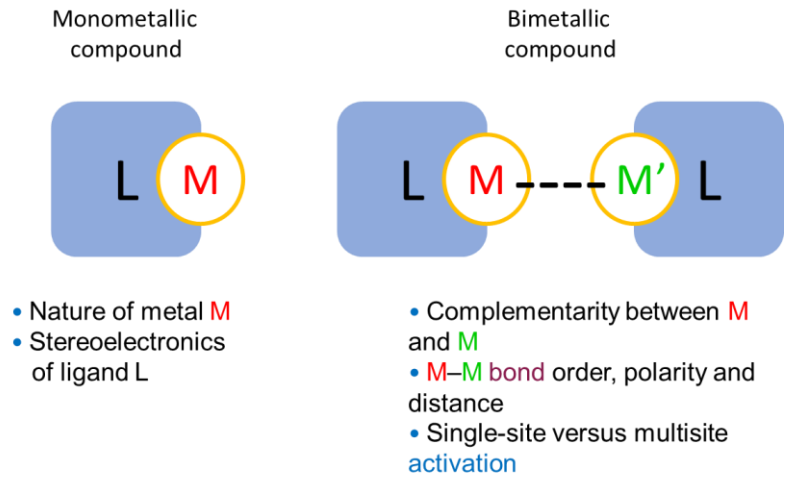

Figure 4. Monometallic vs bimetallic complexes.

Having two metals in close proximity permits routes for bond activation that are unavailable for mononuclear complexes. Thus, apart from single-site activation at one metal centre, multi-site activation by different means is also possible. In general, the modes of cooperative small molecule activation across bimetallic species can be broadly organised into three groups (Figure 3). These three generic mechanistic proposals are based on the structure of the key transition state in which the bond breaking of the substrate takes place. This classification may offer some aid in categorising the wide variety of bimetallic approaches to bond activation and catalysis. However, these categories represent a simplification of mechanistic options that might even coexist for a precise bimetallic design and for which the boundaries may be diffuse.

In the first option the bond cleavage may takes place at one of the two metal centres without direct participation of the second metal (Figure 5A). This scenario is similar to mononuclear systems, and one of the

metals could be considered as a metalloligand. In fact, it is now well recognized that metalolligands may impart electronic features to the active metal site that are difficult to attain by other traditional ligands.[132] Nonetheless, single-site activation at one of the two metals may be followed by migration of one of the activated fragments to the second metal in what may be considered a single-site mechanism for small molecule activation. These aspects will be further discussed in the context of the bimetallic compounds discussed within this Thesis.

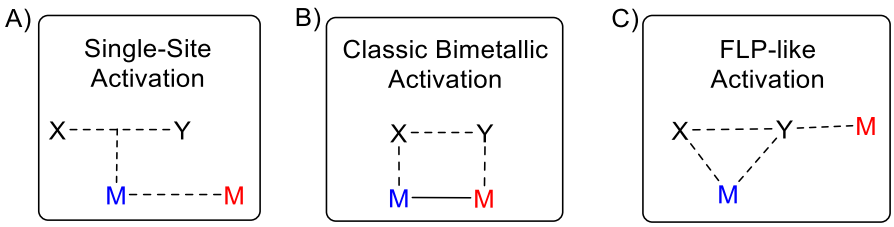

Figure 5. simplification of bimetallic mechanistic to bond activation and catalysis.

The second mechanism implies what can be considered a classical bimetallic activation, that is, the substrate is directly added across the metal-to-metal bond in a concerted way (Figure 5B). In this process the metal-metal bond may also be cleaved (or its bond order reduced) in concert with the formation of the new M-substrate bonds. Also, the molecule can be cleaved by the cooperative action of two independent metallic fragments by a FLP-like mechanism similar to the one discussed in the previous section (Figure 5C), in which there is no metal-metal interaction in the key transition state.

[132] R. J. Eisenhart, L. J. Clouston, C. C. Lu. *Acc. Chem. Res.* **2015**, *48*, 2885–2894.

Given the remarkable complexity and mechanistic possibilities offered by the presence of a second metal in transition metal compounds, it is not surprising that bimetallic cooperativity in homogeneous catalysis occurs more frequently than many had imagined. More sophisticated experimental techniques and computational studies, in many occasions revisiting well-known catalytic process, have revealed that some of those that were believed to proceed by mononuclear active species are indeed mediated by key bimetallic intermediates.[133] Overall, bimetallic structures provide tuneable parameters inaccessible to monometallic species, thus a better knowledge of the factors influencing bimetallic synergies and how to control them will place enormous possibilities within our grasp. The next sections will cover some selected representative examples of the cooperative reactivity across homobimetallic and heterobimetallic compounds, especially for systems that are somewhat related to the subsequent discussion about bimetallic frustrated Lewis pairs, the crux of this Thesis.

[133] a) M. H. Pérez-Temprano, J. A. Casares, A. R. de Lera, R. Alvarez, P. Espinet. *Angew. Chem. Int. Ed.* **2012**, *51*, 4917–4920. b) R. J. Oeschger, P. Chen. *J. Am. Chem. Soc.* **2017**, *139*, 1069–1072. c) C. Chen, C. Hou, Y. Wang, T. S. A. Hor. *Z. Weng. Org. Lett.* **2014**, *16*, 524–527.

I.2.2. Reactivity of Homobimetallic Complexes

For several decades, metal-metal complexes with different bond orders have been involved in binuclear bond activation reactions.[134] In many cases the activation of the substrate across the metal-metal bond results in the formation of monometallic species or, at least, on an alteration on the bond order or nature of the metal-metal bond. However, there are cases in which this interaction remains mostly intact along the bimetallic bond activation process.

The bimetallic complex $[Co_2(CO)_8]$ represents a milestone in the area since it was the first one to catalyze the Pauson-Khand reaction, in which an alkyne, an alkene and CO yield a cyclopentenone in an overall [2+2+1] cycloaddition. This fact represented a paradigmatic example of bimetallic catalysis in which the integrity of the M−M bond remains.[135] The group of Nakamura investigated the mechanism of this transformation by advanced computational studies, providing the mechanistic picture depicted in Scheme 41A.[136] The addition of the alkyne directly takes place at the cobalt centres with no apparent alteration on the Co−Co bond.

More recently, Uyeda published an exhaustive study of dinuclear Ni−Ni compounds as intermediates for the Pauson-Khand reaction.[137] Ligand assisted oxidative addition of Br_2 to the well-defined d^9–d^9 dinickel

[134] a) Y. Chen, S. Sakaki. *Dalton. Trans.* **2014**, *43*, 11478–11492. b) H. Tsurugi, A. Hayakawa, S. Kando, Y. Sugino, K. Mashima. *Chem. Sci.* **2015**, *6*, 3434–3439. c) M. E. Broussard, B. Juma, S. G. Train, W.-G. Peng, S. A. Laneman, G. G. Stanley. *Science* **1993**, *260*, 1784–1788. d) T. Inatomi, Y. Koga, K. Matsubara. *Molecules* **2018**, *23*, 140.
[135] a) I. U. Khand, G. R. Knox, P. L. Pauson, W. E. Watts. *J. Chem. Soc. D.* **1971**, *1*, 36a. b) I. U. Khand, G. R. Knox, P. L. Pauson, W. E. Watts. *J. Chem. Soc. Perkin. Trans. 1*. **1973**, 975–977. c) I. U. Khand, G. R. Knox, P. L. Pauson, W. E. Watts, M. I. Foreman. *J. Chem. Soc. Perkin. Trans. 1*. **1973**, 977–981.
[136] M. Yamanaka, E. Nakamura. *J. Am. Chem. Soc.* **2001**, *123*, 1703–1708.
[137] D. R. Hartline, M. Zeller, C. Uyeda. *Angew. Chem. Int. Ed.* **2016**, *55*, 6084–6087.

complex **85** supported by a naphthyridine-diimine pincer ligand (NDI) was effectively proved, revealing very little changes on the Ni−Ni bond length distances. As in the previous case, these results suggest a minimal change in the metal-metal bond order during the activation of the substrate (Scheme 41B).

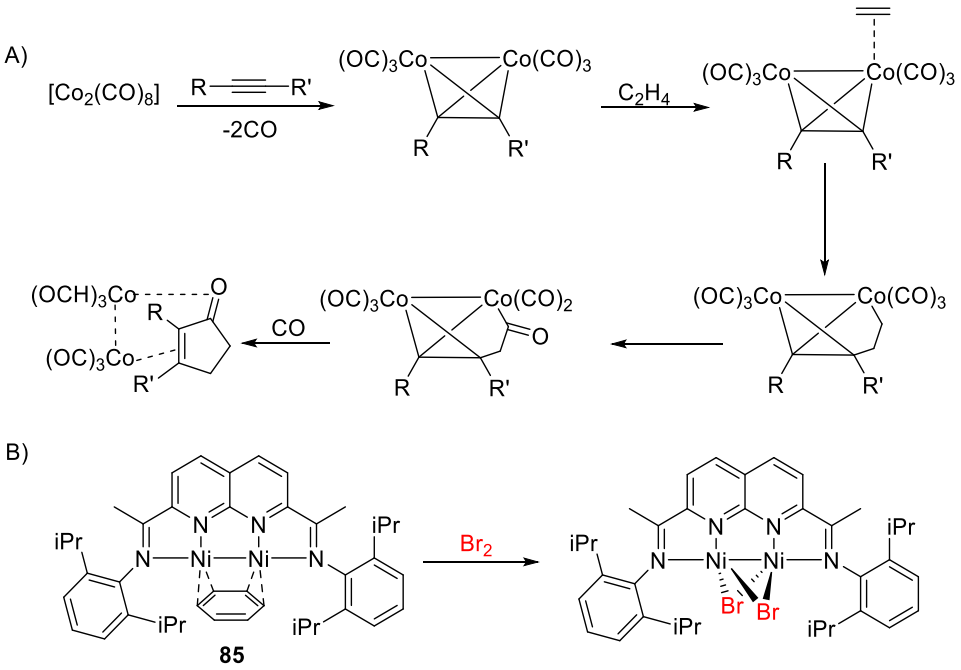

Scheme 41. A) Proposed mechanism for the Pauson-Khand reaction mediated by $[Co_2(CO)_8]$. B) Oxidative addition of Br_2 across dinickel complex **85**.

The reactivity of multiply bonded homobimetallic compounds has also been amply investigated, even for the most exotic members of this family, namely quintuply bonded species. Several groups have explored the chemistry of Cr−Cr and Mo−Mo quintuply bonded complexes stabilized by different nitrogen donor ligands to observe diverse reactivity

with small molecules.[138] Among those the studies reported by Tsai's group should be highlighted. For instance, the reaction of **86** with terminal alkynes evolved to the [2+2+2] cycloaddition products, that is, to the formation of substituted benzene rings. In fact, this process could be performed in a catalytic manner. Nevertheless, with internal alkynes, the [2+2] cycloaddition adducts were formed (Scheme 42).[139] In these new complexes, the two amidinate ligands adopt a bent geometry to accommodate the newly formed dimetallacyclobutene and the Mo–Mo bond order is reduced to four.

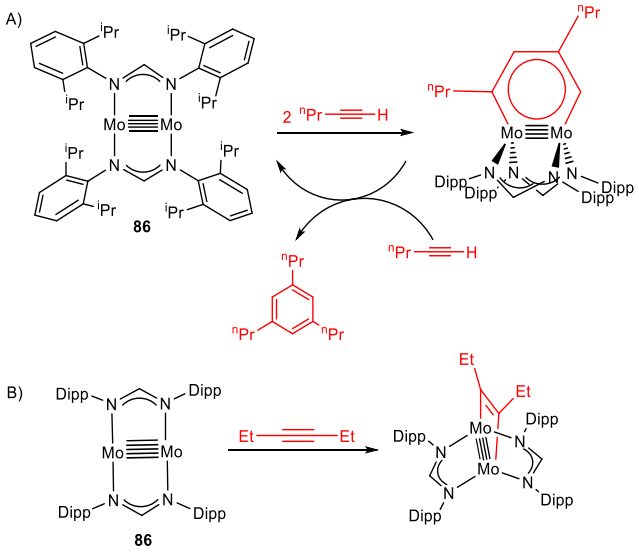

Scheme 42. Reaction of **86** with alkynes examples. A) Terminal alkynes evolve to the [2+2+2] cycloaddition products. B) Internal alkynes to afford the [2+2] cycloaddition product. Dipp = 2,6-Diisopropylphenyl.

[138] a) A. Noor, G. Glatz, R. Müller, M. Kaupp, S. Demeshko, R. Kempe. *Nature Chem.* **2009**, *1*, 322–325. b) C. Ni, B. D. Ellis, G. L. Long, P. P. Power. *Chem. Commun.* **2009**, *17*, 2332–2334. c) C. Schwarzmaier, A. Noor, G. Glatz, M. Zabel, A. Y. Timoshkin, B. M. Cossairt, C. C. Cummins, R. Kempe, M. Scheer. *Angew. Chem. Int. Ed.* **2011**, *50*, 7283–7286.

[139] a) H.-Z. Chen, S.-C. Liu, C. H. Yen, J.-S. K. Yu, Y.-J. Shieh, T.-S. Kuo, Y.-C. Tsai. *Angew. Chem. Int. Ed.* **2012**, *51*, 10342–10346. b) Y. Chen, S. Sakaki. *Dalton Trans.* **2014**, *43*, 11478–11492.

In an interesting study, Sakaki extended the concept of TMFLPs to multiply bonded complexes,[140] for which a polarization of the M–M multiple bond is proposed to parallel the polarization found in encounter complexes of FLP systems. The group focused, from a computational perspective, on the oxidative addition of H−H, C−H and O−H bonds over the quintuply bonded compound **86** (R = H) (Scheme 43). The key orbitals involved in σ-bond cleavage get polarized in the transition state (Scheme 42B) facilitating charge transfer from the M−M bond to the σ^*_{HH} orbital, while weakening the exchange repulsion between the multiple M−M bond and the E–H (E = H, C, O) substrate. This study provides encouragement to investigate other multiply bonded bimetallic compounds that can somehow behave as FLP-like entities due to facile M−M bond polarization.

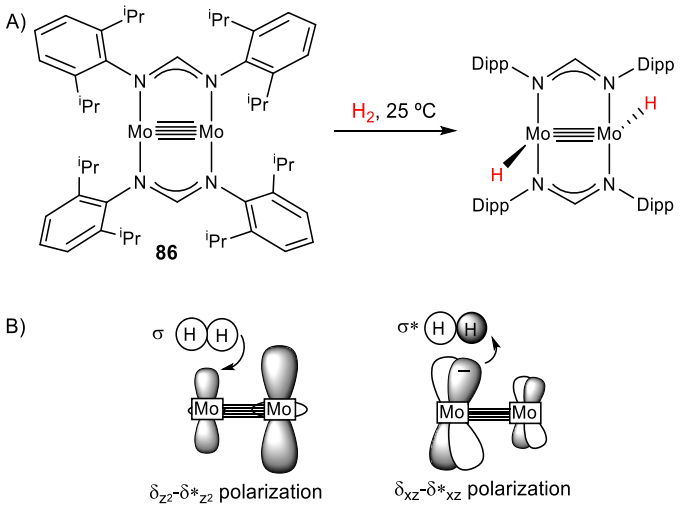

Scheme 43. A) Addition of dihydrogen over the quintuply bonded Mo_2 complex **86**; B) Simplified representation of the polarized δ_{Mo2} orbitals participating in H_2 cleavage reminiscent of FLPs.

[140] Y. Chen, S. Sakaki. *Inorg. Chem.* **2017**, *56*, 4011–4020.

I.2.3. Reactivity of Polar Heterobimetallic Complexes

In some cases, polar M−M bonds exhibit reactivity that is reminiscent of FLP systems. At variance with main group frustrated pairs, the integrity of the M−M bond may remain virtually intact during small molecule activation events, in a manner that could be understood as traditional heterobimetallic activation (Figure 5A). However, it is also possible that the monometallic fragments may coexist in solution due to the lability of the M−M bond, thus enabling FLP-type activation pathways in the same fashion as thermally induced FLPs.[14] The latter situation is more facile in unsupported heterobimetallic compounds, that is, those in which the M−M bond is the sole interaction holding the two metallic fragments together. In this section, some examples of heterobimetallic entities containing bridging ligands and unsupported polarized heterobimatallic complexes are briefly discussed. In addition, the connection between the latter systems and FLPs with will be drawn and discussed when pertinent.

As in homobimetallic compounds, bridging ligands have the utility of keeping the two metal centres tight together in close proximity. Compound **87** constitutes an interesting example of this approach. Bergman explored its bimetallic reactivity towards a variety of small molecules with different polarity (Scheme 44).[141] Although the existence of the Ir−Zr bond in the precursor is beyond any doubt, the mechanism of the bond activation processes was not studied in detail, so there is no information on the step at which the heterobimetallic bond is cleaved.

[141] a) A. M. Baranger, R. G. Bergman. *J. Am. Chem. Soc.* **1994**, *116*, 3822–3835. b) T. A. Hanna, A. M. Baranger, R. G. Bergman. *J. Am. Chem. Soc.* **1995**, *117*, 11363–11364.

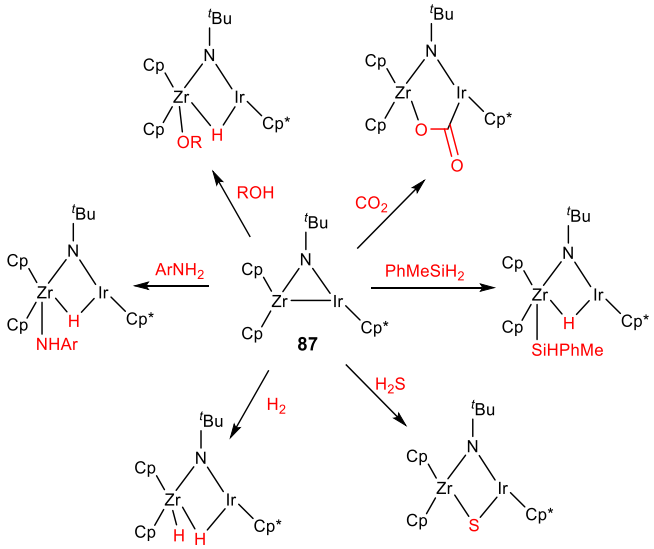

Scheme 44. Cooperative reactivity of the heterodinuclear [(η^5-C_5H_5)$_2$Zr(μ-N^{t}Bu)Ir(η^5-C_5Me_5)] complex with small molecules.

In more contemporary studies, Thomas presented heterobimetallic Zr(IV)/Co(–I) complexes in which two transition metals are linked through a bis- or tris-(phosphinoamide) ligand framework. A wide range of small molecules were activated by compound **88** and others alike (Scheme 45).[142] For example, the reaction with H_2 at room temperature resulted in the addition of two molecules of H_2 with concomitant P−N bond cleavage

[142] a) S. L. Marquard, M. W. Bezpalko, B. M. Foxman, C. M. Thomas. *J. Am. Chem. Soc.* **2013**, *135*, 6018–6021. b) B. Wu, R. Hernández-Sánchez, M. W. Bezpalko, B. M. Foxman, C.M. Thomas. *Inorg. Chem.* **2014**, *53*, 10021–10023. c) H. Zhang, B. Wu, S. L. Marquard, E. D. Litle, D. A. Dickie, M. W. Bezpalko, B. M. Foxman, C. M. Thomas. *Organometallics* **2017**, *36*, 3498–3507. d) H. Zhang, G. P. Hatzis, C. E. Moore, D. A. Dickie, M. W. Bezpalko, B. M. Foxman, C. M. Thomas. *J. Am. Chem. Soc.* **2019**, *141*, 9516–9520.

of the phosphinoamide ligand.[143] On the other hand, the activation of dihydrogen by the related heterobimetallic complex **89**, bearing only two bridging phosphinoamide ligands, progressed directly across the metal-metal bond without any ligand rearrangement and only incorporating one equivalent of H_2.[144]

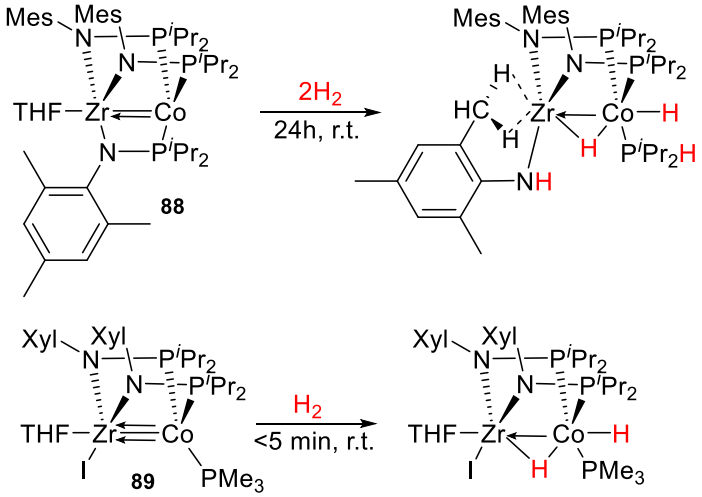

Scheme 45. Hydrogen activation by Zr(IV)/Co(–I) heterobimetallic complexes with tris- and bis-(phosphonamide) bridging ligands.

As aforementioned, the presence of bridging ligands is not always required to access bimetallic structures. Those in which the sole connection between the two metal fragments is a dative metal-metal bond are referred as metal only Lewis pairs (MOLPs),[84] and are highly reminiscent of main group FLPs. In 1967, Nowell and Russell first described a Lewis acid-base compound of this kind by reporting the X-ray molecular structure of

[143] C. M. Thomas, J. W. Napoline, G. T. Rowe, B. M. Foxman. *Chem. Commun.* **2010**, *46*, 5790–5792.
[144] K. M. Gramigna, D. A. Dickie, B. M. Foxman, C. M. Thomas. *ACS Catal.* **2019**, *9*, 3153–3164.

[(η^5-C_5H_5)$(CO)_2$Co→$HgCl_2$].[145] Since then, the interest in bimetallic systems with metal-metal dative bonds has considerably grown, particularly in the last two decades and largely motivated by the investigation of the role of metal-metal interactions in catalytic transformations.[146]

Braunschweig's group has reported the formation of a wide diversity of unsupported dative bonds between transition metal bases with *s*- and *p*-block metal acidic fragments. Several representative examples based on the basic [$Pt(PCy_3)_2$] fragment are depicted in Scheme 46A.[147] In an interesting study, they investigated the exchange of $GaCl_3$ or $AlCl_3$ between different transition metal bases as a method to gauge Lewis basicity (Scheme 46B).[148] These studies proved the lability and dynamic behavior of the M→M bond, implying strong similarities with main group phosphino-borane adducts, and foreseeing a great potential to act as thermally induced FLP systems, an idea that has been exploited within this Thesis.

[145] I. N. Nowell, D. R. Russell. *Chem. Commun.* **1967**, *16*, 817.
[146] M. Ma, A. Sidiropoulos, R. Lalrempuia, A. Stasch, C. Jones. *Chem. Commun.* **2013**, *49*, 48–50.
[147] a) H. Braunschweig, K. Gruss, K. Radacki. *Angew. Chem. Int. Ed.* **2009**, *48*, 4239–4241. b) H. Braunschweig, K. Gruss, K. Radacki. *Angew. Chem. Int. Ed.* **2007**, *46*, 7782–7784. c) H. Braunschweig, K. Gruss, K. Radacki. *Inorg. Chem.* **2008**, *47*, 8595–8597. d) H. Braunschweig, A. Damme, R. D. Dewhurst, F. Hupp, J. O. C. Jimenez-Halla. *Chem. Commun.* **2012**, *48*, 10410–10412.
[148] a) H. Braunschweig, R. D. Dewhurst, F. Hupp, C. Kaufmann, A. K. Phukan, C. Schneider, Q. Ye. *Chem. Sci.* **2014**, *5*, 4099–4104. b) R. Bissert, H. Braunschweig, R. D. Dewhurst, C. Schneider. *Organometallics* **2016**, *35*, 2567–2573.

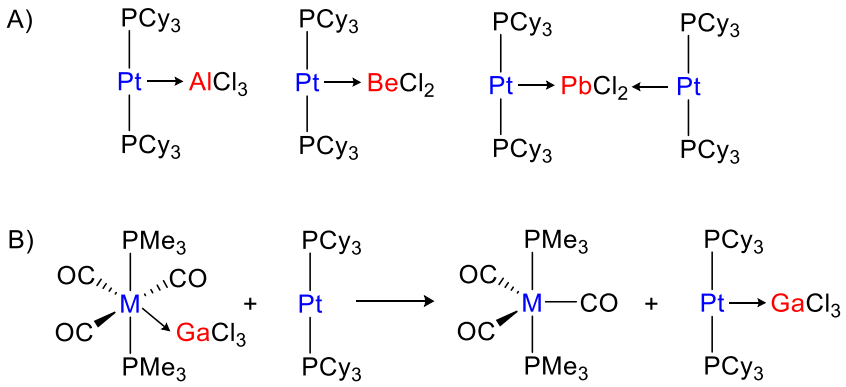

Scheme 46. A) Examples of different MOLPs with Pt(0). B) Transfer of the Lewis acid $GaCl_3$ from M (M = Fe, Ru, Os) carbonyl complexes to $[Pt(PCy_3)_2]$.

In a paradigmatic example, Cutler showed that complexes $[Cp(CO)_2M{-}Zr(Cl)Cp_2]$ (M = Fe, Ru), **90**, react with CO_2 to yield the corresponding bimetallocarboxylates, **91**, $[Cp(CO)_2M(\mu\text{-}\eta^1\text{-}C{:}\eta^2\text{-}O,O')Zr(Cl)Cp_2]$ (Scheme 47). The resemblance to FLP systems is obvious, although the analogy could not be delineated at that time. The bimetallocarboxylates are stabilized by push-pull interactions derived from the Lewis basic group 8 compound and the electrophilic zirconium fragment.[149] Although a traditional bimetallic mechanism involving the insertion of CO_2 into the M−M bond was favored, an alternative pathway through dissociation of the bimetallic compound into monometallic fragments followed by concerted trapping of CO_2 –as a thermally induced TMFLP– could not be ruled out. Subsequent reports further support the aforementioned analogy of the reactivity between polar M−M bonds and

[149] J. R. Pinkes, B. D. Steffey, J. C. Vites, A. R. Cutler. *Organometallics* **1994**, *13*, 21–23.

FLPs.[141,150] Although the authors provided some experimental support for the later activation mechanism, however no computational studies were performed and no information about the M→Zr bond in the suggested transition state was discussed.

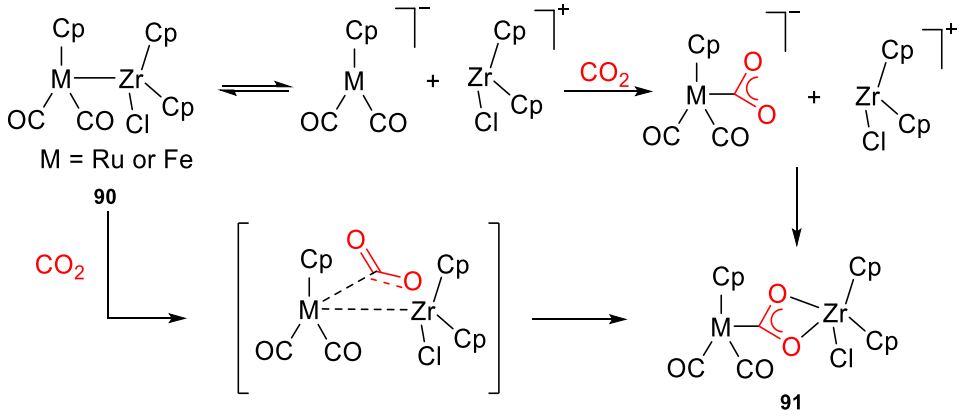

Scheme 47. Bimetallic CO_2 activation by a Zr−M (M = Ru, Fe) metal only Lewis pair.

More recently, the use of metal-only Lewis adduct **92**, $[(P^tBu_3)_2Pt→Cu(NCMe)_n]$, has been described in the context of bond activation (Scheme 48). This complex is capable of activating an O−H

[150] a) H. Memmler, U. Kauper, L. H. Gade, I. J. Scowen, M. McPartlin. *Chem. Commun.* **1996**, 1751–1752. b) A. Schneider, L. H. Gade, M. Breuning, G. Bringmann, I. J. Scowen, M. McPartlin. *Organometallics* **1998**, *17*, 1643–1645. c) L. H. Gade, H. Memmler, U. Kauper, A. Schneider, S. Fabre, I. Bezougli, M. Lutz, C. Galka, I. J. Scowen, M. McPartlin. *Chem. Eur. J.* **2000**, *6*, 692–708. d) B. Findeis, M. Schubart, C. Platzek, L. H. Gade, I. Scowen, M. McPartlin. *Chem. Commun.* **1996**, 219–220. e) J. R. Pinkes, S. M. Tetrick, B. E. Landrum, A. R. Cutler. *J. Organomet. Chem.* **1998**, *556*, 1–7. f) A. Sisak, E. Halmos. *J. Organomet. Chem.* **2007**, *92*, 1817–1824. g) K. Uehara, S. Hikichi, A. Inagaki, M. Akita. *Chem. Eur. J.* **2005**, *11*, 2788–2809. h) J. A. R. Schmidt, E. B. Lobkovsky, G. W. Coates. *J. Am. Chem. Soc.* **2005**, *127*, 11426–11435. i) J. P. Krogman, B. M. Foxman, C. M. Thomas. *J. Am. Chem. Soc.* **2011**, *133*, 14582–14585. j) B. G. Cooper, C. M. Fafard, B. M. Foxman, C. M. Thomas. *Organometallics* **2010**, *29*, 5179–5186. k) I. M. Riddlestone, N. A. Rajabi, J. P. Lowe, M. F. Mahon, S. A. Macgregor, M. K. Whittlesey. *J. Am. Chem. Soc.* **2016**, *35*, 11081–11084.

bond of water (by using wet acetone as a solvent) to generate a cationic Pt(II) hydride and copper hydroxide.[151] The origin of the hydride ligand was corroborated by using D_2O. Although the mechanism could not be unambiguously determined, a cooperative pathway that implies the bimetallic adduct seems more likely.

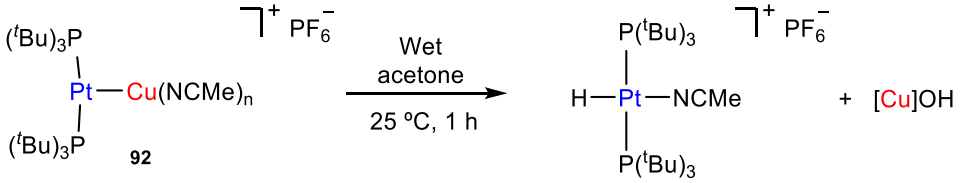

Scheme 48. O−H bond activation at a Pt−Cu MOLP.

In recent years, the group of Mankad has intensively explored a variety of unbridged polarized heterobimetallic systems (**93-96**, Scheme 49),[152] highlighting in many occasions the analogy with frustrated Lewis pairs. For example, compound **93[CuFe]** reacts with dihydrogen,[153] carbon disulfide,[154] iodomethane[152a] and benzyl chlorides,[155] in a way that is highly reminiscent of main group FLPs (Scheme 50). The mechanism for dihydrogen cleavage has been thoroughly investigated by the group with several metal combinations. Computational analysis revealed key orbital interactions involved in dihydrogen splitting that resemble classic FLPs.

[151] S. Jamali, S. Abedanzadeh, N. K. Khaledi, H. Samouei, Z. Hendi, S. Zacchini, R. Kia, H. R. Shahsavari. *Dalton Trans.* **2016**, *45*, 17644–17651.
[152] a) U. Jayarathne, T. J. Mazzacano, S. Bagherzadeh, N. P. Mankad. *Organometallic* **2013**, *32*, 3986–3992. b) S. Banerjee, M. K. Karunananda, S. Bagherzadeh, U. Jayarathne, S. R. Parmelee, G. W. Waldhart, N. P. Mankad. *Inorg. Chem.* **2014**, *53*, 11307–11315. c) M. K. Karunananda, F. X. Vázquez, E. E. Alp, W. Bi, S. Chattopadhyay, T. Shibatade, N. P. Mankad. *Dalton Trans.* **2014**, *43*, 13661–13671.
[153] M. K. Karunananda, N. P. Mankad. *Organometallics* **2017**, *36*, 220–227.
[154] U. Jayarathne, S. R. Parmelee, N. P. Mankad. *Inorg. Chem.* **2014**, *53*, 7730–7737.
[155] M. K. Karunananda, S. R. Parmelee, G. W. Waldhart, N. P. Mankad. *Organometallics* **2015**, *34*, 3857–3864.

Hence, there is donation from the σ_{HH} orbital to a copper valence orbital, with concerted back-donation from the Cu−Fe bond towards the σ^*_{HH} orbital. Experimental observations evinced that Mankad's heterobimetallic systems display dynamic equilibrium in solution towards the individual monometallic fragments, albeit small molecule activation seems to proceed through the M−M bound frameworks.[156] These combined results suggest that modulating the degree of frustration *vs* M−M interaction may be important to tune the activity of polarized heterobimetallic systems.

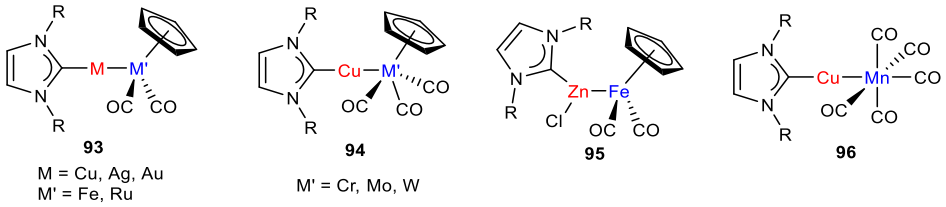

Scheme 49. Selected examples of Mankad's metal-only Lewis pairs (R = Mes, Dipp).

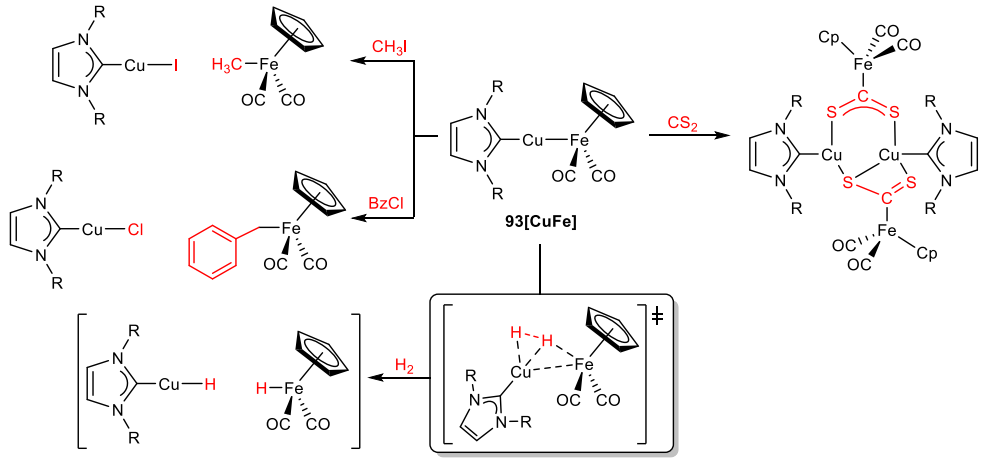

Scheme 50. Heterobimetallic activation of small molecules by **193[CuFe]**, highlighting a proposed key transition state for dihydrogen cleavage.

[156] N. P. Mankad. *Chem. Commun.* **2018**, *54*, 1291–1302.

The heterobimetallic compounds depicted in Scheme 48 revealed important applications in catalysis that capitalize on the cooperative reactivity of the two metals in close proximity. Accordingly, highly efficient processes for *E*-selective alkyne semi-hydrogenation,[157] C−H borylation,[158] or regioselective alkyne hydrostannylation[159] were recently disclosed. As an archetypal example, the proposed mechanism for catalytic C−H borylation mediated by **93[CuFe]** is depicted in Scheme 51.[158b] A comprehensive computational analysis revealed two bimetallic transition states that are crucial for catalytic turnover, being in agreement with experimental observations. In the first, a bimetallic oxidative addition is proposed to occur along the Cu–Fe bond, reminiscent of heterolytic bond cleavage by FLPs. Moreover, the terminal iron hydride that emerges after C–H borylation is proposed to be intercepted by the previously formed copper hydride, regenerating **93[CuFe]** after a bimolecular reductive elimination of H_2 involving an FLP-like transition state (identical to the one shown in Scheme 50).

[157] M. K. Karunananda, N. P. Mankad. *J. Am. Chem. Soc.* **2015**, *137*, 14598–14601.
[158] a) T. J. Mazzacano, N. P. Mankad. *J. Am. Chem. Soc.* **2013**, *135*, 17258–17261. b) S. R. Parmelee, T. J. Mazzacano, Y. Zhu, N. P. Mankad, J. A. Keith. *ACS Catal.* **2015**, *5*, 3689–3699.
[159] L. J. Cheng, N. P. Mankad. *J. Am. Chem. Soc.* **2019**, *141*, 3710–3716.

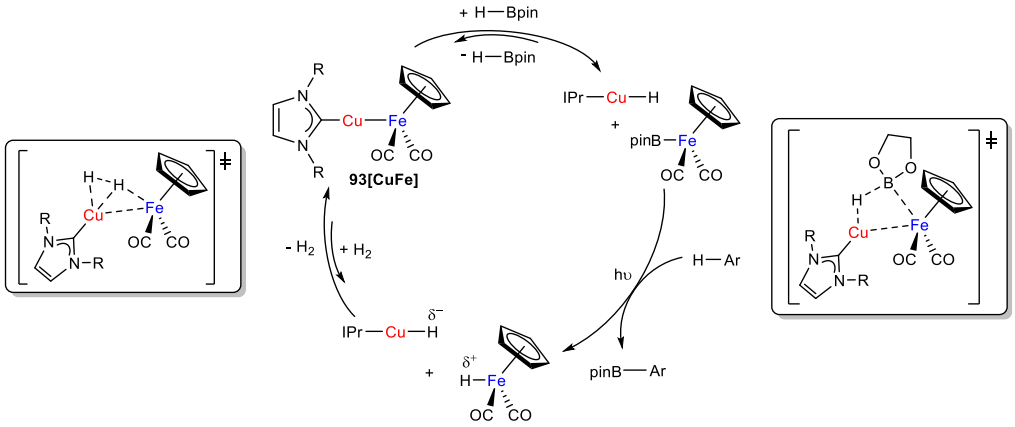

Scheme 51. Proposed catalytic cycle for C−H borylation mediated by polar heterobimetallic compound **93[CuFe]** highlighting key cooperative transition states.

II.4. References

1. a) G. N. Lewis. *Valence and the Structure of Atoms and Molecules.* Chemical Catalogue Company. New York, **1923**.

2. S. G. Shore, R. W. Parry. *J. Am. Chem. Soc.* **1955**, *77*, 6084–6085.

3. a) H. C. Brown, H. I. Schlesinger, S. Z. Cardon. *J. Am. Chem. Soc.* **1942**, *64*, 325–329. b) H. C. Brown, B. Kanner. *J. Am. Chem. Soc.* **1966**, *88*, 986–992.

4. G. Wittig, E. Benz. *Chem. Ber.* **1959**, *92*, 1999–2013.

5. W. Tochtermann. *Angew. Chem. Int. Ed.* **1966**, *5*, 351–371.

6. R. Damico, C. D. Broadus. *J. Org. Chem*. **1966**, *31*, 1607–1612.

7. H. Lankamp, W. T. Nauta, C. MacLean. *Tetrahedron Lett.* **1968**, *9*, 249–254.

8. S. Doering, G. Erker, R. Fröhlich, O. Meyer, K. Bergander. *Organometallics* **1998**, *17*, 2183–2187.

9. G. C. Welch, R. R. S. Juan, J. D. Masuda, D. W. Stephan. *Science* **2006**, *314*, 1124–1126.

10. G. C. Welch, D. W. Stephan. *J. Am. Chem. Soc.* **2007**, *129*, 1880–1881.

11. J. S. J. McCahill, G. C. Welch, D. W. Stephan. *Angew. Chem. Int. Ed.* **2007**, *46*, 4968–4971.

12. P. Spies, G. Erker, G. Kehr, K. Bergander, R. Fröhlich, S. Grimme, D. W. Stephan. *Chem. Commun.* **2007**, 5072–5074.

13. P. A. Chase, G. C. Welch, T. Jurca, D. W. Stephan. *Angew. Chem. Int. Ed.* **2007**, *46*, 8050–8053.

14. T. A. Rokob, A. Hamza, A. Stirling, I. Pápai. *J. Am. Chem. Soc.* **2009**, *131*, 2029–2036.

15. a) G. Skara, F. De Vleeschouwer, P. Geerlings, F. De Proft, B. Pinter. *Sci. Rep.* **2017**, *7*, 16024. b) D. Yepes, P. Jaque, I. Fernández. *Chem. Eur. J.* **2016**, *22*, 18801–18809. c) J. Paradies. *Eur. J. Org. Chem.* **2019**, 283–294.

16. L. L. Liu, L. L. Cao, Y. Shao, G. Ménard, D. W. Stephan. *Chem* **2017**, *3*, 259–267.

17. L. L. Liu, L. L. Cao, Y. Shao, D. W. Stephan. *J. Am. Chem. Soc*. **2017**, *139*, 10062–10071.

18. Some examples: a) A. R. Jupp, D. W. Stephan. *Trends in Chemistry* **2019**, *1*, 35–48. b) D. W. Stephan, G. Erker. *Angew Chem. Int. Ed.* **2015**, *54*, 6400–6441. c) D. W. Stephan, G. Erker. *Chem. Sci.* **2014**, *5*, 2625–2641. d) D. W. Stephan, G. Erker. *Top. Curr. Chem.* **2013**, *332*, 1–311. e) D. W. Stephan, G. Erker. *Top. Curr. Chem.* **2013**, *334*, 1–345. f) J. C. Slootweg, A. R. Jupp. *Molecular Catalysis* **2021**, *2*, 1–408.

19. Some examples: a) M. A. Legare, M. A. Courtemanche, E. Rochette, F. G. Fontaine. *Science* **2015**, *349*, 513–516. b) M. A. Legare, E. Rochette, J. L. Lavergne, N. Bouchard, F. G. Fontaine. *Chem. Commun.* **2016**, *52*, 5387–5390. c) K. Chernichenko, M. Lindqvist, B. Kotai, M. Nieger, K. Sorochkina, I. Pápai, T. Repo. *J. Am. Chem. Soc.* **2016**, *138*, 4860–4868.

20. Some examples: a) C. B. Caputo, D. W. Stephan. *Organometallics* **2012**, *31*, 27–30. b) J. T. Zhu, M. Pérez, D. W. Stephan. *Angew. Chem. Int. Ed.* **2016**, *55*, 8448–8451. c) J. Zhu, M. Pérez, C. B. Caputo, D. W. Stephan. *Angew. Chem. Int. Ed.* **2016**, *55*, 1417–1421.

21. Some examples: a) M. Hong, J. Chen, E. Y.-X. Chen. *Chem. Rev.* **2018**, *118*, 10551–10616. b) L. Chen, R. Liu, Q. Yan. *Angew. Chem. Int. Ed.* **2018**, *57*, 9336–9340. c) T. Wang, C. G. Daniliuc, C. Mück-Lichtenfeld, G. Kehr, G. Erker. *J. Am. Chem. Soc.* **2018**, *140*, 3635–3643.

22. a) M. Ullrich, A. J. Lough, D. W. Stephan. *J. Am. Chem. Soc.* **2009**, *131*, 52−53. b) M. Ullrich, A. J. Lough, D. W. Stephan. *Organometallics* **2010**, *29*, 3647−3654.

23. H. Wang, R. Fröhlich, G. Kehr, G. Erker. *Chem. Commun.* **2008**, 5966−5968.

24. a) S. J. Geier, A. L. Gille, T. M. Gilbert, D. W. Stephan. *Inorg. Chem.* **2009**, *48*, 10466−10474. b) S. J. Geier, D. W. Stephan. *J. Am. Chem. Soc.* **2009**, *131*, 3476−3477.

25. a) P. A. Chase, D. W. Stephan. *Angew. Chem. Int. Ed.* **2008**, *47*, 7433−7437. b) S. J. Geier, P. A. Chase, D. W. Stephan. *Chem. Commun.* **2010**, *46*, 4884−4886. c) D. Holschumacher, T. Bannenberg, C. G. Hrib, P. G. Jones, M. Tamm. *Angew. Chem. Int. Ed.* **2008**, *47*, 7428−7432.

26. a) D. W. Stephan. *Org. Biomol. Chem.* **2012**, *10*, 5740−5746. b) D. W. Stephan, G. Erker. *Angew. Chem. Int. Ed.* **2010**, *49*, 46−76.

27. M. A. Dureen, D. W. Stephan. *J. Am. Chem. Soc.* **2009**, *131*, 8396−8397. b) J. Paradies. *Angew. Chem. Int. Ed.* **2014**, *53*, 3552−3557.

28. M. A. Dureen, C. C. Brown, D. W. Stephan. *Organometallics* **2010**, *29*, 6594−6607.

29. a) S. J. Geier, M. A. Dureen, E. Y. Ouyang, D. W. Stephan. *Chem. Eur. J.* **2010**, *16*, 988−993. b) C. F. Jiang, O. Blacque, H. Berke. *Organometallics* **2010**, *29*, 125−133.

30. M. A. Dureen, C. C. Brown, D. W. Stephan. *Organometallics* **2010**, *29*, 6422−6432.

31. C. M. Mömming, E. Otten, G. Kehr, R. Fröhlich, S. Grimme, D. W. Stephan, G. Erker. *Angew. Chem. Int. Ed.* **2009**, *48*, 6643−6646.

32. X. Zhao, D. W. Stephan. *Chem. Commun.* **2011**, *47*, 1833−1835.

33. M. J. Sgro, J. Domer, D. W. Stephan. *Chem. Commun.* **2012**, *48*, 7253−7255.

34. a) I. Peuser, R. C. Neu, X. Zhao, M. Ulrich, B. Schirmer, J. A. Tannert, G. Kehr, R. Fröhlich, S. Grimme, G. Erker, D. W. Stephan. *Chem. Eur. J.* **2011**, *17*, 9640−9650. b) M. Harhausen, R.

Fröhlich, G. Kehr, G. Erker. *Organometallics* **2012**, *31*, 2801−2809. c) R. C. Neu, G. Ménard, D. W. Stephan. *Dalton Trans.* **2012**, *41*, 9016−9018. d) F. Bertini, V. Lyaskoyskyy, B. J. J. Timmer, F. J. J. de Kanter, M. Lutz, A. W. Ehlers, J. C. Slootweg, K. Lammertsma. *J. Am. Chem. Soc*. **2012**, *134*, 201−204.

35. M. Reißmann, A. Schäfer, S. Jung, T. Müller. *Organometallics* **2013**, *32*, 6736−6744.

36. a) M. Feroci, I. Chiarotto, S. V. Ciprioti, A. Inesi. *Electrochim. Acta* **2013**, *109*, 95−101. b) J. D. Holbrey, W. M. Reichert, I. Tkatchenko, E. Bouajila, O. Walter, I. Tommasi, R. D. Rogers. *Chem. Commun.* **2003**, 28−29. c) E. L. Kolychev, T. Bannenberg, M. Freytag, C. G. Daniliuc, P. G. Jones, M. Tamm. *Chem. Eur. J.* **2012**, *18*, 16938−16946. d) E. Theuergarten, T. Bannenberg, M. D. Walter, D. Holschumacher, M. Freytag, C. G. Daniliuc, P. G. Jones, M. Tamm. *Dalton Trans.* **2014**, *43*, 1651−1662.

37. a) Y. Liu, G. P. Jessop, M. Cunningham, C. A. Eckert, C. L. Liotta, *Science* **2006**, *313*, 958−960. b) P. G. Jessop, D. H. Heldebrant, X. Li, C. A. Eckert, C. L. Liotta. *Nature* **2005**, *436*, 1102. c) D. A. Dickie, M. V. Parkes, R. A. Kemp. *Angew. Chem. Int. Ed.* **2008**, *47*, 9955−9957. d) T. Voss, T. Mahdi, E. Otten, R. Fröhlich, G. Kehr, D. W. Stephan, G. Erker. *Organometallics* **2012**, *31*, 2367−2378.

38. P. A. Chase, T. Jurca, D. W. Stephan. *Chem. Commun.* **2008**, 1701−1703.

39. D. W. Stephan, S. Greenberg, T. W. Graham, P. A. Chase, J. J. Hastie, S. J. Geier, J. M. Farrell, C. C. Brown, Z. M. Heiden, G. C. Welch, M. Ullrich. *Inorg. Chem.* **2011**, *50*, 12338−12348.

40. V. Fasano, M. J. Ingleson. *Synthesis* **2018**, *50*, 1783−1795.

41. J. W. Thomson, J. A. Hatnean, J. J. Hastie, A. Pasternak, D. W. Stephan, P. A. Chase. *Org. Process Res. Dev.* **2013**, *17*, 1287−1292.

42. L. Greb, P. Oña-Burgos, B. Schirmer, S. Grimme, D. W. Stephan, J. Paradies. *Angew. Chem. Int. Ed.* **2012**, *51*, 10164−10168.

43. L. J. Hounjet, C. Bannwarth, C. N. Garon, C. B. Caputo, S. Grimme, D. W. Stephan. *Angew. Chem. Int. Ed.* **2013**, *52*, 7492−7495.

44. L. Greb, C. G. Daniliuc, K. Bergander, J. Paradies. *Angew. Chem. Int. Ed.* **2013**, *52*, 5876−5879.

45. B. Inés, D. Palomas, S. Holle, S. Steinberg, J. A. Nicasio, M. Alcarazo. *Angew. Chem. Int. Ed.* **2012**, *51*, 12367−12369.

46. K. Chernichenko, A. Madarász, I. Pápai, M. Nieger, M. Leskelä, T. A. Repo. *Nat. Chem.* **2013**, *5*, 718−723.

47. T. Mahdi, D. W. Stephan. *Angew. Chem. Int. Ed.* **2013**, *52*, 12418−12421.

48. A. E. Ashley, A. L. Thompson, D. O'Hare. *Angew. Chem. Int. Ed.* **2009**, *48*, 9839−9843.

49. A. Berkefeld, W. E. Piers, M. Parvez. *J. Am. Chem. Soc.* **2010**, *132*, 10660−10661.

50. M. A. Courtemanche, M. A. Legare, L. Maron, F. G. Fontaine. *J. Am. Chem. Soc.* **2013**, *135*, 9326−9329.

51. T. Wang, D. W. Stephan. *Chem. Eur. J.* **2014**, *20*, 3035−3039.

52. C. Li, J. Agarwal, H. T. Schaefer. *J. Phys. Chem. B* **2014**, *118*, 6482−6490.

53. Z. Lu, H. Ye, H. Wang. *New organoboranes in "frustrated Lewis pair" chemistry.* In: G. Erker, D. Stephan (eds) Frustrated Lewis Pairs II. Topics in Current Chemistry. **2012**. Springer, Berlin, Heidelberg, p 59−80.

54. K. P. Keep. *Inorg. Chem.* **2016**, *55*, 9461−9470.

55. a) A. M. Chapman, M. F. Haddow, D. F. Wass. *J. Am. Chem. Soc.* **2011**, *133*, 8826–8829. b) A. M. Chapman, M. F. Haddow, D. F. Wass. *J. Am. Chem. Soc.* **2011**, *133*, 18463−18478. c) A. M.

Chapman, M. F. Haddow, D. F. Wass. *Eur. J. Inorg. Chem.* **2012**, 1546−1554.

56. a) X. Xu, R. Fröhlich, C. G. Daniliuc, G. Kehr, G. Erker. *Chem. Commun.* **2012**, *48*, 6109−6111. b) X. Xu, G. Kehr, C. G. Daniliuc, G. Kehr, G. Erker. *J. Am. Chem. Soc.* **2013**, *135*, 6465−6476.

57. D. W. Stephan. *Org. Biomol. Chem.* **2008**, *6*, 1535−1539.

58. a) N. S. Lambic, R. D. Sommer, E. A. Ison. *J. Am. Chem. Soc.* **2016**, *138*, 4832−4842. b) N. Zwettler, S. P. Walg, F. Belaj, N. C. Mösch-Zanetti. *Chem. Eur. J.* **2018**, *24*, 7149–7160. c) G. Erker. *Dalton Trans.* **2011**, *40*, 7475–7483.

59. H. Yamamoto (Ed). *Lewis acids in organic synthesis.* **2000**. Wiley-VCH, Weinheim.

60. X. Xu, G. Kehr, C. G. Daniliuc, G. Erker. *Angew. Chem. Int. Ed.* **2013**, *52*, 13629–13632.

61. X. Xu, G. Kehr, C. G. Daniliuc, G. Erker. *Organometallics* **2013**, *32*, 7306–7311.

62. a) Z. Mo, A. Rit, J. Campos, E. L. Kolychev, S. Aldridge. *J. Am. Chem. Soc.* **2016**, *138*, 3306–3309. b) Z. Mo, E. L. Kolychev, A. Rit, J. Campos, S. Aldridge. *J. Am. Chem. Soc.* **2015**, *137*, 12227–12230. c) G. Ma, G. Song, Z. H. Li. *Chem. Eur. J.* **2018**, *24*, 13238–13245. d) M. Boudjelel, E. D. Sosa Carrizo, S. Mallet-Ladeira, S. Massou, K. Miqueu, G. Bouhadir, D. Bourissou. *ACS Catal.* **2018**, *8*, 4459–4464.

63. O. J. Metters, S. R. Flynn, C. K. Dowds, H. A. Sparkes, I. Manners, D. F. Wass. *ACS Catal.* **2016**, *6*, 6601–6611.

64. P. M. Treichel, J. W. Johnson, K. P. Wagner. *J. Organomet. Chem.* **1975**, *88*, 227–230.

65. A. Habib, R. S. Tanke, E. M. Holt, R. H. Crabtree. *Organometallics* **1989**, *8*, 1225–1231.

66. Y. Liu, G. Kehr, C. G. Daniliuc, G. Erker. *Organometallics* **2017**, *36*, 3407–3414.

67. P. H. M. Budzelaar, D. L. Hughes, M. Bochmann, A. Macchionic, L. Rocchigiani. *Chem. Commun.* **2020**, *56*, 2542–2545.

68. X. Xu, G. Kehr, C. G. Daniliuc, G. Erker. *Organometallics* **2015**, *34*, 2655–2661.

69. Z. Jian, C. G. Daniliuc, G. Kehr, G. Erker. *Organometallics* **2017**, *36*, 424–434.

70. A. T. Normand, C. G. Daniliuc, B. Wibbeling, G. Kehr, P. Le Gendre, G. Erker. *Chem. Eur. J.* **2016**, *22*, 4285–4293.

71. O. J. Metters, S. J. K. Forrest, H. A. Sparkes, I. Manners, D. F. Wass. *J. Am. Chem. Soc.* **2016**, *138*, 1994–2003.

72. L. Rocchigiani, G. Ciancaleoni, C. Zuccaccia, A. Macchioni. *J. Am. Chem. Soc.* **2014**, *136*, 112–115.

73. S. R. Flynn, O. J. Metters, I. Manners, D. F. Wass. *Organometallics* **2016**, *35*, 847–850.

74. A. M. Chapman, D. F. Wass. *Dalton Trans.* **2012**, *41*, 9067–9072.

75. A. T. Normand, P. Richard, C. Balan, C. G. Daniliuc, G. Kehr, G. Erker, P. L. Gendre. *Organometallics* **2015**, *34*, 2000–2011.

76. A. T. Normand, Q. Bonnin, S. Brandès, P. Richard, P. Fleurat-Lessard, C. H. Devillers, C. Balan, P. L. Gendre, G. Kehr, G. Erker. *Chem. Eur. J.* **2019**, *25*, 2803–2815.

77. M. Fischer, D. Barbul, M. Schmidtmann, R. Beckhaus. *Organometallics* **2018**, *37*, 1979–1991.

78. M. Fischer, K. Schwitalla, S. Baues, M. Schmidtmann, R. Beckhaus. *Dalton Trans.* **2019**, *48*, 1516–1523.

79. S. Zhang, A. M. Appel, R. M. Bullock. *J. Am. Chem. Soc.* **2017**, *139*, 7376–7387.

80. a) E. B. Hulley, K. D. Welch, A. M. Appel, D. L. DuBois, R. M. Bullock. *J. Am. Chem. Soc.* **2013**, *135*, 11736–11739. b) E. B. Hulley, M. L. Helm, R. M. Bullock. *Chem. Sci.* **2014**, *5*, 4729–4741.

81. a) T. Liu, D. L. DuBois, R. M. Bullock. *Nat. Chem.* **2013**, *5*, 228–233. b) T. Liu, X. Wang, C. Hoffmann, D. L. DuBois, R. M. Bullock. *Angew. Chem. Int. Ed.* **2014**, *53*, 5300–5304. c) T. Liu, Q. Liao, M. O. Hagan, E. B. Hulley, D. L. DuBois, R. M. Bullock. *Organometallics* **2015**, *34*, 2747–2764.

82. a) J. C. Fontecilla-Camps, A. Volbeda, C. Cavazza, Y. Nicolet. *Chem. Rev.* **2007**, *107*, 4273–4303. b) W. Lubitz, H. Ogata, O. Rüdiger, E. Reijerse. *Chem. Rev.* **2014**, *114*, 4081–4148.

83. S. Zhang, R. M. Bullock. *Inorg. Chem.* **2015**, *54*, 6397–6409.

84. J. Bauer, H. Braunschweig, R. D. Dewhurst. *Chem. Rev.* **2012**, *112*, 4320–4346.

85. C. Tang, Q. Liang, A. R. Jupp, T. C. Johnstone, R. C. Neu, D. Song, S. Grimme, D. W. Stephan. *Angew. Chem. Int. Ed.* **2017**, *56*, 16588–16592.

86. J. B. Geri, J. P. Shanahan, N. K. Szymczak. *J. Am. Chem. Soc.* **2017**, *139*, 5952–5956.

87. A. Simonneau, R. Turrel, L. Vendier, M. Etienne. *Angew. Chem. Int. Ed.* **2017**, *56*, 12268–12272.

88. a) T. A. Rokob, I. Pápai. *Hydrogen activation by frustrated Lewis pairs: Insights from computational studies.* In: G. Erker, D. Stephan (eds) Frustrated Lewis Pairs I. Topics in Current Chemistry. **2013**. Springer, Berlin, Heidelberg, p 157–212. b) L. Rocchigiani. *Isr. J. Chem.* **2015**, *55*, 134–149. c) L. Liu, B. Lukose, P. Jaque, B. Ensing. *Green Energy & Environment* **2019**, *4*, 20–28.

89. B. M. Hoffman, D. Lukoyanov, Z.-Y. Yang, D. R. Dean, L. C. Seefeldt. *Chem. Rev.* **2014**, *114*, 4041–4062.

90. a) T. T. Thai, D. S. Mérel, A. Poater, S. Gaillard, J. L. Renaud. *Chem. Eur. J.* **2015**, *21*, 7066–7070. b) C. Seck, M. D. Mbaye, S. Coufourier, A. Lator, J. F. Lohier, A. Poater, T. R. Ward, S. Gaillard, J. L. Renaud. *ChemCatChem* **2017**, *9*, 4410–4416. c) A. Lator, Q. G. Gaillard, D. S. Mérel, J. F. Lohier, S. Gaillard, A. Poater, J. L. Renaud. *J. Org. Chem.* **2019**, *84*, 6813–6829.

91. B. L. Conley, M. K. Pennington-Boggio, E. Boz, T. J. Williams. *Chem. Rev.* **2010**, *110*, 2294–2312.

92. a) H. F. T. Klare, M. Oestreich, J.-I. Ito, H. Nishiyama, Y. Ohki, K. Tatsumi. *J. Am. Chem. Soc.* **2011**, *133*, 3312–3315. b) C. D. F. Königs, H. F. T. Klare, Y. Ohki, K. Tatsumi, M. Oestreich. *Org. Lett.* **2012**, *14*, 2842–2845. c) J. Hermeke, H. F. T. Klare, M. Oestreich. *Chem. Eur. J.* **2014**, *20*, 9250–9254. d) C. D. F. Königs, M. F. Müller, N. Aiguabella, H. F. T. Klare, M. Oestreich. *Chem. Commun.* **2013**, *49*, 1506–1508. e) C. D. F. Königs, H. F. T. Klare, M. Oestreich. *Angew. Chem. Int. Ed.* **2013**, *52*, 10076–10079. f) T. T. Metsänen, M. Oestreich. *Organometallics* **2015**, *34*, 543–546. g) T. Stahl, H. F. T. Klare, M. Oestreich. *J. Am. Chem. Soc.* **2013**, *135*, 1248–1251. h) S. Bähr, M. Oestreich. *Organometallics* **2017**, *36*, 935–943.

93. S. Webbolt, M. S. Maji, E. Irran, M. Oestreich. *Chem. Eur. J.* **2017**, *23*, 6213–6219.

94. T. Stahl, P. Hrobárik, C. D. F. Königs, Y. Ohki, K. Tatsumi, S. Kemper, M. Kaupp, H. F. T. Klare, M. Oestreich. *Chem. Sci.* **2015**, *6*, 4324–4334.

95. a) N. Ochi, T. Matsumoto, T. Dei, Y. Nakao, H. Sato K. Tatsumi, S. Sakaki. *Inorg. Chem.* **2015**, *54*, 576–585. b) T. Matsumoto, Y. Nakaya, N. Itakura, K. Tatsumi. *J. Am. Chem. Soc.* **2008**, *130*, 2458–2459.

96. M. Carmona, J. Ferrer, R. Rodríguez, V. Passarelli, F. J. Lahoz, P. García-Orduña, L. Cañadillas-Delgado, D. Carmona. *Chem. Eur. J.* **2019**, *25*, 13665–13670.

97. R. Gareth. *Chem. Soc. Rev.* **2012**, *41*, 3535−3546.

98. W. H. Harman, J. C. Peters. *J. Am. Chem. Soc.* **2012**, *134*, 5080−5082.

99. a) H. Fong, M.-E. Moret, Y. Lee, J. C. Peters. *Organometallics* **2013**, *32*, 3053−3062. b) S. N. MacMillan, W. H. Harman, J. C. Peters. *Chem. Sci.* **2014**, *5*, 590−597. c) W. H. Harman, T.-P. Lin, J. C. Peters. *Angew. Chem. Int. Ed.* **2014**, *53*, 1081–1086.

100. M. A. Nesbit. D. L. M. Suess, J. C. Peters. *Organometallics* **2015**, *34*, 4741−4752.

101. S. J. K. Forrest, J. Clifton, N. Fey, P. G. Pringle, H. A. Sparkes, D. F. Wass. *Angew. Chem. Int. Ed.* **2015**, *54*, 2223−2227.

102. K. Mistry, P. G. Pringle, H. A. Sparkes, D. F. Wass. *Organometallics* **2020**, *39*, 468−477.

103. a) B. R. Barnett, C. E. Moore, A. L. Rheingold, J. S. Figueroa. *J. Am. Chem. Soc.* **2014**, *136*, 10262−10265. b) B. R. Barnett, M. L. Neville, C. E. Moore A. L. Rheingold, J. S. Figueroa. *Angew. Chem. Int. Ed.* **2017**, *56*, 7195−7199.

104. a) C. M. Friend, A. S. K. Hashmi. *Acc. Chem. Res.* **2014**, *47*, 729–730. b) I. Braun, A. M. Asiri, A. S. K. Hashmi. *ACS Catal.* **2013**, *3*, 1902–1907. c) M. Rudolph, A. S. Hashmi. *Chem. Soc. Rev.* **2012**, *41*, 2448–2462. d) N. Krause, C. Winter. *Chem. Rev.* **2011**, *111*, 1994–2009. e) A. Corma, A. Leyva-Pérez, M. J. Sabater. *Chem. Rev.* **2011**, *111*, 1657–1712. f) A. Fürstner. *Chem. Soc. Rev.* **2009**, *38*, 3208–3221. g) C. Obradors, A. M. Echavarren. *Chem. Commun.* **2014**, *50*, 16–28.

105. S. G. Weber, C. Loos, F. Rominger, B. F. Straub. *ARKIVOC* **2012**, *23*, 226–242.

106. S. Arndt, M. M. Hansmann, P. Motloch, M. Rudolph, F. Rominger, A. S. K. Hashmi. *Chem. Eur. J.* **2017**, *23*, 2542–2547.

107. Z. Wang, Y. Wang, L. Zhang. *J. Am. Chem. Soc.* **2014**, *136*, 8887–8890.

108. a) Z. Wang, A. Ying, Z. Fan, C. Hervieu, L. Zhang. *ACS Catal.* **2017**, *5*, 3676–3680. b) X. Li, X. Ma, Z. Wang, P.-N. Liu, L. Zhang. *Angew. Chem. Int. Ed.* **2019**, *58*, 17180–17184. c) X. Cheng, Z. Wang, C. D. Quintanilla, L. Zhang. *J. Am. Chem. Soc.* **2019**, *141*, 3787–3791.

109. R. Anwander, S. Kobayashi, S. Kobayashi(Eds). *Lanthanides: chemistry and use in organic synthesis.* **1999**. Springer, Berlin, Heidelberg.

110. a) A. Berkefeld, W. E. Piers, M. Parvez, L. Castro, L. Maron, O. Eisenstein. *J. Am. Chem. Soc.* **2012**, *134*, 10843–10851. b) A. Berkefeld, W. E. Piers, M. Parvez, L. Castro, L. Maron, O. Eisenstein. *Chem. Sci.* **2013**, *4*, 2152–2162.

111. K. Chang, X. Xu. *Dalton Trans.* **2017**, *46*, 4514–4517.

112. K. Chang, X. Wang, Z. Fan, X. Xu. *Inorg. Chem.* **2018**, *57*, 8568–8580.

113. a) P. Xu, Y. Yao, X. Xu. *Chem. Eur. J.* **2017**, *23*, 1263–1267. b) T. Yao, P. Xu, X. Xu. *Dalton Trans.* **2019**, *48*, 7743–7754.

114. a) H. Yasuda. *J. Organomet. Chem.* **2002**, *647*, 128−138. b) H. Yasuda. *J. Polym. Sci. Part A Polym. Chem.* **2001**, *39*, 1955−1959.

115. a) P. Xu, X. Xu. *ACS Catal.* **2018**, *8*, 198–202. b) P. Xu, L. Wu, L. Dong, X. Xu. *Molecules* **2018**, *2*, 360–369.

116. K. Chang, Y. Dong, X. Xu. *Chem. Commun.* **2019**, *55*, 12777–12780.

117. a) P. L. Arnold, I. A. Marr, S. Zlatogorsky, R. Bellabarbac, R. P. Toozec. *Dalton Trans.* **2014**, *43*, 34–37. b) Z. R. Turner, R. Bellabarba, R. P. Tooze, P. L. Arnold. *J. Am. Chem. Soc.* **2010**, *132*, 4050–4051.

118. P. L. Arnold, Z. R. Turner, A. I. Germeroth, I. J. Casely, G. S. Nichol, R. Bellabarba, R. P. Tooze. *Dalton Trans.* **2013**, *42*, 1333–1337.

119. P. L. Arnold, R. W. F. Kerr, C. Weetman, S. R. Docherty, J. Rieb, F. L. Cruickshank, K. Wang, C. Jandl, M. W. McMullon, A. Pöthig, F. E. Kühn, A. D. Smith. *Chem. Sci.* **2018**, *9*, 8035–8045.

120. X. Sun, W. Su, K. Shi, Z. Xie, C. Zhu. *Chem. Eur. J.* **2020**, *26*, 5354–5359.

121. For general reviews: a) G. B. Kauffman. *Coord. Chem. Rev.* **1973**, *9*, 339–363. b) G. B. Kauffman. *Coord. Chem. Rev.* **1974**, *12*, 105–149. c) G. B. Kauffman. *Coord. Chem. Rev.* **1975**, *15*, 1–92.

122. L. F. Dahl, E. Ishishi, R. E. Rundle. *J. Chem Phys.* **1957**, *26*, 1750–1751.

123. T. Nguyen, A. D. Sutton, M. Brynda, J. C. Fettinger, G. J. Long, P. P. Power. *Science* **2005**, *310*, 844–847.

124. G. Frenking, R. Tonner. *Nature* **2007**, *446*, 276–277.

125. a) S. P. Green, C. Jones, A. Stasch. *Science* **2007**, *318*, 1754–1757. b) A. Stasch, C. Jones. *Dalton Trans.* **2011**, *40*, 5659–5672.

126. I. Resa, E. Carmona, E. Gutierrez-Puebla, A. Monge. *Science* **2004**, *305*, 1136–1138.

127. a) M. Stender, A. D. Phillips, R. J. Wright, P. P. Power. *Angew. Chem. Int. Ed.* **2002**, *41*, 1785–1787. b) P. P. Power. *Organometallics* **2007**, *26*, 4362–4372.

128. L. Pu, B. Twamley, P. P. Power. *J. Am. Chem. Soc.* **2000**, *122*, 3524–3525.

129. B. Cornils, W. A. Herrmann, M. Beller, R. Paciello. *Applied homogeneous catalysis with organometallic compounds: a comprehensive handbook in four volumes.* 3rd ed. **2017**. New York, Wiley.

130. J. Campos. *Nat. Rev. Chem.* **2020**, *4*, 696–702.

131. a) P. Buchwalter, J. Rosé, P. Braunstein. *Chem. Rev.* **2015**, *115*, 28–126. b) N. P. Mankad. *Chem. Eur. J.* **2016**, *22*, 5822–5829. c) I. G. Powers, C. Uyeda. *ACS Catal.* **2017**, *7*, 936–958.

132. R. J. Eisenhart, L. J. Clouston, C. C. Lu. *Acc. Chem. Res.* **2015**, *48*, 2885–2894.

133. a) M. H. Pérez-Temprano, J. A. Casares, A. R. de Lera, R. Alvarez, P. Espinet. *Angew. Chem. Int. Ed.* **2012**, *51*, 4917–4920. b) R. J. Oeschger, P. Chen. *J. Am. Chem. Soc.* **2017**, *139*, 1069–1072. c) C. Chen, C. Hou, Y. Wang, T. S. A. Hor. *Z. Weng. Org. Lett.* **2014**, *16*, 524–527.

134. a) Y. Chen, S. Sakaki. *Dalton. Trans.* **2014**, *43*, 11478–11492. b) H. Tsurugi, A. Hayakawa, S. Kando, Y. Sugino, K. Mashima. *Chem. Sci.* **2015**, *6*, 3434–3439. c) M. E. Broussard, B. Juma, S. G. Train, W.-G. Peng, S. A. Laneman, G. G. Stanley. *Science* **1993**, *260*, 1784–1788. d) T. Inatomi, Y. Koga, K. Matsubara. *Molecules* **2018**, *23*, 140.

135. a) I. U. Khand, G. R. Knox, P. L. Pauson, W. E. Watts. *J. Chem. Soc. D.* **1971**, *1*, 36a. b) I. U. Khand, G. R. Knox, P. L. Pauson, W. E. Watts. *J. Chem. Soc. Perkin. Trans. 1*. **1973**, 975–977. c) I. U. Khand, G. R. Knox, P. L. Pauson, W. E. Watts, M. I. Foreman. *J. Chem. Soc. Perkin. Trans. 1*. **1973**, 977–981.

136. M. Yamanaka, E. Nakamura. *J. Am. Chem. Soc.* **2001**, *123*, 1703–1708.

137. D. R. Hartline, M. Zeller, C. Uyeda. *Angew. Chem. Int. Ed.* **2016**, *55*, 6084–6087.

138. a) A. Noor, G. Glatz, R. Müller, M. Kaupp, S. Demeshko, R. Kempe. *Nature Chem.* **2009**, *1*, 322–325. b) C. Ni, B. D. Ellis, G. L. Long, P. P. Power. *Chem. Commun.* **2009**, *17*, 2332–2334. c) C. Schwarzmaier, A. Noor, G. Glatz, M. Zabel, A. Y. Timoshkin, B. M. Cossairt, C. C. Cummins, R. Kempe, M. Scheer. *Angew. Chem. Int. Ed.* **2011**, *50*, 7283–7286.

139. a) H.-Z. Chen, S.-C. Liu, C. H. Yen, J.-S. K. Yu, Y.-J. Shieh, T.-S. Kuo, Y.-C. Tsai. *Angew. Chem. Int. Ed.* **2012**, *51*, 10342–10346. b) Y. Chen, S. Sakaki. *Dalton Trans.* **2014**, *43*, 11478–11492.

140. Y. Chen, S. Sakaki. *Inorg. Chem.* **2017**, *56*, 4011–4020.

141. a) A. M. Baranger, R. G. Bergman. *J. Am. Chem. Soc.* **1994**, *116*, 3822–3835. b) T. A. Hanna, A. M. Baranger, R. G. Bergman. *J. Am. Chem. Soc.* **1995**, *117*, 11363–11364.

142. a) S. L. Marquard, M. W. Bezpalko, B. M. Foxman, C. M. Thomas. *J. Am. Chem. Soc.* **2013**, *135*, 6018–6021. b) B. Wu, R. Hernández-Sánchez, M. W. Bezpalko, B. M. Foxman, C.M. Thomas. *Inorg. Chem.* **2014**, *53*, 10021–10023. c) H. Zhang, B. Wu, S. L. Marquard, E. D. Litle, D. A. Dickie, M. W. Bezpalko, B. M. Foxman, C. M. Thomas. *Organometallics* **2017**, *36*, 3498–3507. d) H. Zhang, G. P. Hatzis, C. E. Moore, D. A. Dickie, M. W. Bezpalko, B. M. Foxman, C. M. Thomas. *J. Am. Chem. Soc.* **2019**, *141*, 9516–9520.

143. C. M. Thomas, J. W. Napoline, G. T. Rowe, B. M. Foxman. *Chem. Commun.* **2010**, *46*, 5790–5792.

144. K. M. Gramigna, D. A. Dickie, B. M. Foxman, C. M. Thomas. *ACS Catal.* **2019**, *9*, 3153–3164.

145. I. N. Nowell, D. R. Russell. *Chem. Commun.* **1967**, *16*, 817.

146. M. Ma, A. Sidiropoulos, R. Lalrempuia, A. Stasch, C. Jones. *Chem. Commun.* **2013**, *49*, 48–50.

147. a) H. Braunschweig, K. Gruss, K. Radacki. *Angew. Chem. Int. Ed.* **2009**, *48*, 4239–4241. b) H. Braunschweig, K. Gruss, K. Radacki. *Angew. Chem. Int. Ed.* **2007**, *46*, 7782–7784. c) H. Braunschweig, K. Gruss, K. Radacki. *Inorg. Chem.* **2008**, *47*, 8595–8597. d) H. Braunschweig, A. Damme, R. D. Dewhurst, F. Hupp, J. O. C. Jimenez-Halla. *Chem. Commun.* **2012**, *48*, 10410–10412.

148. a) H. Braunschweig, R. D. Dewhurst, F. Hupp, C. Kaufmann, A. K. Phukan, C. Schneider, Q. Ye. *Chem. Sci.* **2014**, *5*, 4099–4104. b)

R. Bissert, H. Braunschweig, R. D. Dewhurst, C. Schneider. *Organometallics* **2016**, *35*, 2567–2573.

149. J. R. Pinkes, B. D. Steffey, J. C. Vites, A. R. Cutler. *Organometallics* **1994**, *13*, 21–23.

150. a) H. Memmler, U. Kauper, L. H. Gade, I. J. Scowen, M. McPartlin. *Chem. Commun.* **1996**, 1751–1752. b) A. Schneider, L. H. Gade, M. Breuning, G. Bringmann, I. J. Scowen, M. McPartlin. *Organometallics* **1998**, *17*, 1643–1645. c) L. H. Gade, H. Memmler, U. Kauper, A. Schneider, S. Fabre, I. Bezougli, M. Lutz, C. Galka, I. J. Scowen, M. McPartlin. *Chem. Eur. J.* **2000**, *6*, 692–708. d) B. Findeis, M. Schubart, C. Platzek, L. H. Gade, I. Scowen, M. McPartlin. *Chem. Commun.* **1996**, 219–220. e) J. R. Pinkes, S. M. Tetrick, B. E. Landrum, A. R. Cutler. *J. Organomet. Chem.* **1998**, *556*, 1–7. f) A. Sisak, E. Halmos. *J. Organomet. Chem.* **2007**, *92*, 1817–1824. g) K. Uehara, S. Hikichi, A. Inagaki, M. Akita. *Chem. Eur. J.* **2005**, *11*, 2788–2809. h) J. A. R. Schmidt, E. B. Lobkovsky, G. W. Coates. *J. Am. Chem. Soc.* **2005**, *127*, 11426–11435. i) J. P. Krogman, B. M. Foxman, C. M. Thomas. *J. Am. Chem. Soc.* **2011**, *133*, 14582–14585. j) B. G. Cooper, C. M. Fafard, B. M. Foxman, C. M. Thomas. *Organometallics* **2010**, *29*, 5179–5186. k) I. M. Riddlestone, N. A. Rajabi, J. P. Lowe, M. F. Mahon, S. A. Macgregor, M. K. Whittlesey. *J. Am. Chem. Soc.* **2016**, *35*, 11081–11084.

151. S. Jamali, S. Abedanzadeh, N. K. Khaledi, H. Samouei, Z. Hendi, S. Zacchini, R. Kia, H. R. Shahsavari. *Dalton Trans.* **2016**, *45*, 17644–17651.

152. a) U. Jayarathne, T. J. Mazzacano, S. Bagherzadeh, N. P. Mankad. *Organometallic* **2013**, *32*, 3986–3992. b) S. Banerjee, M. K. Karunananda, S. Bagherzadeh, U. Jayarathne, S. R. Parmelee, G. W. Waldhart, N. P. Mankad. *Inorg. Chem.* **2014**, *53*, 11307–11315. c) M. K. Karunananda, F. X. Vázquez, E. E. Alp, W. Bi, S. Chattopadhyay, T. Shibatade, N. P. Mankad. *Dalton Trans.* **2014**, *43*, 13661–13671.

153. M. K. Karunananda, N. P. Mankad. *Organometallics* **2017**, *36*, 220–227.

154. U. Jayarathne, S. R. Parmelee, N. P. Mankad. *Inorg. Chem.* **2014**, *53*, 7730–7737.

155. M. K. Karunananda, S. R. Parmelee, G. W. Waldhart, N. P. Mankad. *Organometallics* **2015**, *34*, 3857–3864.

156. N. P. Mankad. *Chem. Commun.* **2018**, *54*, 1291–1302.

157. M. K. Karunananda, N. P. Mankad. *J. Am. Chem. Soc.* **2015**, *137*, 14598–14601.

158. a) T. J. Mazzacano, N. P. Mankad. *J. Am. Chem. Soc.* **2013**, *135*, 17258–17261. b) S. R. Parmelee, T. J. Mazzacano, Y. Zhu, N. P. Mankad, J. A. Keith. *ACS Catal.* **2015**, *5*, 3689–3699.

159. L. J. Cheng, N. P. Mankad. *J. Am. Chem. Soc.* **2019**, *141*, 3710–3716.

CHAPTER II.

Transition Metals Only Frustrated Lewis Pairs (TMOFLPs)

II.1. Introduction

Chapter 1 describes FLP examples in which transition metal elements act as either Lewis bases or acids within a frustrated framework. It also discusses general concepts and reactivity of bimetallic systems, drawing special attention to their connection with FLPs. Combining these two areas results in the obvious target of designing frustrated Lewis pairs in which the two components are based on transition metals. This kind of cooperative systems are rather rare, despite the fact that many polarized heterobimetallic complexes exhibit cooperative reactivity that is reminiscent of FLPs.[1]

In a first attempt towards an all-transition metal FLP, the group of Wass anticipated the use of a phosphinoaryloxide zirconocene as a suitable architecture to coordinate an electron rich Pt(0) center through its pendant phosphine. However, contrary to the expected Zr(IV)/Pt(0) FLP, a new heterobimetallic compound is formed instead by formal insertion of the platinum center into a Zr−C bond (Scheme 1).[2]

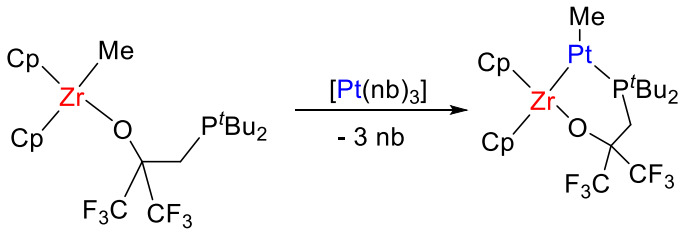

Scheme 1. Reaction of a phosphinoaryloxide zirconocene with [Pt(nb)$_3$] (nb = norbornene).

[1] a) D. W. Stephan. *Coord. Chem. Rev.* **1989**, *95*, 41–107. b) N. Wheatley, P. Kalck. *Chem. Rev.* **1999**, *99*, 3379–3420. c) L. H. Gade. *Angew. Chem. Int. Ed.* **2000**, *39*, 2658–2678. d) B. G. Cooper, J. W. Napoline , C. M. Thomas. *Catalysis Reviews* **2012**, *54*, 1–40. e) M. Herberhold, G.-X. Jin. *Angew. Chem. Int. Ed.* **1994**, *33*, 964–966.
[2] A. M. Chapman, S. R. Flynn, D. F. Wass. *Inorg. Chem.* **2016**, *55*, 1017–1021.

It is also possible to access bimetallic FLPs in which only one of the components is based on a transition metal, while the other corresponds to a main group metal. The Bourissou group reported a cyclometalated compound comprised of a basic platinum site and an acidic aluminum fragment, which constitutes a representative example.[3] The presence of a Pt→Al dative bond was confirmed by X-ray diffraction studies and computational analysis. However, the strain associated to the four-membered metallacycle facilitates the insertion of several small molecules along the Pt−Al bond in an FLP-manner. Thus, this pair reacts with CO_2 and CS_2 to provide the corresponding adducts stabilized by push-pull forces, while oxidative addition of N−H and H−H bonds is found after addition of an amide or dihydrogen, respectively. Theoretical studies on the mechanism of H_2 activation provided evidence of an FLP-like transition state in which dihydrogen coordinates side-on to the acidic Al center and end-on to the basic Pt nucleus to obtain the transhydrido-aluminohydride Pt(II) complex (Scheme 2).

[3] M. Devillard, R. Declercq, E. Nicolas, A. W. Ehlers, J. Backs, N. Saffon-Merceron, G. Bouhadir, J. C. Slootweg, W. Uhl, D. Bourissou. *J. Am. Chem. Soc*. **2016**, *138*, 4917–4926.

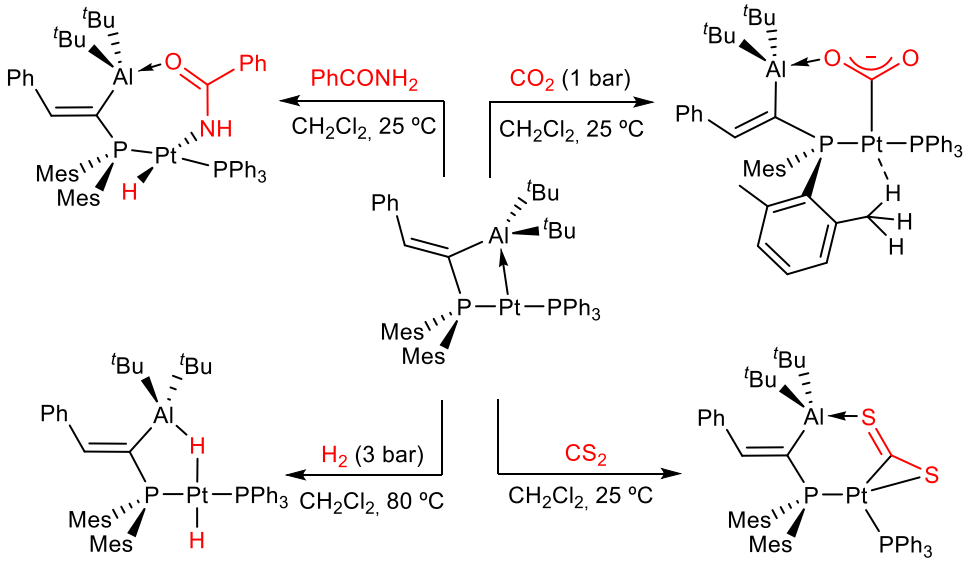

Scheme 2. FLP-like small molecule activation along a constraint Pt→Al bond.

Inspired by Bourissou's work, Brewster recently explored a series of aluminum/transition metal bimetallic complexes with bridging pyridine ligands. The heterobimetallic iridium-aluminum and rhodium-aluminum complexes were capable to activate dihydrogen generating the corresponding alkanes by reductive elimination of alkyl ligands. However, mechanistic investigations indicated that the activation of dihydrogen proceeds through direct oxidative addition at the rhodium or iridium center forming the dihydride species, rather than through a cooperative pathway. The authors discussed that the cooperative hydrogenolysis mechanism is

energetically unfeasible, probably because the transition metal center and the aluminum center are not in close enough proximity.[4,5]

A year earlier, our group described for the first time a transition metal only frustrated Lewis pair (TMOFLP) by combining $[(PMe_2Ar^{Dipp2})Au(I)]NTf_2$ (**1b**; Ar^{Dipp2} = C_6H_3-2,6-(C_6H_3-2,6-$^iPr_2)_2$; NTf_2^- = $[N(SO_2CF_3)_2]^-$) and $[Pt(P^tBu_3)_2]$ (**2**), motivated by their proven Lewis acidic and basic character, respectively.[6] The choice of bulky phosphine ligands was essential to avoid the formation of a metal-only Lewis pair (MOLP). Activation of dihydrogen and acetylene was studied with this system in order to demonstrate its potential FLP-like reactivity. In the case of hydrogen, it is important to remark that neither gold nor platinum precursors reacted with hydrogen by themselves even under forcing conditions, while in the presence of the two metals dihydrogen activation took place immediately at room temperature. In the case of acetylene two different isomers, a vinylene and bridging acetylide were obtained in a 1:4 ratio (Scheme 3).

This gold-platinum system has been largely expanded in this Thesis with three main goals: (i) investigating ligand effects on the activity and selectivity towards small molecule activation; (ii) carry out mechanistic investigations to demonstrate the truly genuine FLP nature of the bimetallic pair; (iii) extend the reactivity studies to other small molecules. The results of these investigations are collected in this Chapter.

[4] T. P. Brewster, T. H. Nguyen, Z. Li, W. T. Eckenhoff, N. D. Schley, N. J. DeYonker. *Inorg. Chem.* **2018**, *57*, 1148–1157.
[5] R. M. Charles III, T. W. Yokley, N. D. Schley, N. J. DeYonker, T. P. Brewster. *Inorg. Chem.* **2019**, *58*, 12635–12645.
[6] J. Campos. *J. Am. Chem. Soc.* **2017**, *139*, 2944–2947.

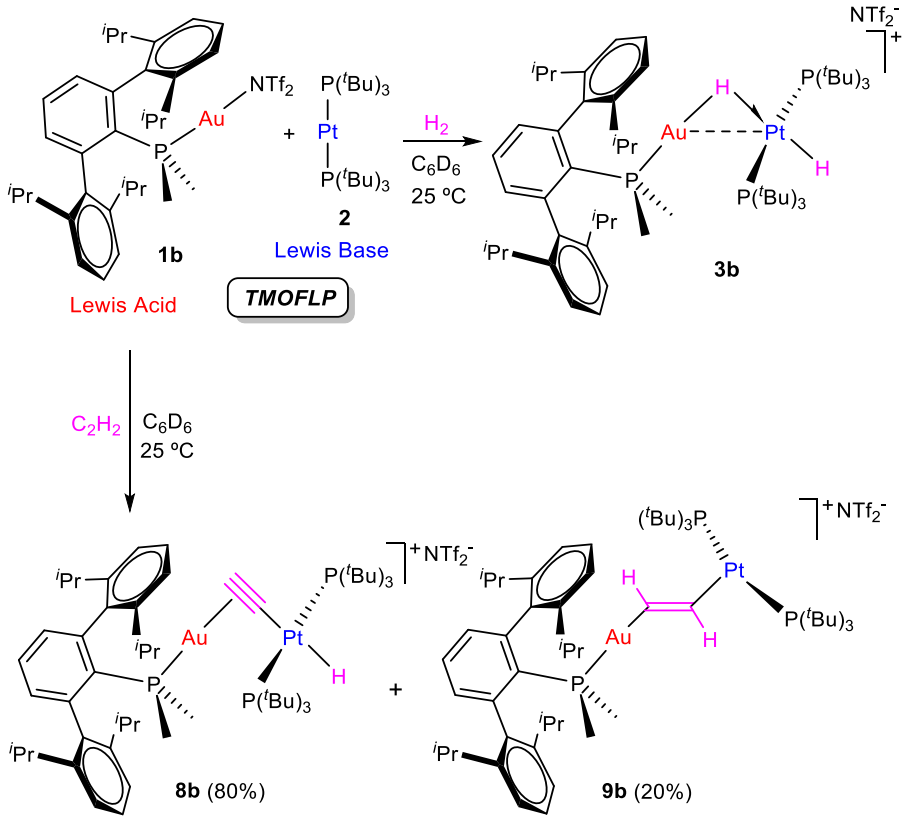

Scheme 3. First example of TMOFLP and hydrogen activation Hydrogen and acetylene activation by a Au(I)/Pt(0) transition metal-only frustrated Lewis pair (TMOFLP) (NTf_2^- (triflimide)= $[N(SO_2CF_3)_2]^-$).[6]

II.2. Results and Discussion

II.2.1. Frustration Versus Adduct Formation

An important aspect when studying mechanisms in FLP systems is the presence of acid-base interactions. Avoiding the formation of a dative bond between the Lewis acid and the Lewis base was once considered a *sine qua non* condition for FLP reactivity. However, a number of studies demonstrate that the already mentioned and so-called 'thermally induced FLPs',[7] in which the resting state is a Lewis adduct, are competent for small molecule activation.[8,9] In fact, these systems may even outperform their fully frustrated versions in catalytic applications.[10] Thus, a precise control of the degree of frustration can be directly associated with catalytic efficiency (i.e. turnover frequency).[11] With this in mind and in the light of the FLP-like reactivity exhibited by heterodinuclear complexes with an explicit M−M bond,[12] we decided to investigate in this Thesis the effects derived from finely tuning the balance between metal-metal bond formation[13] and complete metallic frustration in the gold(I)/platinum(0) system previously

[7] T. A. Rokob, A. Hamza, A. Stirling, I. Pápai. *J. Am. Chem. Soc*. **2009**, *131*, 2029−2036.
[8] F.-G. Fontaine, D. W. Stephan. *Philos. Trans. R. Soc. A,* **2017**, *375*, 20170004.
[9] a) T. Mahdi, D. W. Stephan. *J. Am. Chem. Soc*. **2014**, *136*, 15809−15812. b) D. J. Scott, M. J. Fuchter, A. E. Ashley. *J. Am. Chem. Soc.* **2014**, *136*, 15813–15816. c) M. A. Légaré, E. Rochette, J. Légaré Lavergne, N. Bouchard, F.-G. Fontaine. *Chem. Commun*. **2016**, *52*, 5387–5390.
[10] J. Légaré Lavergne, A. Jayaraman, L. C. Misal Castro, E. Rochette, F.-G. Fontaine. *J. Am. Chem. Soc.* **2017**, *139*, 14714−14723.
[11] M. V. Mane, K. Vanka. *ChemCatChem* **2017**, *9*, 3013−3022.
[12] See for example: a) M. K. Karunananda, S. R. Parmelee, G. W. Waldhart, N. P. Mankad. *Organometallics* **2015**, *34*, 3857−3864. b) L.-J. Cheng, N. P. Mankad. *J. Am. Chem. Soc.* **2019**, *141*, 3710−3716. c) I. M. Riddlestone, N. A. Rajabi, J. P. Lowe, M. F. Mahon, S. A. Macgregor, M. K. Whittlesey. *J. Am. Chem. Soc*. **2016**, *138*, 11081−11084. d) K. M. Gramigna, D. A. Dickie, B. M. Foxman, C. M. Thomas. *ACS Catalysis*, **2019**, *9*, 3153−3164. e) A. M. Baranger, R. G. Bergman. *J. Am. Chem. Soc*. **1994**, *116*, 3822– 3835. f) C. M. Thomas, J. W. Napoline, G. T. Rowe, B. M. Foxman. *Chem. Commun*. **2010**, *46*, 5790– 5792.
[13] J. Bauer, H. Braunschweig, R. D. Dewhurst. *Chem. Rev.* **2012**, *112*, 4329−4346.

reported by our group. To switch between the two extreme scenarios three Lewis acidic gold complexes stabilized by terphenyl phosphines, PR_2Ar' (R = alkyl; Ar' = C_6H_3-2,6-Ar_2), whose steric parameters were recently investigated by our group (Figure 1), have been investigated in this Thesis.[14]

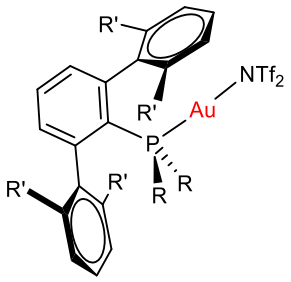

1a: R = Me; R' = Me
1b: R = Me; R' = ^{i}Pr
1c: R = Cyp; R' = Me

Figure 1. Lewis acidic gold complexes stabilized by terphenyl phosphines used in this Chapter (Cyp = cyclopentyl).

To study the equilibrium between the formation of a dative Au←Pt bond and complete bimetallic frustration we examined the interaction between Pt(0) compound **2** and Au(I) triflimide complexes **1a-c** (Figure 1) bearing phosphines PMe_2Ar^{Xyl2} (**1a**), PMe_2Ar^{Dipp2} (**1b**) and $PCyp_2Ar^{Xyl2}$ (**1c**) (Cyp = cyclopentyl). Compound **1b** was readily prepared by chloride abstraction from $(PMe_2Ar^{Xyl2})AuCl$ with silver triflimidate[15] and similar procedure was followed with complexes **1a** and **1c**. The steric shielding provided by these phosphines follows the order $PCyp_2Ar^{Xyl2}$ > PMe_2Ar^{Dipp2} > PMe_2Ar^{Xyl2},[14] which has a direct impact on the reactivity of their gold

[14] M. Marín, J. J. Moreno, M. M. Alcaide, E. Álvarez, J. López-Serrano, J. Campos, M. C. Nicasio, E. Carmona. *J. Organomet. Chem.* **2019**, *896*, 120−128.
[15] M. F. Espada, J. Campos, J. López-Serrano, M. L. Poveda, E. Carmona. *Angew. Chem. Int. Ed.* **2015**, *54*, 15379−15384.

triflimide complexes with compound **2**, as will be discussed in detail in the following sections. For instance, when compound **1a**, based on the less congested phosphine, is combined with an equimolar mixture of **2**, the corresponding bimetallic Lewis adduct **4a** is formed (Scheme 4). However, compound **1b** bearing the intermediate size phosphine (PMe_2Ar^{Dipp2}), seems to be in equilibrium between adduct formation and monometallic fragments. This dynamic behavior is strongly affected by solvent, as previously investigated in detail for traditional FLP systems.[16] In C_6D_6 solution, the ^1H and $^{31}P\{^1H\}$ NMR spectra of compounds **1b** and **2** remained unaltered when mixed together, albeit using the more polar CD_2Cl_2 resulted in broadening of both of their $^{31}P\{^1H\}$ NMR signals, an observation that we attributed to the existence of the aforementioned equilibrium.[6] Thus, Lewis adduct formation appears slightly favored under the more polar environment provided by CD_2Cl_2, as expected for the formation of two ionic species (**4b** and NTf_2^-). Moreover, we found that the addition of 10 equivalents of methanol results in rapid formation of **4b**. This result suggests that the role of methanol may be facilitating triflimide solvation, promoting the formation of the Au←Pt bond.

[16] L. X. Dang, G. K. Schenter, T.-M. Chang, S. M. Kathmann, T. Autrey. *J. Phys. Chem. Lett.* **2012**, *3*, 3312−3319.

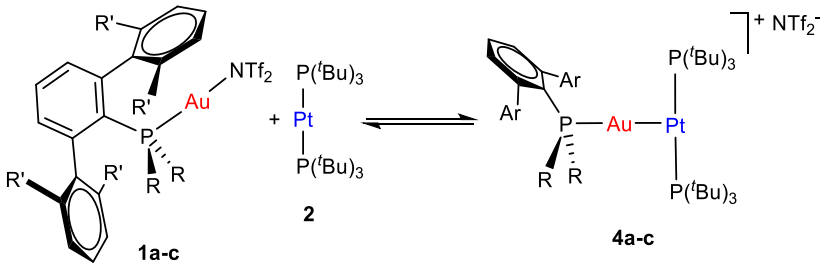

Solvent	**1a + 2 → 4a**	**1b + 2 → 4b**	**1c + 2 → 4c**
	Adduct formation (by NMR)		
C_6D_6	✓	X	X
CD_2Cl_2	✓	*Equilibrium*	X
CD_2Cl_2/MeOH	✓	✓	X
	ΔG⁰ solvent (DFT, kcal·mol⁻¹)		
C_6H_6	-2.5	+1.7	+17.5
CH_2Cl_2	-7.2	-2.4	+10.8

Scheme 4. Solution equilibria for adduct formation vs full frustration in Au(I)/Pt(0) bimetallic pairs as a function of ligand steric and solvent conditions.

Formation of the unsupported heterobimetallic compound **4b** was confirmed on the basis of ^{1}H and $^{31}P\{^{1}H\}$ NMR data. For the latter case, a doublet at 94.5 ppm ($^{1}J_{PPt}$ = 3159 Hz) with a small $^{3}J_{PP}$ coupling constant of 2 Hz was accompanied by a triplet at -34.2 ppm, highly shifted to lower frequencies with respect to gold compound **1b** (δ = -11.5 ppm) and also exhibiting an identical coupling constant of 2 Hz. (Figure 2). Besides, the latter signal arises from the phosphine directly bound to the gold centre but features a relatively strong coupling to platinum ($^{2}J_{PPt}$ = 1984 Hz). This $^{31}P\{^{1}H\}$ NMR pattern supports the fact that a new Pt→Au dative bond is present in compound **4b**.

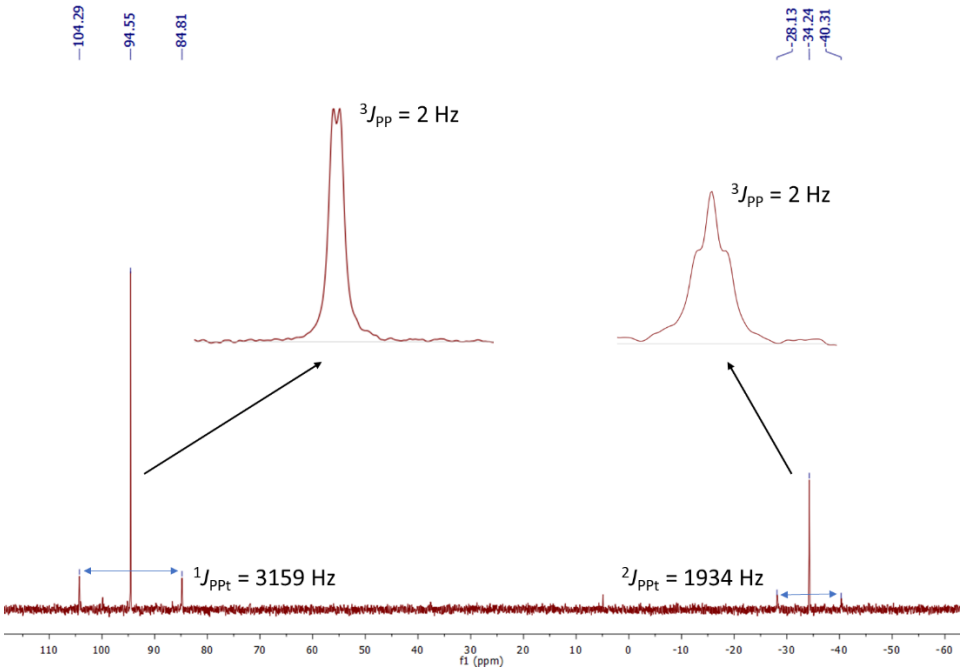

Figure 2. $^{31}P\{^1H\}$ NMR (160 MHz, CD_2Cl_2, 25 °C) of complex **4b**.

The proposed molecular structure of **4b** was also confirmed by single-crystal X-ray diffraction studies (Figure 3). The platinum centre exhibits a slightly distorted T-shaped coordination environment, with a relatively reduced P−Pt−P bond of 167.59(5)° likely due to the bulkiness of the Au(PMe_2Ar^{Dipp2}) unit bound to the Pt(0) centre. The Pt−Au distance amounts to 2.575(1) Å, significantly shortened when compared to its related heterobimetallic dihydride compound,[17] but marginally longer than in

[17] a) A. M. Chapman, M. F. Haddow, D. F. Wass. *Eur. J. Inorg. Chem.* **2012**, *9*, 1546–1554. b) O. J. Metters, S. J. K. Forrest, H. A. Sparkes, I. Manners, D. W. Wass. *J. Am. Chem. Soc.* **2016**, *138*, 1994–2003. c) A. M. Chapman, M. F. Haddow, D. F. Wass. *J. Am. Chem. Soc.* **2011**, *133*, 18463–18478. d) S. R. Flynn, O. J. Metters, I. Manners, D. F. Wass. *Organometallics* **2016**, *35*, 847–850. e) O. J. Metters, S. R. Flynn, C. K. Dowds, H. A. Sparkes, I. Manners, D. F. Wass. *ACS Catal.* **2016**, *6*, 6601–6611. f) H. B. Hamilton, A. M. King, H. A. Sparkes, N. E. Pridmore, D. F. Wass. *Inorg. Chem.* **2019**, *58*, 6399−6409.

compound $[(PCy_3)_2Pt]\rightarrow Au(PCy_3)$ ($d_{Au\text{-}Pt}$ = 2.54Å), the only other unsupported Pt(0)−Au(I) species structurally characterized to date.[18]

The analogous complex based on PMe_2Ar^{Xyl2} (**4a**) revealed similar ^1H and $^{31}P\{^1H\}$ NMR patterns, with characteristic $^{31}P\{^1H\}$ NMR resonances at 96.4 ($^1J_{PPt}$ = 3140, $^3J_{PP}$ = 3 Hz) and -32.5 ($^1J_{PPt}$ = 1933, $^3J_{PP}$ = 3 Hz) ppm. As in compound **4b**, the resonance due to the terphenyl phosphine appears highly shifted to lower frequencies with respect to its gold precursor **1a** (δ = -7.0 ppm). The molecular formulation of **4a** was further validated by single crystal X-ray diffraction analysis (Figure 3), evincing a distorted T-shaped coordination at the platinum center. The P−Pt−P angle of 169.97(3)° and Au−Pt bond distance of 2.561(1) Å are slightly widened and shortened, respectively, compared to **4b** (P−Pt−P = 167.59(5)°; d_{AuPt} = 2.575(1) Å), as expected for the smaller xylyl-based terphenyl substituent on the phosphine.

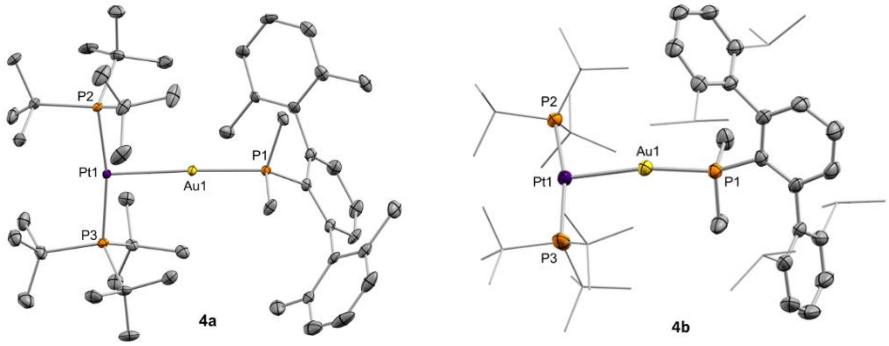

Figure 3. ORTEP diagrams of compound **4a** and **4b**; for the sake of clarity hydrogen atoms and triflimide anion are excluded, while thermal ellipsoids are set at 50% probability. *Tert*-butyl and *iso*-propyl substituents have been drawn in wireframe format in **4b**.

[18] J. Bauer, H. Braunschweig, A. Damme, K. Radacki. *Angew. Chem. Int. Ed*. **2012**, *51*, 10030–10033.

In the case of the analogous reaction based on **1c**, the formation of a new Au←Pt dative bond is not observed by NMR even under more forcing conditions (up to 80 °C with 100 equiv. of methanol). This contrasts with previous examples based on related $[Pt(0)(PR_3)]_2$ species, which in all cases led to the formation of metal-only Lewis pairs.[18,19] Interestingly, while combining **1a** or **1b** with Pt(0) precursor **2** results in a distinct bright yellow color of the resulting solutions, the addition of **1c** over benzene or chlorinated solutions of **2** did not alter the colorless appearance of the mixture, which we attribute to the absence of adduct **4c**. The steric pressure exerted by the two cyclopentyl substituents in $PCyp_2Ar^{Xyl2}$ is likely responsible for quenching bimetallic Lewis adduct formation, which suggests a fully frustrated nature. These findings are in perfect agreement with DFT computational studies (ωB97XD/6-31G(d,p)[SDD], see Scheme 4) carried out by Dr. Juan José Moreno, another member of our research group. These studies revealed that the formation of the bimetallic adduct in CH_2Cl_2 (SMD model)[20] is clearly exergonic for the systems based on PMe_2Ar^{Xyl2} (ΔG = -7.2 kcal·mol^{-1}) and PMe_2Ar^{Dipp2} (ΔG = -2.4 kcal·mol^{-1}), while for the latter the process turns to be endergonic when changing the solvent to benzene, as observed experimentally. In contrast, accessing

[19] a) H. Braunschweig, K. Radacki, K. Schwab. *Chem. Commun*. **2010**, *46*, 913–915. b) J. Bauer, H. Braunschweig, P. Brenner, K. Kraft, K. Radacki, K. Schwab. *Chem. Eur. J*. **2010**, *16*, 11985−11992. c) M. Ma, A. Sidiropoulos, L. Ralte, A. Stasch, C. Jones. *Chem. Commun.* **2013**, *49*, 48–50. d) H. Braunschweig, R. D. Dewhurst, F. Hupp, C. Schneider. *Chem. Commun*. **2014**, *50*, 15685–15688. e) B. R. Barnett, C. E. Moore, P. Chandrasekaran, S. Sproules, A. L. Rheingold, S. DeBeerde, J. S. Figueroa. *Chem. Sci*. **2015**, *6*, 7169−7178.

[20] A. V. Marenich, C. J. Cramer, D. G. Truhlar. *J. Phys. Chem. B* **2009**, *113*, 6378−6396.

compound **4c** based on $PCyp_2Ar^{Xyl2}$ is endergonic with respect to the monometallic fragments even in CH_2Cl_2 (10.8 kcal·mol^{-1}).

Altogether, we have in hand a bimetallic pair where the M−M interaction/frustration balance can be rationally tuned from expeditious M−M dative bond formation in PMe_2Ar^{Xyl2} to complete frustration in $PCyp_2Ar^{Xyl2}$, through an intermediate and adjustable equilibrium situation in PMe_2Ar^{Dipp2}. The effects of controlling this balance on the bimetallic reactivity and selectivity towards dihydrogen and acetylene activation are discussed in the next sections.

II.2.2. TMOFLPs Reactivity with Dihydrogen

The activation of dihydrogen has continuously been examined as the prime benchmark reaction to demonstrate FLP behavior in main group systems. However, the variety of potential chemical pathways to account for the bimetallic H_2 splitting depicted in Scheme 3 prevented our group from providing a solid mechanistic picture during preliminary investigations.[6] In fact, the mechanisms by which TMFLPs operate remain underexplored compared to phosphine-borane and related main group designs. As an archetypical example, a vast amount of work has emerged to gain fundamental mechanistic understanding of the heterolytic cleavage of dihydrogen with traditional FLPs.[21] Nonetheless, and despite being the simplest molecule to activate, the precise mechanism remains a matter of intense debate.[22] Focusing on metal-containing systems, most relevant information derives from the concept of metal-ligand cooperation and from the examination of prominent cooperative catalysts for hydrogenation reactions (typically containing pendant Lewis acid or basic sites), whose reactivity resembles that of TMFLPs, as already discussed in Chapter 1.[23,24]

[21] a) T. A. Rokob, I. Pápai. *Top. Curr. Chem.* **2013**, *332*, 157−211. b) J. Paradies. *Eur. J. Org. Chem*. **2019**, 283–294. c) L. Rocchigiani. *Isr. J. Chem*. **2015**, *55*, 134–149. d) L. Liu, B. Lukose, P. Jaque, B. Ensing. *Green Energy Environ.* **2019**, *4*, 20–28.
[22] a) G. Skara, F. De Vleeschouwer, P. Geerlings, F. De Proft, B. Pinter. *Sci. Rep*. **2017**, *7*, 16024. b) J. Daru, I. Bakó, A. Stirling, I. Pápai. *ACS Catal.* **2019**, *9*, 6049−6057. c) S. Grimme, H. Kruse, L. Goerigk, G. Erker. *Angew. Chem. Int. Ed.* **2010**, *49*, 1402–1405. d) D. Yepes, P. Jaque, I. Fernández. *Chem. Eur. J.* **2016**, *22*, 18801–18809. e) L. Liu, L. L. Cao, Y. Shao, G. Ménard, D. W. Stephan. *Chem*, **2017**, *3*, 259–267. f) H. B. Hamilton, D. F. Wass. *Chem*, **2017**, *3*, 198–210. g) T. A. Rokob, I. Bakó, A. Stirling, A. Hamza, I. Pápai. *J. Am. Chem. Soc.* **2013**, *135*, 4425−4437. h) G. Bistoni, A. A. Auer, F. Neese. *Chem. Eur. J.* **2017**, *23*, 865–873.
[23] S. R. Flynn, D. F. Wass. *ACS Catal.* **2013**, *3*, 2574–2581.
[24] a) R. M. Bullock, G. M. Chambers. *Phil. Trans. R. Soc. A*, **2017**, *375*, 20170002. b) M. K. Karunanan, N. P. Mankad. *ACS Catal.* **2017**, *7*, 6110−6119. c) E. R. M. Habraken, A. R. Jupp, M. B. Brands, M. Nieger, A. W. Ehlers, C. J. Slootweg. *Eur. J. Inorg. Chem.* **2019**, 2436–2442.

In the same vein, the mechanistic knowledge regarding TMOFLPs is virtually nonexistent, albeit significant insights may be inferred from polar heterobimetallic complexes (see Section I.2.3.).[25]

In this context, one of the goals of this Thesis has been to investigate the activation of the H−H bond by TMOFLP **1b**/**2** to confirm its FLP-like reactivity. To gain a deeper mechanistic knowledge we have extended the original system based on PMe_2Ar^{Dipp2} to also investigate the metal-only Lewis pair **4a**, as well as the fully frustrated TMOFLP **1c**/**2**, with the aim of highlighting the relevance of M···M interactions. Although the H−H bond in dihydrogen is the simplest covalent bond to activate, we observe quite different product speciation for the three investigated Au(I)/Pt(0) systems (Scheme 5 and Table 1), despite the fact that they only differ on the substituents of the terphenyl phosphine.

[25] a) N. P. Mankad. *Chem. Commun*. **2018**, *54*, 1291–1302. b) I. G. Powers, C. Uyeda. *ACS Catal.* **2017**, *7*, 936−958. c) R. C. Cammarota, L. J. Clouston, C. C. Lu. *Coord. Chem. Rev*. **2017**, *334*, 100–111. d) J. Berry, C. C. Lu. *Inorg. Chem.* **2017**, *56*, 7577−7581. e) N. P. Mankad. *Chem. Eur. J.* **2016**, *22*, 5822–5829.

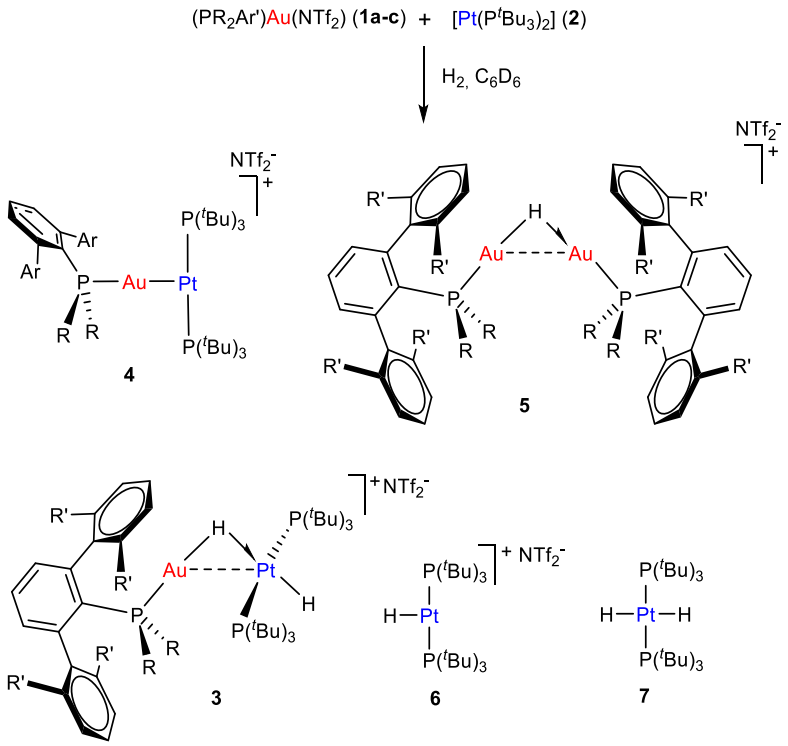

Scheme 5. Reactivity of **1**:**2** TMOFLPs towards hydrogen.

Entry	Gold	T	Product speciation (Yields (%))[a] [Au]		[Au:Pt]		[Pt]		
			1	**5**	**3**	**4**	**2**	**6**	**7**
1		5 min	-	-	-	100	-	-	-
2	**1a**	12 h	-	-	38	62	-	-	-
3		48 h	-	-	99	1	-	-	-
4	**1b**	5 min	-	99	<1	-	50	50	-
5		12 h	-	<1	>95	-	-	<1	-
6	**1c**	5 min	89	11	-	-	47	11	42
7		18 h	-	95	-	-	8[b]	14[b]	48[b]

[a]Yields were calculated by ^{1}H and $^{31}P\{^{1}H\}$ NMR spectroscopy relative to each of the metals (Au or Pt) as appropriate; [b] Unknown Pt-containing species account for the remaining percentage of Pt in solution by ^{31}P NMR

Table 1. Product speciation during FLP-like activation of H_2 by **1:2** pairs.

It is important to note that neither complex **2** nor gold precursors **1** evolved when their C_6D_6 solutions were exposed to dihydrogen (1 bar) even under harsher reaction conditions (80 °C, up to 1 week) to those attempted with the metallic pairs. In stark contrast, TMOFLPs **1b**/**2** and **1c**/**2** readily react with H_2 (1 bar, 25 °C), with the former pair exhibiting faster H−H cleavage. Complete consumption of **1b** was observed by the time spectra were recorded rapidly after sample preparation (<5min) to yield a 1:1:1 mixture of the hydride-bridged digold compound **5b**, platinum hydride $[Pt(P^tBu_3)_2(H)]^+$ (**6**)[26] and unreacted **2** (Table 1, entry 4). Low-temperature ^1H and $^{31}P\{^1H\}$ NMR monitoring revealed the extreme reactivity of TMOFLP **1b**/**2** towards H_2, since H−H cleavage is observed even at -20 °C, with a half-life for compound **1b** of *ca.* 120 min at that temperature. The foregoing mixture evolved to the heterobimetallic dihydride **3b** after 12 hours at 25 °C as the only discernible product by NMR spectroscopy (entry 5).

Although proceeding at a lower rate, TMOFLP **1c**:**2** built on $PCyp_2Ar^{Xyl2}$ exhibited smooth reactivity towards H_2 even after short reaction times, with conversion of one tenth of **1c** and more than half of **2** (entry 6) by the time NMR spectra were recorded (*ca.* 5 min). The formation of platinum dihydride **7**,[27] which was not observed when combining **1b** and **2**, accounts for the dissimilar conversion rate of Pt(0) complex **2** compared to Au(I) species **1c**. This finding suggests an unconventional catalytic role of gold for the hydrogenation of **2** towards **7**.[28] We demonstrated this by exposing C_6D_6 solutions of **2** to H_2 atmosphere (0.5 bar) under variable

[26] R. G. Goel, R. C. Srivastava. *Can. J. Chem.* **1983**, *61*, 1352−1359.
[27] R. G. Goel, W. O. Ogiri, R. C. Srivastava. *Organometallics* **1982**, *1*, 819–824.
[28] a) C. González-Arellano, A. Corma, M. Iglesias, F. Sánchez. *Chem. Commun*. **2005**, 3451–3453. b) A. Comas-Vives, G. Ujaque. *J. Am. Chem. Soc.* **2013**, *135*, 1295−1305.

catalytic amounts of **1c** (Scheme 6). Intriguingly, best yields for the hydrogenated product (*ca.* 80% of **7**) derived from using 10 mol% of gold catalyst **1c**, whereas increasing its amount to 30% had a detrimental effect (only 17% of **7** formed) under otherwise identical conditions. This may result from a complex series of solution equilibrium processes existing after FLP-like H−H bond cleavage (see Scheme7). For this system, the main gold containing species (*ca.* 95%) in the long term (18 hours) is the hydride-bridged digold compound **5c**, while half of the platinum precursor was converted into dihydride **7** after that time, accompanied by smaller amounts (*ca.* 10%) of unreacted **2** and monohydride **6**, along with other unidentified Pt-containing species (entry 7). No signals of a presumed heterobimetallic dihydride **3c** were detected, likely due steric reasons on account of $PCyp_2Ar^{Xyl2}$.

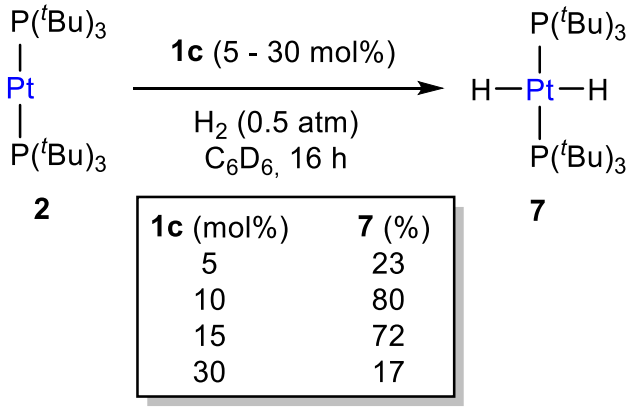

1c (mol%)	**7** (%)
5	23
10	80
15	72
30	17

Scheme 6. Catalytic hydrogenation of **2** mediated by **1c**.

Product speciation is considerably simplified with the less hindered system (**1a**:**2**) based on PMe_2Ar^{Xyl2}, which immediately yielded the metal-only Lewis pair **4a** even in the presence of dihydrogen. H−H bond activation

proceeds at a considerably slower pace, with full conversion to **3a** reached after two days at 25 °C (entries 1−3), while no intermediates were detected by ^{1}H or $^{31}P\{^{1}H\}$ NMR methods. Overall, the rate of H−H bond cleavage follows the trend **1b**:**2** (PMe_2Ar^{Dipp2}) > **1c**:**2** ($PCyp_2Ar^{Xyl2}$) > **1a**:**2** (PMe_2Ar^{Xyl2}). As discussed later in deeper detail, this trend supports the notion of a genuine FLP-type H−H cleavage, since the existence of a Au←Pt dative bond (**1a**; PMe_2Ar^{Xyl2}) handicaps H_2 activation, while forcing complete frustration by steric clash (**1c**; $PCyp_2Ar^{Xyl2}$) somehow diminishes the rate of activation compared to the intermediate interaction/frustration situation found for the **1b**:**2** pair based on PMe_2Ar^{Dipp2}.

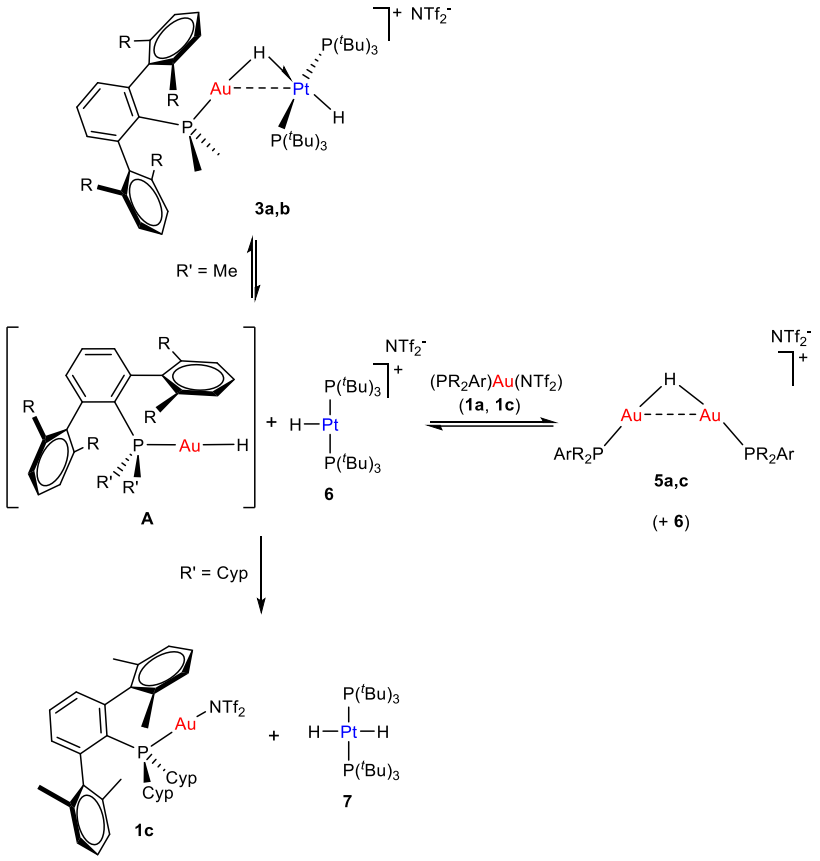

Scheme 7. Proposed reaction pathways taking place after H−H cleavage by **1:2** pairs.

As aforementioned, we assume metal speciation after H_2 splitting to result from a series of equilibria that are likely controlled by steric reasons. We have not been able to spectroscopically observe a gold monohydride species **A** (Scheme 7) that would arise from heterolytic H−H cleavage, since it seems to be rapidly trapped by still unreacted gold triflimide **1** to yield digold hydrides **5**, as it also occurs when treating compounds **1** with $SiEt_3H$. Nevertheless, in the case of the less hindered **1a**, direct access to heterobimetallic dihydride **3a** is kinetically favored. The reduced size of PMe_2Ar^{Xyl2} may facilitate the approach of platinum complex **6** to give the

thermodynamic product, **3a**. In turn, the reversible formation of compounds **5** would accounts for the slow formation (*ca.* 12 h) of **3b** by trapping the continuously liberated monohydride **A** (from **5b**) by **2**. However, the more sterically congested system based on $PCyp_2Ar^{Xyl2}$ precludes the observation of **3c**, likely due to steric reasons. Thus, an alternative pathway involving hydride abstraction by cationic platinum **6** to produce **7** and generate gold triflimide **1c**, becomes available. This would explain the catalytic role of gold for the hydrogenation of Pt(0) **2**. Overall, the prevalence of each of the interrelated reactions seems to be controlled by steric reasons and is responsible for the product speciation observed with the three investigated terphenyl phosphines.

The molecular formulation of compound **3a** was ascertained by multinuclear NMR spectroscopy, where distinctive ^{1}H NMR resonances at -1.75 ($^{2}J_{HP}$ = 110 Hz, $^{1}J_{HPt}$ = 516 Hz) and -10.39 ppm, due to the bridging and terminal hydride, respectively, were recorded (Figure 4). Both low-frequency signals where flanked by ^{195}Pt satellites with coupling constants of 516 and 1030 Hz, respectively. Besides, ^{195}Pt satellites accompanying the corresponding $^{31}P\{^{1}H\}$ NMR signals at 91.5 ($^{1}J_{PPt}$ = 2713 Hz, $P(^{t}Bu)_3$) and 5.7 ($^{2}J_{PPt}$ = 208 Hz, PMe_2Ar^{Xyl2}) evinced the presence of a Au···Pt interaction in **3a** (Figure 5). These data compared well with its related compound **3b** (δ_{1H} = -1.67 ($^{2}J_{HP}$ = 112 Hz, $^{1}J_{HPt}$ = 503 Hz)), -11.39 ($^{1}J_{HPt}$ = 1053 Hz); δ_{31P} = 90.0 ($^{1}J_{PPt}$ = 2744 Hz), 7.2 ($^{2}J_{PPt}$ = 200 Hz), which was previously reported by our group.[6]

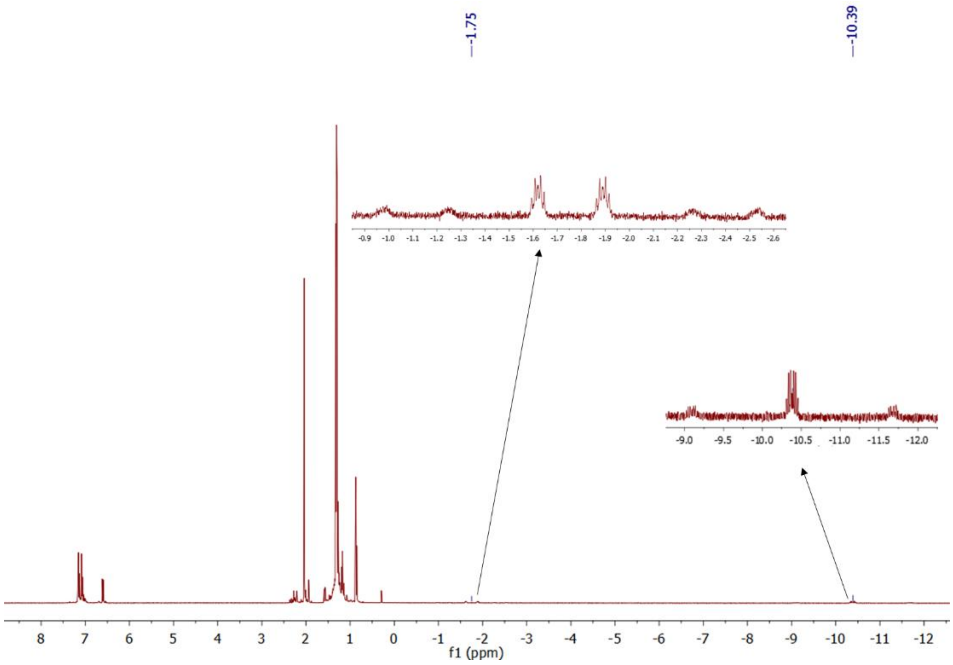

Figure 4. ^{1}H NMR (400 MHz, C_6D_6, 25 °C) of complex **3a**.

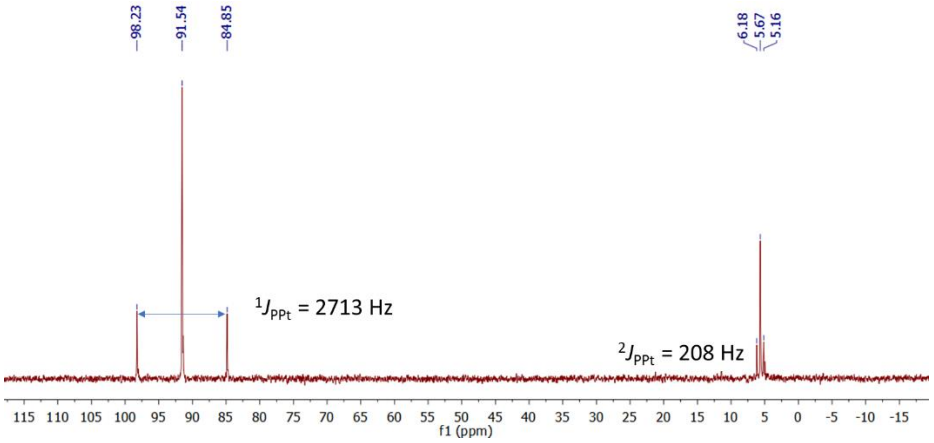

Figure 5. ^{31}P{^{1}H} NMR (160 MHz, C_6D_6, 25 °C) of complex **3a**.

With regards to compound **5b**, our group previously assumed a digold hydride-bridged formulation as the main gold containing species for the PMe_2Ar^{Dipp2} system after short periods of time (Table 1, entry 4).[6] This statement was made exclusively based on NMR data, particularly on a

distinctive ^{1}H NMR signal at 2.83 ppm that appears as a triplet ($^{2}J_{HP}$ = 99.5 Hz) and was attributed to the bridging hydride. However, all attempts to isolate this compound in the past proved unsuccessful due to formation of $[Au(PMe_2Ar^{Dipp2})_2]^+$ with concomitant release of hydrogen and appearance of gold nanoparticles ($t_{1/2}$ at 25 °C ≈ 3 h). In stark contrast, the steric shrouding provided by $PCyp_2Ar^{Xyl2}$ allowed us to isolate in this Thesis work the first stable compound of type $[Au_2(\mu\text{-H})(PR_3)_2]^+$ (**5c**) authenticated by single-crystal X-ray diffraction (Figure 6).

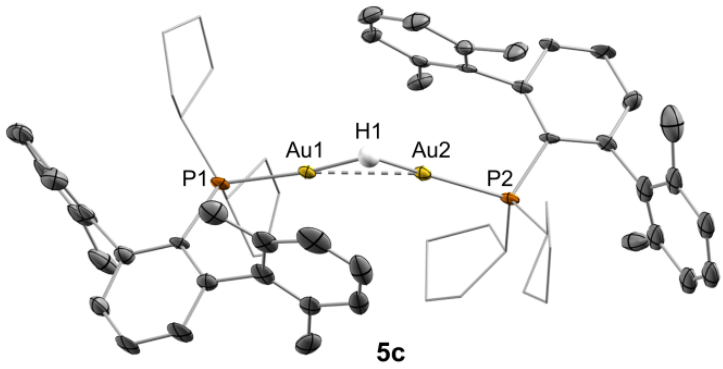

Figure 6. ORTEP diagram of compound **5c**; for the sake of clarity hydrogen atoms (except the gold hydride) and triflimide anion are excluded and cyclopentyl substituents have been represented in wireframe format, while thermal ellipsoids are set at 50% probability.

This compound was independently prepared by reacting **1c** and $SiEt_3H$.[29] A short Au−Au distance of 2.748(1) Å suggests the existence of a

[29] a) E. Y. Tsui, P. Muller, J. P. Sadighi. *Angew. Chem. Int. Ed.* **2008**, *47*, 8937–8940. b) A. Escalle, G. Mora, F. Gagosz, N. Mezailles, X. F. Le Goff, Y. Jean, P. Le Floch. *Inorg. Chem.* **2009**, *48*, 8415–8422. c) R. J. Harris, R. A. Widenhoefer. *Angew. Chem. Int. Ed*. **2014**, *53*, 9369–9371.

strong aurophilic interaction,[30] being comparable to other hydride-bridged digold complexes (2.70-2.78 Å).29[b,31] In its ^{1}H NMR spectrum (Figure 7), the bridging hydride appears as a triplet at 4.78 ppm and features a strong coupling with the ^{31}P nuclei ($^{2}J_{HP}$ = 90.9 Hz), comparable to **5b** and to a related species based on P(^{t}Bu)$_2$(*o*-biphenyl)29[c] and thus further supporting the formulation priorly proposed by our group.

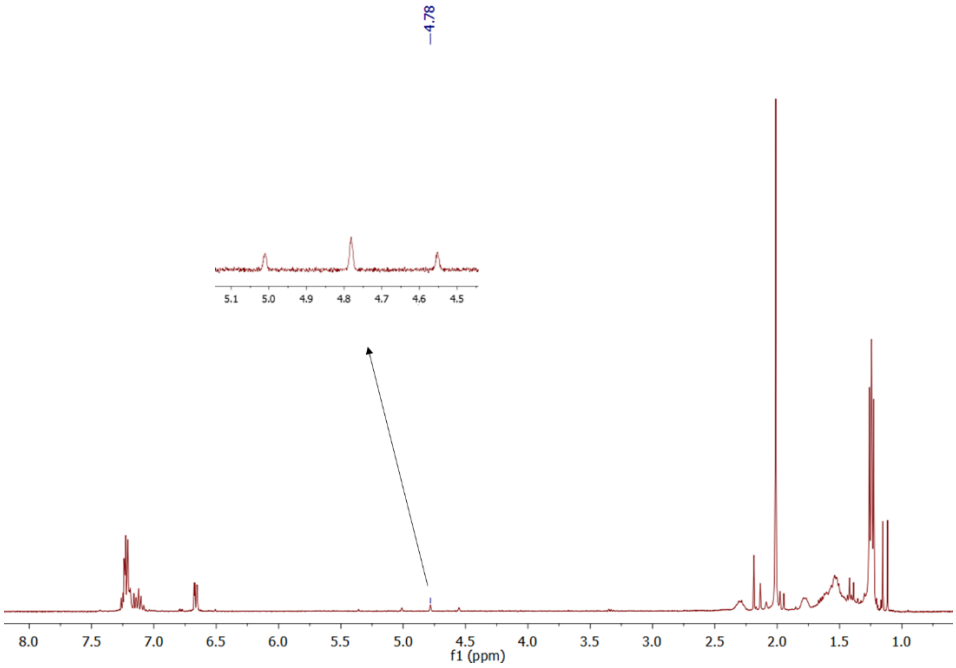

Figure 7. ^{1}H NMR (400 MHz, C_6D_6, 25 °C) of compound **5c**.

As discussed in the introduction, the mechanism of H−H bond cleavage for a variety of cooperative systems has been extensively investigated.[22,24] In the context of heterobimetallic designs, three main

[30] H. Schmidbaurab, A. Schiera. *Chem. Soc. Rev*. **2012**, *41*, 370–412.
[31] N. Phillips, T. Dodson, R. Tirfoin, J. I. Bates, S. Aldridge. *Chem. Eur. J.* **2014**, *20*, 16721–16731.

scenarios can be envisaged. Those are represented in Scheme 8 with regards to our Au(I)/Pt(0) pairs and relates to the ones discussed in Figure 5 of Chapter 1. In the first, dihydrogen is added across the Au−Pt bond to yield two monometallic hydrides which, after rapid rearrangement, would lead to the final heterobimetallic dihydride **3** (Scheme 8a). Alternatively, the H−H bond could be cleaved by the cooperative action of the two independent metallic fragments, that is, by a truly FLP-type mechanism (Scheme 8b). As before, the resulting monohydrides could readily evolve towards **3**. The third possible route involves the orthogonal reactivity of a metal fragment that initially activates the dihydrogen molecule and subsequently evolves to the final heterobimetallic compound in the presence of the second metal fragment (Scheme 8c). In principle, this mechanism may operate both in the presence or absence of a Au−Pt bond.

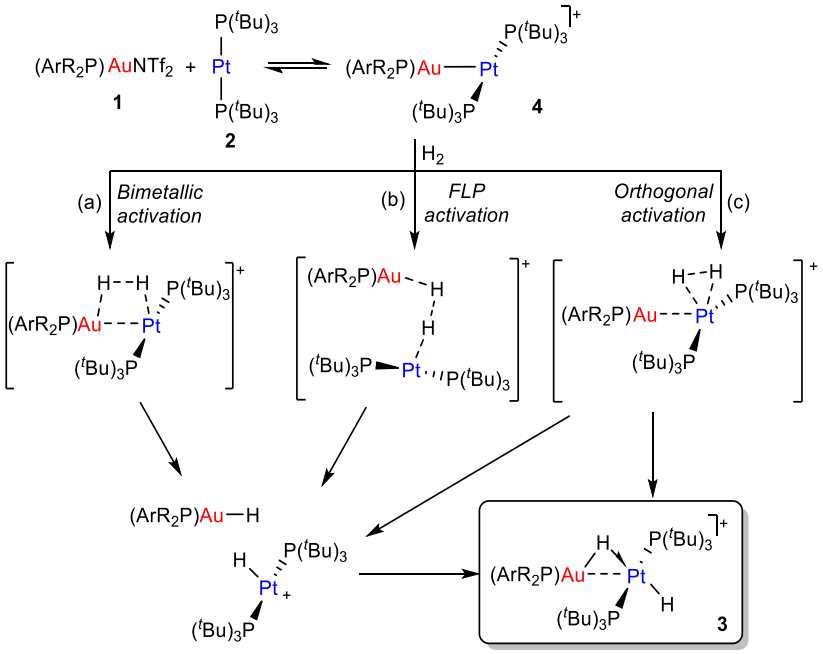

Scheme 8. Cooperative H_2 activation involving (a) traditional bimetallic activation across a M−M bond; (b) transition metal-only FLP activation and (c) orthogonal reactivity.

Our group had tentatively proposed a genuine FLP pathway as in Scheme 6b for the pair **1b**:**2** before the beginning of this Thesis,[6] though there was not enough data to unambiguously discern between the three alternatives described in Scheme 8. We have now investigated the potential role of these mechanisms in deeper detail by a combined experimental/computational approach, being the computational studies developed by Dr. Joaquín López-Serrano and Dr. Juan José Moreno, other members of our research group.

We have particularly focused on the pair **1a**:**2**, which reacts with H_2 (1 bar, 25 °C) at a considerably slower rate and thus facilitates kinetic

analysis. It is important to remark that this is the only pair in which the existence of the Au←Pt bond is unequivocal under all experimental conditions, suggesting the need to access the independent Au(I) and Pt(0) fragments for the H−H cleavage to take place (as in Scheme 8b). In fact, we observed that hydrogen activation with **1a**:**2** proceeds at a slower rate when using an excess of either the Au(I) or Pt(0) fragments (Figure 8). When an excess of 0.5 equiv. of the platinum precursor **2** is added, the appearance of heterobimetallic dihydride **3a** is decelerated (Figure 8, green line), while formation of [Pt(P^tBu_3)$_2$(H)$_2$] (**7**) becomes noticeable. At variance, the latter species is absent when using a 1:1 mixture of **1a** and **2** under the same conditions. Interestingly, after *ca.* 6 hours at room temperature the excess of Pt(0) precursor **2** is fully converted to compound **7**, after which time the kinetic profile parallels the one that results from an equimolar ratio of Au(I)/Pt(0). Likewise, the kinetic profile derived from using an excess (0.5 equiv) of Au(I) evinces a detrimental effect on the H_2 activation rate (orange line). These findings further support the notion of a genuine FLP mechanism which requires the initial cleavage of the Au←Pt bond in **4a**. This would also explain why gold precursors **1b** and **1c**, for which no metallic Lewis adducts with [Pt(P^tBu_3)$_2$] are observed under identical conditions (i. e. not involving an energetic penalty for M−M bond cleavage) do activate H_2 considerably faster.

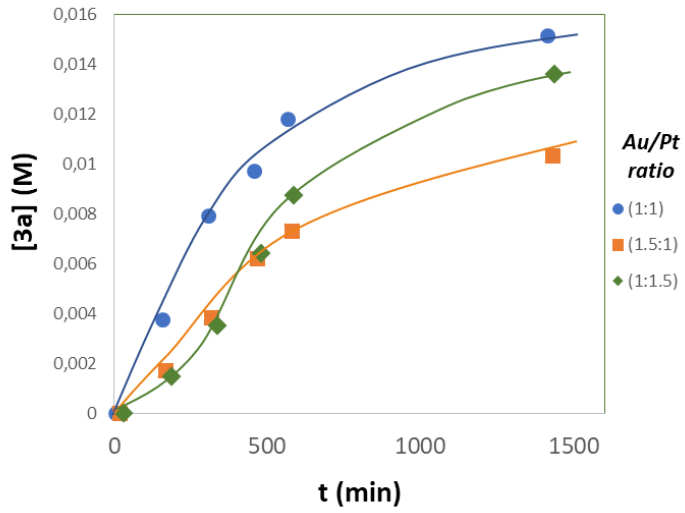

Figure 8. Reaction profile of hydrogen activation (1 bar, 25 °C) by **1a**:**2** to yield **3a** at variable Au/Pt ratios monitored by ^{1}H and $^{31}P\{^{1}H\}$ NMR (lines drawn to guide the eye).

As part of our kinetic studies, we found of interest to investigate the kinetic isotopic effect derived from using deuterium instead of hydrogen. For the sake of reproducibility, we performed these experiments with crystalline samples of compound **4a** and the reactions were performed in triplicate. The kinetic profiles were monitored by ^{1}H and $^{31}P\{^{1}H\}$ NMR using hexamethylbenzene, triphenylphosphine oxide or PPh_3 as internal standards and after exposure to H_2 or D_2 (2 bar) at 25 °C (see Figure 32 in the Experimental Section). To our surprise, we found a strongly inverse KIE of 0.46 ± 0.04. Puzzled by this result we performed low-temperature NMR kinetics (-20 °C) for the activation of H_2 with the **1b**:**2** couple and found an analogous strong inverse KIE that accounts for 0.50 ± 0.02, suggesting that both systems may share a common mechanism. Inverse KIEs are rather

uncommon in the context of FLPs[32] and bimetallic systems,[33] though a very recent report from Mankad and Ess revealed an akin inverse KIE of 0.6 for the heterobimetallic *trans*-hydro(deutero)genation of alkynes using a polar ruthenium-silver complex containing a Ru−Ag bond.[34] For that system, formation of a terminal ruthenium hydride with low-energy binding modes that contributes to an inverse equilibrium isotopic effect (EIE) is proposed to be responsible of the measured inverse KIE. In contrast to the Ru/Ag system where an inverse EIE preequilibirum is responsible for an overall inverse KIE, here we propose that our system has an inverse KIE effect in the rate-limiting transition state.[35]

We have considered the three scenarios for H−H cleavage shown in Scheme 8 for the less hindered system **1a**:**2**, for which the formation of a Lewis adduct, **4a**, was confirmed experimentally. As discussed above, calculations are consistent with this observation and indicate that **4a** is 5.2 kcal·mol^{-1} (ΔG^{o}) more stable than the FLP in benzene (2.5 kcal·mol^{-1} more stable than the separated metal fragments; Scheme 4). Interestingly, the anion (NTf_2^-) plays a key role in the reactivity of the pair as it assists the cleavage of both the Au−Pt bond of **4a** ($\Delta G^{\ddagger}$ = 14.4 kcal·mol^{-1}) and the H−H bond by the FLP, as we shall see later. Regardless, metal-metal cooperativity was also confirmed to be instrumental in H_2 activation. Firstly, while H_2 oxidative addition to **2** yields the *cis*-Pt(II) dihydride through an accessible energy barrier ($\Delta G^{\ddagger}$ = 24.4 kcal·mol^{-1}), the step is endergonic and *cis*/*trans*

[32] S. Tussing, L. Greb, S. Tamke, B. Schirmer, C. Muhle-Goll, B. Luy, J. Paradies. *Chem. Eur. J.* **2015**, *21*, 8056–8059.
[33] A. J. Esswein, A. S. Veige, P. M. B. Piccoli, A. J. Schultz, D. G. Nocera. *Organometallics* **2008**, *27*, 1073–1083.
[34] Y. Zhang, M. K. Karunananda, H.-C. Yu, K. J. Clark, W. Williams, N. P. Mankad, D. H. Ess. *ACS Catal.* **2019**, *9*, 2657−2663.
[35] Computational studies at the ωB97xD/6-31g(d,p)+SDD level carried out by Drs. Joaquín López Serrano and Juan José Moreno.

isomerization to form **7** is not feasible ($\Delta G^{\ddagger}$ = 46.6 kcal·mol^{-1}). This agrees with the absence of reactivity between H_2 and **2** alone. Similarly, orthogonal reactivity, route 'c' in Scheme 8, presents a barrier of 30 kcal·mol^{-1} towards the heterobimetallic dihydride **3a**, which is too high to be consistent with our experimental results.

Regarding route 'a', addition of H_2 across the Au−Pt bond of adduct **4a**[36] yields an intermediate, **B** (see Figure 9), in which the expected pair of monometallic dihydrides (PR_2Ar')AuH (**A**), and **6** are connected by a dihydride bond. Considering recent studies highlighting the key role of triflimidate and triflate counteranions in related bond activation processes,[37] NTf_2^- was explicitly considered for this calculations, which provided an overall barrier for H−H cleavage of 21.3 kcal·mol^{-1} (Figure 9). This transition state features Au−H (1.85 Å) and Au−Pt (4.28 Å) distances, in addition to an elongated H−H (0.92 Å) distance and a short Au···NTf_2^- (2.58 Å) contact (Figure 10). We propose here an FLP-type H−H cleavage which is concomitant with dissociation of the Au−NTf_2^- bond of the Lewis acidic fragment. In addition, the intermediate preceding this TS is an encounter complex, **Int$_{H-H,FLP}$**, in which the H_2 molecule approaches both the metal centers of **1a** and **2** in an end on fashion (Au−H−H and Pt−H−H angles 136º and 176º, Figure 10). Side on coordination of H_2 to the acidic fragment of an FLP, with the basic fragment populating the high-lying σ*(H−H) orbital, has been associated to high-energy "late" transition states

[36] The calculations yield a geometry for **6b** with a different conformation of the terphenyl phosphine that is 9.9 kcal·mol^{-1} above than the most stable conformation used as the origin of energies. See M. Marín, J. J. Moreno, C. Navarro-Gilabert, E. Álvarez, C. Maya, R. Peloso, M. C. Nicasio, E. Carmona. *Chem. Eur. J.* **2019**, *25*, 260–272.

[37] A recent study on H_2 activation by a N/Sn Lewis pair supports a related role for the couteranion (OTf^-) to the acidic $^{i}Pr_3Sn^+$ fragment: S. Das, S. Mondal, S. K. Pati. *Chem. Eur. J.* **2018**, *24*, 2575–2579.

for H_2 splitting by phosphine-borane pairs, whereas low-energy "early" transition states feature "linearized" $L_A{-}H{-}H{-}L_B$ motifs. Inefficient orbital overlap in the latter is compensated by polarization of the H−H bond in a strong electrostatic field generated by the acid and the base.[22a] In our case, H···H distances suggest that **TS'$_{\mathbf{H-H,FLP}}$** is a "geometrically late" transition state. This discussion relates to the two somehow antagonistic views on H_2 activation by FLPs, one advocating that an orbital-based interaction, mainly populating of the σ*(H−H) by the base, leads to destabilization of the H−H bond in an electron transfer process, and the other attributing the main role to polarization of the H_2 molecule within the electric field of the Lewis pair, as discussed in Section I.1.1 of Chapter 1.[21b,22f,38] NBO analysis of the encounter complex, **Int$_{\mathbf{H-H,FLP}}$**, and **TS'$_{\mathbf{H-H,FLP}}$** discloses a synergistic transfer of electron density from one *d* orbital on the Pt to the *σ**(H−H) orbital and a second donor-acceptor interaction of similar energy between the *σ*(H−H) orbital and an empty orbital (of *s* character) on the Au center. This relay of electron density occurs as the H−H bond becomes polarized at the TS, as reflected by atomic charges of -0.17 and +0.07 e- for the Au···H and H···Pt hydrogens respectively, compared to values close to zero in the encounter complex (-0.04 e^- for both H). This two aspects seem to indicate that both mechanisms contribute to a certain extent to the reaction.

[38] J. J. Cabrera-Trujillo, I. Fernández. *Inorg. Chem.* **2019**, *58*, 7828−7836.

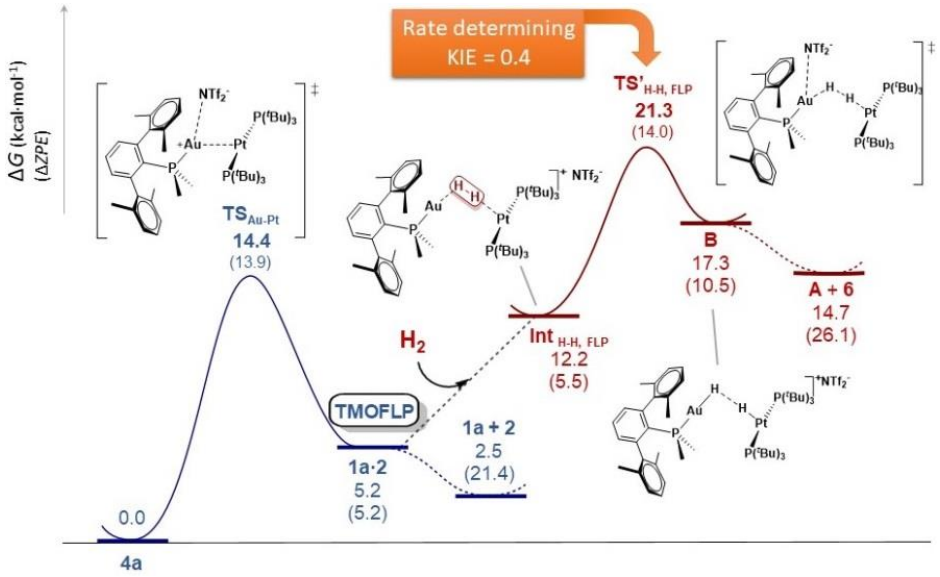

Figure 9. Calculated Free Energy Profile for FLP-like, NTf_2^--assisted H−H cleavage by **4a**. Zero-Point Energies are given in parentheses.

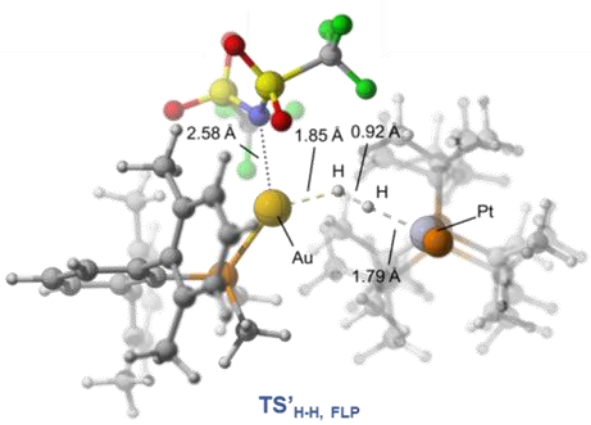

Figure 10. Transition state (**TS'$_{H-H, FLP}$**) for heterolytic H−H cleavage.

Once established a reasonable mechanism for H_2 cleavage, we wondered whether our model could explain the inverse primary KIE measured experimentally. We thus began by analyzing the overall energy profile for NTf_2 assisted H−H cleavage. Starting from the reactants, **4a** + H_2, Au−Pt bond cleavage to form a thermally induced FLP, **1a·2**, is represented in blue trace in Figure 9. The H−H cleavage by the FLP is represented in red. Supposing that insertion of H_2 into the FLP to give the encounter complex $\mathbf{Int_{H-H,FLP}}$ is easy, $\mathbf{TS'_{H-H,FLP}}$ would be rate-determining. We confirmed that the latter rearrangement of metallic monohydrides towards **4a** was easy by reacting the cationic Pt hydride **6** with digold hydride **5a** (prepared *in situ* by adding $SiEt_3H$ to **1a** at -30 °C). This reaction is fast at 25 °C to yield an equimolar mixture of **3a** and **1a**, while it offers no evidence for the formation of the Lewis adduct or H_2 release.

Following the above considerations, our computational collaborators calculated the KIE for the reaction from the zero-point Energy differences ($\Delta\Delta ZPE$) between the reactants, **4a** + H_2/D_2, and $\mathbf{TS'_{H-H,FLP}}$ to find an inverse primary KIE $k_H/k_D = 0.40$, in good agreement with the experiments. An (inverse) isotope effect implies the forming/breaking of E−H(D) (E = H(D) or metal atom) bonds in the rate-determining step. In our case, $\mathbf{TS'_{H-H,FLP}}$ involves partial breaking of the H−H (D−D) bond and formation of two Au−H(D) and Pt−H(D) bonds. Since primary KIEs arise mainly from a balance between the changes in vibrational frequencies or bond strengths (*force constant*) between the isotopomers in the reactants and the products, our result implies stronger bonds (larger *force constants*) at the TS than in H−H/D−D. However, a normal KIE could be initially anticipated since the force constant for H−H stretching is higher than those for M−H stretching. Nevertheless, it must be recognized that all isotopically sensitive modes

(∑ν(H/D)), including bending modes, contribute to the ZPE at the TS, i.e. it is the sum of all vibrational modes involving the forming Au−H and Pt−H and the breaking H−H bonds at the TS, not only stretching modes, that determine the inverse KIE in our case (Figure 11).[34,39]

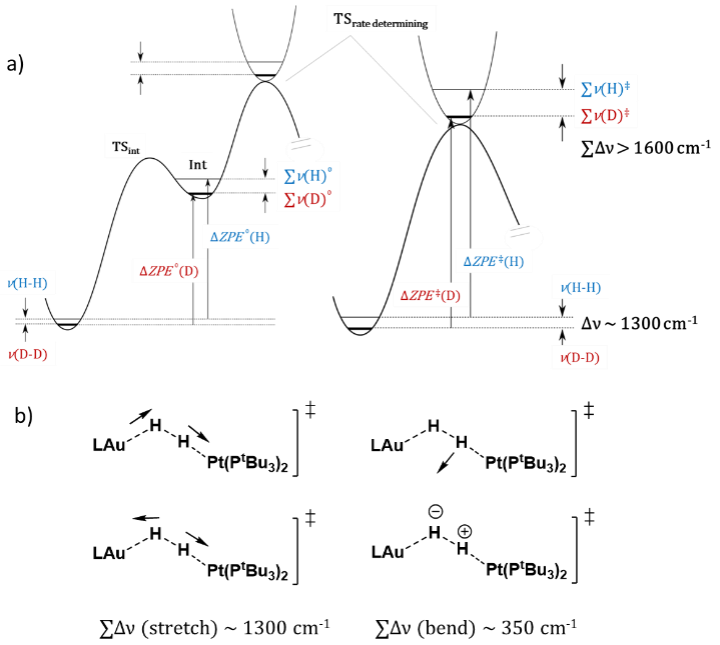

Figure 11. a) Graphical illustration of the origin of the traditional inverse KIE arising from the combination of an inverse equilibrium isotopic effect (EIE) and a normal KIE (left) *versus* direct one-step inverse KIE as occurs in the reported Au:Pt system (right), and b) difference in selected E−H/D vibrational frequencies (Δν) and vector displacements at TS'$_{HH,FLP}$.

The occurrence of inverse KIEs was anticipated long ago,[40] and these have been shown to occur in reactions in which a preequilibrium is followed

[39] a) T.-Y. Cheng, R. M. Bullock. *J. Am. Chem. Soc.* **1999**, *121*, 3150−3155. b) H. C. Lo, A. Haskel, M. Kapon, E. Keinan. *J. Am. Chem. Soc.* **2002**, *124*, 3226−3228.
[40] J. Bigeleisen. *J. Pure. Appl. Chem.* **1964**, *8*, 217−223.

by an irreversible rate-determining step (Figure 11, left) and, although less common, there are also examples of reactions involving a single rate-determining step (Figure 11, right).[41] In the first case, the inverse KIE arises from the combination of normal KIEs and an inverse equilibrium isotope effect (EIE) resulting from the higher energy intermediate in the preequilibrium having higher *force constants* than the reactants [thus $\Delta ZPE^{o}(H) > \Delta ZPE^{o}(D)$].[42] In the second case, inverse KIEs can take place when it is the TS for the single rate-determining step which has higher force constants than the ground state [$\Delta ZPE^{\ddagger}(H) > \Delta ZPE^{\ddagger}(D)$]), being also associated with product-like transition states.39 As already stated, we do not see evidence for a pre-equilibrium and the barrier for the evolution of the monometallic hydrides to the product must be lower than the calculated reverse barrier from **B** to the encounter complex. Therefore, the observed inverse KIE should be related to $\Delta G^{\ddagger}$ ($\Delta ZPE^{\ddagger}$) for the FLP-type H−H cleavage and its origin should be attributed to the collective isotopically sensitive vibrational modes ($\sum\nu$(H/D)) at the TS which is rate-determining.

[41] M. Gómez-Gallego, M. A. Sierra. *Chem. Rev.* **2011**, *111*, 4857–4963.
[42] For some selected examples see: a) R. A. Periana, R. G. Bergman. *J. Am. Chem. Soc*. **1986**, *108*, 7332−7346 and reference 14 therein. b) D. G. Churchill, K. E. Janak, J. S. Wittenberg, G. Parkin. *J. Am. Chem. Soc.* **2003**, *125*, 1403−1420. c) O. T. Northcutt, D. D. Wick, A. J. Vetter, W. D. Jones. *J. Am. Chem. Soc*. **2001**, *123*, 7257−7270.

II.2.3. TMOFLPs Reactivity with Alkynes

Prior results from our group demonstrated that the Au/Pt pair **1b**:**2** reacts with acetylene to produce a mixture of a bridging σ,π-acetylide (**8b**) and a rather unusual heterobimetallic vinylene (-CH=CH-) (**9b**) in a 4:1 ratio (Scheme 3). To investigate regioselectivity effects during alkyne activation we decided to examine the three Au/Pt bimetallic pairs **1:2** towards acetylene activation. In the case of **1b:2**, when a dichloromethane or benzene solution of the latter pair is exposed to acetylene (0.5 bar, 25 °C) a rapid color change from bright yellow to intense orange takes place. As aforesaid, compounds **8b** and **9b** are produced in a 4:1 ratio (Scheme 9). These metallic species are highly reminiscent of the organic products derived from the reactivity of traditional phosphine/borane FLPs with alkynes, where the prevalence of one or the other isomer typically depends on the basicity of the phosphine (see Chapter 1, Scheme 8).[43]

In this Thesis we have examined the analogous reactivity using gold precursors [(PMe_2Ar^{Xyl2})Au(NTf_2)] **1a** and [($PCyp_2Ar^{Xyl2}$)Au(NTf_2)] **1c** in our search for regioselectivity effects while keeping unaltered the basicity of the metallic base (**2**). Moreover, the acidity of the gold precursors **1a-c** barely differs from one another,[14] thus any anticipated outcomes mostly build on steric grounds. In fact, we found a drastic change in product distribution from the less hindered system (**1a**, PMe_2Ar^{Xyl2}) to the more congested one (**1c**, $PCyp_2Ar^{Xyl2}$), as determined by NMR spectroscopy. While the former yields around 95% of the bridging Au/Pt acetylide **8a** and only a residual amount of the vinylene (**9a**, <5%), the more hindered pair

[43] See for example: a) M. A. Dureen, D. W. Stephan. *J. Am. Chem. Soc.* **2009**, *131*, 8396–8397. b) S. J. Geier, M. A. Dureen, E. Y. Ouyang, D. W. Stephan. *Chem. Eur. J.* **2010**, *16*, 988–993.

comprising the $[(PCyp_2Ar^{Xyl2})Au]^+$ fragment (**1c**) fully reversed the selectivity towards the exclusive formation of the corresponding vinylene **9c** (Scheme 9). Attempts to isolate **8c** by the reaction of independently prepared compounds $[(PCyp_2Ar^{Xyl2})Au(C{\equiv}CH)]$ (**10c**) and $[Pt(P^tBu_3)_2H][NTf_2]$[26] (**6**) proved unsuccessful and resulted in intractable mixtures.

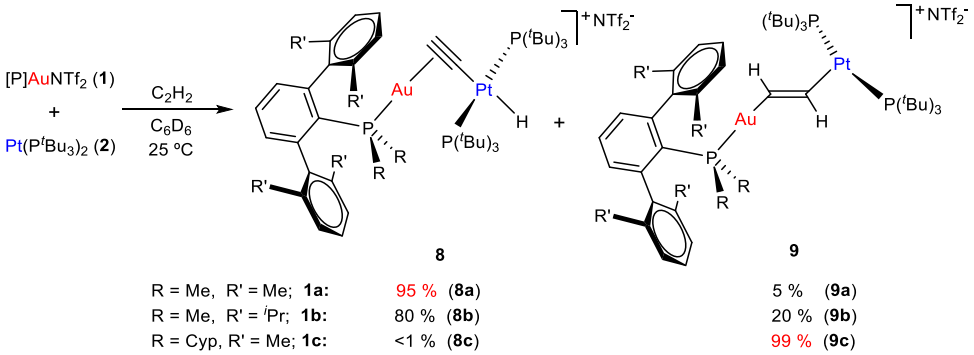

Scheme 9. Regioselectivity in the activation of acetylene by TMOFLPs **1**:**2**.

As aforesaid, this dramatic shift in regioselectivity seems to be dominated by steric effects, which contrasts with prior strategies to modulate alkyne activation by FLPs that mostly rely on phosphine basicity. More importantly, it evinces the potential of FLP systems that incorporate transition metal Lewis acids to easily tune the selectivity during bond activation processes and, as such, in subsequent catalytic applications that incorporate those activation events. As pointed out earlier, this could be seen as a key advantage compared to traditional FLP designs that usually involve fluorinated boranes, since accessing these moieties already entails substantial synthetic challenges and limitations, not to mention their limited stability towards moisture and air.[44] In stark contrast, the preparation of

[44] Z. Lu, H. Y. He, H. Wang. *Top. Curr. Chem.* **2012**, *334*, 59–80.

terphenyl phosphines PR_2Ar' is straightforward and highly versatile,[45] while the resulting gold precursors **1** are readily obtained in high yields and exhibit stability towards water or under moderate oxidizing conditions.[15]

The nature of the new heterobimetallic compounds **8a** and **9c** was ascertained by comparison of their ^{1}H and $^{31}P\{^{1}H\}$ NMR signals with those derived from their analogous species based on PMe_2Ar^{Dipp2}, that is, **3b** and **4b**, respectively.[6] The heterobimetallic nature of compounds **9** is evinced by the ^{195}Pt satellites that flank the $^{31}P\{^{1}H\}$ resonances associated to terphenyl phosphines, which appear at 2.1 (**9b**, $^{4}J_{PPt}$ = 282 Hz) and 51.7 (**9c**, $^{4}J_{PPt}$ = 277 Hz) ppm (Figure 12). The bridging vinylene (-CH=CH-) moiety displays a distinctive pair of ^{1}H NMR signals in the region between 4.0 and 4.5 ppm that reveal scalar coupling to the ^{195}Pt center in the range 120–200 Hz (Figure 13). By analogy, we attribute a $^{31}P\{^{1}H\}$ NMR resonance at 3.67 ppm to the minor species (*ca.* 5%) in the PMe_2Ar^{Xyl2} system (**9a**), with an identical ^{1}H NMR pattern comprised of signals at 4.54 and 4.37 ppm, though their corresponding ^{195}Pt satellites could not be observed due to the low concentration of isomer **9a**. Corresponding ^{13}C NMR resonances for compounds **9b** and **9c** emerge at *ca.* 155 ($^{1}J_{CH} \approx 175$ Hz) and 115 ($^{1}J_{CH} \approx 190$ Hz) ppm, supporting the proposed formulation and the sp^2 hybridization of the carbon atoms.

[45] L. Ortega-Moreno, M. Fernández-Espada, J. J. Moreno, C. Navarro, J. Campos, S. Conejero, J. López-Serrano, C. Maya, R. Peloso, E. Carmona. *Polyhedron*, **2016**, *116*, 170–181.

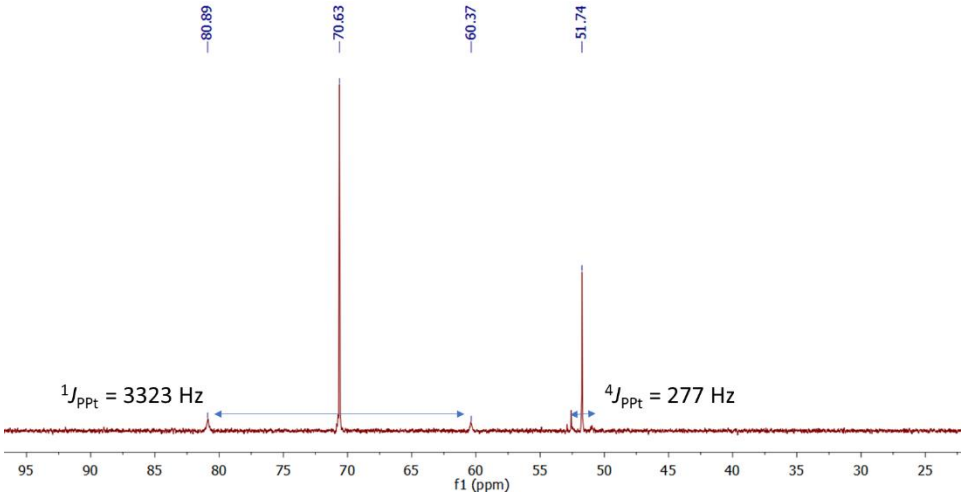

Figure 12. $^{31}P\{^1H\}$ NMR (160 MHz, C_6D_6, 25 °C) of compound **9c**.

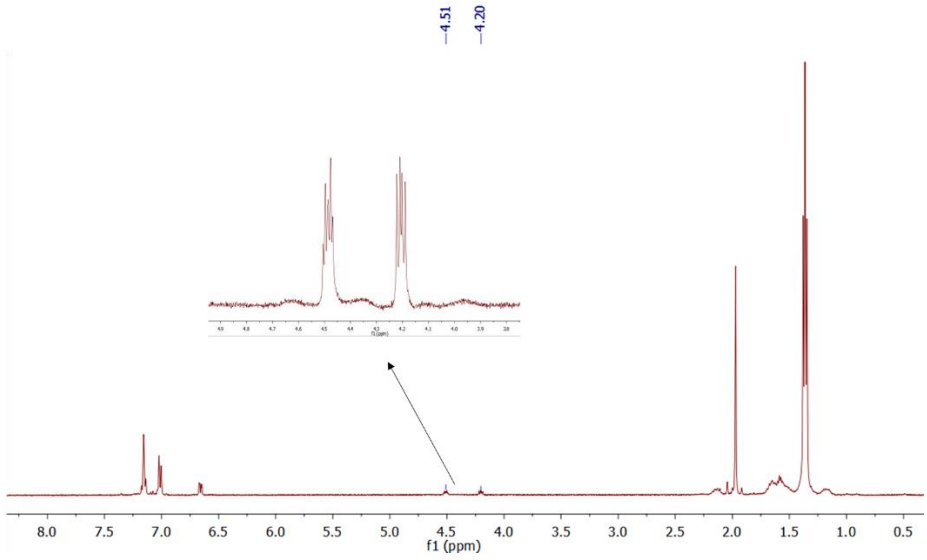

Figure 13. ^1H NMR (400 MHz, C_6D_6, 25 °C) of compound **9c**.

The molecular structure of compounds **8a** and **9c** was further corroborated by X-ray diffraction studies (Figure 14). The presence of the σ,π-acetylide or vinylene linkers distorts the platinum center towards a

T-shaped conformation characterized by P−Pt−P angles of around 165° that shifted from the ideal 180° due to the steric pressure exerted by the bulky gold fragment. The Pt1−C1 (2.016(6) Å) and Au1−C1 (2.311(5) Å) bond distances in **8a** appear slightly shortened compared to **8b** (d_{Pt-C1} = 2.044(7) Å; d_{Au-C1} = 2.360(7) Å). The average C=C bond distances of the vinylene linkers in the two crystallographically independent molecules of **9c** accounts for 1.278(13) Å, comparable to **9b** (1.287(11) Å) and another related species.[46]

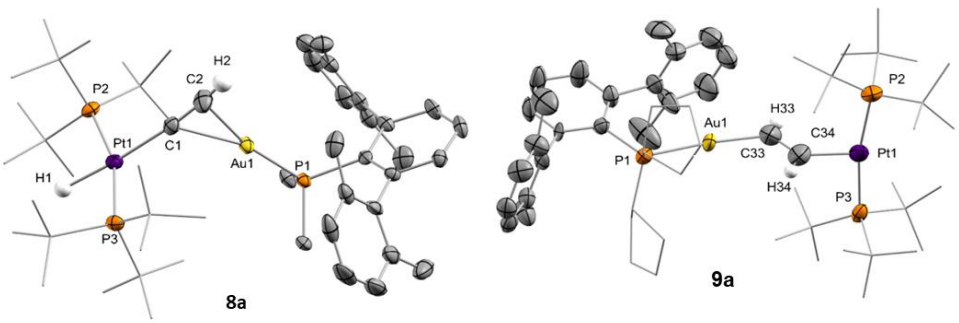

Figure 14. ORTEP diagrams of compounds **8a** and **9c**; for the sake of clarity most hydrogen atoms and triflimide anions are excluded and some substituents have been represented in wireframe format, while thermal ellipsoids are set at 50% probability.

We have already discussed in the previous section that the three investigated terphenyl phosphines permit to control the equilibrium between complete frustration and bimetallic adduct formation. Thus, while a dative Pt→Au bond is immediately formed between [(PMe_2Ar^{Xyl2})Au(NTf_2)] (**1a**) and [Pt(P^tBu_3)$_2$] (**2**), the formation of an identical adduct based on

[46] D. Steinborn, A. M. A. Aisa, F. W. Heinemann, S. Lehmann. *J. Organomet. Chem.* **1997**, *527*, 239–245.

($PCyp_2Ar^{Xyl2}$) is endergonic and could not be experimentally detected. An intermediate situation is reached for the medium-sized phosphine (PMe_2Ar^{Dipp2}), where the prevalence of the monometallic fragments or the bimetallic adduct depends upon experimental conditions. In this context, we have observed that TMOFLPs (**1**:**2**) based on gold precursors [(PMe_2Ar^{Dipp2})Au(NTf_2)] (**1b**) and [($PCyp_2Ar^{Xyl2}$)Au(NTf_2)] (**1c**) are considerably more active towards alkyne activation than the one built on [(PMe_2Ar^{Xyl2})Au(NTf_2)] (**1a**). While full conversion towards compounds **8** and **9** was recorded by the time of placing the sample in the NMR probe (<5 min) in the case of using **1b**:**2** or **1c**:**2**, the analogous transformation essayed with **1a** required up to 24 hours to reach completion under otherwise identical conditions (C_2H_2, 0.5 bar, 25 °C, toluene or C_6D_6). This fact speaks in favor of a genuine FLP mechanism that imposes an energetic demand to overcome the Pt→Au bond cleavage prior to acetylene activation, a requirement that only applies to the less hindered gold precursor **1a**.

In addition, it is key to highlight that the cooperative reactivity depicted in Scheme 9 contrasts with that of the individual Au(I) or Pt(0) fragments (Scheme 10). For instance, [Pt(P^tBu_3)$_2$] (**2**) readily catalyzes acetylene polymerization, evinced by the rapid formation of a purple-black solid accompanied by the disappearance of a ^{1}H NMR resonance at 1.34 ppm due to C_2H_2, while signals due to **2** remained unchanged. At variance, no indication of polyacetylene formation is apparent when gold is also present in solution. In the case of the individual gold compounds **1** there is no sign of chemical transformation in the short term (*ca.* 30 min), while at longer reaction times the gold triflimide precursors evolve to bridging

σ,π-acetylide compounds **11** (Scheme 10A),[47] albeit only in moderate yields and accompanied by other unidentified gold-containing species.

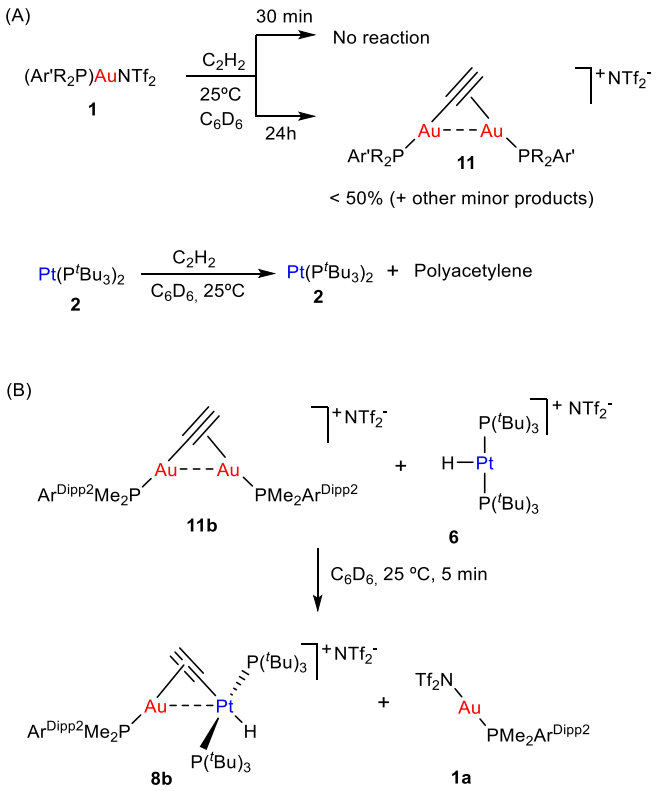

Scheme 10. (A) Reactivity of individual gold (**1**) and platinum (**2**) compounds towards acetylene; (B) Reaction of σ,π-acetylide **11b** and T-shaped platinum hydride **6**.

Having the previous experimental findings on hand, we were interested in further understanding the cooperative action of TMOFLPs **1:2** to gain fundamental knowledge of significance for future catalytic applications. As such, we initially wondered about the possible role of

[47] T. J. Brown, R. A. Widenhoefer. *Organometallics* **2011**, *30*, 6003–6009.

acetylide-bridged digold compounds like **11** as precursors towards complexes **8** and **9**. In fact, the reaction between **11b** and $[Pt(P^tBu_3)_2H][NTf_2]$ (**6**) immediately yielded the corresponding heterobimetallic σ,π-acetylide compound **8b**, where the unsaturated linker is now σ-bonded to the platinum center instead of the gold nucleus (Scheme 10).

Nevertheless, the complete absence of the vinylene isomer **9b** during the latter reaction would require an additional competing route to provide access to this unusual bimetallic motif, which actually is the exclusive isolated isomer for the bulkier $PCyp_2Ar^{Xyl2}$-based system (Scheme 9). Moreover, formation of compounds **11** requires several hours to proceed to appreciable conversions, while the activation of acetylene by **1**:**2** pairs is immediate (<5 min), except for the gold precursor **1b** bearing PMe_2Ar^{Xyl2}, which as noted earlier takes around 24 hours to convert into **8a** in the presence of $[Pt(P^tBu_3)_2]$ (**2**).

To further investigate the mechanism and the reasons for the drastically different regioselectivity observed computational studies (ωB97XD/6-31G(d,p) + SDD) were once more carried by Dr. Joaquín López-Serrano and Dr. Juan José Moreno. Focusing on the system based on PMe_2Ar^{Dipp2}, we began searching for initial acetylene activation steps by approaching the acetylene molecule to the individual Au(I) (**1b**) and Pt(0) (**2**) fragments, assuming that Au−Pt dissociation is a prerequisite for alkyne activation, as deduced from the reduced reactivity of the pair **1a**:**2** compared to **1b**:**2** and **1c**:**2**, and the reactivity already discussed with dihydrogen. Interestingly, formation of **8** and **9** seems to share a common intermediate, namely a Au(I) acetylene adduct of formula $[(PR_2Ar')Au(C_2H_2)]^+$ (**12**). The formation of this type of π-complexes has

been previously proposed in the context of alkyne[48,43a] and alkene[49] activation by P/B pairs, but no experimental proofs of their existence have been reported. In an attempt to spectroscopically identify such an intermediate, we recorded the formation of a new gold-containing species by low temperature NMR (-80 °C) as the major species (*ca.* 80%) upon exposing a CD_2Cl_2 solution of **1b** to acetylene atmosphere. This species exhibits a distinctive ^{1}H NMR signal at 3.43 ppm that correlates with a ^{31}P NMR resonance at -0.3 ppm (compared to δ_P = -9.9 ppm for **1b**) and presents dynamic exchange with free acetylene (δ_H = 2.11 ppm) as seen by EXSY NMR experiments, while other ^{1}H NMR resonances are comparable to those of **1b**. This finding constitutes an additional benefit of TMFLPs for mechanistic investigations in frustrated systems, since they provide additional modes of stabilizing otherwise fleeting intermediates.

Starting from acetylene adduct **12b**, calculations indicate that the attack of the platinum compound **2** over **12b** leads to either of the two bimetallic isomers **8b** and **9b** depending on the trajectory followed by **2** while approaching **9b** (Figure 15). Thus, if **2** approaches the acetylene adduct along the Au-C_2H_2 direction the corresponding vinylene **9b** forms ($\Delta G^{\ddagger}$ = 22.2 kcal·mol^{-1}), in a process somehow reminiscent of the gold-mediated nucleophilic attack over activated alkynes (e. g. gold-catalyzed hydroamination).[50]

[48] C. F. Jiang, O. Blacque, H. Berke. *Organometallics* **2010**, *29*, 125−133.
[49] Y. Guo, S. Li. *Eur. J. Inorg. Chem.* **2008**, 2501–2505.
[50] a) W. Debrouwer, T. S. A. Heugebaert, B. I. Roman, C. V. Stevens. *Adv. Synth. Catal*. **2015**, *357*, 2975–3006. b) A. Couce-Rios, A. Lledós, I. Fernández, G. Ujaque. *ACS Catal.* **2019**, *9*, 848–858.

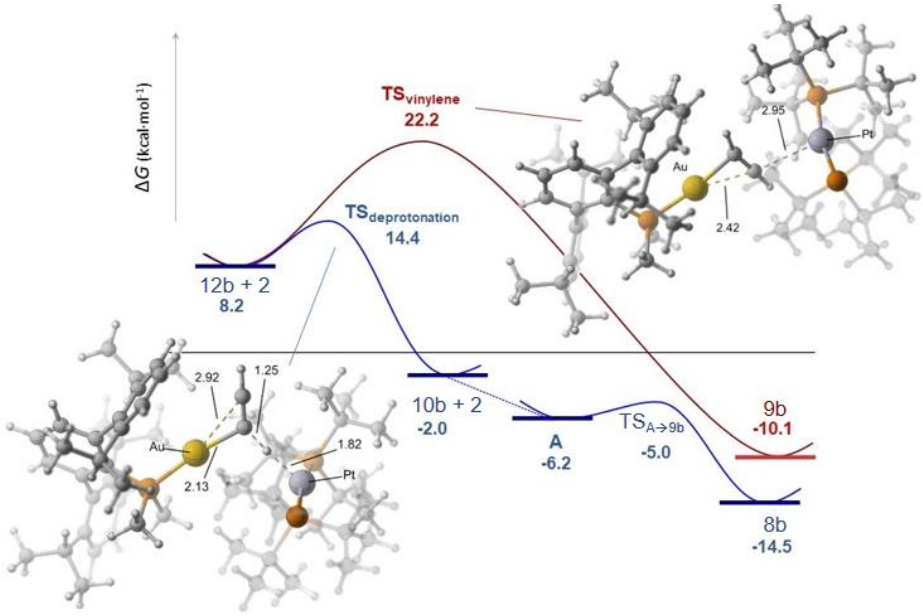

Figure 15. Energy profiles for the formation of the acetylide and vinylene complexes **8b** and **9b** from the common intermediate **12b** and platinum(0) compound **2**.

In contrast, the alignment of the basic **2** in an orthogonal disposition with respect to the Au−C_2H_2 bond results in deprotonation of the activated acetylene (14.4 kcal·mol^{-1} for the pair **1b**:**2**) to yield the corresponding Au(I) terminal acetylide [(PMe_2Ar^{Dipp2})Au(C≡CH)] (**10b**) and [Pt(P^tBu_3)$_2$H][NTf_2] (**6**). These two fragments readily rearrange to intermediates [(PR_2Ar')Au(μ-η^1:η^2-C≡CH)Pt(H)(P^tBu_3)$_2$]$^+$ (**A**) that subsequently evolve to compounds **8** by rapid σ,π-isomerization of the bridging μ-C≡CR unit. In experimental agreement, reaction of independently synthesized [(PMe_2Ar^{Dipp2})Au(C≡CH)] (**10b**) and [Pt(P^tBu_3)$_2$H][NTf_2] (**6**) rapidly yields complex **8b**. As mentioned above, this does not apply to compound **10c**, whose reaction with **6** resulted in a

complex mixture of products that include decomposition into black gold. Nevertheless, the corresponding [(PCyp$_2$Ar^{Xyl2})Au(μ-η^2:η^1-C≡CH)Pt(H)(P^{t}Bu$_3$)$_2$]$^+$ (**8c**) has not been detected during the bimetallic activation of acetylene.

Information on the activation of the simplest alkyne (C_2H_2) by FLPs is rather scarce.[48] For the sake of completeness and to better compare our results with prior studies on main group FLPs, we decided to test other more commonly employed triply bonded hydrocarbons. Regarding internal alkynes, all our attempts to access bimetallic vinylenes were unsuccessful. Reaction of **1**:**2** pairs with diphenylacetylene, 2-butyne and 1,4-Diphenylbutadiyne did not result in the formation of any new species even under more forcing experimental conditions. At variance, addition of phenylacetylene to equimolar mixtures of **1** and **2** provided phosphine-dependent divergent outcomes derived from C(sp)−H bond cleavage (Scheme 11). Paralleling acetylene activation with the more congested pairs based on **1b** and **1c**, reaction of these systems with PhC≡CH was also immediate. In contrast, while acetylene activation took up to 24 hours for the non-frustrated **1a**:**2** pair, the reaction was complete after around 15 min in the case of phenylacetylene.

The appearance of a distinctive low-frequency ^{1}H NMR resonance at around -10 ppm flanked by ^{197}Pt satellites ($^1J_{HPt}$ = 608 Hz, **1a**:**2**; $^1J_{HPt}$ = 533 Hz, **1b**:**2** and **1c**:**2**) prompted us to believe that the corresponding heterobimetallic σ,π-acetylide complex was formed in all cases. However, a more careful analysis revealed unexpected differences in product distribution for the less bulky terphenyl phosphine (PMe$_2$Ar^{Xyl2}) compared to the more hindered systems (Scheme 11). Extracting the reaction crudes

with pentane permitted isolation of the same platinum containing compound **13** for the pairs **1b**:**2** and **1c**:**2**, while the less hindered gold fragment **1a** did not led to any metallic species soluble in non-polar hydrocarbon solvents. An infrared band at 2090 cm^{-1} was recorded for a Pt-hydride ligand in **13**, while characteristic ^{13}C NMR resonances at 118.8 and 117.6 ppm accounted for a σ-bonded acetylide ligand.

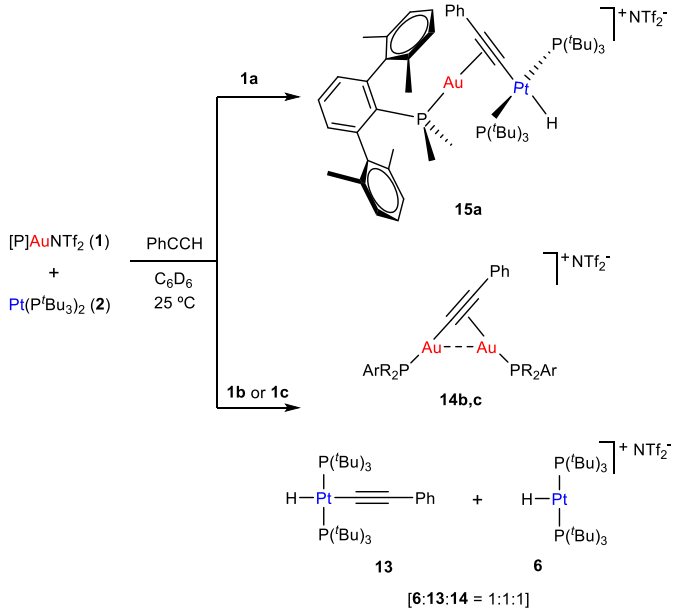

Scheme 11. Product distribution from the activation of phenylacetylene by TMOFLP pairs **1**:**2**.

Based on these spectroscopic features and its high solubility we proposed a molecular formulation for **13** as [Pt(P^tBu_3)$_2$(H)(C≡CPh)], that is, the formal oxidative addition of phenylacetylene over Pt(0) compound **2**. This assumption was further corroborated by X-ray diffraction analysis (Figure 16). Nevertheless, it is important to remark that compound **2** does not react with phenylacetylene even after longer reaction times (48 h) or at

elevated temperatures (80 ºC), which suggest a cooperative action between platinum and gold to account for alkyne C−H activation.

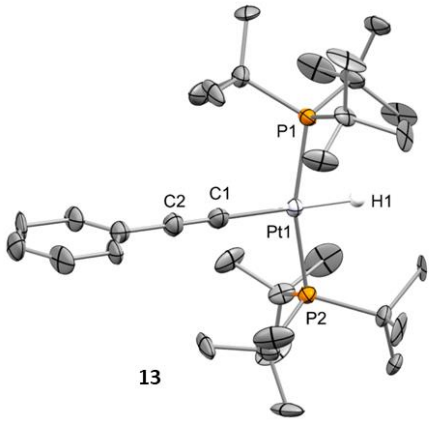

Figure 16. ORTEP diagram of compound **13**; for the sake of clarity most hydrogen atoms are excluded. Thermal ellipsoids are set at 50% probability.

The only detectable gold-containing species in these reactions were assigned to the corresponding bridging σ,π-acetylide digold complexes (**14**). Those where characterized by $^{31}P\{^{1}H\}$ NMR signals at 0.4 (**14b**) and 53.9 (**14c**), shifted at higher frequencies with respect to their precursors **1** (*c.f.* -11.9, **1b**; 48.8 ppm, **1c**), in agreement to other related examples.[51] Also similar to those, the presence of a single ^{31}P resonance for each compound suggests rapid exchange of the σ,π-coordination in solution. The process is frozen though in the solid-state. An ORTEP representation of the molecular

[51] See for example: a) A. Gimeno, A. B. Cuenca, S. Suárez-Pantiga, C. R. De Arellano, M. Medio-Simýn, G. Asensio. *Chem. Eur. J.* **2014**, *20*, 683–688. b) M. M. Hansmann, F. Rominger, M. P. Boone, D. W. Stephan, A. S. K. Hashmi. *Organometallics* **2014**, *33*, 4461–4470. c) A. Grirrane, H. García, A. Corma, E. Álvarez. *Chem. Eur. J.* **2013**, *19*, 12239–12244. d) C. Obradors, A. M. Echavarren,. *Chem. Eur. J.* **2013**, *19*, 3547–3551. e) A. Grirrane, H. García, A. Corma, E. Álvarez. *ACS Catal.* **2011**, *1*, 1647–1653. f) A. Gómez-Suárez, S. Dupuy, A. M. Z. Slawin, S. P. Nolan. *Angew. Chem. Int. Ed.* **2013**, *52*, 938–942.

structure of **1b** is shown in Figure 17. The σ,π-coordination of the acetylide is reflected by a non-symmetric arrangement characterized by bond distances of 2.021(10) and 2.209(9) Å for the Au2−C1 and Au1−C1 bond distances, respectively. The Au1 center is also connected to C2 by a slightly longer bond distance of 2.310(9) Å. The presence of an aurophilic interaction can be inferred from a Au1−Au2 distance of 3.366(1) Å, which is faintly elongated compared to its related acetylide analogue ([Au_2{μ-C≡CH}], $d_{Au1\text{-}Au2}$ = 3.31 Å), likely as a result of the higher steric pressure exerted by phenylacetylide. Digold complexes **14b** and **14c** were accompanied by equimolar amounts of $[Pt(P^tBu_3)_2(H)]^+$ (**6**) that could not be washed out with pentane, as evinced by a broad low-frequency ^{1}H NMR resonance at 1.16 ppm ($^1J_{PPt}$ = 6.5Hz).

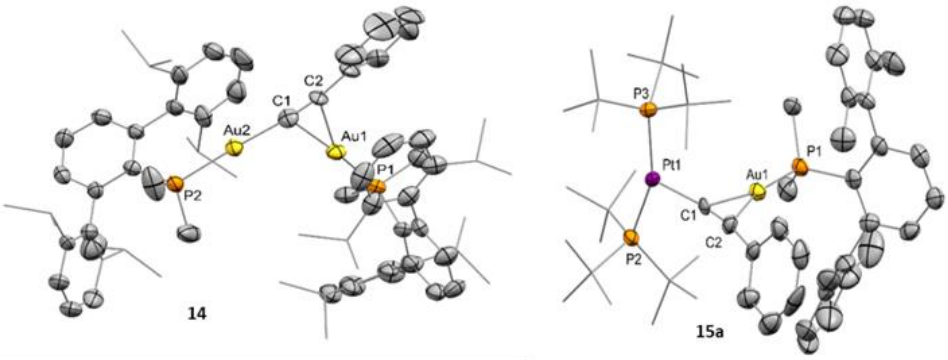

Figure 17. ORTEP diagrams of compounds **14b** and **15a**; for the sake of clarity hydrogen atoms, solvent molecules and triflimide anions are excluded and some substituents have been represented in wireframe format, while thermal ellipsoids are set at 50% probability. The hydride ligand bound to platinum in **15a** could not be located in the Fourier electron density map.

As noted earlier, the reaction of the less hindered **1a**:**2** pair with phenylacetylene yielded a divergent result. C(sp)−H activation became

evident by the presence of a distinctive hydridic ^{1}H NMR (Figure 18) resonance at -10.4 ppm ($^{2}J_{HP}$ = 14 Hz, $^{1}J_{HPt}$ = 608 Hz). However, a single platinum complex was formed in this case, which resonates at 82.2 ppm ($^{1}J_{PPt}$ = 2810 Hz) in its ^{31}P{^{1}H} NMR spectrum and could not be washed out using non-polar hydrocarbon solvents. The corresponding C≡C stretching frequency rendered a band shifted to lower wavenumbers ($\nu_{C\equiv C}$ = 1982 cm^{-1}; *c.f.* 2048, **14b**; 2029, **14c**; 2090 cm^{-1}, **13**), while sp-hybridized carbon atoms resonate at lower frequencies (91.1 and 85.9 ppm) compared to compounds **14b**, **14c** and **13** (116-125 ppm). These observations expose the divergent product distribution derived from using phosphines with different steric profiles. Since the recorded parameters equate with heterobimetallic σ,π-acetylide compounds **8**, we assumed an analogous structure for this complex (**15a**), a premise that we could substantiate by X-ray diffraction analysis (Figure 17). The bulkier nature of the phenylacetylide moiety with respect to the unsubstituted acetylide in **3a** is likely the cause of a more intense distortion of the T-shape platinum fragment, where a P−Pt−P angle of 156.71(8)º is recorded (*c.f.* 162.76(5)º for **3a**). The close proximity between the acetylide phenyl fragment and the *ortho* substituents of one of the flanking aryl rings of the terphenyl moiety may be responsible for the dissimilar product distribution found between PMe_2Ar^{Xyl2} *vs* PMe_2Ar^{Dipp2}/$PCyp_2Ar^{Xyl2}$.

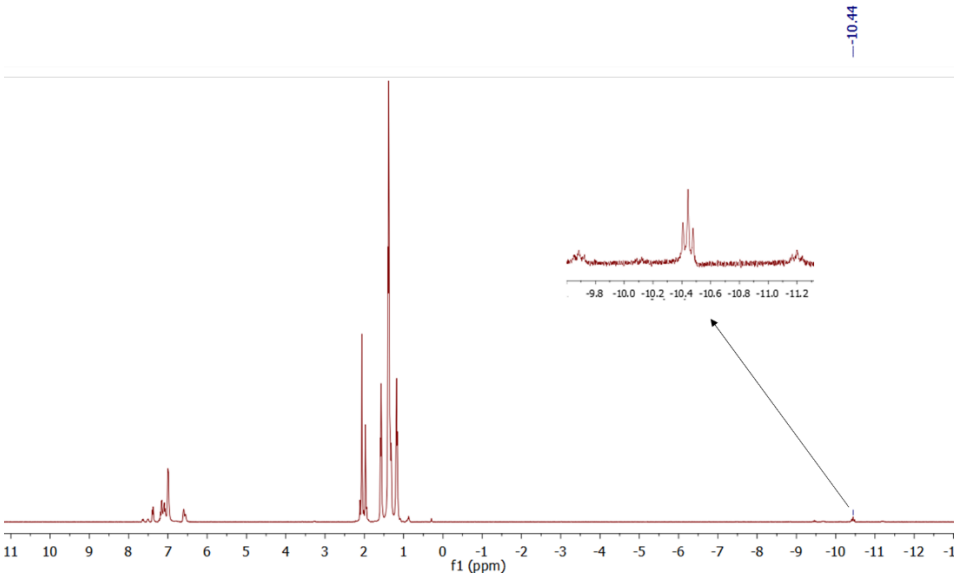

Figure 18. ^{1}H NMR (400 MHz, C_6D_6, 25 ºC) of compound **15a**.

Based on our experimental and computational studies on acetylene activation, initial formation of a gold-alkyne adduct like **12** seems most plausible. The slightly higher acidity of phenylacetylene, as well as its higher size, may account for the prevalence of the deprotonation pathway in detriment of the 1,2-addition route towards vinylene structures, which were not detected. In turn, the dissimilar reaction products depicted in Scheme 11 might be understood according to steric grounds. Thus, selective formation of compounds **14** for the bulkier PMe_2Ar^{Dipp2}/$PCyp_2Ar^{Xyl2}$-based systems could be the result of a higher steric clash between the *tert*-butyl substituents on the platinum fragment and the terphenyl moiety of the gold-bound phosphine. In contrast, the reduced steric pressure introduced by PMe_2Ar^{Xyl2} may permit easier access to the heterobimetallic compound **15a**, analogous to its unsubstituted acetylide version (**8a**).

We thought of interest to carry out several further experiments to shed some light into the operating cooperative mechanism. In the same manner as we observed for acetylene activation, the reactivity of the individual metallic fragments starkly contrasts with that of the bimetallic pairs. Accordingly, platinum compound **2** does not exhibit any reactivity towards phenylacetylene even after heating at 80 ºC for 48 hours (Scheme 12A). In turn, compounds **1** promote C(sp)−H cleavage of the alkyne to form the corresponding digold σ,π-acetylide complexes **14**, but at a considerably slower pace (24 h at 25 ºC: **1a**, 9% of **14a**; **1b**, 70% of **14b**; **1c**, 12% of **14c**; NMR spectroscopic yields).

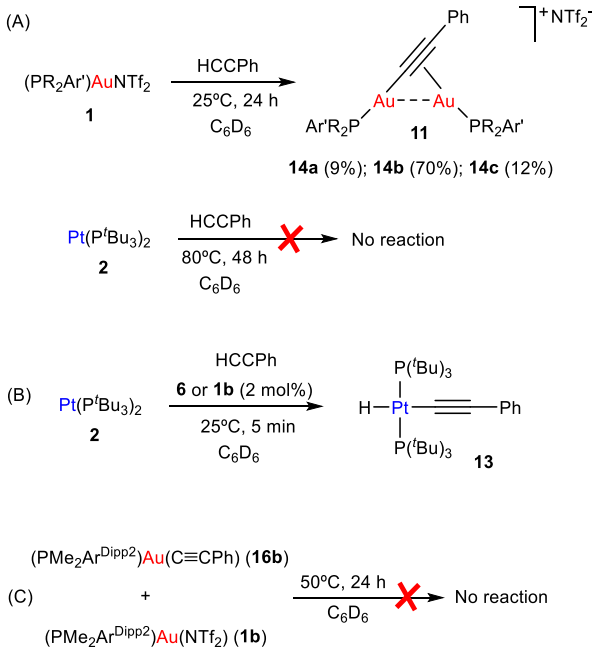

Scheme 12. Selected experiments carried out to provide information about the mechanism of phenylacetylene activation mediated by TMOFLPs **1**:**2**.

To account for the origin of **13**, we performed the reaction of **2** with equivalent amounts of phenylacetylene and catalytic quantities of **1**. In addition, we also tested the same transformation but using **6** as the catalyst, since this presumably forms in situ after protonation of **2** by small amounts of $HNTf_2$ derived from the reaction of **1** and phenylacetylene toward **14**. Catalytic amounts of compound **6** may also derive from the cooperative Au/Pt C(sp)−H activation of phenylacetylene by a deprotonation mechanism. As anticipated, immediate conversion of **2** into **13** was observed at room temperature using either **1** or **6** in catalytic amounts as low as 2 mol% (Scheme 12B). The reaction of the independently prepared **13** with 1a leads to **8a** as the major species by NMR analysis, though other unidentified side products are also formed. The reaction of the independently synthesized neutral σ-acetylide compound [(PMe2ArDipp2)Au-(C≡CPh)] (**16b**; ORTEP diagram Figure 19) with **1b** yielded the expected digold σ,π-acetylide **14b** under mild conditions (Scheme 12C). This result parallels the reactivity previously described for NHC-based gold complexes, where the latter transformation proceeds smoothly,[51f] as also occurs with the parent unsubstituted acetylide (C≡CH) fragment,[17b] terminal acetylides of type **16** may be regarded as key intermediates toward compounds **14** during the activation of PhC≡CH.

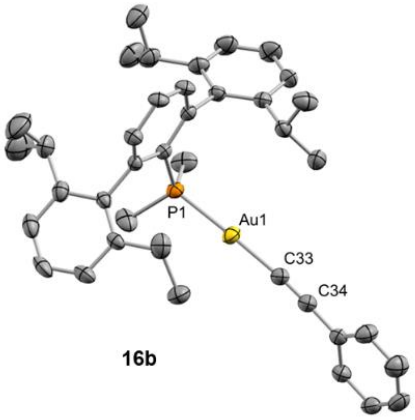

Figure 19. ORTEP diagram of compound **16b**; for the sake of clarity hydrogen atoms are excluded. Thermal ellipsoids are set at 50% probability.

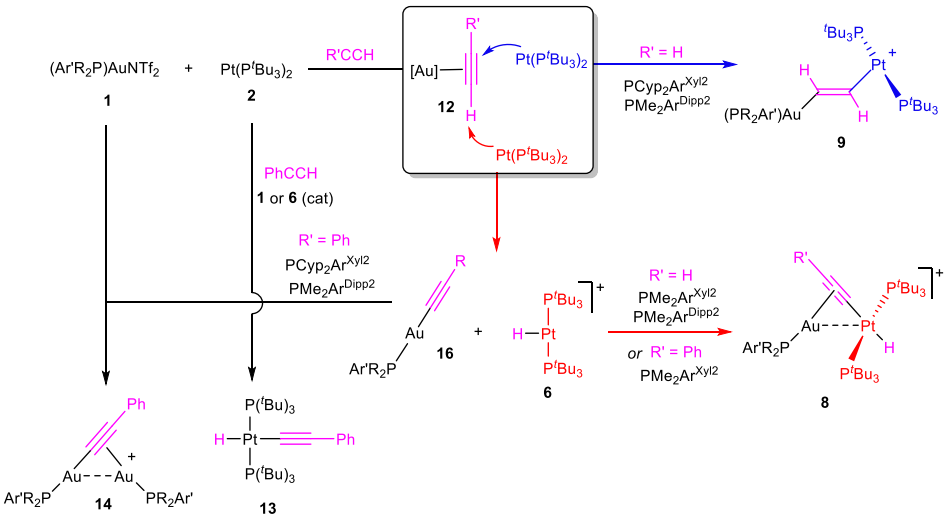

Scheme 13. Overall representation of the proposed pathway to account for product distribution during alkyne activation. Counteraions have been excluded for clarity.

On consideration of all the information discussed above, Scheme 13 contains an overall mechanistic picture to account for the phosphine-dependent product distribution during the activation of alkynes. The common gold acetylene adduct **12** is proposed to be a key intermediate. While both deprotonation and 1,2-addition mechanisms (blue and red in Scheme 13, respectively) are viable for acetylene, only the deprotonation pathway seems to be operative in the case of the more acidic phenyl-substituted alkyne. Once the latter is deprotonated to form an equimolar mixture of **16** and **6**, steric factors appear to dominate the final product distribution. The combination of the more hindered terphenyl phosphines with the bulkier phenylacetylene prevents formation of the corresponding Au/Pt heterobimetallic adducts likely due to a steric clash, while the latter is the only observed complex in the PMe_2Ar^{Xyl2} system. In turn, terminal gold acetylides **16**, although unable to react with $[Pt(P^tBu_3)_2H]^+$ (**6**), rapidly yield the corresponding digold σ,π-acetylides **11** upon combination with still unreacted triflimide complexes **1**. We can also infer from our experimental observations that several of the transformations depicted in Scheme 13 constitute dynamic equilibria that are dependent on reaction conditions.

II.2.4. Reactivity of TMOFLPs with Germanium and Tin Dihalides

The use of molecular donor-acceptor pairs has served as a fruitful tool to stabilize or intercept reactive inorganic species with ambiphilic character.[52] The strategy has been particularly successful in the study of heavier tetrylenes, $:EX_2$ (E = Si, Ge, Sn, Pb), compounds based on a divalent heavier group 14 element, which possess relatively reduced HOMO-LUMO gaps and dual nucleophilic (lone electron pair) and electrophilic (empty p orbital) nature. The cooperative stabilization conferred by a donor and an acceptor that mutually bind an ambiphilic molecule is understood in terms of the electronic push-pull bonding scheme that emerges. Representative examples of otherwise highly unstable tetrylene fragments include $:E(CH_3)_2$[53], $:EH_2$[54] or $:SiCl_2$[55], which have been characterized by this approach, providing fundamental understanding of their bonding and reactivity. Stabilizing heavier tetrylenes by intra- or intermolecular donors

[52] E. Rivard. *Dalton Trans.* **2014**, *43*, 8577−8586.
[53] a) T. J. Marks. *J. Am. Chem. Soc*. **1971**, *93*, 7090−7091. b) T. J. Marks, A. R. Newman. *J. Am. Chem. Soc.* **1973**, *95*, 769−773. c) C. Eisenhut, T. Szilvasi, G. Dübek, N. C. Breit, S. Inoue. *Inorg. Chem*. **2017**, *56*, 10061−10069. d) S. K. Grumbine, D. A. Straus, T. D. Tilley, A. L. Rheingold. *Polyhedron* **1995**, *14*, 127−148.
[54] a) M. Y. Abraham, Y. Wang, Y. Xie, P. Wei, H. F. Schaefer, P. V. R. Schleyer, G. H. Robinson. *J. Am. Chem. Soc.* **2011**, *133*, 8874−8876. b) K. C. Thimer, S. M. I. Al-Rafia, M. J. Ferguson, R. McDonald, E. Rivard. *Chem. Commun*. **2009**, 7119−7121. c) A. K. Swarnakar, S. M. McDonald, K. C. Deutsch, P. Choi, M. J. Ferguson, R. McDonald, E. Rivard. *Inorg. Chem*. **2014**, *53*, 8662−8671. d) S. M. I. Al-Rafia, A. C. Malcolm, S. K. Liew, M. J. Ferguson, E. Rivard. *J. Am. Chem. Soc*. **2011**, *133*, 777−779. e) S. M. I. Al-Rafia, O. Shynkaruk, S. M. McDonald, S. K. Liew, M. J. Ferguson, R. McDonald, R. H. Herber, E. Rivard. *Inorg. Chem*. **2013**, *52*, 5581−5589.
[55] a) R. S. Ghadwal, H. W. Roesky, S. Merkel, D. Stalke. *Chem. Eur. J.* **2010**, *16*, 85−88. b) R. Azhakar, G. Tavcar, H. W. Roesky, J. Hey, D. Stalke. *Eur. J. Inorg. Chem*. **2011**, 475− 477. c) S. M. I. Al-Rafia, A. C. Malcolm, R. McDonald, M. J. Ferguson, E. Rivard. *Chem. Commun*. **2012**, *48*, 1308−1310. d) R. S. Ghadwal, R. Azhakar, K. Pröpper, J. J. Holstein, B. Dittrich, H. W. Roesky. *Inorg. Chem*. **2011**, *50*, 8502−8508.

has also been exploited in their use as more robust ligands in coordination chemistry.[56]

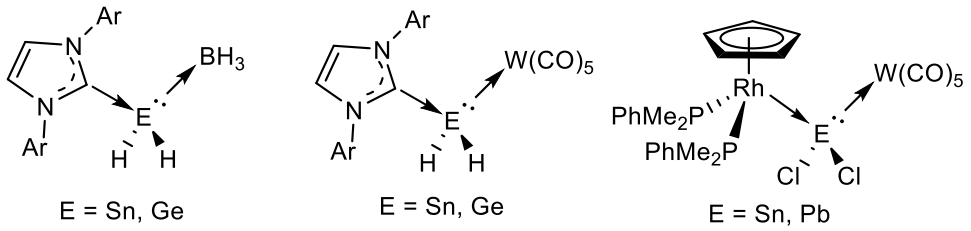

Figure 20. Selected representative examples of tetrylenes stabilized by push-pull interactions reported by the Rivard's group.

From a related perspective, this electronic push-pull stabilization highly resembles the chemistry of frustrated Lewis pairs (FLPs). However, the presence of heavier group 14 elements within the field of FLPs mostly focuses on their use as acidic partners,[57] while reactivity studies of traditional FLP systems towards the tetrel series finds little precedent.[58]

Somehow related metal-only donor-acceptor pairs have been recently employed by Rivard to stabilize low-valent group 14 species.[59] A Rh/W pair that stabilizes $SnCl_2$ and $PbCl_2$ is shown in Figure 20. Encouraged by these results we decided to explore the reactivity of our Au(I)/Pt(0) **1b:2**

[56] a) J. A. Cabeza, P. García-Álvarez, D. Polo. *Eur. J. Inorg. Chem.* **2016**, 10−22. b) M. F. Lappert, R. S. Rowe. *Coord. Chem. Rev*. **1990**, *100*, 267−292. c) W. Petz. *Chem. Rev*. **1986**, *86*, 1019−1047.
[57] a) B. Michelet, C. Bour, V. Gandon. *Chem. Eur. J.* **2014**, *20*, 14488−14492. b) J. A. B. Abdalla, I. M. Riddlestone, R. Tirfoin, S. Aldridge. *Angew. Chem. Int. Ed.* **2015**, *54*, 5098−5102. c) J. Backs, M. Lange, J. Possart, A. Wollschlager, C. Muck-Lichtenfeld, W. Uhl. *Angew. Chem. Int. Ed.* **2017**, *56*, 3094−3097. d) Y. Yu, J. Li, W. Liu, O. Yeb, H. Zhu, *Dalton Trans.* **2016**, *45*, 6259−6268.
[58] a) A. Jana, I. Objartel, H. W. Roesky, D. Stalke. *Inorg. Chem*. **2009**, *48*, 7645−7649. b) A. Jana, G. Tavčar, H. W. Roesky, C. Schulzke. *Dalton Trans.* **2010**, *39*, 6217−6220.
[59] A. K. Swarnakar, M. J. Ferguson, R. McDonald, E. Rivard. *Dalton Trans*. **2016**, *45*, 6071−6078.

FLP towards simple forms of low-valent group 14 compounds, particularly $GeCl_2$ and $SnCl_2$. We focused mostly on the PMe_2Ar^{Dipp2} system based on the results discussed along the previous sections, from which it is inferred that it is this 'medium-size' phosphine the best behaved in terms of FLP-type reactivity. It is also pertinent to note that after push-pull stabilization, germanium and tin dihalides could serve as suitable precursors towards their corresponding dialkyl53 or dihydride54 derivatives, which in turn can be the source of functional nanomaterials.[60] We will firstly present the reactivity of germanium and tin dihalides with the gold and platinum single components of the FLP. The discussion will then be continued by describing their combined reactivity. In addition, the present studies reveal the key role of tin dichloride in promoting phosphine exchange reactions for the platinum component of the metallic FLP.

[60] a) H. Yang, J. Zhao, M. Qiu, P. Sun, D. Han, L. Niu, G. Cui. *Biosens. Bioelectron*. **2019**, *124-125*, 191−198. b) L. Wang, E. Guan, J. Zhang, J. Yang, Y. Zhu, Y. Han, M. Yang, C. Cen, G. Fu, B. C. Gates, F.-S. Xiao. *Nature Comm.* **2018**, *9*, 1362.

II.2.4.1. Reactivity of $GeCl_2$ and $SnCl_2$ Towards Gold Compound 1b

We began our studies by exploring the reactivity of germanium and tin dihalides towards gold compound (PMe_2Ar^{Dipp2})Au(NTf_2), **1b**. In both cases reactions proceed readily to yield compounds **17** and **18** after the respective insertion of $GeCl_2$ or $SnCl_2$ into the Au-N(SO_2CF_3)$_2$ bond of **1b** (Scheme 14) in quantitative spectroscopic yield. These species were isolated as white powders and their purity confirmed by microanalysis. While **17** features a broad ^{31}P NMR resonance in CD_2Cl_2 at 4.8 ppm, shifted to higher frequency by about 16 ppm relative to **1b** (δ = -11.5 ppm), the analogous broad signal due to **18** appears at -9.3 ppm. These resonances become sharp upon cooling the NMR probe to -40 °C suggesting fluxional behaviour for both compounds likely due to the lability of the triflimide anion. Similarly, all the resonances observed in their ^{1}H NMR spectra become sharper when recorded at low temperatures and do not exhibit any relevant features that differ from those of precursor **1b**. Fluxional behaviour seems to be hampered in THF-d_8 solution, where the ^{31}P NMR resonances of the gold germyl and stannyl compounds shift to higher frequencies (**17·THF**, 6.7 ppm; **18·THF**, -3.1 ppm) likely due to the displacement of the weakly coordinating triflimide anion by a solvent molecule (Scheme 14). As introduced above, the bonding scheme in these cationic complexes may be understood in terms of the push-pull interactions provided by the Au/THF pair to the :ECl_2 moiety. However, while **18·THF** remains stable in solution for at least one day, its germanium analogue is acidic enough to readily promote the electrophilic ring-opening polymerization of THF.[61]

[61] a) A. Aouissi, S. S. Al-Deyab, H. Al-Shahri. *Molecules* **2010**, *15*, 1398−1407. b) B. Pan, F. P. Gabbaï. *J. Am. Chem. Soc.* **2014**, *136*, 9564−9567.

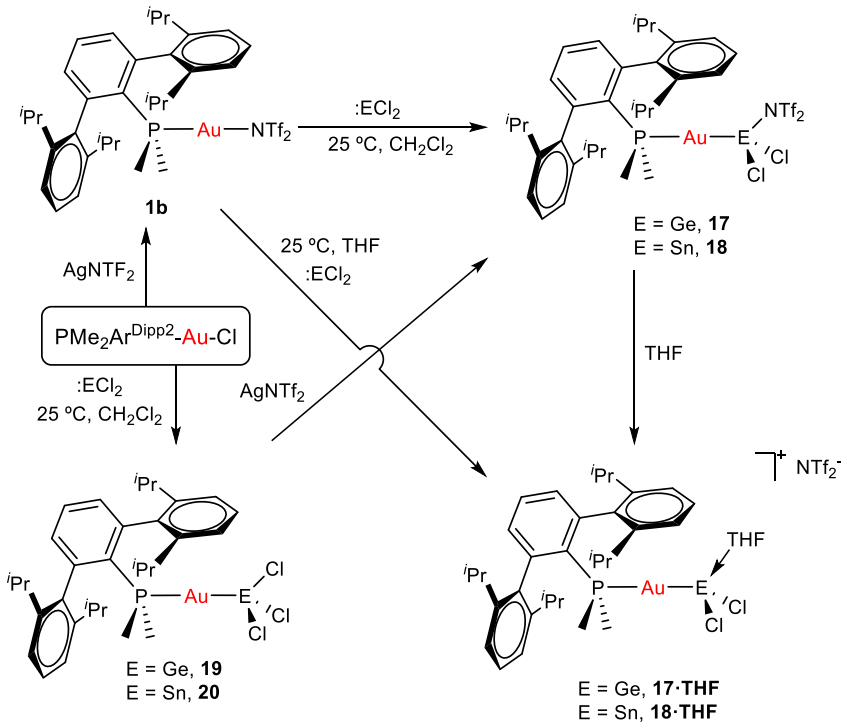

Scheme 14. Reactivity of tetrylene dihalides with gold compounds bearing a terphenyl phosphine.

Despite our efforts, we were unable to grow single crystals of enough quality to authenticate the proposed formulation for compounds **17** and **18**. Nevertheless, the insertion of germylenes and stannylenes into gold-halide and other related bonds is well-documented. In fact, the same reactivity is observed when $GeCl_2$·dioxane or $SnCl_2$ are added to dichloromethane solutions of the gold chloride compound (PMe_2Ar^{Dipp2})AuCl,[15] precursor of **1b** via salt metathesis with $AgNTf_2$ (Scheme 14). The resulting gold-tetryl species are characterized by ^{31}P NMR resonances at 5.0 and -2.2 ppm due to the germyl (**19**) and stannyl (**20**) insertion products respectively, while their ^{1}H NMR spectra match with those of their precursor, as well as with other gold derivatives previously described by our group.[6] Subsequent chloride

abstraction by silver triflimide results in quantitative formation of compounds **17** and **18**, respectively, as expected for the proposed molecular formulations collected in Scheme 14. The insertion of tetrylenes into gold-halide bonds has provided complexes with Au−E (E = Ge, Sn) bonds with a variety of geometries and coordination environments,[62] as well as interesting photophysical properties.[63] Most examples rely on the use of sterically unhindered phosphines that permit the formation of supramolecular aggregates by aurophilic and other non-covalent interactions. The former interactions have indeed been suggested as key for the reported photoluminiscent properties of these species. The solid-state structure of complex **19** is depicted in Figure 21, revealing that no gold aggregates are formed. At variance with prior examples, gold-gold and gold-chloride contacts are replaced by a weak Au···C_{arene} interaction with the *ipso* carbon of a lateral terphenyl ring ($d_{Au\text{-}Cipso}$ = 2.95(4) Å), a common feature for gold complexes of biaryl phosphines.[6,64] This forces the coordination geometry around gold to bend from linearity (P−Au−Ge 171.30(4)°), while other distances and angles lie within normal values. The two flanking aryl rings of the terphenyl fragment are equivalent by NMR, while the $^{13}C\{^1H\}$ NMR resonance of the interacting *ipso*-carbon (138.1 ppm, $^3J_{CP}$ = 6 Hz) lies close to the analogous one in the free phosphine (142.5 ppm, $^3J_{CP}$ = 5 Hz). This data, along with the long Au···C_{Arene} distance, suggests that the secondary interaction is weak. For the sake of comparison, we aimed to examine the

[62] a) A. Bauer, A. Schier, H. Schmidbaur. *J. Chem. Soc. Dalton Trans.* **1995**, 2919−2920. b) A. Bauer, H. Schmidbaur. *J. Am. Chem. Soc.* **1996**, *118*, 5324–5325. c) J. A. Dilts, M. P. Johnson. *Inorg. Chem.* **1966**, *5*, 2079–2081.

[63] a) R. V. Bojan, J. M. López-de-Luzuriaga, M. Monge, M. E. Olmos, R. Echeverría, O. Lehtonen, D. Sundholm. *ChemPlusChem* **2016**, *81*, 176–186. b) R. V. Bojan, J. M. López-de-Luzuriaga, M. Monge, M. E. Olmos, R. Echeverria, O. Lehtonen, D. Sundholm. *ChemPlusChem* **2014**, *79*, 67–76.

[64] P. Pérez-Galán, N. Delpont, E. Herrero-Gómez, F. Maseras, A. M. Echavarren. *Chem. Eur. J.* **2010**, *16*, 5324–5332.

supramolecular structure of a compound analogous to **19** but constructed around the less hindered terphenyl phosphine PMe_2Ar^{Xyl2} (where Ar^{Xyl2} = C_6H_3-2,6-(C_6H_3-2,6-Me_2)$_2$), in which the isopropyl groups of the lateral aryl rings were replaced by methyl groups. The related gold germyl compound was prepared in good yields (*ca.* 90%) by the same strategy followed to access its bulkier counterpart. Its solid-state structure was almost identical to **19** and exhibits a similar secondary Au-arene interaction characterized by a $d_{Au\text{-}Cipso}$ of 3.05(4) Å and a reduced P−Au−Ge angle of 165.77(2)° (Figure 21, $\mathbf{19^{Xyl}}$).

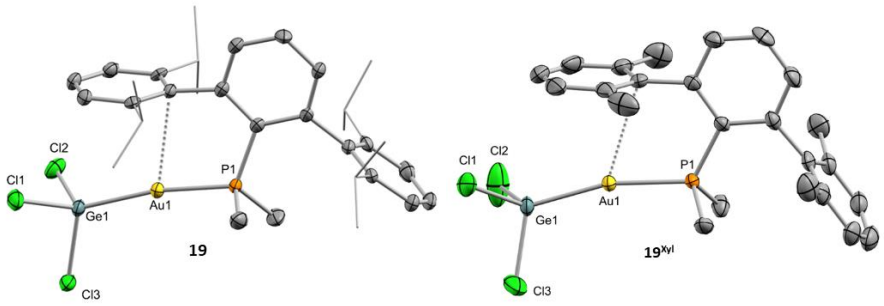

Figure 21. ORTEP diagram of compound **6**; for the sake of clarity hydrogen atoms are excluded and some substituents have been represented in wireframe format, while thermal ellipsoids are set at 50% probability.

Drawing on the same theme, we wondered if the steric properties of terphenyl phosphines would still permit the insertion of bulkier tetrylenes across the gold-chloride/triflimide bond.[65] We chose stannylene $Sn[N(SiMe_3)]_2$ to carry out these experiments since its insertion into Au−Cl

[65] a) U. Anandhi, P. R. Sharp. *Inorg. Chim. Acta* **2006**, *359*, 3521–3526. b) J. A. Cabeza, J. M. Fernández-Colinas, P. García-Álvarez, D. Polo. *Inorg. Chem*. **2012**, *51*, 3896–3903. c) M. Walewska, J. Hlina, W. Gaderbauer, H. Wagner, J. Baumgartner, C. Marschner. *Z. Anorg. Allg. Chem*. **2016**, *642*, 1304–1313.

bonds was recently documented.65[b] Its addition to benzene solutions of **1b** and their precursor indeed resulted in almost quantitative formation of compounds **22** and **21**, respectively (Scheme 15). Trace amounts of another gold complex were detected, as discussed below. The new Au−Sn heterobimetallic compounds are characterized by a higher-frequency shift of their ^{31}P NMR resonances (**21**, 15.4 ppm; **22**, 13.8 ppm) of around 23 ppm with respect to their precursors. The ^{31}P NMR signal of compound **21** exhibits a strong two-bond coupling due to the *trans* tin centre ($^{2}J_{PSn}$ = 3201 Hz) (Figure 22A). A new intense signal in the ^{1}H NMR spectrum is collected at around 0.47 ppm due to the trimethylsilyl groups for both **21** and **22**, while the rest of their ^{1}H NMR spectra is comparable to other related samples described in this section.

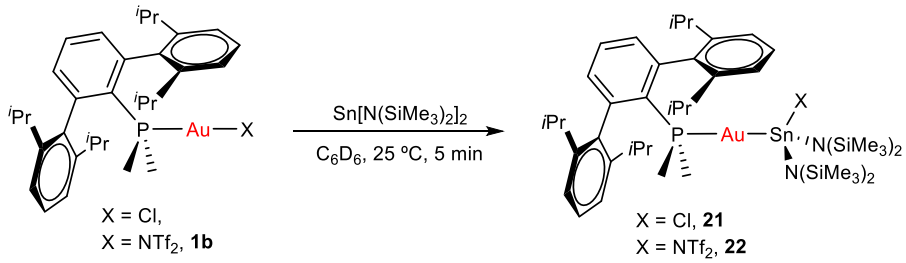

Scheme 15. Reaction of stannylene Sn[N(SiMe$_3$)]$_2$ with gold precursors.

Authenticating the proposed molecular structures proved challenging due to the poor quality of the crystals grown with the selected phosphine system. However, we succeeded in growing crystals with a related bulkier phosphine, namely PCyp$_2$Ar^{Xyl2} (Cyp = C_5H_9). Thus, compound **21^{Cyp}** was isolated in moderate yield as a white crystalline material following the same synthetic procedure described to access **21**. Its

$^{31}P\{^{1}H\}$ NMR resonance displays a $^{2}J_{PSn}$ coupling constant of 2846 Hz, somewhat smaller relative to compounds **21** (Figure 22B).

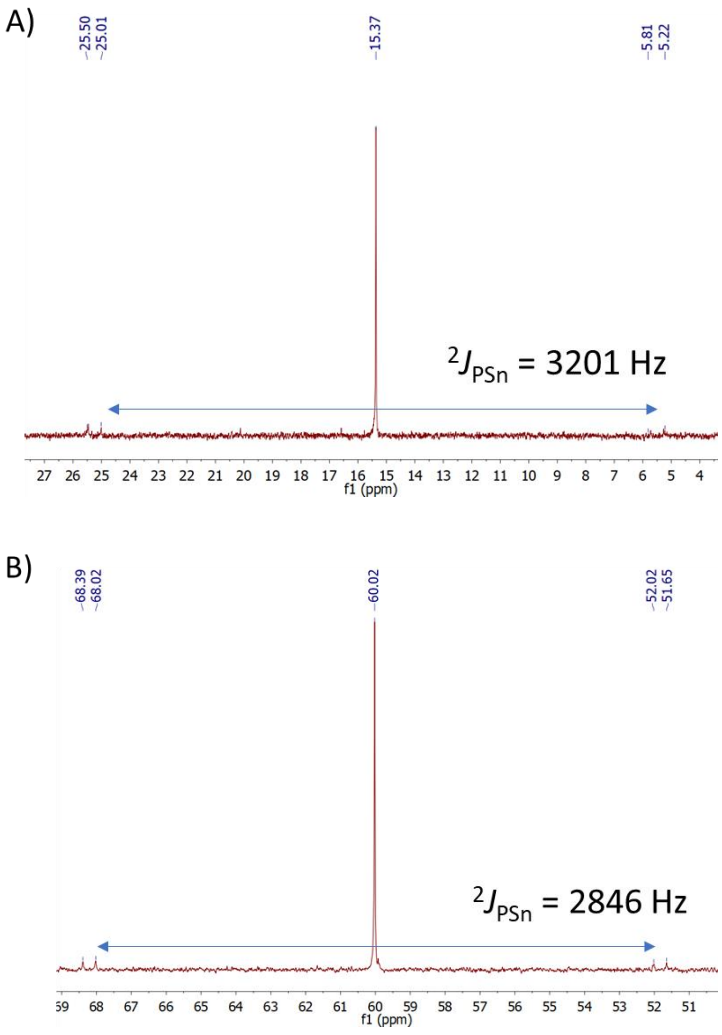

Figure 22. (a) $^{31}P\{^{1}H\}$NMR of complex **21**. (b) $^{31}P\{^{1}H\}$NMR of complex **21^{Cyp}**.

This decreased of the $^{1}J_{PSn}$ coupling constant may result from the steric pressure exerted by the cyclopentyl substituents of the phosphorus

centre onto the bulky bis(trimethylsilyl)amido fragments, which could weaken the metal-metal bond. In fact, its X-ray diffraction structure (Figure 23) reveals a Au−Sn bond distance that accounts for 2.65(1) Å, relatively elongated compared to previous linear gold-tin complexes (*ca.* 2.57 Å).[66]

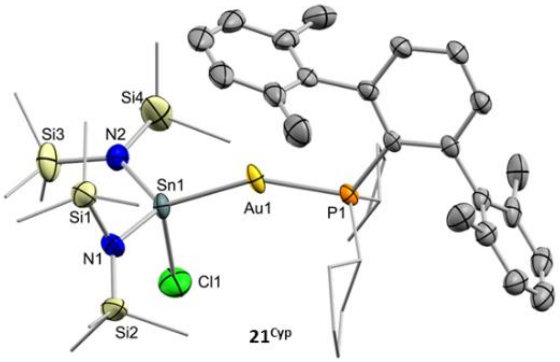

Figure 23. ORTEP diagram of compound **21^{Cyp}**; for the sake of clarity hydrogen atoms are excluded and some substituents have been represented in wireframe format, while thermal ellipsoids are set at 50% probability.

In addition, we could isolate the main side product resulting from the reactions represented in Scheme 12 (<5% by $^{31}P\{^{1}H\}$ NMR spectroscopy), which consists of an amido-bridged cationic digold complex of formula $[Au_2(\mu\text{-}N(SiMe_3)_2)(PMe_2Ar^{Dipp2})_2]$ due to the transfer of a trimethylsilylamido substituent from stannylene to a gold centre. This compound could be independently synthesized by mixing equimolar amounts of gold-triflimide **1b** and $[PMe_2Ar^{Dipp2}]Au[N(SiMe_3)_2]$, prepared

[66] a) J. Hlina, H. Arp, M. Walewska, U. Florke, K. Zangger, C. Marschner, J. Baumgartner. *Organometallics* **2014**, *33*, 7069–7077. b) B. Findeis, M. Contel, L. H. Gade, M. Laguna, M. C. Gimeno, I. J. Scowen, M. McPartlin. *Inorg. Chem.* **1997**, *36*, 2386–2390. c) C. Marschner, J. Baumgartner, H. Arp, K. Rasmussen, N. Siraj, P. Zark, T. Muller. *J. Am. Chem. Soc.* **2013**, *135*, 7949–7959.

by reaction of gold-chloride, (PMe_2Ar^{Dipp2})AuCl, and Li[$N(SiMe_3)_2$]. The molecular formulation of the amido-bridged digold compound based on PMe_2Ar^{Xyl2} phosphine was further confirmed by single-crystal X-ray diffraction studies (Figure 24) and represents an uncommon example of this motif in the context of gold chemistry.[67]

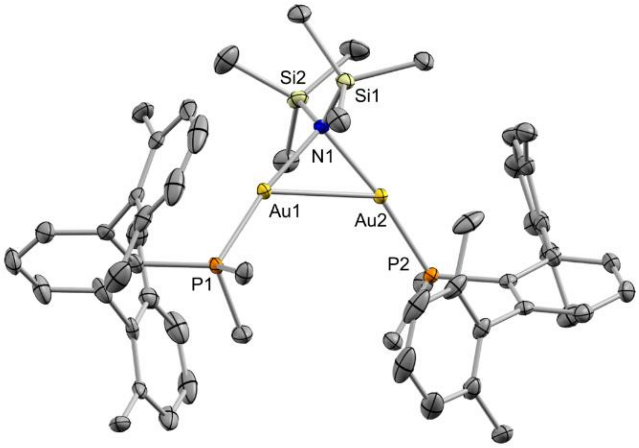

Figure 24. ORTEP diagram of compound [Au_2(μ-$N(SiMe_3)_2$)(PMe_2Ar^{Xyl2})$_2$]; hydrogen atoms and the triflimide counteraion have been excluded for clarity. Thermal ellipsoids are set at 50% probability.

[67] a) S. D. Bunge, O. Just, W. S. Rees. *Angew. Chem. Int. Ed.* **2000**, *39*, 3082–3084. b) K. Angermaier, H. Schmidbaur. *Chem. Ber.* **1995**, *128*, 817. c) A. Shiotani, H. Schmidbaur. *J. Am. Chem. Soc.* **1970**, *92*, 7003–7004. d) S. D. Bunge, J. L. Steele. *Inorg. Chem*. **2009**, *48*, 2701–2706.

II.2.4.2. Reactivity of $GeCl_2$ and $SnCl_2$ Towards Platinum Compound 2

The reaction of tetrel dihalides[68], as well as aluminum trichloride,[19b,69] with linear platinum(0) compounds has been investigated by Braunschweig and co-workers. In those studies the reactions of :$GeCl_2$ and :$SnCl_2$ with [$Pt(PCy_3)_2$] (Cy = cyclohexyl) yielded the corresponding mononuclear dihalogermylene and -stannylene compounds $(PCy_3)_2Pt{=}ECl_2$ (E = Ge, Sn). In stark contrast, reactions of equimolar amounts of :ECl_2 and [$Pt(P^tBu_3)_2$] (**2**) did not result in major alterations of the resonances recorded by ^1H and $^{31}P\{^1H\}$ NMR spectroscopy relative to reactant **2**, although a rapid colour change from colourless to dark red was noticeable in both cases. The dissimilar reactivity of compound **2** and its PCy_3 analogue towards :ECl_2 is reminiscent to their reaction with H_2, which is rapid for [$Pt(PCy_3)_2$][70] but impracticable for **2** unless gold complex **1** is present, in which case the FLP-like H_2 splitting discussed in section II.2.2. We ascribe the lack of reactivity of **2** to the high steric shielding provided by the *tert*-butyl phosphines.

Although the Pt(0) compound **2** remained practically unchanged, we observed a new $^{31}P\{^1H\}$ NMR signal at 94.5 ppm after the addition of one equivalent of :$GeCl_2$·dioxane to its CD_2Cl_2 solution, but it accounted for only around 5% of the overall phosphorus content, preventing the observation of a $^{195}Pt–^{31}P$ coupling constant (Scheme 16A). Based on its chemical shift and in comparison with prior studies by Braunschweig this signal could be tentatively assigned to a Pt germylene compound analogous

[68] a) F. Hupp, M. Ma, F. Kroll, J. O. C. Jimenez-Halla, R. D. Dewhurst, K. Radacki, A. Stasch, C. Jones, H. Braunschweig. *Chem. Eur. J.* **2014**, *20*, 16888–16898. b) H. Braunschweig, M. A. Celik, R. D. Dewhurst, M. Heid, F. Huppa, S. S. Sen. *Chem. Sci*. **2015**, *6*, 425–435.
[69] a) H. Braunschweig, K. Gruss, K. Radacki. *Angew. Chem. Int. Ed*. **2007**, *46*, 7782–7784.
[70] T. Yoshida, S. Otsuka. *J. Am. Chem. Soc*. **1977**, *99*, 2134–2140.

to $(PCy_3)_2Pt{=}GeCl_2$.68[b] However, addition of excess :$GeCl_2$ did not lead to a major increase in the proportion of this species, which remained as the minor product (<10%) under all attempted conditions. We decided to examine whether an equilibrium towards the formation of a Pt germylene could be observed at variable temperature. Low-temperature multinuclear NMR spectroscopic studies revealed dynamic behaviour in solution, although the proportion of the suggested Pt germylene remained practically unaltered. However, an additional broad ^{31}P NMR resonance at 119.4 ppm exhibiting a large $^{1}J_{PPt}$ coupling constant of 4670 Hz became discernible below -20 °C and reached a proportion of around 20% at -60 °C. Although we are unsure of the nature of this new species, it seems to result from the dissociation of a phosphine ligand, as evinced by a $^{31}P\{^{1}H\}$ NMR signal at 59.9 ppm of intensity equal to the newly formed compound and corresponding to P^tBu_3. Based on the analogous reactivity with :$SnCl_2$ (*vide infra*) we tentatively suggest the formation of a dinuclear platinum compound stabilized by bridging germanium halides.

Although treatment of CD_2Cl_2 solutions of **2** with equimolar amounts of :$SnCl_2$ led to an immediate colour change to dark red, we could not observe the formation of Pt stannylene or the existence of an equilibrium with such a species by low-temperature ^{1}H and $^{31}P\{^{1}H\}$ NMR monitoring. Identical results were derived from reactions in tetrahydrofuran where tin dichloride exhibits better solubility. In contrast, the addition of a second equivalent of :$SnCl_2$ in chlorinated solutions drastically changed the reaction outcome. Complete disappearance of Pt(0) compound **2** is immediately recorded upon addition of the second equivalent of tin dichloride at room temperature to yield a complex mixture of species, in which we could unambiguously identify several platinum compounds (Scheme 16B).

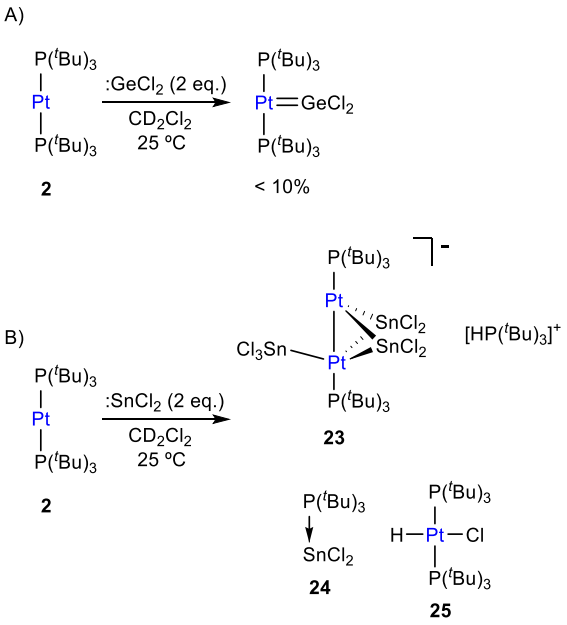

Scheme 16. Reactivity of Pt(0) compound **2** with 2 equivalents :$GeCl_2$ (A) of :$SnCl_2$ (B).

A $^{31}P\{^1H\}$ resonance recorded at 52.8 ppm and exhibiting a $^1J_{PSn}$ coupling-constant of 1855 Hz accounts for the formation of the tin-phosphine adduct **24**, confirmed by the independent reaction between :$SnCl_2$ and P^{t}Bu$_3$. It is worth mentioning that in all experiments described herein variable amounts of [PtClH(P^{t}Bu$_3$)$_2$] (**25**) were formed, likely due to reaction of **2** with hydrochloric acid produced by adventitious traces of water in the presence of :$SnCl_2$. Phosphonium cation [H(P^{t}Bu$_3$)]$^+$ was produced by the same reason and displays a distinctive ^{1}H NMR doublet at 6.02 ppm ($^1J_{HP}$ = 408 Hz). More interestingly, the higher-frequency region of the $^{31}P\{^1H\}$ spectra reveals the formation of a major compound (**23**) that resonates at 128.3 ppm and is accompanied by both ^{119}Sn ($^2J_{PSn}$ = 110 Hz) and ^{195}Pt ($^1J_{PPt}$ = 4874 Hz) satellites (Figure 25).

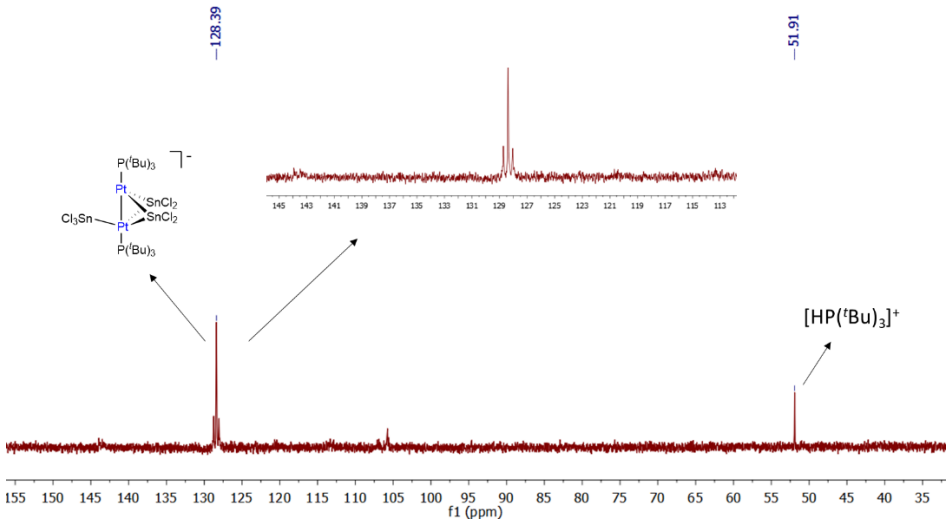

Figure 25. $^{31}P\{^{1}H\}$ NMR spectra of compound **23**.

We managed to grow crystals from the crude dichloromethane reaction mixtures that exhibit an intense dark red colour by slow diffusion of pentane at -30 ºC. X-ray diffraction studies proved the formation of a dinuclear Pt(0) compound **23** in which each metal bears a single tri(*tert*-butyl)phosphine ligand (Figure 26). The capacity of tin chloride to promote phosphine dissociation has been examined in more detail and will be discussed later.

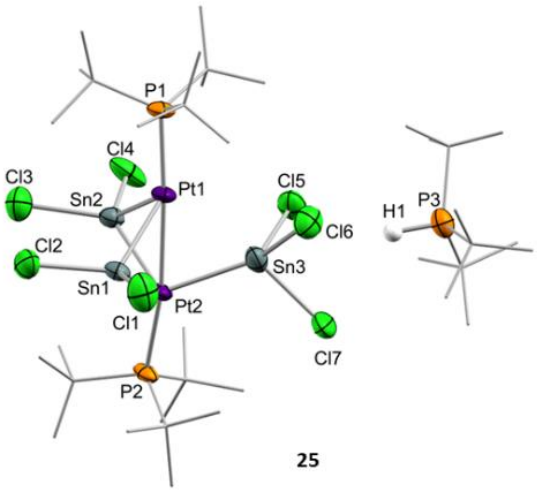

Figure 26. ORTEP diagram of compound **25**; for the sake of clarity most hydrogens have been omitted and *tert*-butyl substituents have been represented in wireframe format. Thermal ellipsoids are set at 50% probability.

The dinuclear platinum fragment in **23** is held together by three tin chloride units, one of which formally appears as an anionic bridging stannyl fragment. A phosphonium cation $[H(P^tBu_3)]^+$ linked to the Pt-cluster by $P{-}H^+\cdot\cdot Cl$ interactions (average $d_{H\text{-}Cl}$ 3.0 Å) compensates the anionic character of the Pt_2Sn_3 cluster . The anionic part of the molecular structure depicted in Figure 26 can be described as a distorted trigonal bypiramid with a missing Pt−Sn edge and characterized by an average Pt−Pt distance of 2.706(1) Å. The average Pt−Sn bond distances accounts for 2.58 Å, except for the $SnCl_3^-$ termini, for which one of the two Pt−Sn contacts is elongated to 2.998(2) Å. The P−Pt−Pt−P escapes from linearity due to the presence of the stannyl-bridged group, which distorts the ideal symmetry. Thus, one of the phosphine ligands tilts to accommodate the $SnCl_3^-$ group resulting in a Pt−Pt−P bond angle of 171.2 Å. A somehow related structure

has been previously described in which the bridging divalent tin nuclei are stabilized by acetylacetonate ligands.[71] As in prior cases, the highly reduced character of the heteropolymetallic cluster is likely responsible for its high instability.[72]

We found of interest to interrogate the bonding scheme in diplatinum **23** by computational methods. Optimization of its molecular geometry at the ωB97XD/6-31G(d,p) level of theory was carried out by Dr. Juan José Moreno, and found perfect agreement with the solid state structure, with Pt-Pt and Pt-Sn bond distances of 2.77 and 2.63−2.69 Å, respectively, except for the $SnCl_3^-$ group, for which one of the two Pt−Sn contacts is elongated to 3.21 Å. Analysis of the computed electron density (QTAIM) performed at the same level of theory disclosed bond critical points (BCPs) and the corresponding bond paths (BPs) connecting each $SnCl_2$ fragment to both Pt atoms, while the $SnCl_3^-$ group binds to a single Pt centre (Pt(2)) (Figure 27). Additionally, one BCP was located at the path between the Pt atoms, supporting the bonding interaction suggested by the short solid state Pt−Pt distance.

[71] G. W. Bushnell, D. T. Eadie, A. Pidcock, A. R. Sam, R. D. Holmes-Smith, S. R. Stobart, E. T. Brennan, T. S. Cameron. *J. Am. Chem. Soc.* **1982**, *104*, 5837–5839.
[72] Z. Béni, R. Scopelliti, R. Roulet. *Inorg. Chem. Commun.* **2005**, *8*, 99–101.

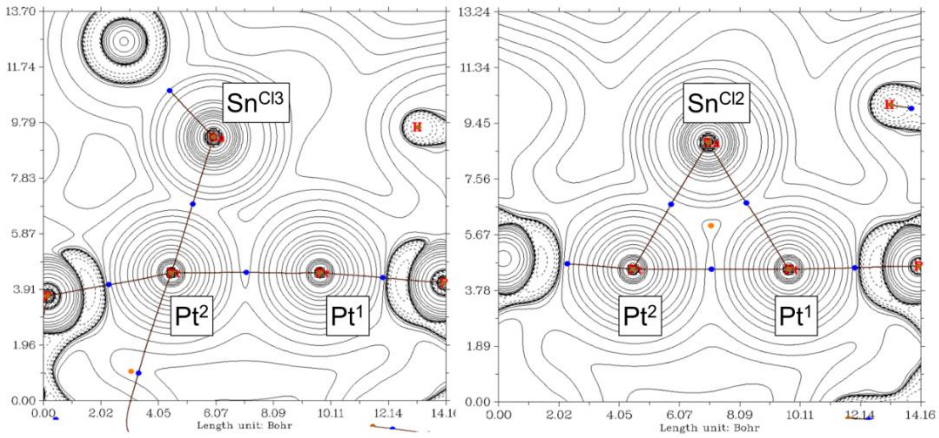

Figure 27. Plot of the laplacian of the electron density, $\nabla^2\rho$, of complex **23** in the Pt(1)−Pt(2)−$SnCl_3$ (left) and the Pt(1)−Pt(2)−$SnCl_2$ (right) planes calculated with the ωB97X-D functional. The solid and dashed lines correspond to positive and negative values of $\nabla^2\rho$, respectively. In plane BCPs and BPs of the electron density are superimposed.

The analysis of the electron density was complemented with an analysis of localized molecular orbitals to rationalize the interactions between the [Pt(P^{t}Bu$_3$)], $SnCl_2$ and $SnCl_3^-$ fragments, following the Pipek-Mezey[73] and NBO criteria. Both localization schemes provide similar information revealing that the three $SnCl_n$ fragments donate electron density to one of the platinum atoms, Pt(2), whereas Pt(1) acts as a donor by delocalizing *d*-electron density onto empty *p* orbitals of the two $SnCl_2$ fragments (Figure 28A). Besides, Pt(1) also behaves as an acceptor, since the Pt−Pt interaction arises from electron delocalization from one *d* orbital on Pt(2) onto Pt(1) as seen in Figure 28B. Overall, the bonding in compound **23** could be rationalize by the schematic representation depicted in Figure

[73] J. Pipek, P. G. Mezey. *J. Chem. Phys.* **1989**, *90*, 4916–4926.

28A, where each metal atom (except for $SnCl_3^-$) exhibits ambiphilic donor-acceptor character.

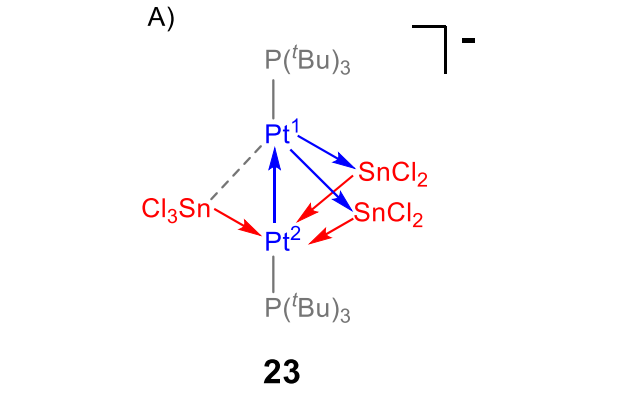

23

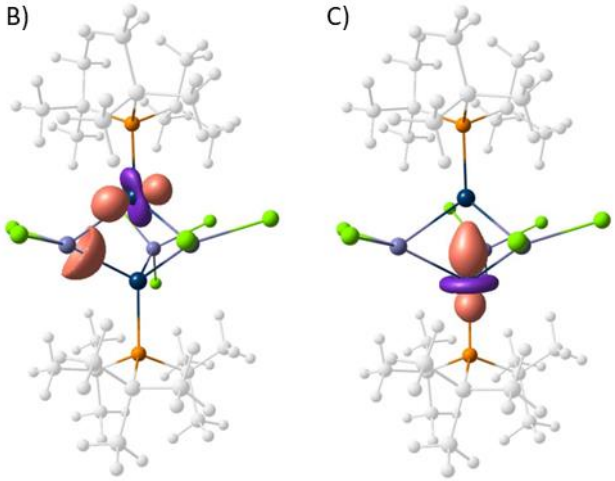

Figure 28. A) Simplified bonding scheme representation of compound **10**, where arrows describe electron donation between metal centres; (B,C) Representative localized molecular orbitals (Pipek-Mezey) involved in the Pt−Sn (B) and the Pt−Pt bonding (C).

II.2.4.3. Reactivity of $GeCl_2$ and $SnCl_2$ Towards the Au/Pt FLP 1b:2

After examining the reactivity of tetrylene dihalides with compounds **1b** and **2** we moved to investigate their chemistry with the two metallic fragments in cooperation. Before describing the details of these experiments it must be noted that the reaction outcomes were independent of the order in which the three components were mixed together. In other words, the reaction of platinum compound **2** with pre-formed germyl or stannyl derivatives **17** and **18**, respectively, led to identical product distributions than those detected after the addition of gold compound **1b** to dichloromethane solutions of **2** and the corresponding tetrylene. As previously discussed, NMR line-broadening upon mixing **1b** and **2** supports the formation of a bimetallic adduct **4b** (see Scheme 4 in section II.2.1.), though the individual components prevail in solution. To our surprise, treatment of dichloromethane solutions of the **1b:2** pair with one equivalent of :$GeCl_2$·dioxane cleanly generated adduct **4b** (Scheme 17). The tetrylene seems to be key in withdrawing the triflimide anion from gold, likely by formation of $NTf_2 \rightarrow GeCl_2$, as observed before upon addition of methanol (see Section II.2.1.). The formulation of the unsupported heterobimetallic compound **4b** was ascertained by NMR spectroscopy and validated by microanalysis.

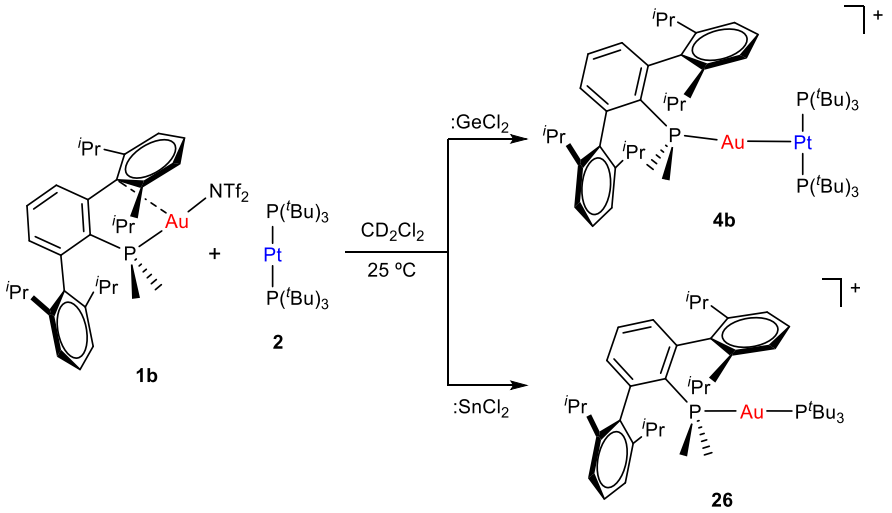

Scheme 17. Combined reactivity of compounds **1b** and **2** towards germanium and tin dihalides. The triflimide counteranion has been excluded for clarity.

As briefly noted earlier, compound **4b** was alternatively synthesized by treatment of gold germyl **17** with [Pt(P^tBu_3)$_2$] **2**, which reflects the lability of the Au−Ge bond in these species. However, the reactivity of :$SnCl_2$ with Au/Pt **1b:2** pair markedly differs and no metal-only Lewis adduct **4b** was detected in any of our experiments. Instead, tin dichloride promoted an interesting phosphine exchange to yield the heteroleptic compound [(PMe_2Ar^{Dipp2})Au(P^tBu_3)]$^+$ (**26**) as the only gold-containing species. $^{31}P\{^1H\}$ NMR spectroscopy revealed the immediate formation of compound **26** upon mixing the three reaction components, as evidenced by two set of doublets at 100.6 and 14.6 ppm, characterized by a two-bond coupling-constant of 312 Hz, analogous to other cationic and heteroleptic

diphosphine gold derivatives.[74] We could not observe, however, any other signal by $^{31}P\{^{1}H\}$ NMR corresponding to the remaining Pt-bound tri-*tert*-butylphosphine (Figure 29).

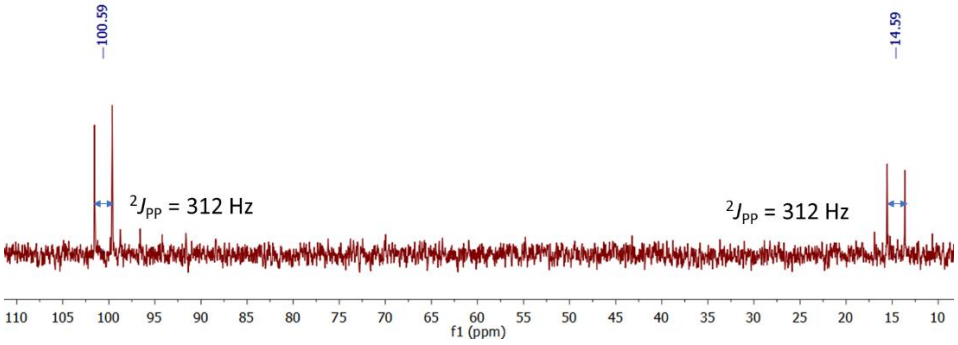

Figure 29. $^{31}P\{^{1}H\}$ NMR of compound **26**.

[74] a) S. Arndt, M. M. Hansmann, P. Motloch, M. Rudolph, F. Rominger, A. S. K. Hashmi, *Chem. Eur. J.* **2017**, *23*, 2542–2547. b) R. Uson, J. Gimeno, J. Fornies, F. Martinez, C. Fernandez. *Inorg. Chim. Act.* **1982**, *63*, 91–96. c) H. El-Amouri, A. A. Bahsoun, J. Fischer, J. A. Osborn, M.-T. Youinou. *Organometallics* **1991**, *10*, 3582–3588.

II.2.4.4. Tin-Promoted Phosphine Exchange Reactions

The ability of :$SnCl_2$ to mediate the transfer of a phosphine ligand from Pt(0) to Au(I) prompted us to investigate the possibility of accessing heteroleptic diphosphine Pt(0) compounds, of which there are very few reported examples.[3,75] Prior studies have shown that ligand-exchange reactions between [$Pt(PCy_3)_2$] and several N-heterocyclic carbenes (NHCs) provide access to heteroleptic NHC−Pt−PCy_3 derivatives,[19b] but the analogous substitution reaction to incorporate bulky phosphines into P−Pt(0) −P' structures remains unknown. To carry out these studies we chose three bulky phosphines, more precisely PCy_3, whose stannylene-platinum chemistry has already been outlined by Braunschweig,[68a] as well as $PMeXyl_2$ (Xyl = 2,6-$Me_2C_6H_3$) and PMe_2Ar^{Dtbp2} (Ar^{Dtbp2} = C_6H_3-2,6-(C_6H_3-3,5-$(CMe_3)_2$)), whose coordination chemistry and reactivity has been reported by our group.[76] The progress of the exchange reactions can be easily monitored by $^{31}P\{^1H\}$ NMR spectroscopy. Heating equimolar solutions of Pt(0) compound **2** and each of the three aforementioned phosphine ligands at 80 °C for several days did not result in any apparent transformation in view of the resulting NMR spectra, except for PCy_3, where minor amounts of unknown species were detected. Likewise, the inertness of **2** towards ligand substitution stands unaltered under excess of the free phosphine (up to 10 equivalents). In stark contrast, the addition of one equivalent of :$SnCl_2$ to the previous solutions led to rapid phosphine-exchange reactions that had in common the appearance of free

[75] B. E. Cowie, F. A. Tsao, D. J. H. Emslie. *Angew. Chem. Int. Ed*. **2015**, *54*, 2165–2169.
[76] a) J. Campos, R. Peloso, E. Carmona. *Angew. Chem. Int. Ed.* **2012**, *51*, 8255–8258. b) J. Campos, L. Ortega-Moreno, S. Conejero, R. Peloso, J. López-Serrano, C. Maya, E. Carmona. *Chem. Eur. J.* **2015**, *21*, 8883–8896. c) M. Marín, J. J. Moreno, C. Navarro-Gilabert, E. Álvarez, Celia Maya, R. Peloso, M. C. Nicasio, E. Carmona. *Chem. Eur. J.* **2019**, *25*, 260–272.

P^{t}Bu$_3$ as the main side-product. Best yields were obtained by the use of 1.5 equivalents of :SnCl$_2$. In the case of PCy$_3$, instead of the aimed heteroleptic Pt(0) compound, immediate formation of (PCy$_3$)$_2$Pt=SnCl$_2$ at 25 °C was evinced by ^{31}P{^{1}H} NMR spectroscopy (Scheme 18). A characteristic broad singlet at 51.4 ppm flanked by ^{195}Pt satellites ($^1J_{PPt}$ = 3525 Hz), as previously described by Braunschweig,68[a] demonstrated its formation, which became quantitative when performing the reaction with 2.1 equivalents of PCy$_3$. The formation of (PCy$_3$)$_2$Pt=SnCl$_2$ was accompanied by the presence of unbound P^{t}Bu$_3$ in a 1:2 ratio, with a ^{31}P{^{1}H} NMR signal at 59.9 ppm.

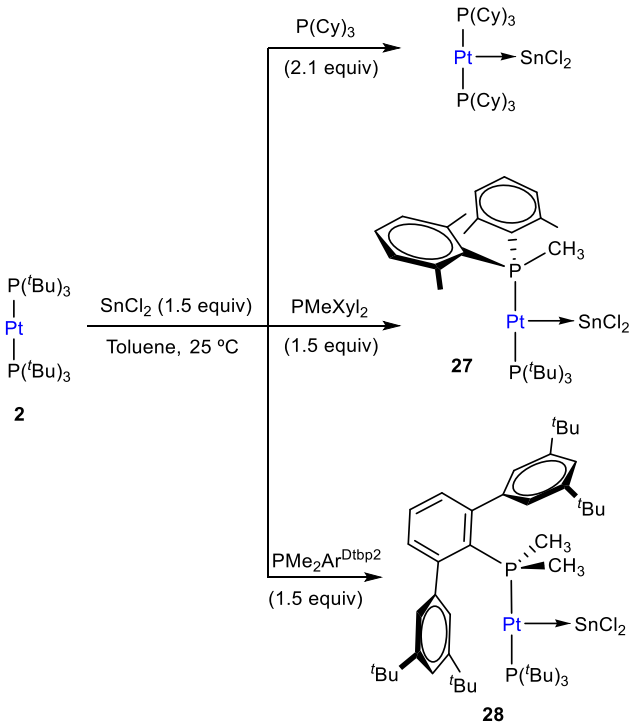

Scheme 18. Tin-mediated phosphine exchange reactions at Pt(0) **2**.

The reaction of $PMeXyl_2$ and Pt(0) **2** in the presence of $:SnCl_2$ (1.5 equiv.) proceeds rapidly towards compound **27** in quantitative spectroscopic yield (Scheme 18). At variance with PCy_3, the use of $PMeXyl_2$ permitted the formation of the desired heteroleptic Pt(0) species in which only one of the two P^tBu_3 ligands was substituted by the incoming phosphine. In fact, using an excess of $PMeXyl_2$ did not lead to the homoleptic Pt(0) compound analogous to $(PCy_3)_2Pt{=}SnCl_2$ even under moderate heating. The use of the bulkier phosphine PMe_2Ar^{Dtbp2} bearing a terphenyl group led to the formation of heteroleptic platinum stannylene **28** (Scheme 18), though it required longer reaction times. The high-resolution mass spectra of **27** and **28** fit exactly to their proposed formulation (see Experimental Section, II.3.1), albeit without the bound $SnCl_2$ fragment, not surprisingly given the lability of the Pt→Sn bond. Both compounds feature similar $^{31}P\{^1H\}$ NMR spectra characterized by two doublets exhibiting $^2J_{PP}$ of around 300 Hz, indicating the *trans* disposition of the two phosphines. Compound **27** leads to resonances at 94.6 and 6.3 ppm due to P^tBu_3 and $PMeXyl_2$, respectively, while the analogous signals appear at 97.3 and 12.6 ppm due to P^tBu_3 and PMe_2Ar^{Dtbp2} in compound **28**. These resonances are flanked by ^{195}Pt satellites with strong coupling constants (**27**: $^1J_{PPt}$ = 3776 and 3244 Hz; **28**: $^1J_{PPt}$ = 3788 and 3504 Hz). The presence of a tin centre bound to platinum was inferred in the two compounds from the satellites that escort the P^tBu_3 doublet ($^2J_{PSn}$ *ca.* 250 Hz). In ^{195}Pt NMR spectra, their platinum centres resonate at about -5000 ppm as double doublets and, in the case of **27**, we could detect a large $^1J_{PtSn}$ coupling constant of 3210 Hz that further corroborates the coordination of tin (Figure 30).

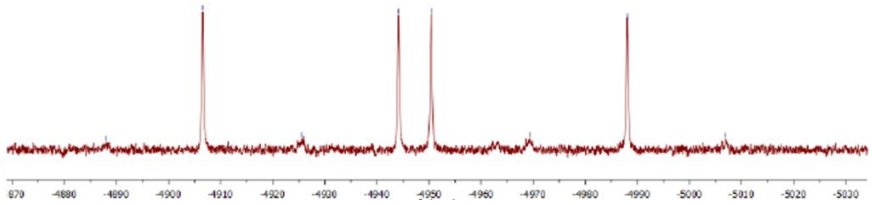

Figure 30. ^{195}Pt NMR spectra of complex **27**.

Our attempts to record ^{119}Sn{^{1}H} NMR resonances were unsuccessful, though this is not unexpected due to the high asymmetry of the ^{119}Sn centres in these compounds, which results in an increased effect of chemical shift anisotropy in the relaxation of their NMR signals.[77] Coupling to the variety of neighbouring NMR-active nuclei adds to the difficulty of observing ^{119}Sn{^{1}H} NMR signals for **27** and **28**.

As a side note, we observed that the methyl group directly bound to the phosphorus centre in compound **27** resonates at 2.93 ppm (dd, $^{3}J_{HPt}$ = 50.7, $^{2}J_{HP}$ = 9.0, $^{4}J_{HP}$ = 2.5 Hz) in the ^{1}H NMR spectrum, shifted to surprisingly higher frequency compared to free phosphine (1.63 ppm)[78] or to other Pt−PMeXyl$_2$ compounds previously reported by us (*ca.* 1.5−1.7 ppm).76 However, its corresponding ^{13}C{^{1}H} resonance appears at 21.0 ppm ($^{1}J_{CP}$ = 37 Hz), that is, within the expected range for a Ar$_2$P*Me* group. The unexpected ^{1}H NMR chemical shift served though to validate the proposed molecular structure of **27** by means of computational studies carried out by Dr. Juan José Moreno. A conformational analysis was calculated at the ωB97XD/6-31G(d,p) level of theory and disclosed no close contacts between the P−CH$_3$ moiety and the Sn or Pt centres. The geometric

[77] R. R. Sharp, J. W. Tolan. *J. Chem. Phys.* **1976**, *65*, 522–530.
[78] J. Campos, M. F. Espada, J. López-Serrano, E. Carmona. *Inorg. Chem*. **2013**, *52*, 6694–6704.

parameters of the minimum energy conformer of complex **27** are also comparable to previous platinum(0) diphosphine stannylene systems.68 With this model in hand, the theoretical ^{1}H NMR chemical shifts of **27** were calculated by means of the GIAO method (ωB97XD/6-311+G(2d,p)//ωB97XD/6-31G(d,p)).[79] To calibrate these results ^{1}H NMR data of compounds **2**, [Pt(PCy$_3$)$_2$(SnCl$_2$)]68[a] and [Pt(IMes)(PCy$_3$)(SnCl$_2$)]68[a] (IMes = 1,3-dimesitylimidazol-2-ylidene) were also evaluated. The linear relationship found between calculated and experimental proton chemical shifts (R^2 = 0.996, Figure 31) gives an expected δ of 2.71 ppm for the PMe moiety in complex **27**, in reasonable agreement with the experimental value (2.93 ppm).

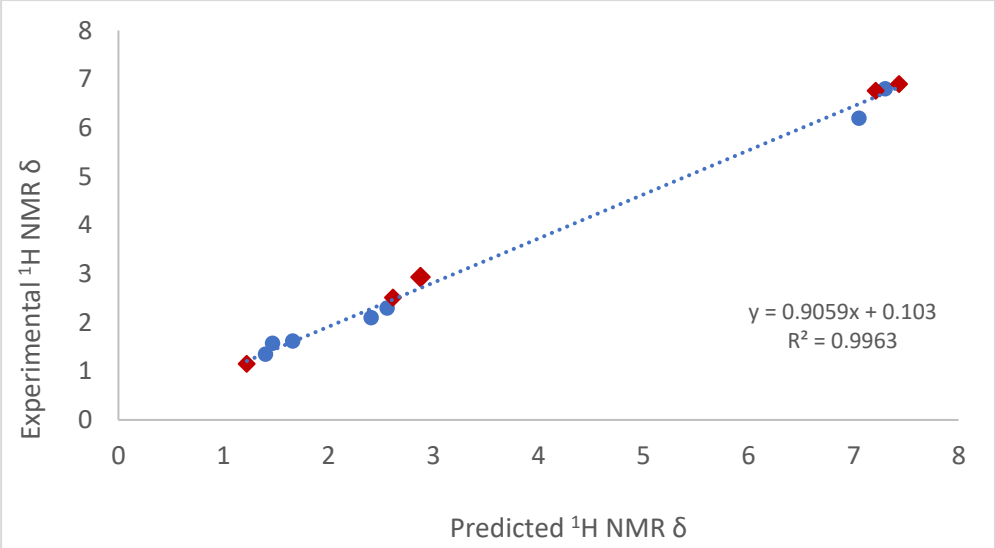

Figure 31. Predicted and experimental ^{1}H NMR data relative to complexes **27** (red diamond), benchmarked against **2**, [Pt(PCy$_3$)$_2$(SnCl$_2$)]68[a] and [Pt(IMes)(PCy$_3$)(SnCl$_2$)]68[a]

[79] a) K. Wolinski, J. F. Hinton, P. Pulay. *J. Am. Chem. Soc.* **1990**, *112*, 8251–8260. b) M. Häser, R. Ahlrichs, H. P. Baron, P. Weiss, H. Horn. *Theor. Chim. Acta* **1992**, *83*, 455–470.

III.3. Experimental Section

II.3.1. Synthesis and Characterization of New Compounds

General considerations

All preparations and manipulations were carried out using standard Schlenk and glove-box techniques, under an atmosphere of argon and of high purity nitrogen, respectively. All solvents were dried, stored over 3 Å molecular sieves, and degassed prior to use. Toluene (C_7H_8) and n-pentane (C_5H_{12}) were distilled under nitrogen over sodium. Tetrahydrofuran (THF) and diethyl ether were distilled under nitrogen over sodium/benzophenone. [D_6]Benzene was dried over molecular sieves (3 Å) and CD_2Cl_2 over CaH_2 and distilled under argon. [AuCl(THT)] (THT =tetrahydrothiophene),[80] phosphine ligands PMe_2Ar^{Dipp2},[45] PMe_2Ar^{Xyl2},[76c] $PCyp_2Ar^{Xyl2}$,[76c] PMe_2Ar^{Dtbp2}[76c] and compounds **1a**,[15] **2**,[81] **6**[26]**, 8b**,[6] **9b**,[6] **10b**[6] were prepared as described previously. Other chemicals were commercially available and used as received. Solution NMR spectra were recorded on Bruker AMX-300, DRX-400 and DRX-500 spectrometers. Spectra were referenced to external $SiMe_4$ (δ: 0 ppm) using the residual proton solvent peaks as internal standards (^{1}H NMR experiments), or the characteristic resonances of the solvent nuclei (^{13}C NMR experiments), while ^{31}P was referenced to H_3PO_4. Spectral assignments were made by routine one- and two-dimensional NMR experiments where appropriate. Infrared spectra were recorded on a Bruker Vector 22 spectrometer and sampling preparation was made in Nujol. For

[80] R. Uson, A. Laguna, M. Laguna, D. A. Briggs, H. H. Murray, J. P. Fackler. *Inorg. Synth.* **2007**, *26*, 85–91.
[81] H. R. C. Jaw, W. R. Mason. *Inorg. Chem.* **1989**, *28*, 4370–4373.

elemental analyses a LECO TruSpec CHN elementary analyzer, was utilized. Supplementary crystallographic data for all the structurally characterized compounds described in this Thesis can be obtained free of charge from The Cambridge Crystallographic Data Centre. CCDC: 19655523, 1965524, 1965525, 1965526, 1986501, 1986502, 1986503, 1986504, 1897306, 1897307, 1897308, 1897309, 1897310, 1897311.

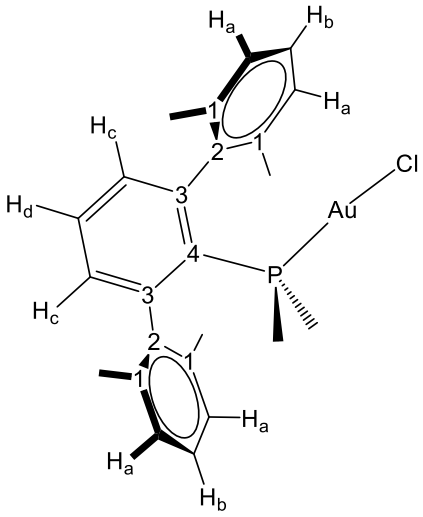

(PMe$_2$Ar^{Xyl2})AuCl. A solution of the phosphine PMe$_2$Ar^{Xyl2} (500 mg, 1.44 mmol) in toluene (15 mL) was added over a suspension of [Au(THT)Cl] (386 mg, 1.20 mmol) in toluene (10 mL). The initial white suspension became a solution after several hours and was stirred for an overall period of 8 hours. The solvent was then removed under vacuum and the resulting white solid washed with pentane and dried to give (PMe$_2$Ar^{Xyl2})AuCl as a fine white powder (630 mg, 90%).

Anal. Calcd. for $C_{24}H_{27}AuClP$: C, 49.8; H, 4.7. **Found:** C, 49.7; H, 4.7.

^{1}H NMR (400 MHz, CD_2Cl_2, 25 ºC) δ: 7.63 (td, 1 H, $^3J_{HH}$ = 7.6 Hz, $^5J_{HP}$ = 1.8 Hz, H_d), 7.28 (t, 2 H, $^3J_{HH}$ = 7.6 Hz, H_b), 7.16 (d, 4 H, $^3J_{HH}$ = 7.6 Hz, H_a), 7.13 (dd, 2 H, $^3J_{HH}$ = 7.6 Hz, $^4J_{HP}$ = 3.5 Hz, H_c), 2.13 (s, 12 H, Me_{Xyl}), 1.20 (d, 6 H, $^2J_{HP}$ = 10.4 Hz, PMe_2).

^{13}C{^{1}H} NMR (100 MHz, CD_2Cl_2, 25 ºC) δ: 146.5 (d, $^2J_{CP}$ = 10 Hz, C_3), 141.0 (d, $^3J_{CP}$ = 5 Hz, C_2), 136.7 (C_1), 132.3 (d, $^4J_{CP}$ = 2 Hz, CH_d), 131.6 (d, $^3J_{CP}$ = 8 Hz, CH_c), 128.8 (CH_b), 128.4 (CH_a), 127.6 (d, $^1J_{CP}$ = 57 Hz, C_4), 21.9 (Me_{Xyl}), 17.5 (d, $^1J_{CP}$ = 40 Hz, PMe_2).

^{31}P{^{1}H} NMR (160 MHz, CD_2Cl_2, 25 ºC) δ: -3.2.

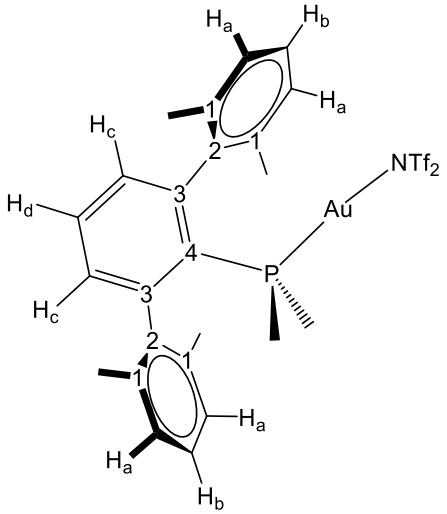

Compound 1a. To a suspension of (PMe_2Ar^{Xyl2})AuCl (300 mg, 0.517 mmol) in toluene (10 mL) was added one equivalent of $AgNTf_2$ (200 mg, 0.517 mmol) under N_2 atmosphere and the mixture covered with aluminum foil and stirred at room temperature for 1 hour. The solution was filtered and the volatiles were removed in vacuo to yield complex **1a** as white powder (350 mg, 82%).

Anal. Calcd. for $C_{26}H_{27}AuF_6NO_4PS_2$: C, 37.9; H, 3.3; N, 1.7; S, 7.8. **Found:** C, 37.9; H, 3.3; N, 1.7; S, 8.0.

^{1}H NMR (400 MHz, C_6D_6, 25 ºC) δ: 7.06 (t, 2 H, $^3J_{HH}$ = 7.6 Hz, H_b), 6.96 (d, 4 H, $^3J_{HH}$ = 7.6 Hz, H_a), 6.92 (td, 1 H, $^3J_{HH}$ = 7.6 Hz, $^5J_{HP}$ = 1.9 Hz, H_d), 6.50 (dd, 2 H, $^3J_{HH}$ = 7.6 Hz, $^4J_{HP}$ = 3.6 Hz, H_c), 1.97 (s, 12 H, Me_{Xyl}), 0.56 (d, 6 H, $^2J_{HP}$ = 11 Hz, PMe_2).

^{13}C{^{1}H} NMR (100 MHz, C_6D_6, 25 ºC) δ: 146.1 (d, $^2J_{CP}$ = 10 Hz, C_3), 140.2 (d, $^3J_{CP}$ = 4 Hz, C_2), 136.2 (C_1), 132.2 (d, $^4J_{CP}$ = 2 Hz, CH_d), 131.1 (d, $^3J_{CP}$ = 9 Hz, CH_c), 129.2 (CH_b), 128.4 (CH_a), 125.3 (d, $^1J_{CP}$ = 60 Hz, C_4), 120.4 (q, $^1J_{CF}$ = 323 Hz, CF_3), 21.7 (Me_{Xyl}), 16.7 (d, $^1J_{CP}$ = 42 Hz, PMe_2).

^{31}P{^{1}H} NMR (160 MHz, C_6D_6, 25 ºC) δ: -7.0.

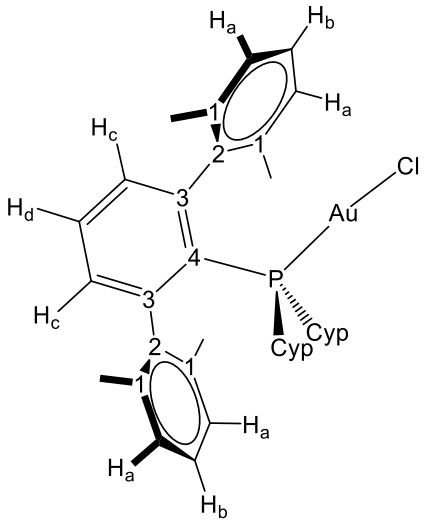

(PCyp$_2$Ar^{Xyl2})AuCl. A solution of PCyp$_2$Ar^{Xyl2} (500 mg, 1.10 mmol) in toluene (15 mL) was added over a suspension of [Au(THT)Cl] (294 mg, 0.92 mmol) in toluene (10 mL). The initial white suspension became a solution after several hours and was stirred for an overall period of 8 hours. The solvent was then removed under vacuum and the resulting white solid washed with pentane and dried to give (PCyp$_2$Ar^{Xyl2})AuCl as a fine white powder (572 mg, 90%).

Anal. Calcd. for $C_{32}H_{39}AuClP$: C, 55.9; H, 5.7. **Found:** C, 55.9; H, 5.7.

^{1}H NMR (400 MHz, CD_2Cl_2, 25 ºC) δ: 7.58 (td, 1 H, $^3J_{HH}$ = 7.6 Hz, $^5J_{HP}$ = 1.9 Hz, H_d), 7.29 (t, 2 H, $^3J_{HH}$ = 7.6 Hz, H_b), 7.13 (dd, 2 H, $^3J_{HH}$ = 7.6 Hz, $^4J_{HP}$ = 3 Hz, H_c), 7.12 (d, 4 H, $^3J_{HH}$ = 7.6 Hz, H_a), 2.17-2.09 (m, 2 H, PCH), 2.06 (s, 12 H, Me_{Xyl}), 1.82-1.25 (m, 16 H, CH_2).

^{13}C{^{1}H} NMR (100 MHz, CD_2Cl_2, 25 ºC) δ: 148.4 (d, $^2J_{CP}$ = 10 Hz, C_3), 141.9 (d, $^3J_{CP}$ = 4 Hz, C_2), 136.9 (C_1), 132.7 (d, $^3J_{CP}$ = 7 Hz, CH_c), 131.7 (d, $^4J_{CP}$ = 2 Hz, CH_d), 129.0 (d, $^1J_{CP}$ = 48 Hz, C_4), 128.5 (CH_b), 128.1 (CH_a),

38.5 (d, $^{1}J_{CP}$ = 35 Hz, PCH), 35.6 (d, $^{2}J_{CP}$ = 8 Hz, CH_2), 32.9 (d, $^{2}J_{CP}$ = 8 Hz, CH_2), 25.5 (d, $^{2}J_{CP}$ = 12 Hz, CH_2), 25.2 (d, $^{2}J_{CP}$ = 14 Hz, CH_2), 21.7 (Me_{Xyl}).

$^{31}P\{^{1}H\}$ NMR (160 MHz, CD_2Cl_2, 25 ºC) δ: 53.3.

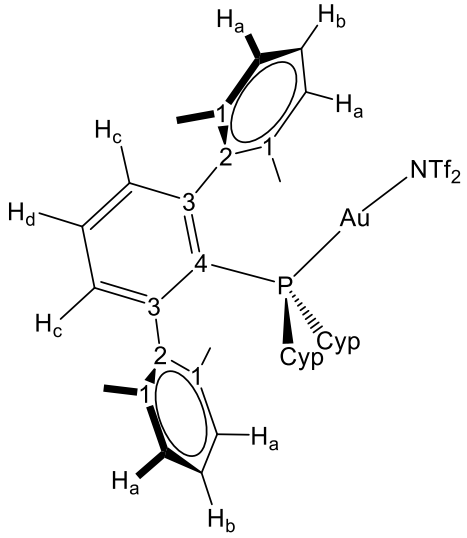

Compound 1c. To a suspension of ($PCyp_2Ar^{Xyl2}$)AuCl (300 mg, 0.437 mmol) in toluene (10 mL) was added one equivalent of $AgNTf_2$ (169 mg, 0.437 mmol) under N_2 atmosphere and the mixture covered with aluminum foil and stirred at room temperature for 1 hour. The solution was filtered and the volatiles were removed in vacuo to yield complex **1c** as white powder (285 mg, 70%).

Anal. Calcd. for $C_{34}H_{39}AuF_6NO_4PS_2$: C, 43.8; H, 4.2; N, 1.5; S, 6.9. **Found:** C, 44.0; H, 4.4; N, 1.8; S, 6.8.

^{1}H NMR (400 MHz, C_6D_6, 25 ºC) δ: 7.19 (t, 2 H, $^3J_{HH}$ = 7.6 Hz, H_b), 7.06 (d, 4 H, $^3J_{HH}$ = 7.6 Hz, H_a), 6.93 (td, 1 H, $^3J_{HH}$ = 7.6 Hz, $^5J_{HP}$ = 1.8 Hz, H_d), 6.57 (dd, 2 H, $^3J_{HH}$ = 7.6 Hz, $^4J_{HP}$ = 3.3 Hz, H_c), 2.06-1.95 (m, 2 H, PCH), 1.90 (s, 12 H, Me_{Xyl}), 1.72-1.15 (m, 16 H, CH_2).

^{13}C{^{1}H} NMR (100 MHz, C_6D_6, 25 ºC) δ: 148.2 (d, $^2J_{CP}$ = 10 Hz, C_3), 141.1 (d, $^3J_{CP}$ = 5 Hz, C_2), 136.4 (C_1), 132.3 (d, $^3J_{CP}$ = 7 Hz, CH_c), 131.6 (d, $^4J_{CP}$ = 2 Hz, CH_d), 128.7 (CH_b), 128.6 (CH_a), 126.4 (d, $^1J_{CP}$ = 50 Hz, C_4), 120.4 (q, $^1J_{CF}$ = 323 Hz, CF_3), 38.4 (d, $^1J_{CP}$ = 36 Hz, PCH), 35.6

(d, $^{3}J_{CP}$ = 7 Hz, CH_2), 32.8 (d, $^{3}J_{CP}$ = 6.6 Hz, CH_2), 25.4 (d, $^{2}J_{CP}$ = 12 Hz, CH_2), 25.2 (d, $^{2}J_{CP}$ = 13 Hz, CH_2), 21.5 (Me_{Xyl}).

$^{31}P\{^{1}H\}$ NMR (160 MHz, C_6D_6, 25 ºC) δ: 48.8.

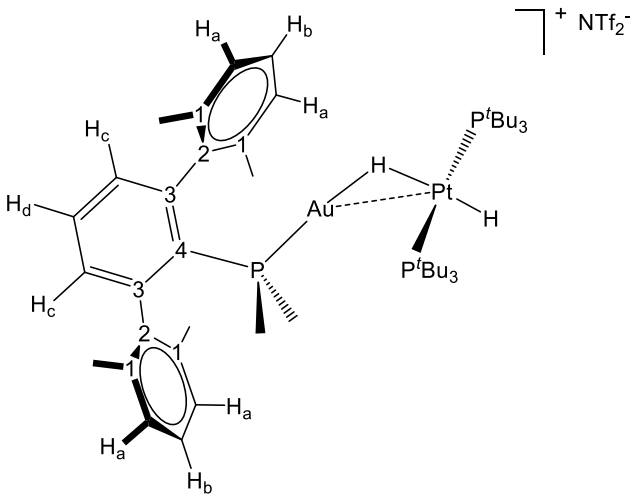

Compound 3a. A mixture of compounds **1a** (100 mg, 0.121 mmol) and **2** (73 mg, 0.121 mmol) was placed in a Schlenk inside a dry box, dissolved in toluene (5 mL) and stirred at room temperature for 48 hours under H_2 atmosphere (1 bar). The solution was layered with pentane (10 mL) and stored at -30 °C overnight to yield compound **3a** as yellow crystals (86 mg, 50%).

Anal. Calcd. for $C_{50}H_{83}AuF_6NO_4P_3PtS_2$: C, 42.1; H, 5.9; N, 1.0; S, 4.5. **Found**: C, 42.5; H, 5.8; N, 0.9; S, 4.1.

^{1}H NMR (400 MHz, C_6D_6, 25 °C) δ: 7.15 (t, 2 H, $^3J_{HH}$ = 7.6 Hz, H_b), 7.07 (d, 4 H, $^3J_{HH}$ = 7.6 Hz, H_a), 7.05 (td, 1 H, $^3J_{HH}$ = 7.6 Hz, $^5J_{HP}$ = 1.8 Hz, H_d), 6.60 (dd, 2 H, $^3J_{HH}$ = 7.6 Hz, $^4J_{HP}$ = 3.4 Hz, H_c), 2.04 (s, 12 H, Me_{Xyl}), 1.31 (vt, 54 H, $^3J_{HP}$ = 6.4 Hz, ^{t}Bu), 1.28 (d, 6 H, $^2J_{HP}$ = 9.5 Hz, PMe_2), -1.75 (m, 1 H, $^2J_{HP}$ = 110 Hz, $^1J_{HPt}$ = 516 Hz, Au(μ-H)Pt), -10.39 (m, 1 H, $^1J_{HPt}$ = 1030 Hz, Pt−H).

^{13}C{^{1}H} NMR (100 MHz, C_6D_6, 25 °C) δ: 146.6 (d, $^2J_{CP}$ = 10 Hz, C_3), 140.8 (d, $^3J_{CP}$ = 4 Hz, C_2), 136.5 (C_1), 132.1 (CH_d), 131.3 (d, $^3J_{CP}$ = 7 Hz, CH_c), 129.1 (CH_b), 128.5 (CH_a), 121.4 (q, $^1J_{CF}$ = 323 Hz, CF_3), 39.4 (vt,

$^{1}J_{CP}$ = 8 Hz, $^{2}J_{CPt}$ = 30 Hz, Pt−*C*(CH_3)$_3$), 32.9 (Pt−C(*C*H_3)$_3$), 22.1 (Me_{Xyl}), 17.4 (d, $^{1}J_{CP}$ = 7 Hz, PMe_2). The quaternary carbon C_4 could not be located neither in the $^{13}C\{^{1}H\}$ NMR spectrum or by two-dimensional ^{1}H-^{13}C correlations.

$^{31}P\{^{1}H\}$ NMR (160 MHz, C_6D_6, 25 °C) δ: 91.5 ($^{1}J_{PPt}$ = 2713 Hz, P(^{t}Bu)$_3$), 5.7 ($^{2}J_{PPt}$ = 208 Hz, Au−P).

IR (Nujol): ν(Pt/Au−H) 2290, 2165 cm^{-1}.

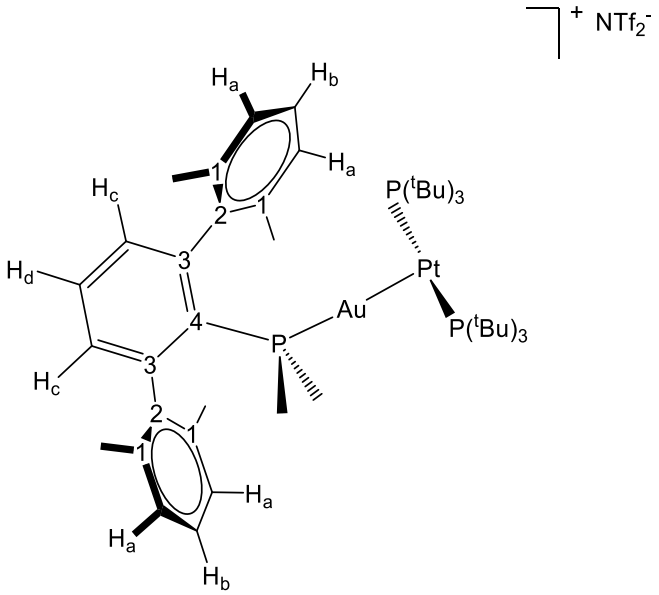

Compound 4a. To a solid mixture of **1a** (100 mg, 0.121 mmol) and **2** (73 mg, 0.121 mmol) was added 5 mL of toluene and the solution stirred at room temperature for 10 minutes. Addition of pentane (10 mL) caused precipitation of an orange solid (160 mg, 93%) that was washed with pentane. Single crystals of **4a** suitable for X-ray diffraction studies were grown by diffusion of pentane into a toluene solution of **4a** (1:2 by vol.) at -20 °C.

Anal. Calcd. for $C_{50}H_{81}AuF_6NO_4P_3PtS_2$: C, 42.2; H, 5.7; N, 1.0; S, 4.5. **Found**: C, 42.4; H, 5.6; N, 1.0; S, 4.4.

^{1}H NMR (400 MHz, CD_2Cl_2, 25 °C) δ: 7.62 (td, 1 H, $^3J_{HH}$ = 7.6 Hz, $^5J_{HP}$ = 1.8 Hz, H_d), 7.26 (t, 2 H, $^3J_{HH}$ = 7.6 Hz, H_b), 7.13 (d, 4 H, $^3J_{HH}$ = 7.6 Hz, H_a), 7.03 (dd, 2 H, $^3J_{HH}$ = 7.6 Hz, $^4J_{HP}$ = 3.3 Hz, H_c), 2.11 (s, 12 H, Me_{Xyl}), 1.52 (vt, 54 H, $^3J_{HP}$ = 6.5 Hz, ^{t}Bu), 1.08 (d, 6 H, $^2J_{HP}$ = 10 Hz, PMe_2).

$^{13}C\{^{1}H\}$ NMR (100 MHz, CD_2Cl_2, 25 °C) δ: 145.8 (d, $^{2}J_{CP}$ = 10 Hz, C_3), 141.2 (d, $^{3}J_{CP}$ = 4 Hz, C_2), 136.7 (C_1), 132.3 (CH_d), 132.2 (d, $^{3}J_{CP}$ = 7 Hz, CH_c), 129.0 (CH_b), 128.4 (CH_a), 126.2 (d, $^{1}J_{CP}$ = 52 Hz, C_4), 122.2 (q, $^{1}J_{CF}$ = 323 Hz, CF_3), 39.4 (vt, $^{1}J_{CP}$ = 8 Hz, $^{2}J_{CPt}$ = 20 Hz, Pt−P(*C*$(CH_3)_3$), 33.8 (Pt−P(C(*C*$H_3)_3$), 22.3 (Me_{Xyl}), 18.7 (d, $^{1}J_{CP}$ = 36 Hz, PMe_2).

$^{31}P\{^{1}H\}$ NMR (160 MHz, CD_2Cl_2, 25 °C) δ: 96.4 (d, $^{3}J_{PP}$ = 3 Hz, $^{1}J_{PPt}$ = 3140 Hz, P(^{t}Bu)$_3$), -32.5 (t, $^{3}J_{PP}$ = 3 Hz, $^{2}J_{PPt}$ = 1933 Hz, Au−P).

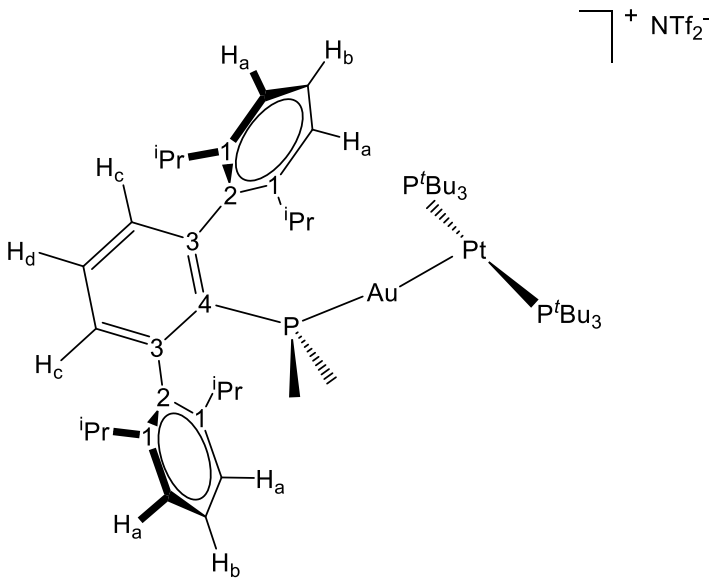

Compound 4b. A mixture of compounds **4** (100 mg, 0.106 mmol) and **1** (64 mg, 0.106 mmol) was placed in a Schlenk inside a dry box, disolved in CH_2Cl_2 (5 mL). To the solution was added 3 equivalent of MeOH (13 µL) and stirred at room temperature for 15 minutes. Addition of pentane (10 mL) cause precipitation of an orange solid (130 mg, 80%) that was washed with pentane and, if necessary, recrystallized from CH_2Cl_2/pentane at -20 ºC.

Alternative Synthesis: A solid mixture of compounds **1b** (100 mg, 0.106 mmol), **2** (64 mg, 0.106 mmol) and :$GeCl_2$·dioxane (25 mg, 0.106 mmol) was placed in a Schlenk flask inside a dry box, dissolved in CH_2Cl_2 (5 mL) and stirred at room temperature for 15 minutes. Addition of pentane (10 mL) caused precipitation of **4b** as an orange solid that was washed with pentane (150 mg, 92%).

Anal. Calcd. for $C_{58}H_{97}AuF_6NO_4P_3PtS_2$: C, 45.4; H, 6.4; N, 0.9; S, 4.2. **Found:** C, 45.8; H, 6.2; N, 0.8; S, 4.0.

^{1}H NMR (400 MHz, CD_2Cl_2, 25 ºC) δ: 7.52 (td, 1 H, $^{3}J_{HH}$ = 7.6 Hz, $^{5}J_{HP}$ = 2.0 Hz, H_d), 7.42 (t, 2 H, $^{3}J_{HH}$ = 7.6 Hz, H_b), 7.26 (d, 4 H, $^{3}J_{HH}$ = 7.6 Hz, H_a), 7.14 (dd, 2 H, $^{3}J_{HH}$ = 7.6 Hz, $^{4}J_{HP}$ = 3.6 Hz, H_c), 2.56 (sept, 4 H, $^{3}J_{HH}$ = 6.5 Hz, ^{i}Pr(CH)), 1.50 (vt, 54 H, $^{3}J_{HP}$ = 6.4 Hz, ^{t}Bu), 1.3 (d, 12 H, $^{3}J_{HH}$ = 6.7 Hz, ^{i}Pr(CH_3)), 1.19 (d, 6 H, $^{2}J_{HP}$ = 10 Hz, PMe_2), 1.00 (d, 12 H, $^{3}J_{HH}$ = 6.7 Hz, ^{i}Pr(CH_3)).

^{13}C{^{1}H} NMR (100 MHz, CD_2Cl_2, 25 ºC) δ: 146.8 (C_1), 144.4 (d, $^{2}J_{CP}$ = 10 Hz, C_3), 139.2 (d, $^{5}J_{CP}$ = 3 Hz, C_2), 134.8 (d, $^{3}J_{CP}$ = 9 Hz, CH_c), 130.0 (CH_b), 129.2 (CH_d), 127.4 (d, $^{1}J_{CP}$ = 41 Hz, C_4), 124.1 (CH_a), 120.5 (q, $^{1}J_{CF}$ = 323 Hz, CF_3), 39.5 (vt, $^{1}J_{CP}$ = 8 Hz, $^{2}J_{CPt}$ = 20 Hz, Pt−P(*C*(CH_3)$_3$), 33.8 (Pt−P(C(*C*H_3)$_3$), 31.5 (^{i}Pr(CH), 25.9 (^{i}Pr(CH_3), 23.8 (^{i}Pr(CH_3), 19.7 (d, $^{1}J_{CP}$ = 35 Hz, PMe_2).

^{31}P{^{1}H} NMR (160 MHz, CD_2Cl_2, 25 ºC) δ: 94.5 ($^{1}J_{PPt}$ = 3159 Hz), -34.2 ($^{2}J_{PPt}$ = 1984 Hz)

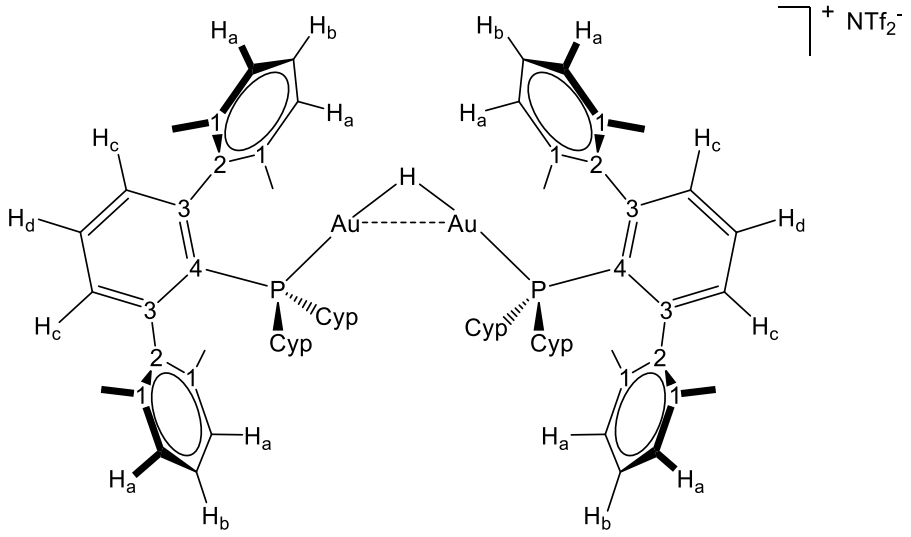

Compound 5c. A mixture of compounds **1c** (100 mg, 0.107 mmol) and **2** (64 mg, 0.107 mmol) was placed in a Schlenk inside a dry box, dissolved in toluene (5 mL) and stirred at room temperature for 48 hours under H_2 atmosphere (1 bar). The solution was layered with pentane and stored at -20 °C overnight to yield compound **5c** as yellow crystals (94 mg, 56%).

Alternative Synthesis: Compound **5c** can be synthesized by adding $SiEt_3H$ (51 μL, 0.321 mmol) to a toluene solution (10 mL) of **1c** (100 mg, 0.107 mmol) after stirring at room temperature for 30 minutes. Subsequent addition of pentane (10 mL) caused precipitation of a white solid that was washed with pentane and dried to provide compound **5c** (147 mg, 87%).

^{1}H NMR (400 MHz, C_6D_6, 25 °C) δ: 7.22 (m, 12 H, $^3J_{HH}$ = 7.6 Hz, H_a, H_b), 7.12 (td, 2 H, $^3J_{HH}$ = 7.6 Hz, $^5J_{HP}$ = 1.6 Hz, H_d), 6.66 (dd, 4 H, $^3J_{HH}$ = 7.6 Hz, $^4J_{HP}$ = 3.0 Hz, H_c), 4.78 (t, 1 H, $^2J_{HP}$ = 90.9 Hz, Au−H−Au), 2.36-2.24 (m, 4 H, PCH), 2.01 (s, 24 H, Me_{Xyl}), 1.82-1.34 (m, 32 H, CH_2).

^{13}C{^{1}H} NMR (100 MHz, C_6D_6, 25 °C) δ: 148.1 (d, $^2J_{CP}$ = 9 Hz, C_3), 141.1 (d, $^3J_{CP}$ = 5 Hz, C_2), 136.8 (C_1), 136.5 (d, $^3J_{CP}$ = 7 Hz, CH_c), 132.4 (d,

$^{4}J_{CP}$ = 8 Hz, CH_d), 131.9 (d, $^{1}J_{CP}$ = 40 Hz, C_4), 129.1 (CH_b), 128.7 (CH_a), 120.4 (q, $^{1}J_{CF}$ = 323 Hz, CF_3), 38.4 (d, $^{1}J_{CP}$ = 33 Hz, PCH), 35.6 (d, $^{2}J_{CP}$ = 10 Hz, CH_2), 32.8 (d, $^{2}J_{CP}$ = 10 Hz, CH_2), 25.4 (d, $^{2}J_{CP}$ = 10 Hz, CH_2), 25.2 (d, $^{2}J_{CP}$ = 10 Hz, CH_2), 21.5 (Me_{Xyl}).

$^{31}P\{^{1}H\}$ NMR (160 MHz, C_6D_6, 25 °C) δ: 58.0.

IR (Nujol): ν(Au−H) 1922 cm^{-1}.

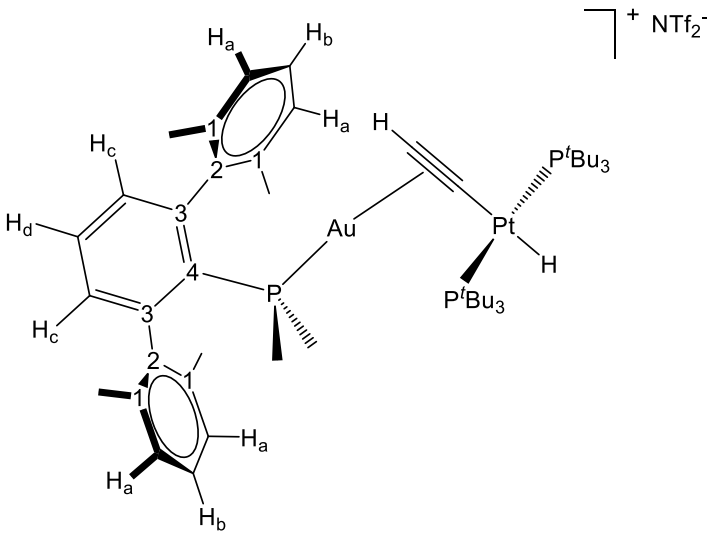

Compound 8a. A solid mixture of **1a** (100 mg, 0.121 mmol) and **2** (73 mg, 0.121 mmol) was dissolved in 5 mL of toluene and stirred at room temperature for 12 hours under C_2H_2 atmosphere (0.5 bar). The solution was layered with pentane (10 mL) and stored at -30 °C overnight to yield compound **8a** as colorless crystals (115 mg, 66%).

Anal. Calcd. for $C_{52}H_{83}AuF_6NO_4P_3PtS_2$: C, 43.1; H, 5.8; N, 1.0; S, 4.4. **Found:** C, 43.1; H, 5.5; N, 1.1; S, 4.4.

^{1}H NMR (400 MHz, C_6D_6, 25 °C) δ: 7.26 (t, 2 H, $^3J_{HH}$ = 7.6 Hz, H_b), 7.18 (m, 1 H, H_d), 7.15 (d, 4 H, $^3J_{HH}$ = 7.6 Hz, H_a), 6.71 (dd, 2 H, $^3J_{HH}$ = 7.5 Hz, $^4J_{HP}$ = 3.5 Hz, H_c), 2.98 (m, 1 H, C≡CH), 2.15 (s, 12 H, Me_{Xyl}), 1.52 (d, 6 H, $^2J_{HP}$ = 9.5 Hz, PMe_2), 1.49 (vt, 54 H, $^3J_{HP}$ = 6.4 Hz, ^{t}Bu), -10.27 (m, 1H, $^2J_{HP}$ = 14 Hz, $^1J_{HPt}$ = 571 Hz, Pt−H).

^{13}C{^{1}H} NMR (100 MHz, C_6D_6, 25 °C) δ: 146.8 (d, $^2J_{CP}$ = 10 Hz, C_3), 141.1 (d, $^3J_{CP}$ = 4 Hz, C_2), 136.8 (C_1), 132.4 (CH_d), 131.4 (d, $^3J_{CP}$ = 8 Hz, CH_c), 129.3 (CH_b), 128.8 (CH_a), 127.4 (d, $^1J_{CP}$ = 57 Hz, C_4), 126.6 (d, $^2J_{CP}$ = 79 Hz, *C*≡CH), 121.4 (q, $^1J_{CF}$ = 323 Hz, CF_3), 108.2 (d, $^2J_{CP}$ = 20 Hz,

C≡*C*H), 41.2 (vt, $^{1}J_{CP}$ = 8 Hz, Pt−*C*(CH_3)$_3$), 33.1 (Pt−(C(*C*H_3)$_3$)), 21.8 (Me_{Xyl}), 17.0 (d, $^{1}J_{CP}$ = 38 Hz, PMe_2).

^{31}P{^{1}H} NMR (160 MHz, C_6D_6, 25 °C) δ: 82.9 ($^{1}J_{PPt}$ = 2768 Hz, P(^{t}Bu)$_3$), 0.8 (Au−P).

IR (Nujol): ν(≡C−H) 3171, ν(C≡C) 1843 cm^{-1}.

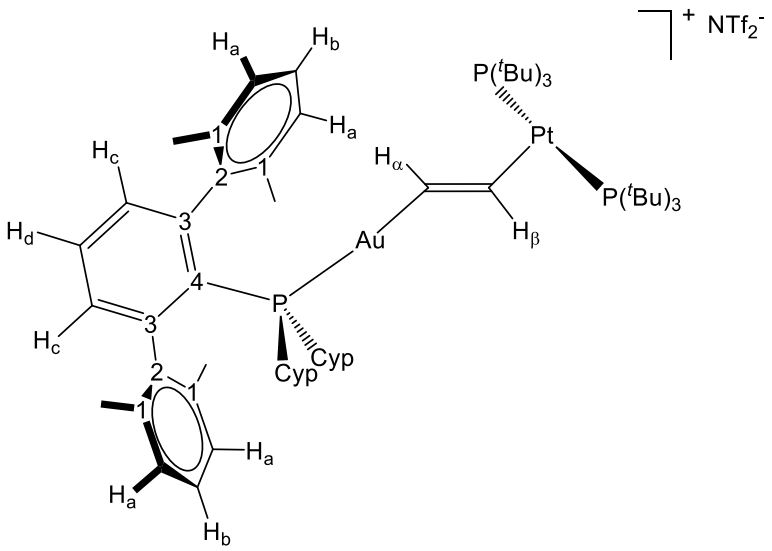

Compound 9c. A mixture of compounds **1c** (100 mg, 0.107 mmol) and **2** (64 mg, 0.107 mmol) was dissolved in toluene (5 mL) and the argon atmosphere was replaced by C_2H_2 (0.5 bar), upon which the bright yellow solution changed to an intense orange color. The solution was then filtered, layered with pentane and stored at -20 °C overnight to yield compound **9c** as orange crystals (68 mg, 41%).

Anal. Calcd. for $C_{60}H_{95}AuF_6NO_4P_3PtS_2$: C, 46.3; H, 6.1; N, 1.0; S, 4.1. **Found:** C, 45.9; H, 5.7; N, 1.0; S, 3.8.

^{1}H NMR (400 MHz, C_6D_6, 25 °C) δ: 7.19-7.08 (m, 3 H, H_b, H_d), 7.01 (d, 4 H, $^3J_{HH}$ = 7.6 Hz, H_a), 6.66 (dd, 2 H, $^3J_{HH}$ = 7.7 Hz, $^4J_{HP}$ = 2.7 Hz, H_c), 4.51 (dt, 1 H, $^3J_{HH}$ = 7.6 Hz, $^3J_{HP}$ = 3.4 Hz, $^2J_{HPt}$ = 110 Hz, H_β), 4.20 (dd, 1 H, $^3J_{HH}$ = 7.6 Hz, $^3J_{HP}$ = 6.4 Hz, $^3J_{HPt}$ = 194 Hz, H_α), 2.22-2.09 (m, 2 H, CH), 1.97 (s, 24 H, Me_{Xyl}), 1.71-1.47 (m, 12 H, CH_2), 1.36 (vt, 54 H, $^3J_{HP}$ = 6.5 Hz, ^{t}Bu), 1.24-1.09 (m, 4H, CH_2).

^{13}C{^{1}H} NMR (100 MHz, C_6D_6, 25 °C) δ: 159.4 (d, $^2J_{CP}$ = 113, $^1J_{CH}$ = 198 Hz, *C*H_α), 148.9 (d, $^2J_{CP}$ = 10 Hz, C_3), 142.4 (d, $^3J_{CP}$ = 5 Hz, C_2),

137.9 (C_1), 137.0 (d, $^3J_{CP}$ = 6 Hz, CH_c), 132.4 (d, $^4J_{CP}$ = 8 Hz, CH_d), 131.6 (d, $^1J_{CP}$ = 40 Hz, C_4), 129.3 (CH_a), 125.7 (CH_b), 121.7 (q, $^1J_{CF}$ = 322 Hz, CF_3), 115.5 (d, $^3J_{CP}$ = 24, $^1J_{CH}$ = 193 Hz, CH_β), 41.2 (vt, $^1J_{CP}$ = 8 Hz, Pt−$C(CH_3)_3$), 38.0 (d, $^1J_{CP}$ = 28 Hz, PCH), 35.0 (d, $^2J_{CP}$ = 10 Hz, CH_2), 33.1 (Pt−(C(CH_3)$_3$)), 32.5 (d, $^2J_{CP}$ = 10 Hz, CH_2), 26.0 (d, $^2J_{CP}$ = 10 Hz, CH_2), 25.7 (d, $^2J_{CP}$ = 10 Hz, CH_2), 21.4 (Me_{Xyl}).

$^{31}P\{^1H\}$ NMR (160 MHz, C_6D_6, 25 °C) δ: 70.6 ($^1J_{PPt}$ = 3323 Hz, P(^{t}Bu)$_3$), 51.7 ($^4J_{PPt}$ = 277 Hz, Au−P).

IR (Nujol): ν(=C−H) 3172, ν(C=C) 1645 cm^{-1}.

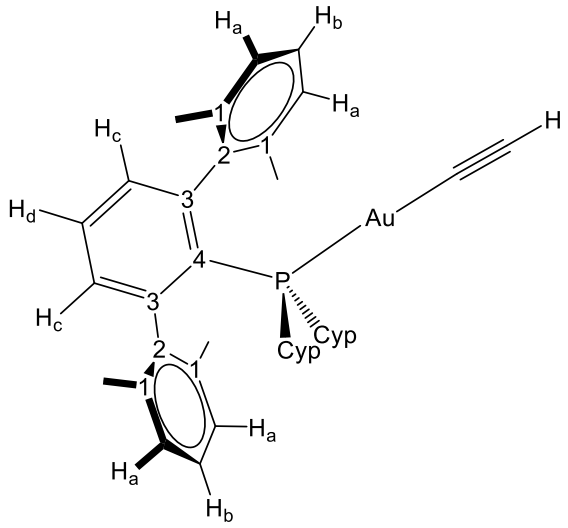

Compound 10c. A suspension of ($PCyp_2Ar^{Xyl2}$)AuCl (200 mg, 0.29 mmol) in toluene (10 mL) was cooled to -40 ºC and a toluene solution containing a small excess (1.2 eq.) of Mg(C≡CH)Br was added dropwise. The mixture was stirred for additional 2 hours at -40 ºC. The volatiles were removed in vacuo and the residue extracted with pentane. Evaporation of the solvent led to compound **10c** as a white powder (35 mg, 18 %). Gold acetylides are potentially explosive and should be handle with caution.

Anal. Calcd. for $C_{34}H_{40}AuP$: C, 60.4; H, 6.0. **Found:** C, 60.4; H, 5.8.

^{1}H NMR (400 MHz, C_6D_6, 25 ºC) δ: 7.29 (t, 2 H, $^3J_{HH}$ = 7.6 Hz, H_b), 7.09 (d, 4 H, $^3J_{HH}$ = 7.56 Hz, H_a), 6.94 (td, 1 H, $^3J_{HH}$ = 7.6 Hz, $^5J_{HP}$ = 1.6 Hz, H_d), 6.64 (dd, 2 H, $^3J_{HH}$ = 7.6 Hz, $^4J_{HP}$ = 2.7 Hz, H_c), 2.17-2.05 (m, 2 H, PCH), 1.97 (s, 12 H, Me_{Xyl}), 1.78 (d, 1H, $^4J_{HP}$ = 5.5 Hz, AuC≡CH), 1.7-1.1 (m, 16 H, CH_2).

^{13}C{^{1}H} NMR (100 MHz, C_6D_6, 25 ºC) δ: 148.8 (d, $^2J_{CP}$ = 10 Hz, C_3), 141.9 (d, $^3J_{CP}$ = 5 Hz, C_2), 136.3 (C_1), 132.0 (d, $^3J_{CP}$ = 7 Hz, CH_c), 130.8 (d, $^4J_{CP}$ = 5 Hz, CH_d), 130.2 (d, $^2J_{CP}$ = 158 Hz, Au*C*≡CH), 128.9 (d,

$^{1}J_{CP}$ = 48 Hz, C_4), 128.7 (CH_b), 128.4 (CH_a), 86.6 (d, $^{3}J_{CP}$ = 25 Hz, $^{1}J_{CH}$ = 233 Hz, AuC≡*C*H), 38.3 (d, $^{1}J_{CP}$ = 31 Hz, PCH), 35.1 (d, $^{2}J_{CP}$ = 10 Hz, CH_2), 32.4 (d, $^{2}J_{CP}$ = 10 Hz, CH_2), 25.4 (d, $^{2}J_{CP}$ = 11 Hz, CH_2), 25.3 (d, $^{2}J_{CP}$ = 13 Hz, CH_2), 21.6 (Me_{Xyl}).

$^{31}P\{^{1}H\}$ NMR (160 MHz, C_6D_6, 25 ºC) δ: 55.5.

IR (Nujol): ν(≡C−H) 3286, ν(C≡C) 1944 cm^{-1}.

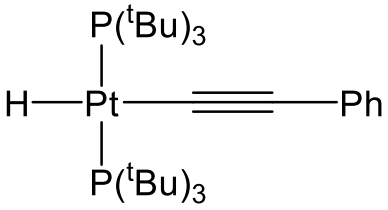

Compound 13. A toluene (5 mL) solution of **2** (64 mg, 0.107 mmol), phenylacetylene (11 μL, 0.107 mmol) and **1b** or **1c** (2 mg, 0.002 mmol) was stirred at room temperature for 15 minutes. The volatiles were removed in vacuo and the residue extracted with pentane (3x5 mL). Evaporation of the solvent yield compound **13** as colorless oil (26 mg, 35%). Suitable crystals for X-ray diffraction studies can be obtained by slow pentane evaporation at room temperature.

Anal. Calcd. for $C_{32}H_{60}P_2Pt$: C, 54.8; H, 8.6. **Found:** C, 54.9; H, 8.4.

^{1}H NMR (400 MHz, C_6D_6, 25 ºC) δ: 7.64 (d, 2 H, $^3J_{HH}$ = 7.3 Hz, *o*-C_6H_5), 7.21 (t, 2 H, $^3J_{HH}$ = 8.2 Hz, *m*-C_6H_5), 7.02 (t, 1 H, $^3J_{HH}$ = 7.3 Hz, *p*-C_6H_5), 1.58 (vt, 54 H, $^3J_{HP}$ = 6.3 Hz, ^{t}Bu), -9.46 (t, 1 H, $^2J_{HP}$ = 15.4, $^1J_{HPt}$ = 532.9 Hz, Pt−H).

^{13}C{^{1}H} NMR (100 MHz, C_6D_6, 25 ºC) δ: 131.3 (CH-Ar), 130.7 (CH-Ar), 129.3 (C-Ar), 124.2 (CH-Ar), 118.8 (C≡C−Ph), 117.6 (C≡C−Ph), 40.4 (vt, $^1J_{CP}$ = 8 Hz, $^2J_{CPt}$ = 35 Hz, Pt−P(*C*(CH_3)$_3$), 33.1 (Pt−P(C(*C*H_3)$_3$).

^{31}P{^{1}H} NMR (160 MHz, C_6D_6, 25 ºC) δ: 81.3 ($^1J_{PPt}$ = 2880 Hz).

IR (Nujol): ν(C≡C) 2090 cm^{-1}.

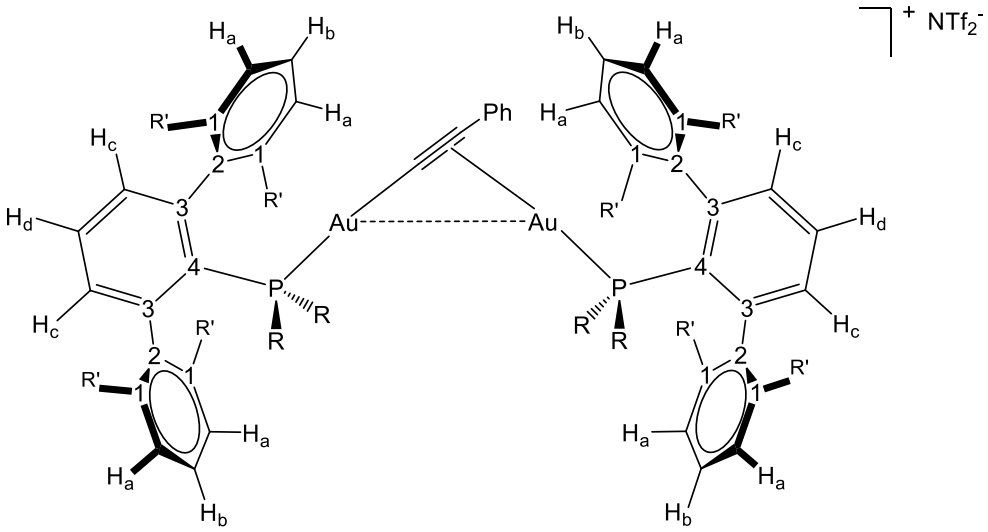

Compound 14. To a solution of compounds **1** (100 mg, 0.107 mmol) and **2** (64 mg, 0.107 mmol) in toluene (5 mL) was added one equivalent of phenylacetylene (11 µL, 0.107 mmol) and the mixture stirred at room temperature for 15 minutes. The volatiles were removed in vacuo and the residue washed with pentane (3x5 mL). The resulting fine white powder (60 mg, **14b**; 65 mg,**14c**) contain a mixture of compounds **14** and **6**, the latter which could not be separated by common methods but whose spectroscopic features did not hamper full characterization of compounds **14**. Single crystal of **14b** suitable for X-ray diffraction studies were grown by slow diffusion of pentane into toluene solution (2:1 by vol.) at -30 ºC.

Compound **14b** could be synthesized free of **6**: to a solution of **1b** (100 mg, 0.107 mmol) in toluene (5 mL) was added one equivalent of phenylacetylene (11 µL, 0.107 mmol) and the mixture stirred at room temperature for 18 hours. The volatiles were removed in vacuo and the residue was washed with pentane (3x5 mL) to yield **14b** as a white powder (90 mg, 50 %).

Compound 14b.

^{1}H NMR (400 MHz, C_6D_6, 25 ºC) δ: 7.55 (d, 2 H, $^{3}J_{HH}$ = 7.6 Hz, *o*-C_6H_5), 7.35 (m, 2 H, *m*-C_6H_5), 7.26 (t, 4 H, $^{3}J_{HH}$ = 7.6 Hz, H_b), 7.09 (d, 8 H, $^{3}J_{HH}$ = 7.8 Hz, H_a), 7.02 (t, 1 H, $^{3}J_{HH}$ = 8.4 Hz, *p*-C_6H_5), 6.93 (m, 6 H, H_c, H_d), 2.54 (sept, 8 H, $^{3}J_{HH}$ = 6.7 Hz, ^{i}Pr(CH)), 1.57 (d, 12 H, $^{2}J_{HP}$ = 9.8 Hz, PMe_2), 1.29 (d, 24 H, $^{3}J_{HH}$ = 6.7 Hz, ^{i}Pr(CH_3)), 0.90 (d, 24 H, $^{3}J_{HH}$ = 6.7 Hz, ^{i}Pr(CH_3)).

^{13}C{^{1}H} NMR (100 MHz, C_6D_6, 25 ºC) δ: 146.6 (C_1), 146.0 (d, $^{2}J_{CP}$ = 10 Hz, C_3), 138.6 (d, $^{5}J_{CP}$ = 3 Hz, C_2), 134.5 (d, $^{3}J_{CP}$ = 9 Hz, CH_c), 133.0 (CH-Ar), 131.5 (d, $^{1}J_{CP}$ = 43 Hz, C_4), 130.7 (CH-Ar), 130.1 (CH_b), 129.7 (C-Ar), 129.3 (CH_d), 125.7 (CH-Ar), 124.0 (CH_a), 120.9 (q, $^{1}J_{CF}$ = 323 Hz, CF_3), 119.9 (C≡C−Ph), 116.4 (C≡C−Ph), 31.6 (^{i}Pr(CH), 25.5 (^{i}Pr(CH_3), 23.1 (^{i}Pr(CH_3), 17.2 (d, $^{1}J_{CP}$ = 38 Hz, PMe_2).

^{31}P{^{1}H} NMR (160 MHz, C_6D_6, 25 ºC) δ: 0.4.

IR (Nujol): ν(C≡C) 2048 cm^{-1}.

Compound 14c.

^{1}H NMR (400 MHz, C_6D_6, 25 ºC) δ: 7.42 (d, 2 H, $^{3}J_{HH}$ = 8 Hz, *o*-C_6H_5), 7.24 (t, 4 H, $^{3}J_{HH}$ = 7.6 Hz, H_b), 7.08 (d, 8 H, $^{3}J_{HH}$ = 7.6 Hz, H_a), 7.05 (m, 5 H, $^{3}J_{HH}$ = 7.6 Hz, H_d, *m*-C_6H_5, *p*-C_6H_5), 6.63 (dd, 4 H, $^{3}J_{HH}$ = 7.6 Hz, $^{4}J_{HP}$ = 3.3 Hz, H_c), 1.94 (s, 24 H, Me_{Xyl}), 2.25-2.13 (m, 4 H, PCH), 1.87-1.22 (m, 32 H, CH_2).

^{13}C{^{1}H} NMR (100 MHz, C_6D_6, 25 ºC) δ: 148.1 (d, $^{2}J_{CP}$ = 10 Hz, C_3), 141.5 (d, $^{3}J_{CP}$ = 5 Hz, C_2), 136.8 (C_1), 133.6 (d, $^{3}J_{CP}$ = 7 Hz, CH_c), 132.5 (d, $^{4}J_{CP}$ = 2 Hz, CH_d), 131.9 (CH-Ar), 130.6 (CH-Ar), 129.3 (CH_b), 129.1 (CH_a), 128.8 (C-Ar), 126.5 (d, $^{1}J_{CP}$ = 46 Hz, C_4), 125.7 (CH-Ar), 124.2

(C≡C−Ph), 121.6 (C≡C−Ph), 120.1 (q, $^{1}J_{CF}$ = 323 Hz, CF_3), 40.2 (d, $^{1}J_{CP}$ = 36 Hz, PCH), 38.7 (d, $^{3}J_{CP}$ = 7 Hz, CH_2), 38.4 (d, $^{3}J_{CP}$ = 6.6 Hz, CH_2), 35.8 (d, $^{2}J_{CP}$ = 12 Hz, CH_2), 32.9 (d, $^{2}J_{CP}$ = 13 Hz, CH_2), 21.6 (Me_{Xyl}).

$^{31}P\{^{1}H\}$ NMR (160 MHz, C_6D_6, 25 ºC) δ: 53.9.

IR (Nujol): ν(C≡C) 2029 cm^{-1}.

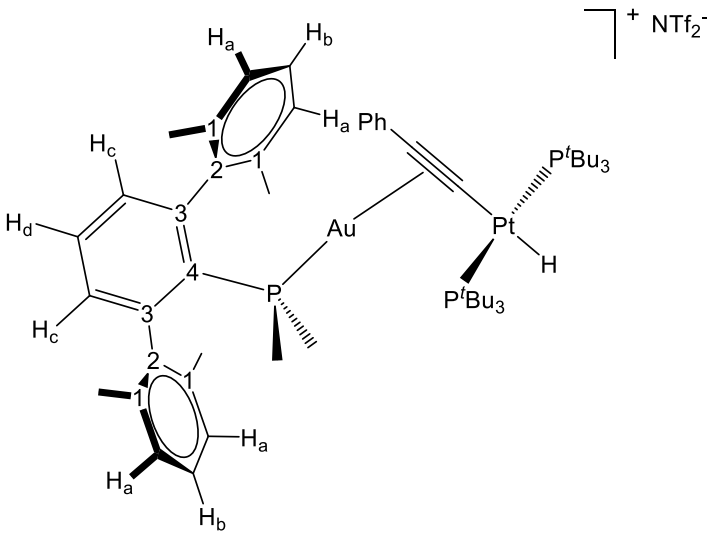

Compound 15a. To a solution of **1a** (100 mg, 0.121 mmol) and **2** (73 mg, 0.121 mmol) in toluene (5 mL) was added one equivalent of phenylacetylene (13 µL, 0.121 mmol) and the mixture stirred at room temperature for 15 minutes. The volatiles were removed in vacuo and the residue washed with pentane (3x5 mL) to yield compound **15a** as a white powder (70 mg, 38%).

Anal. Calcd. for $C_{58}H_{87}AuF_6NO_4P_3PtS_2$: C, 45.7; H, 5.8; N, 0.9; S, 4.2. **Found:** C, 45.9; H, 5.6; N, 1.1; S, 4.3.

^{1}H NMR (400 MHz, C_6D_6, 25 ºC) δ: 7.39 (d, 2 H, $^3J_{HH}$ = 7.3 Hz, *o*-C_6H_5), 7.15 (m, 3 H, *m*-C_6H_5, *p*-C_6H_5), 7.09 (m, 5 H, H_b, H_d), 6.99 (d, 4 H, $^3J_{HH}$ = 7.6 Hz, H_a), 6.58 (dd, 2 H, $^3J_{HH}$ = 7.6 Hz, $^4J_{HP}$ = 3.3 Hz, H_c), 2.06 (s, 12 H, Me_{Xyl}), 1.38 (vt, 54 H, $^3J_{HP}$ = 6.3 Hz, ^{t}Bu), 1.33 (d, 6 H, $^2J_{HP}$ = 10 Hz, PMe_2), -10.40 (m, 1H, $^2J_{HP}$ = 14 Hz, $^1J_{HPt}$ = 608 Hz, Pt−H).

^{13}C{^{1}H} NMR (100 MHz, C_6D_6, 25 ºC) δ: 145.9 (d, $^2J_{CP}$ = 10 Hz, C_3), 140.5 (d, $^3J_{CP}$ = 4 Hz, C_2), 137.9 (C_1), 136.6 (CH-Ar), 132.2 (d, $^4J_{CP}$ = 2 Hz, CH_d), 131.2 (CH-Ar), 129.3 (d, $^3J_{CP}$ = 9 Hz, CH_c), 129.2 (C-Ar), 128.9 (CH_b), 128.6 (CH_a), 125.7 (d, $^1J_{CP}$ = 60 Hz, C_4), 124.2 (CH-Ar), 121.3 (q,

$^{1}J_{CF}$ = 323 Hz, CF_3), 91.1 (C≡C−Ph), 85.9 (C≡C−Ph), 41.0 (vt, $^{1}J_{CP}$ = 8 Hz, $^{2}J_{CPt}$ = 35 Hz, Pt−P(*C*$(CH_3)_3$), 33.1 (Pt−P(C(*C*$H_3)_3$), 32.2 (Me_{Xyl}), 21.9 (d, $^{1}J_{CP}$ = 36 Hz, PMe_2).

$^{31}P\{^{1}H\}$ NMR (160 MHz, C_6D_6, 25 ºC) δ: 82.2 ($^{1}J_{PPt}$ = 2810 Hz, P(^{t}Bu)$_3$), 3.3 (Au−P).

IR (Nujol): ν(C≡C) 1982 cm^{-1}.

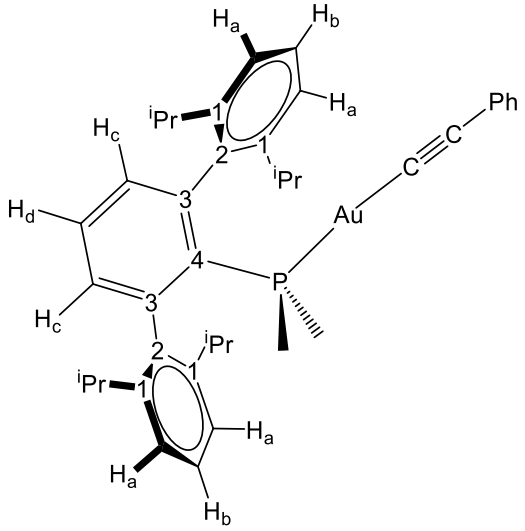

Compound 16b. Following a previously reported method,[82] to a solution of phenylacetylene (36 µL, 0.325 mmol) and KOH (18 mg, 0.325 mmol) in 15 mL of methanol was added a suspension of (PMe_2Ar^{Dipp2})AuCl (150 mg, 0.216 mmol). The solution was stirred for 20 hours at room temperature, and the solid filtered and washed with diethyl ether (2x5 mL) to yield compound **16b** as a white solid (139 mg, 85%). Gold acetylides are potentially explosive and should be handle with caution.

Anal. Calcd. for $C_{40}H_{48}AuP$: C, 63.5; H, 6.4. **Found:** C, 63.2; H, 6.7.

^{1}H NMR (400 MHz, C_6D_6, 25 ºC) δ: 7.74 (d, 2 H, $^3J_{HH}$ = 7.3 Hz, *o*-C_6H_5), 7.36 (t, 2 H, $^3J_{HH}$ = 7.8 Hz, *m*-C_6H_5), 7.17 (d, 4 H, $^3J_{HH}$ = 7.8 Hz, H_a), 7.06 (t, 1 H, $^3J_{HH}$ = 8.3 Hz, *p*-C_6H_5), 6.99 (m, 5 H, H_b, H_c, H_d), 2.64 (sept, 4 H, $^3J_{HH}$ = 6.5 Hz, ^{i}Pr(CH)), 1.34 (d, 12 H, $^3J_{HH}$ = 6.5 Hz, ^{i}Pr(CH_3)), 0.92 (d, 12 H, $^3J_{HH}$ = 6.5 Hz, ^{i}Pr(CH_3)), 0.90 (d, 6 H, $^2J_{HP}$ = 10 Hz, PMe_2).

[82] X.-K. Wan, X.-L. Cheng, Q. Tang, Y.-Z. Han, G. Hu, D. Jiang, Q.-M. Wang. *J. Am. Chem. Soc.* **2017**, *139*, 9451–9554.

$^{13}C\{^{1}H\}$ NMR (100 MHz, C_6D_6, 25 ºC) δ: 146.6 (CH-Ar), 145.7 (d, $^{2}J_{CP}$ = 11 Hz, C_3), 139.0 (d, $^{3}J_{CP}$ = 4 Hz, C_2), 135.8 (C_1), 134.3 (CH-Ar), 132.8 (d, $^{3}J_{CP}$ = 7 Hz, CH_c), 132.6 (d, $^{4}J_{CP}$ = 2 Hz, CH_d), 130.4 (d, $^{1}J_{CP}$ = 47 Hz, C_4), 129.8 (CH_b), 128.9 (CH_a), 125.9 (C-Ar), 123.8 (CH-Ar), 123.0 (C≡C−Ph), 102.4 (C≡C−Ph), 31.6 (^{i}Pr(CH), 25.7 (^{i}Pr(CH_3), 23.2 (^{i}Pr(CH_3), 16.9 (d, $^{1}J_{CP}$ = 35 Hz, PMe_2).

$^{31}P\{^{1}H\}$ NMR (160 MHz, C_6D_6, 25 ºC) δ: 9.7.

IR (Nujol): ν(C≡C) 2115 cm^{-1}.

MS-ESI (m/z): calcd for $C_{40}H_{48}AuPt$: 756.76, found: [M + H] 757.3, [M + Na] 779.3, [M + K] 795.3.

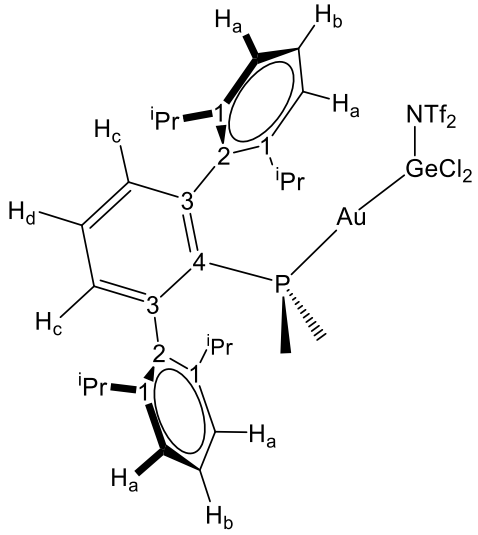

Compound 17. A solution of **1b** (30 mg, 0.03 mmol) in CD_2Cl_2 (0.5 mL) was treated with :$GeCl_2$·dioxane (7.4 mg, 0.03 mmol) in a *J. Young* NMR tube. The tube was shaken resulting in the immediate formation of compound **17**, which could be crystallized by slow diffusion of pentane at -20 ºC (15 mg, 46%).

Anal. Calcd. for $C_{34}H_{43}AuCl_2F_6GeNO_4PS_2$: C, 37.8; H, 4.0; N, 1.3; S, 5.9. **Found:** C, 38.2; H, 4.2; N, 1.5; S, 5.5.

^{1}H NMR (400 MHz, CD_2Cl_2, 25 ºC) δ: 7.60 (t, 1 H, $^3J_{HH}$ = 7.6 Hz, H_d), 7.47 (t, 2 H, $^3J_{HH}$ = 7.6 Hz, H_b), 7.4 (d, 4 H, $^3J_{HH}$ = 7.6 Hz, H_a), 7.26 (dd, 2 H, $^3J_{HH}$ = 7.6 Hz, $^4J_{HP}$ = 3.7 Hz, H_c), 2.48 (sept, 4 H, $^3J_{HH}$ = 6.8 Hz, ^{i}Pr(CH)), 1.37 (d, 6 H, $^2J_{HP}$ = 10 Hz, PMe_2), 1.36 (d, 12 H, $^3J_{HH}$ = 6.8 Hz, ^{i}Pr(CH_3)), 1.06 (d, 12 H, $^3J_{HH}$ = 6.7 Hz, ^{i}Pr(CH_3)).

^{13}C{^{1}H} NMR (100 MHz, CD_2Cl_2, 25 ºC) δ: 147.2 (C_1), 146.2 (d, $^2J_{CP}$ = 12 Hz, C_3), 138.2 (d, $^3J_{CP}$ = 6 Hz, C_2), 133.2 (d, $^3J_{CP}$ = 8 Hz, CH_c), 131.1 (CH_d), 130.4 (CH_b), 129.0 (d, $^1J_{CP}$ = 82 Hz, C_4), 124.8 (CH_a), 119.7

(q, $^{1}J_{CF}$ = 323 Hz, CF_3), 31.7 (^{i}Pr(CH)), 25.5 (^{i}Pr(CH_3)), 23.1 (^{i}Pr(CH_3)), 16.2 (d, $^{1}J_{CP}$ = 36 Hz, PMe_2).

$^{31}P\{^{1}H\}$ NMR (160 MHz, CD_2Cl_2, 25 ºC) δ: 4.8.

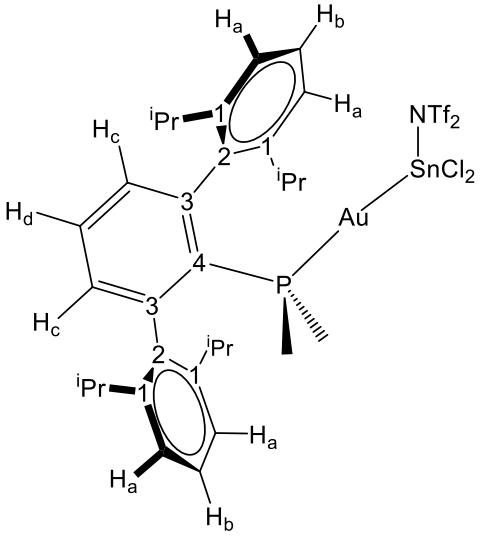

Compound 18. In an NMR tube, a solution of **1b** (30 mg, 0.03 mmol) in CD_2Cl_2 (0.5 mL) was treated with tin(II) chloride (6.0 mg, 0.03 mmol). The tube was shaken resulting in the immediate formation of compound **18**, which could be crystallized by slow diffusion of pentane at -20 ºC (17 mg, 48%).

Anal. Calcd. for $C_{34}H_{43}AuCl_2F_6NO_4PS_2Sn$: C, 36.3; H, 3.9; N, 1.2; S, 5.7. **Found:** C, 36.3; H, 3.9; N, 1.5; S, 5.5.

Spectroscopic data for compound **18·THF**:

^{1}H NMR (400 MHz, THF-d_8, 25 ºC) δ: 7.58 (td, 1 H, $^3J_{HH}$ = 7.6 Hz, $^5J_{HP}$ = 1.9 Hz, H_d), 7.42 (t, 2 H, $^3J_{HH}$ = 7.6 Hz, H_b), 7.29 (dd, 2 H, $^3J_{HH}$ = 7.6 Hz, $^4J_{HP}$ = 3.4 Hz, H_c), 7.25 (d, 4 H, $^3J_{HH}$ = 7.6 Hz, H_a), 2.62 (sept, 4 H, $^3J_{HH}$ = 6.7 Hz, ^{i}Pr(CH)), 1.35 (d, 12 H, $^3J_{HH}$ = 7.0 Hz, ^{i}Pr(CH_3)), 1.27 (d, 6 H, $^2J_{HP}$ = 10.4 Hz, PMe_2), 1.03 (d, 12 H, $^3J_{HH}$ = 7.0 Hz, ^{i}Pr(CH_3)).

^{13}C{^{1}H} NMR (100 MHz, THF-d_8, 25 ºC) δ: 147.1 (C_1), 145.7 (d, $^2J_{CP}$ = 11 Hz, C_3), 139.4 (d, $^3J_{CP}$ = 5 Hz, C_2), 133.7 (d, $^3J_{CP}$ = 8 Hz, CH_c), 130.2 (CH_d), 130.0 (CH_b), 129.3 (d, $^1J_{CP}$ = 56 Hz, C_4), 124.0 (CH_a), 121.0

(q, $^{1}J_{CF}$ = 320 Hz, CF_3), 31.9 (^{i}Pr(CH)), 25.6 (^{i}Pr(CH_3)), 23.1 (^{i}Pr(CH_3)), 17.9 (d, $^{1}J_{CP}$ = 38 Hz, PMe_2).

$^{31}P\{^{1}H\}$ NMR (160 MHz, THF-d_8, 25 ºC) δ: -3.1.

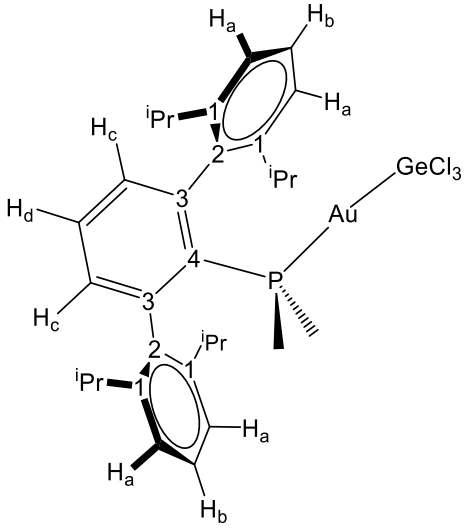

Compound 19. A THF (5 mL) solution of (PMe_2Ar^{Dipp2})AuCl (150 mg, 0.22 mmol) was added under argon atmosphere over a solution of :$GeCl_2$·dioxane (50 mg, 0.22 mmol) in THF (5 mL), then stirred for 30 minutes at room temperature. The solvent was then removed under vacuum to give compound **19** as a fine white powder (161 mg, 88%). Crystals suitable for X-ray studies were grown by slow diffusion of pentane into a dichloromethane solution of **19**.

Anal. Calcd. for $C_{32}H_{43}AuCl_3GeP$: C, 46.1; H, 5.2. **Found:** C, 45.8; H, 5.5.

^{1}H NMR (400 MHz, CD_2Cl_2, 25 ºC) δ: 7.58 (td, 1 H, $^3J_{HH}$ = 7.6 Hz, $^5J_{HP}$ = 1.6 Hz, H_d), 7.47 (t, 2 H, $^3J_{HH}$ = 7.6 Hz, H_b), 7.38 (d, 4 H, $^3J_{HH}$ = 7.6 Hz, H_a), 7.24 (dd, 2 H, $^3J_{HH}$ = 7.6 Hz, $^4J_{HP}$ = 3.5 Hz, H_c), 2.48 (sept, 4 H, $^3J_{HH}$ = 6.8 Hz, ^{i}Pr(CH)), 1.36 (d, 12 H, $^3J_{HH}$ = 6.8 Hz, ^{i}Pr(CH_3)), 1.33 (d, 6 H, $^2J_{HP}$ = 10 Hz, PMe_2), 1.05 (d, 12 H, $^3J_{HH}$ = 6.8 Hz, ^{i}Pr(CH_3)).

^{13}C{^{1}H} NMR (100 MHz, CD_2Cl_2, 25 ºC) δ: 146.9 (C_1), 146.4 (d, $^2J_{CP}$ = 11 Hz, C_3), 138.1 (d, $^3J_{CP}$ = 6 Hz, C_2), 133.1 (d, $^3J_{CP}$ = 7 Hz, CH_c),

130.8 (CH_d), 130.4 (CH_b), 127.5 (d, $^1J_{CP}$ = 52 Hz, C_4), 124.6 (CH_a), 31.7 (^{i}Pr(CH)), 25.6 (^{i}Pr(CH_3)), 23.1 (^{i}Pr(CH_3)), 16.5 (d, $^1J_{CP}$ = 33 Hz, PMe_2).

$^{31}P\{^1H\}$ NMR (160 MHz, CD_2Cl_2, 25 ºC) δ: 5.0.

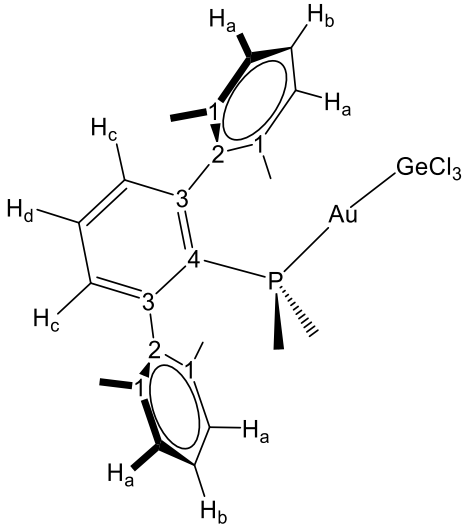

Compound 19^{Xyl}. A solution of (PMe$_2$Ar^{Xyl2})AuCl (150 mg, 0.26 mmol) in THF (5 mL) was added over a solution of germanium chloride dioxane complex (59 mg, 0.26 mmol) in THF (5 mL). The mixture was stirred for 30 minutes at room temperature. The solvent was then removed under vacuum to give compound **19^{Xyl}**, as a fine white powder (169 mg, 90%). Crystals suitable for X-ray analysis were grown by slow diffusion of pentane into a THF solution of **19^{Xyl}**.

Anal. Calcd. for $C_{24}H_{27}AuCl_3GeP$**:** C, 39.9; H, 3.8. **Found:** C, 39.7; H, 3.8.

^{1}H NMR (400 MHz, CD_2Cl_2, 25 ºC) δ: 7.67 (td, 1 H, $^3J_{HH}$ = 7.6 Hz, $^5J_{HP}$ = 1.6 Hz, H_d), 7.28 (m, 6 H, H_a, H_b), 7.16 (dd, 2 H, $^3J_{HH}$ = 7.6 Hz, $^4J_{HP}$ = 3.5 Hz, H_c), 2.09 (s, 12 H, Me_{Xyl}), 1.28 (d, 6 H, $^2J_{HP}$ = 9.5 Hz, PMe_2).

^{13}C{^{1}H} NMR (100 MHz, CD_2Cl_2, 25 ºC) δ: 147.3 (d, $^2J_{CP}$ = 11 Hz, C_3), 140.5 (d, $^3J_{CP}$ = 5 Hz, C_2), 136.5 (C_1), 133.1 (CH_d), 131.7 (d, $^3J_{CP}$ = 8 Hz, CH_c), 129.4 (CH_b), 128.8 (CH_a), 126.0 (d, $^1J_{CP}$ = 51 Hz, C_4), 21.8 (Me_{Xyl}), 16.2 (d, $^1J_{CP}$ = 34 Hz, PMe_2).

^{31}P{^{1}H} NMR (160 MHz, CD_2Cl_2, 25 ºC) δ: 6.8.

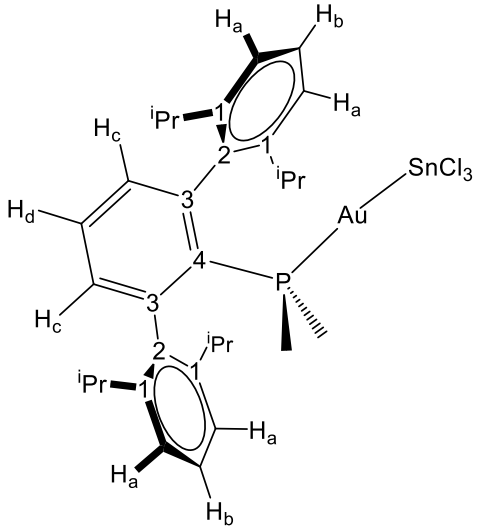

Compound 20. A THF (5mL) solution of (PMe_2Ar^{Dipp2})AuCl (150 mg, 0.22 mmol) was added under argon atmosphere over a solution of tin(II) chloride (41 mg, 0.22 mmol) in THF (5 mL), then stirred for 30 minutes at room temperature. The solvent was then removed under vacuum to give compound **20** as a fine white powder (172 mg, 89%).

Anal. Calcd. for $C_{32}H_{43}AuCl_3PSn$: C, 43.6; H, 4.9. **Found:** C, 43.5; H, 5.1.

^{1}H NMR (400 MHz, CD_2Cl_2, 25 ºC) δ: 7.56 (td, 1 H, $^3J_{HH}$ = 7.6 Hz, $^5J_{HP}$ = 1.8 Hz, H_d), 7.47 (t, 2 H, $^3J_{HH}$ = 7.6 Hz, H_b), 7.33 (d, 4 H, $^3J_{HH}$ = 7.6 Hz, H_a), 7.24 (dd, 2 H, $^3J_{HH}$ = 7.6 Hz, $^4J_{HP}$ = 3.5 Hz, H_c), 2.52 (sept, 4 H, $^3J_{HH}$ = 6.8 Hz, ^{i}Pr(CH)), 1.35 (d, 12 H, $^3J_{HH}$ = 6.8 Hz, ^{i}Pr(CH_3)), 1.33 (d, 6 H, $^2J_{HP}$ = 10 Hz, PMe_2), 1.05 (d, 12 H, $^3J_{HH}$ = 6.8 Hz, ^{i}Pr(CH_3)).

^{13}C{^{1}H} NMR (100 MHz, CD_2Cl_2, 25 ºC) δ: 147.0 (C_1), 146.0 (d, $^2J_{CP}$ = 11 Hz, C_3), 138.7 (d, $^3J_{CP}$ = 4 Hz, C_2), 133.2 (d, $^3J_{CP}$ = 7 Hz, CH_c), 130.5 (CH_d), 130.0 (CH_b), 124.2 (CH_a), 31.7 (^{i}Pr(CH)), 25.6 (^{i}Pr(CH_3)), 23.1 (^{i}Pr(CH_3)), 17.4 (d, $^1J_{CP}$ = 38 Hz, PMe_2). The quaternary carbon *C4* could

not be located neither in the $^{13}C\{^{1}H\}$ NMR spectrum or by two-dimensional ^{1}H-^{13}C correlations.

$^{31}P\{^{1}H\}$ NMR (160 MHz, CD_2Cl_2, 25 ºC) δ: -2.2.

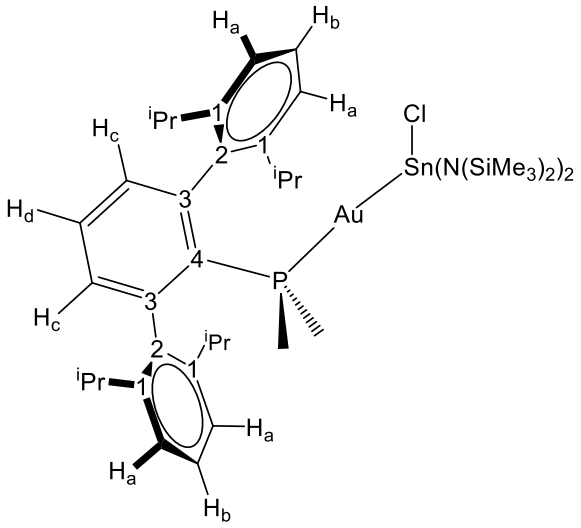

Compound 21. In an NMR tube, a solution of (PMe_2Ar^{Dipp2})AuCl (30 mg, 0.04mmol) in C_6D_6 (0.5 mL) was treated with tin(II) bis(trimethylsilyl)amide (19 mg, 0.04 mmol). The tube was shaken resulting in the formation of compound **21** after 5 minutes. The compound could be isolated as a white powder after removing the solvent under reduced pressure (22 mg, 48%).

Anal. Calcd. for $C_{44}H_{79}AuClNPSi_4Sn$: C, 47.3; H, 7.1; N, 1.3. **Found:** C, 47.3; H, 6.9; N, 1.6.

^{1}H NMR (400 MHz, C_6D_6, 25 ºC) δ: 7.45 (t, 2 H, $^3J_{HH}$ = 7.6 Hz, H_b), 7.24 (d, 4 H, $^3J_{HH}$ = 7.6 Hz, H_a), 7.15 (dd, 2 H, $^3J_{HH}$ = 7.6 Hz, $^4J_{HP}$ = 3.5 Hz, H_c), 6.98 (td, 1 H, $^3J_{HH}$ = 7.6 Hz, $^5J_{HP}$ = 1.8 Hz, H_d), 2.52 (sept, 4 H, $^3J_{HH}$ = 6.8 Hz, ^{i}Pr(CH)), 1.30 (d, 12 H, $^3J_{HH}$ = 6.8 Hz, ^{i}Pr(CH_3)) 1.10 (d, 6 H, $^2J_{HP}$ = 10 Hz, PMe_2), 0.90 (d, 12 H, $^3J_{HH}$ = 6.8 Hz, ^{i}Pr(CH_3)), 0.57 (s, $^2J_{HSi}$ = 15.3 Hz, $^4J_{HSn}$ = 6.5 Hz, $SiMe_3$).

^{13}C{^{1}H} NMR (100 MHz, C_6D_6, 25 ºC) δ: 146.9 (C_1), 146.3 (C_3), 137.8 (d, $^3J_{CP}$ = 6 Hz, C_2), 132.6 (d, $^3J_{CP}$ = 7 Hz, CH_c), 130.7 (CH_d), 129.6 (CH_b),

124.3 (CH_a), 123.2 (d, $^1J_{CP}$ = 60 Hz, C_4), 31.6 (^{i}Pr(CH)), 25.6 (^{i}Pr(CH_3)), 23.2 (^{i}Pr(CH_3)), 17.1 (d, $^1J_{CP}$ = 30 Hz, PMe_2), 7.27 ($^1J_{CSi}$ = 55 Hz, $^3J_{CSn}$ = 16 Hz, $SiMe_3$).

^{31}P{^{1}H} NMR (160 MHz, C_6D_6, 25 ºC) δ: 15.4 ($^2J_{PSn}$ = 3201 Hz).

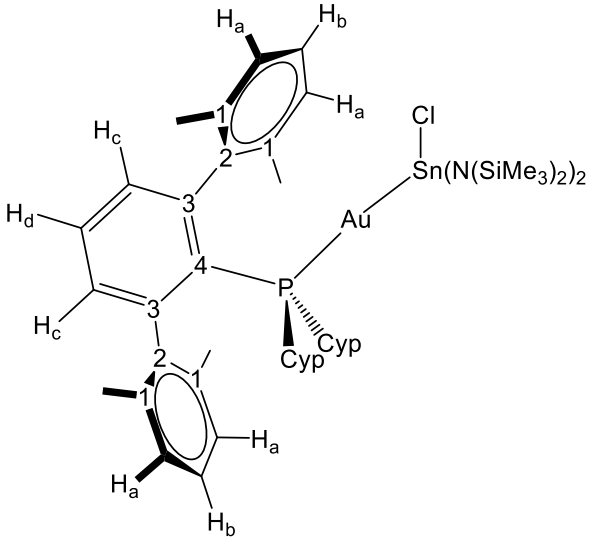

Compound 21^{Cyp}. In a NMR tube, a solution of (PCyp$_2$Ar^{Xyl2})AuCl (30 mg, 0.04 mmol) in C_6D_6 (0.5 mL) was added tin bis(trimethylsilyl)amide (19 mg, 0.04 mmol). The mixture gives compound **21^{Cyp}** after 5 minutes. It can be crystallized by slow diffusion of pentane into a C_6D_6 solution (2:1 by vol.) (23 mg, 51%).

^{1}H NMR (400 MHz, C_6D_6, 25 ºC) δ: 7.29 (t, 2 H, $^3J_{HH}$ = 7.6 Hz, H_b), 7.14 (d, 4 H, $^3J_{HH}$ = 7.6 Hz, H_a), 6.94 (td, 1 H, $^3J_{HH}$ = 7.6 Hz, $^5J_{HP}$ = 1.5 Hz, H_d), 6.57 (dd, 2 H, $^3J_{HH}$ = 7.6 Hz, $^4J_{HP}$ = 2.7 Hz, H_c), 2.27-2.17 (m, 2 H, PCH), 1.94 (s, 12 H, Me_{Xyl}), 1.8-1.25 (m, 16 H, CH_2), 0.58 (s, 36 H, $SiMe_3$).

^{13}C{^{1}H} NMR (100 MHz, C_6D_6, 25 ºC) δ: 148.5 (d, $^2J_{CP}$ = 10 Hz, C_3), 141.1 (d, $^3J_{CP}$ = 4 Hz, C_2), 136.1 (C_1), 136.1 (d, $^3J_{CP}$ = 6 Hz, CH_c), 131.1 (d, $^4J_{CP}$ = 2 Hz, CH_d), 129.6 (CH_b), 128.9 (CH_a), 38.9 (d, $^1J_{CP}$ = 27 Hz, PCH), 35.2 (d, $^2J_{CP}$ = 10 Hz, CH_2), 32.6 (d, $^2J_{CP}$ = 9 Hz, CH_2), 25.1 (d, $^2J_{CP}$ = 10 Hz, CH_2), 24.8 (d, $^2J_{CP}$ = 10 Hz, CH_2), 21.6 (Me_{Xyl}), 7.21 ($SiMe_3$).

^{31}P{^{1}H} NMR (160 MHz, C_6D_6, 25 ºC) δ: 59.9 ($^2J_{PSn}$ = 2846 Hz).

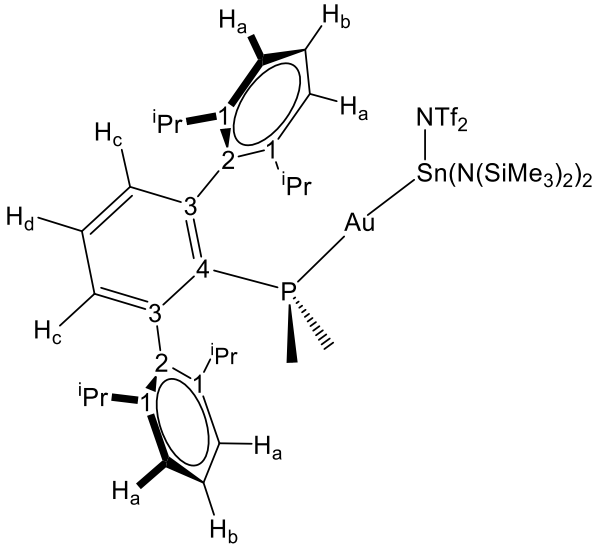

Compound 22. In an NMR tube, a solution of **1b** (30 mg, 0.03 mmol) in C_6D_6 (0.5 mL) was treated with tin(II) bis(trimethylsilyl)amide (14 mg, 0.03 mmol). The tube was shaken resulting in the formation of **22** after 5 minutes. The compound could be isolated as a white powder after removing the solvent under reduced pressure (20 mg, 48%).

Anal. Calcd. for $C_{46}H_{79}AuF_6N_3O_4PS_2Si_4Sn$: C, 40.2; H, 5.8; N, 3.1; S, 4.7. **Found:** C, 40.4; H, 5.8; N, 2.7; S, 4.8.

^{1}H NMR (400 MHz, C_6D_6, 25 ºC) δ: 7.26 (m, 3 H, H_d, H_b), 7.14 (d, 4 H, $^3J_{HH}$ = 7.6 Hz, H_a), 6.94 (m, 2 H, H_c), 2.56 (sept, 4 H, $^3J_{HH}$ = 6.8 Hz, ^{i}Pr(CH)), 1.58 (d, 6 H, $^2J_{HP}$ = 10 Hz, PMe_2), 1.28 (d, 12 H, $^3J_{HH}$ = 6.8 Hz, ^{i}Pr(CH_3)), 0.89 (d, 12 H, $^3J_{HH}$ = 6.8 Hz, ^{i}Pr(CH_3)), 0.47 (s, $SiMe_3$).

^{13}C{^{1}H} NMR (100 MHz, C_6D_6, 25 ºC) δ: 146.6 (C_1), 145.9 (d, $^2J_{CP}$ = 10 Hz, C_3), 138.3 (d, $^3J_{CP}$ = 5 Hz, C_2), 132.9 (d, $^3J_{CP}$ = 7 Hz, CH_c), 130.0 (CH_d), 129.6 (CH_b), 124.3 (CH_a), 120.0 (q, $^1J_{CF3}$ = 322 Hz, CF_3), 31.6 (^{i}Pr(CH)), 25.6 (^{i}Pr(CH_3)), 23.2 (^{i}Pr(CH_3)), 16.6 (d, $^1J_{CP}$ = 33 Hz, PMe_2), 6.7 ($^1J_{CSi}$ = 55 Hz, $^3J_{CSn}$ = 16 Hz, $SiMe_3$).

$^{31}P\{^{1}H\}$ NMR (160 MHz, C_6D_6, 25 ºC) δ: 13.8.

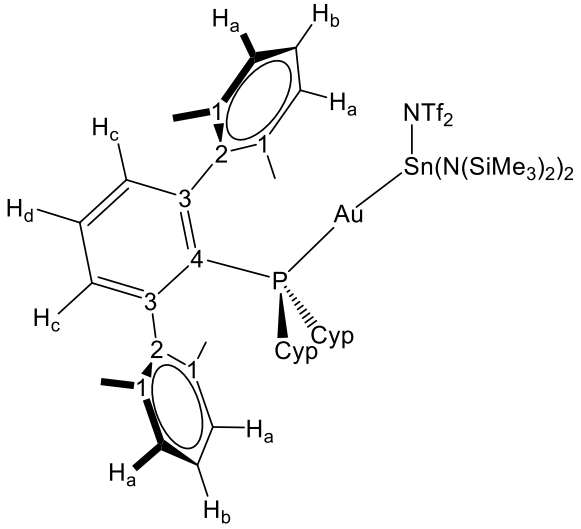

Compound 22^{Cyp}. In a NMR tube, a solution of Au[P(Cyp)$_2$Ar^{Xyl2}]NTf$_2$ (30 mg, 0.03 mmol) in C_6D_6 (0.5 mL) was added tin bis(trimethylsilyl)amide (14 mg, 0.03 mmol). The mixture gives compound **22^{Cyp}** after 5 minutes. It can be crystallized by slow diffusion of pentane into a C_6D_6 solution (2:1 by vol.) (20 mg, 49%).

^{1}H NMR (400 MHz, C_6D_6, 25 ºC) δ: 7.15 (t, 2 H, $^3J_{HH}$ = 7.6 Hz, H_b), 7.03 (d, 4 H, $^3J_{HH}$ = 7.6 Hz, H_a), 6.93 (td, 1 H, $^3J_{HH}$ = 7.6 Hz, $^5J_{HP}$ = 1.5 Hz, H_d), 6.51 (dd, 2 H, $^3J_{HH}$ = 7.6 Hz, $^4J_{HP}$ = 3 Hz, H_c), 2.35-2.23 (m, 2 H, PCH), 1.91 (s, 12 H, Me_{Xyl}), 1.79-1.25 (m, 16 H, CH_2), 0.49 (s, 36 H, $SiMe_3$).

^{13}C{^{1}H} NMR (100 MHz, C_6D_6, 25 ºC) δ: 147.8 (d, $^2J_{CP}$ = 10 Hz, C_3), 141.5 (d, $^3J_{CP}$ = 4 Hz, C_2), 136.6 (C_1), 132.3 (d, $^3J_{CP}$ = 6 Hz, CH_c), 131.3 (CH_d), 128.7 (CH_b), 128.4 (CH_a), 120.4 (q, $^1J_{CF}$ = 323 Hz, CF_3), 38.9 (d, $^1J_{CP}$ = 29 Hz, PCH), 35.9 (d, $^2J_{CP}$ = 10 Hz, CH_2), 32.8 (d, $^2J_{CP}$ = 7 Hz, CH_2), 25.3 (d, $^2J_{CP}$ = 10 Hz, CH_2), 24.4 (d, $^2J_{CP}$ = 10 Hz, CH_2), 21.6 (Me_{Xyl}), 6.74 ($^1J_{CSi}$ = 55 Hz, $^3J_{CSn}$ = 18 Hz, $SiMe_3$).

^{31}P{^{1}H} NMR (160 MHz, C_6D_6, 25 ºC) δ: 60.0 ($^2J_{PSn}$ = 2654 Hz).

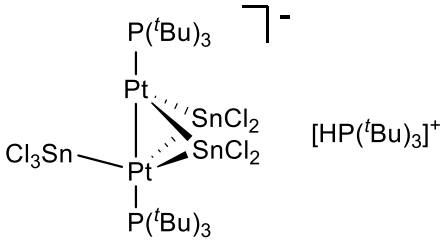

Compound 23. A CH_2Cl_2 (3 mL) solution of **2** (90 mg, 0.15 mmol) was added under argon atmosphere over tin(II) chloride (56 mg, 0.30 mmol) and the resulting red solution was stirred for 5 minutes at room temperature. Compound **23** could be crystallized by slow diffusion of hexane at -30 ºC (26 mg, 11%).

^{1}H NMR (400 MHz, CD_2Cl_2, 25 ºC) δ: 6.15 (d, 1 H, $^{1}J_{HP}$ = 452 Hz, *H*−P(C(CH$_3$)$_3$), 1.69 (d, 27 H, $^{3}J_{HP}$ = 15.0 Hz, H−P(C(C*H*$_3$)), 1.55 (d, 54 H, $^{3}J_{HP}$ = 13.0 Hz, Pt−P(C(CH$_3$)$_3$)).

^{13}C{^{1}H} NMR (100 MHz, CD_2Cl_2, 25 ºC) δ: 40.5 (vt, $^{1}J_{CP}$ = 7 Hz, Pt−P(*C*(CH$_3$)$_3$), 38.0 (d, $^{1}J_{CP}$ = 28 Hz, H−P(*C*(CH$_3$)$_3$), 33.6 (Pt−P(C(*C*H$_3$)$_3$), 30.6 (H−P(C(*C*H$_3$)$_3$).

^{31}P{^{1}H} NMR (160 MHz, CD_2Cl_2, 25 ºC) δ: 128.3 ($^{2}J_{PSn}$ = 110 Hz, $^{1}J_{PPt}$ = 4874 Hz, Pt−P(C(CH$_3$)$_3$), 51.9 (H−P(^{t}Bu)$_3$).

UV-vis (CH_2Cl_2) λ_{max} (ε [cm^{-1} M^{-1}]): 572 nm (102).

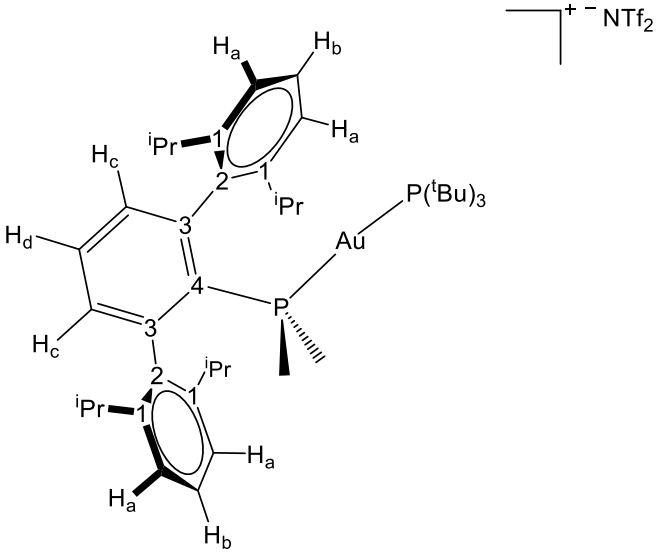

Compound 26. A dichloromethane (5 mL) solution of compound **1b** (50 mg, 0.05 mmol) was treated with P^{t}Bu$_3$ (10.7 mg, 0.05 mmol) under argon atmosphere. The solution was stirred at -80 ºC for 5 min and the temperature was slowly raised to 25 ºC. Compound **26** was precipitated by the addition of pentane as a white solid that was further washed with the same solvent (49 mg, 86%).

^{1}H NMR (400 MHz, CD_2Cl_2, 25 ºC) δ: 7.60 (td, 1 H, $^3J_{HH}$ = 7.6 Hz, $^5J_{HP}$ = 1.7 Hz, H_d), 7.44 (t, 2 H, $^3J_{HH}$ = 7.6 Hz, H_b), 7.31 (d, 4 H, $^3J_{HH}$ = 7.6 Hz, H_a), 7.23 (dd, 2 H, $^3J_{HH}$ = 7.6 Hz, $^4J_{HP}$ = 3.4 Hz, H_c), 2.53 (sept, 4 H, $^3J_{HH}$ = 6.8 Hz, ^{i}Pr(CH)), 1.57 (d, 6 H, $^2J_{HP}$ = 10.4 Hz, PMe_2), 1.35 (d, 27 H, $^3J_{HP}$ = 15 Hz, ^{t}Bu), 1.23 (d, 12 H, $^3J_{HH}$ = 7.0 Hz, ^{i}Pr(CH_3)), 1.06 (d, 12 H, $^3J_{HH}$ = 7.0 Hz, ^{i}Pr(CH_3)).

^{13}C{^{1}H} NMR (100 MHz, CD_2Cl_2, 25 ºC) δ: 146.6 (C_1), 146.1 (d, $^2J_{CP}$ = 10 Hz, C_3), 137.7 (d, $^3J_{CP}$ = 3 Hz, C_2), 132.9 (d, $^3J_{CP}$ = 7 Hz, CH_c), 129.9 (CH_d), 125.2 (CH_b), 123.8 (CH_a), 119.7 (q, $^1J_{CF}$ = 323 Hz, CF_3), 39.9

(d, $^{1}J_{CP}$ = 16 Hz, P(*C*(CH_3)$_3$), 32.3 (P(C(*C*H_3)$_3$), 31.3 (^{i}Pr(CH)), 25.0 (^{i}Pr(CH_3)), 22.9 (^{i}Pr(CH_3)), 16.0 (d, $^{1}J_{CP}$ = 34 Hz, PMe_2).

^{31}P{^{1}H} NMR (160 MHz, CD_2Cl_2, 25 ºC) δ: 100.6 ($^{2}J_{PP}$ = 312 Hz), 14.6 ($^{2}J_{PP}$ = 312 Hz).

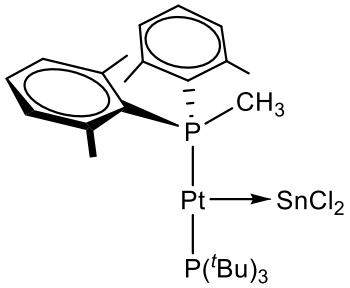

Compound 27. An NMR tube was charged with $PMeXyl_2$ (18 mg, 0.075 mmol), $Pt(P^tBu_3)_2$ (30 mg, 0.05 mmol), tin(II) dichloride (14.4 mg, 0.075 mmol) and deuterated benzene or toluene (0.5 mL). The initial white suspension became a red solution after several hours and was stirred for an overall period of 8 hours. (85% NMR yield).

HRMS (electrospray, m/z): **calcd** for $C_{29}H_{49}P_2Pt$: $[M - SnCl_2 + H]^+$ 654.7249, **found** 654.2952.

^{1}H NMR (400 MHz, tol-d_8, 25 ºC) δ: 6.90 (t, 2 H, $^3J_{HH}$ = 7.4 Hz, *p*-C_6H_3), 6.76 (dd, 4 H, $^3J_{HH}$ = 7.4 Hz, $^4J_{HP}$ = 3.6 Hz, *m*-C_6H_3), 2.93 (dd, 3 H, $^3J_{HPt}$ = 50.7 Hz, $^2J_{HP}$ = 9.0 Hz, $^4J_{HP}$ = 2.5 Hz, PMe), 2.51 (s, 12 H, Me_{Xyl}), 1.15 (d, 27 H, $^3J_{HP}$ = 12.6 Hz, ^{t}Bu).

^{13}C{^{1}H} NMR (100.6 MHz, C_6D_6, 25 ºC) δ: 141.6 (d, $^2J_{CP}$ = 9 Hz, *o*-C_6H_3), 134.0 (d, $^1J_{CP}$ = 48 Hz, *ipso*-C_6H_3), 130.0 (d, $^3J_{CP}$ = 8 Hz, *m*-C_6H_3), 129.1 (d, $^4J_{CP}$ = 2 Hz, *p*-C_6H_3), 39.2 (d, $^1J_{CP}$ = 13, $^2J_{CPt}$ = 55 Hz, Pt−P(*C*$(CH_3)_3$), 32.2 (Pt−P(C(*C*$H_3)_3$), 25.1 (d, $^3J_{CP}$ = 7 Hz, Me_{Xyl}), 21.0 (d, $^1J_{CP}$ = 37 Hz, PMe).

^{31}P{^{1}H} NMR (161.98 MHz, tol-d_8, 25 ºC) δ: 94.6 (d, $^1J_{PPt}$ = 3776 Hz, $^2J_{PP}$ = 299 Hz, $^2J_{PSn}$ = 250 Hz, P^tBu_3), 6.3 (d, $^1J_{PPt}$ = 3244 Hz, $^2J_{PP}$ = 299 Hz, PMeXyl).

^{195}Pt{^{1}H} NMR (86.16 MHz, tol-d_8, 25 ºC) δ: -4947 (dd, $^{1}J_{PPt}$ = 3776 Hz, $^{1}J_{PtP}$ = 3244 Hz, $^{1}J_{PtSn}$ = 3210 Hz).

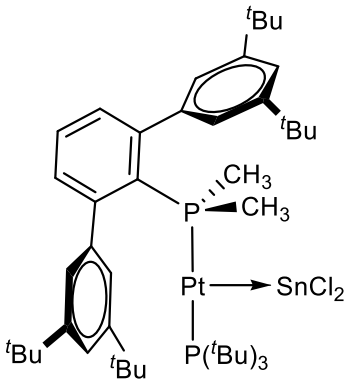

Compound 28. An NMR tube was charged with PMe_2Ar^{Dtbp2} (38.7 mg, 0.075 mmol), compound **2** (30 mg, 0.05 mmol), tin(II) dichloride (14.4 mg, 0.075 mmol) and deuterated benzene or toluene (0.5 mL). The initial white suspension became a red solution after several hours and was stirred for an overall period of one day after which we determined a spectroscopic yield of *ca*. 50%.

HRMS (electrospray, m/z): **calcd** for $C_{48}H_{78}P_2Pt$: [M – $SnCl_2$] 912.1584, **found** 912.5291.

^{1}H NMR (400 MHz, C_6D_6, 25 ºC) δ: 7.27-7.23 (m, 8H, Ar), 7.07 (td, 1H, $^3J_{HH}$ = 7.5 Hz, $^5J_{HP}$ = 1.5 Hz, *p*-C_6H_3), 1.98 (dd, 6 H, $^2J_{HP}$ = 10.0 Hz, $^4J_{HP}$ = 1.9 Hz, PMe_2), 1.49 (br, 36 H, ^{t}Bu (PMe_2Ar^{Dtbp2})), 1.34 (d, 27 H, $^3J_{HP}$ = 12.6 Hz, ^{t}Bu (P^tBu_3)).

^{13}C{^{1}H} NMR (100.6 MHz, C_6D_6, 25 ºC) δ: 151.7 (s, *m*-Dtbp), 149.9 (d, $^2J_{CP}$ = 10 Hz, *o*-C_6H_3), 141.7 (d, $^3J_{CP}$ = 4 Hz, *ipso*-Dtbp), 131.7 (d, $^1J_{CP}$ = 8 Hz, *ipso*-C_6H_3), 130.7 (d, $^4J_{CP}$ = 7 Hz, *m*-C_6H_3), 127.8 (*p*-C_6H_3), 124.6 (s, *o*-Dtbp), 121.6 (s, *p*-Dtbp), 39.6 (d, $^1J_{CP}$ = 12, $^2J_{CPt}$ = 42 Hz, Pt−P(*C*(CH_3)$_3$), 34.8 (s, *C*(CH_3)), 32.4 (Pt−P(C(*C*H_3)$_3$), 31.9 (s, C(*C*H_3)), 19.5 (d, $^1J_{CP}$ = 36 Hz, PMe_2).

$^{31}P\{^{1}H\}$ NMR (161.98 MHz, C_6D_6, 25 ºC) δ: 97.3 (d, $^{1}J_{PPt}$ = 3788 Hz, $^{2}J_{PP}$ = 307 Hz, $^{2}J_{PSn}$ = 255 Hz, P^{t}Bu$_3$), 12.6 (d, $^{1}J_{PPt}$ = 3504 Hz, $^{2}J_{PP}$ = 307 Hz, PAr^{tBu}).

$^{195}Pt\{^{1}H\}$ NMR (86.16 MHz, C_6D_6, 25 ºC) δ: -5067 (dd, $^{1}J_{PPt}$ = 3788 Hz, $^{1}J_{PtP}$ = 3504 Hz).

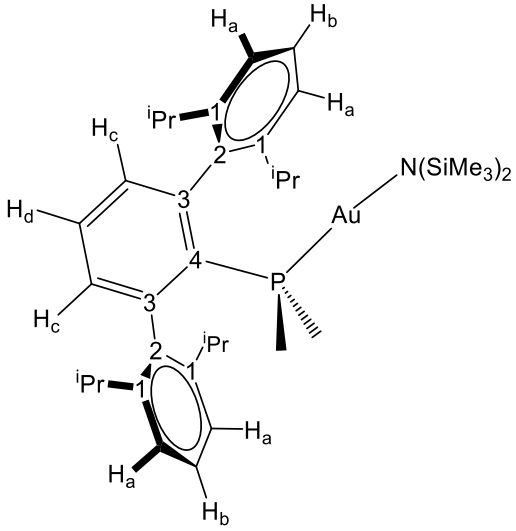

[PMe$_2$Ar^{Dipp2}]Au[N(SiMe$_3$)$_2$]. A solid mixture of compound (PMe$_2$Ar^{Dipp2})AuCl (30 mg, 0.043 mmol) and Li[N(SiMe$_3$)$_2$] (7 mg, 0.043 mmol) was suspended in toluene inside a dry box. The solution was stirred for 30 min, filtered and the solvents evaporated under vacuum. The white residue was washed with pentane to yield [PMe$_2$Ar^{Dipp2}]Au[N(SiMe$_3$)$_2$] as a white solid (28 mg, 80%).

^{1}H NMR (400 MHz, C$_6$D$_6$, 25 ºC) δ: 7.28 (t, 2 H, $^3J_{HH}$ = 7.6 Hz, H$_b$), 7.12 (d, 4 H, $^3J_{HH}$ = 7.6 Hz, H$_a$), 6.93 (m, 2 H, H$_c$), 6.85 (m, 1 H, H$_d$), 2.77 (sept, 4 H, $^3J_{HH}$ = 6.8 Hz, ^{i}Pr(CH)), 1.39 (d, 12 H, $^3J_{HH}$ = 6.8 Hz, ^{i}Pr(CH$_3$)), 0.98 (d, 12 H, $^3J_{HH}$ = 6.8 Hz, ^{i}Pr(CH$_3$)), 0.88 (d, 6 H, $^2J_{HP}$ = 10 Hz, PMe$_2$), 0.41 (s, 18 H, SiMe$_3$).

^{13}C{^{1}H} NMR (100 MHz, C$_6$D$_6$, 25 ºC) δ: 146.9 (C$_1$), 143.8 (d, $^2J_{CP}$ = 10 Hz, C$_3$), 139.2 (d, $^3J_{CP}$ = 5 Hz, C$_2$), 132.9 (d, $^3J_{CP}$ = 8 Hz, CH$_c$), 130.1 (d, $^1J_{CP}$ = 46 Hz, C$_4$), 129.6 (CH$_d$), 128.6 (CH$_b$), 123.6 (CH$_a$), 31.5 (^{i}Pr(CH)), 25.7 (^{i}Pr(CH$_3$)), 23.6 (^{i}Pr(CH$_3$)), 18.1 (d, $^1J_{CP}$ = 37 Hz, PMe$_2$), 6.7 ($^1J_{CSi}$ = 38 Hz, SiMe$_3$).

^{31}P{^{1}H} NMR (160 MHz, C$_6$D$_6$, 25 ºC) δ: 3.1.

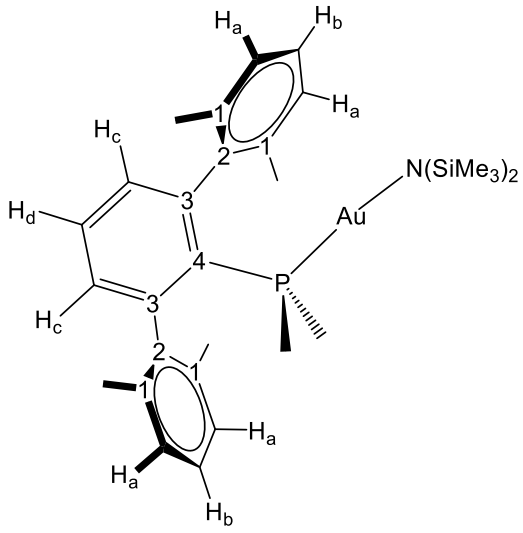

[PMe$_2$Ar^{Xyl2}]Au[N(SiMe$_3$)$_2$]. A solid mixture of compound (PMe$_2$Ar^{Xyl2})AuCl (35 mg, 0.06 mmol) and Li[N(SiMe$_3$)$_2$] (10 mg, 0.04 mmol) was suspended in toluene inside a dry box. The solution was stirred for 30 min, filtered and the solvents evaporated under vacuum. The white residue was washed with pentane to yield [PMe$_2$Ar^{Xyl2}]Au[N(SiMe$_3$)$_2$] as a white solid (29 mg, 69%).

^{1}H NMR (400 MHz, C_6D_6, 25 ºC) δ: 7.08 (t, 2 H, $^3J_{HH}$ = 7.6 Hz, H_b), 6.99 (d, 4 H, $^3J_{HH}$ = 7.6 Hz, H_a), 6.95 (td, 1 H, $^3J_{HH}$ = 7.6 Hz, $^5J_{HP}$ = 1.7 Hz, H_d), 6.58 (dd, 2 H, $^3J_{HH}$ = 7.6 Hz, $^4J_{HP}$ = 3.1 Hz, H_c), 2.11 (s, 12 H, Me_{Xyl}), 0.67 (d, 6 H, $^2J_{HP}$ = 9.4 Hz, PMe_2), 0.48 (s, 18 H, $SiMe_3$).

^{13}C{^{1}H} NMR (100 MHz, C_6D_6, 25 ºC) δ: 145.6 (d, $^2J_{CP}$ = 9 Hz, C_3), 141.3 (d, $^3J_{CP}$ = 3 Hz, C_2), 136.5 (C_1), 130.9 (CH_d), 130.8 (CH_c), 129.6 (d, $^1J_{CP}$ = 60 Hz, C_4), 128.7 (CH_b), 128.4 (CH_a), 22.2 (Me_{Xyl}), 17.2 (d, $^1J_{CP}$ = 38 Hz, PMe_2), 6.8 ($^1J_{CSi}$ = 53 Hz, $SiMe_3$).

^{31}P{^{1}H} NMR (160 MHz, C_6D_6, 25 ºC) δ: 1.5.

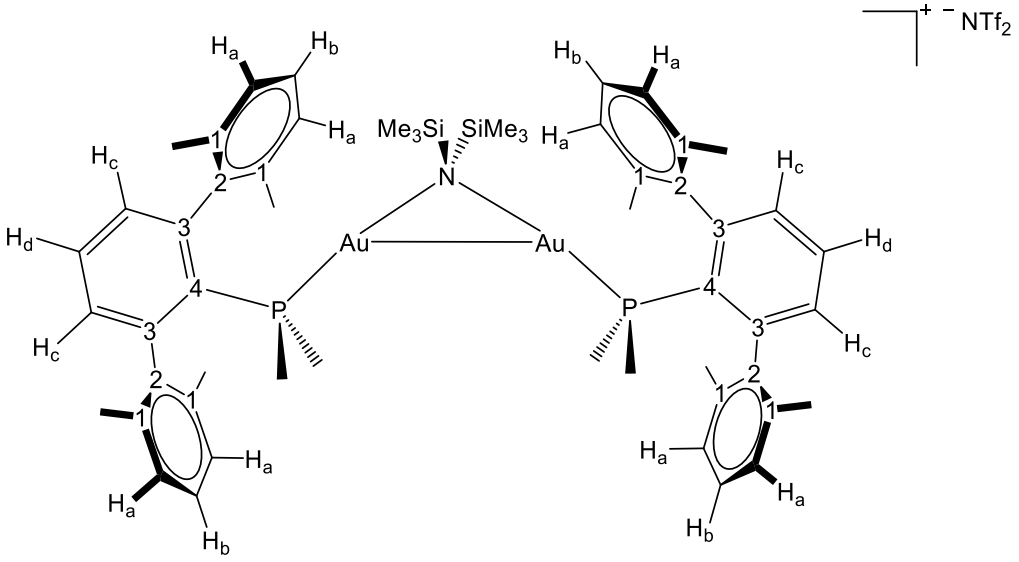

[Au$_2$(μ-N(SiMe$_3$)$_2$)(PMe$_2$Ar^{Xyl2})$_2$]. A solid mixture of compounds **1a** (35 mg, 0.04 mmol) and [PMe$_2$Ar^{Xyl2}]Au[N(SiMe$_3$)$_2$] (30 mg, 0.04 mmol) was dissolved in toluene inside a dry box. The solution was stirred for 30 min and the solvents evaporated under vacuum. The white residue was washed with pentane to yield [Au$_2$(μ-N(SiMe$_3$)$_2$)(PMe$_2$Ar^{Xyl2})$_2$] as a white solid (44 mg, 88%).

^{1}H NMR (400 MHz, C_6D_6, 25 ºC) δ: 7.16 (t, 2 H, $^3J_{HH}$ = 7.6 Hz, H_b), 7.03 (d, 4 H, $^3J_{HH}$ = 7.6 Hz, H_a), 6.95 (td, 1 H, $^3J_{HH}$ = 7.6 Hz, $^5J_{HP}$ = 1.7 Hz, H_d), 6.61 (dd, 2 H, $^3J_{HH}$ = 7.6 Hz, $^4J_{HP}$ = 3.1 Hz, H_c), 1.98 (s, 12 H, Me_{Xyl}), 0.87 (d, 6 H, $^2J_{HP}$ = 10.0 Hz, PMe_2), 0.25 (s, 18 H, $SiMe_3$).

^{13}C{^{1}H} NMR (100 MHz, C_6D_6, 25 ºC) δ: 146.11 (d, $^2J_{CP}$ = 10 Hz, C_3), 140.8 (C_2), 140.1 (C_1), 136.3 (CH_d), 132.1 (CH_c), 125.4 (d, $^1J_{CP}$ = 55 Hz, C_4), 131.1 (CH_b), 129.1 (CH_a), 120.3 (q, $^1J_{CF}$ = 323 Hz, CF_3), 21.7 (Me_{Xyl}), 17.7 (d, $^1J_{CP}$ = 43 Hz, PMe_2), 6.6 ($SiMe_3$).

^{31}P{^{1}H} NMR (160 MHz, C_6D_6, 25 ºC) δ: -3.4.

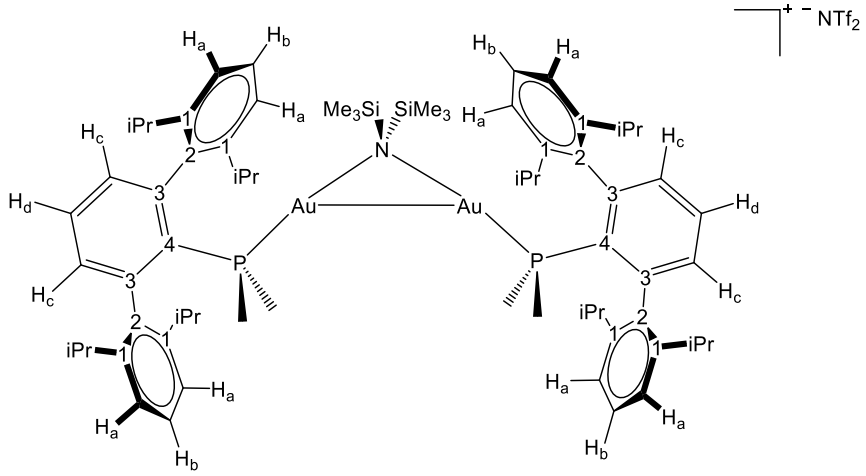

[Au$_2$(μ-N(SiMe$_3$)$_2$)(PMe$_2$Ar^{Dipp2})$_2$]. A solid mixture of compounds **1b** (36 mg, 0.04 mmol) and [PMe$_2$Ar^{Dipp2}]Au[N(SiMe$_3$)$_2$] (32 mg, 0.04 mmol) was dissolved in toluene inside a dry box. The solution was stirred for 30 min and the solvents evaporated under vacuum. The white residue was washed with pentane to yield [Au$_2$(μ-N(SiMe$_3$)$_2$)(PMe$_2$Ar^{Dipp2})$_2$] as a white solid (49 mg, 83%).

^{1}H NMR (400 MHz, C_6D_6, 25 ºC) δ: 7.31 (t, 2 H, $^3J_{HH}$ = 7.6 Hz, H_b), 7.14 (d, 4 H, $^3J_{HH}$ = 7.6 Hz, H_a), 6.96 (m, 2 H, H_c, H_d), 2.56 (sept, 4 H, $^3J_{HH}$ = 6.8 Hz, ^{i}Pr(CH)), 1.33 (d, 12 H, $^3J_{HH}$ = 6.7 Hz, ^{i}Pr(CH$_3$)), 0.95 (d, 12 H, $^3J_{HH}$ = 6.6 Hz, ^{i}Pr(CH$_3$)), 0.14 (s, 18 H, SiMe$_3$).

^{13}C{^{1}H} NMR (100 MHz, C_6D_6, 25 ºC) δ: 146.6 (C_1), 145.4 (d, $^2J_{CP}$ = 10 Hz, C_3), 138.2 (d, $^3J_{CP}$ = 5 Hz, C_2), 133.3 (d, $^3J_{CP}$ = 8 Hz, CH_c), 130.3 (CH_d), 129.8 (d, $^1J_{CP}$ = 47 Hz, C_4), 127.4 (CH_b), 124.1 (CH_a), 120.5 (q, $^1J_{CF}$ = 323 Hz, CF_3), 31.6 (^{i}Pr(CH)), 25.5 (^{i}Pr(CH$_3$)), 23.6 (^{i}Pr(CH$_3$)), 19.3 (d, $^1J_{CP}$ = 39 Hz, PMe$_2$), 7.6 (SiMe$_3$).

^{31}P{^{1}H} NMR (160 MHz, C_6D_6, 25 ºC) δ: -7.8.

II.3.2. Kinetic Studies for the Activation of Dihydrogen

Kinetic studies were carried out to determine the kinetic isotopic effect (KIE) of dihydrogen activation by both the bimetallic pair **1b**:**2** and the presynthesized Lewis adduct **4a**. Reaction progress was monitored by ^{1}H and $^{31}P\{^{1}H\}$ NMR spectroscopy following a similar procedure for the two systems:

- **TMOFLP 1b:2:** In a *J. Young* NMR tube, a mixture of compounds **1b** (8 mg, 0.008 mmol) and **2** (5 mg, 0.008 mmol) was dissolved in toluene-d_8 (0.5 mL) at -80 ºC. H_2 or D_2 (2 bar) was added and the solution was shaken. The progress of the reaction was monitored by ^{1}H and $^{31}P\{^{1}H\}$ NMR spectroscopy at -20 ºC by means of the disappearance of compound **2** and using hexamethylbenzene or triphenylphosphine oxide as internal standards.

- **Adduct 4a**: In a *J. Young* NMR tube, adduct **4a** (10 mg, 0.007 mmol) was dissolved in C_6D_6 (0.5 mL) at room temperature. H_2 or D_2 (2 bar) was added and the solution was shaken. The progress of the reaction was monitored by ^{1}H and $^{31}P\{^{1}H\}$ NMR spectroscopy at 25 ºC by means of the disappearance of adduct **4a** and using hexamethylbenzene or PPh_3 as internal standards.

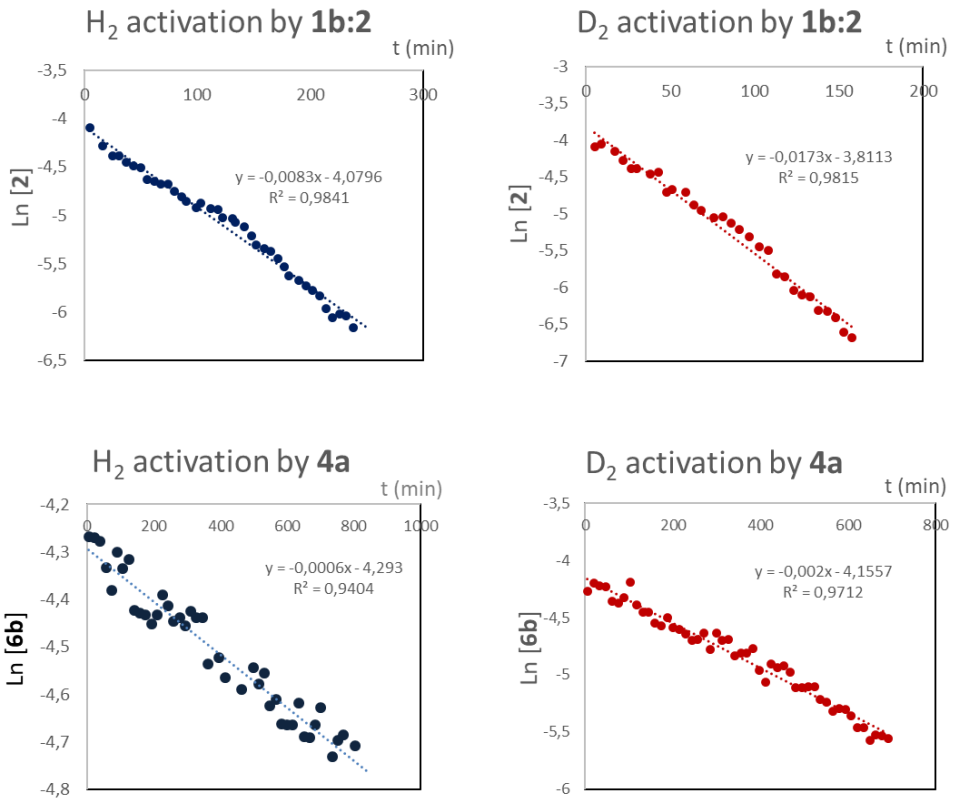

Figure 32. Representative examples of the kinetic profiles for the activation of H_2 or D_2 in the two examined systems.

II.3.3. Computational Details

DFT calculations were perfomed by Dr. Joaquín López Serrano and Dr. Juan José Moreno Díaz. Geometry optimization of minima and transition states was carried out with the Gaussian software package.[83] Optimizations were carried out without symmetry restrictions using the ωB97xD functional[84] that includes empirical dispersion corrections.[85] The 6-31g(d,p) basis set[86] was used for non-metal atoms, Au and Pt atoms were described with the SDD basis and associated electron core potential (ECP).[87] Bulk solvent effects (benzene and dichloromethane) were included during optimization with the SMD continuum model.[20] Free energies were corrected (ΔG_{qh}) to account for errors associated with the harmonic oscillator approximation. Thus, according to Truhlars's quasi harmonic approximation, all vibrational frequencies below 100 cm^{-1} were set to this

[83] Gaussian 09, Revision B.01, M. J. Frisch, G. W. Trucks, H. B. Schlegel, G. E. Scuseria, M. A. Robb, J. R. Cheeseman, G. Scalmani, V. Barone, B. Mennucci, G. A. Petersson, H. Nakatsuji, M. Caricato, X. Li, H. P. Hratchian, A. F. Izmaylov, J. Bloino, G. Zheng, J. L. Sonnenberg, M. Hada, M. Ehara, K. Toyota, R. Fukuda, J. Hasegawa, M. Ishida, T. Nakajima, Y. Honda, O. Kitao, H. Nakai, T. Vreven, J. A. Montgomery Jr., J. E. Peralta, F. Ogliaro, M. Bearpark, J. J. Heyd, E. Brothers, K. N. Kudin, V. N. Staroverov, T. Keith, R. Kobayashi, J. Normand, K. Raghavachari, A. Rendell, J. C. Burant, S. S. Iyengar, J. Tomasi, M. Cossi, N. Rega, J. M. Millam, M. Klene, J. E. Knox, J. B. Cross, V. Bakken, C. Adamo, J. Jaramillo, R. Gomperts, R. E. Stratmann, O. Yazyev, A. J. Austin, R. Cammi, C. Pomelli, J. W. Ochterski, R. L. Martin, K. Morokuma, V. G. Zakrzewski, G. A. Voth, P. Salvador, J. J. Dannenberg, S. Dapprich, A. D. Daniels, O. Farkas, J. B. Foresman, J. V. Ortiz, J. Cioslowski, and D. J. Fox, Gaussian, Inc., Wallingford CT, **2010**.
[84] J.-D. Chai, M. Head-Gordon. *Phys. Chem. Chem. Phys*. **2008**, *10*, 6615–6620.
[85] S. Grimme. *J. Comp. Chem.* **2006**, *27*, 1787–1799.
[86] a) R. Ditchfield, W. J. Hehre, J. A. Pople. *J. Chem. Phys.* **1971**, *54*, 724–728. b) W. J. Hehre, R. Ditchfield, J. A. Pople. *J. Chem. Phys.* **1972**, *56*, 2257–2261. c) P. C. Hariharan, J. A. Pople. *Theor. Chim. Acta* **1973**, *28*, 213–222. d) M. M. Francl, W. J. Pietro, W. J. Hehre, J. S. Binkley, M. S. Gordon, D. J. DeFrees, J. A. Pople. *J. Chem. Phys.* **1982**, *77*, 3654–3665.
[87] D. Andrae, U. Haeussermann, M. Dolg, H. Stoll, H. Preuss. *Theor. Chim. Acta* **1990**, *77*, 123–141.

value so that the entropy contribution is not overestimated.[88] These anharmonic corrections were calculated with the Goodvibes code.[89] NBO analysis was performed with the NBO6.0 suite.[90] Analysis of the electron density was performed within the Atoms In Molecules (AIM) theory of R. F. W. Bader[91] using the Multiwfn program.[92] The CYLview visualization software has been used to create some of the figures.[93]

[88] R. F. Ribeiro, A. V. Marenich, C. J. Cramer, D. G. Truhlar. *J. Phys. Chem. B* **2011**, *115*, 14556–14562.

[89] I. Funes-Ardoiz, R. S. Paton, (2016). Goodvibes: Goodvibes 2.0.2 http://doi.org/10.5281/zenodo.595246

[90] NBO 6.0. E. D. Glendening, J. K. Badenhoop, A. E. Reed, J. E. Carpenter, J. A. Bohmann, C. M. Morales, C. R. Landis, and F. Weinhold (Theoretical Chemistry Institute, University of Wisconsin, Madison, WI, 2013); http://nbo6.chem.wisc.edu/

[91] R. F. W. Bader, Atom in Molecules: A Quantum Theory; Oxford University Press: Oxford, UK, 1995.

[92] a) Multiwfn: A multifunctional wavefunction analyser. T. Lu, F. Chen. *J. Comput. Chem.* **2012**, 33, 580–592. b) Multiwfn 3.6, http://sobereva.com/multiwfn/

[93] CYLview, 1.0b; Legault, C. Y., Université de Sherbrooke, 2009 (http://www.cylview.org)

II.4. References

1. a) D. W. Stephan. *Coord. Chem. Rev.* **1989**, *95*, 41–107. b) N. Wheatley, P. Kalck. *Chem. Rev.* **1999**, *99*, 3379–3420. c) L. H. Gade. *Angew. Chem. Int. Ed.* **2000**, *39*, 2658–2678. d) B. G. Cooper, J. W. Napoline , C. M. Thomas. *Catalysis Reviews* **2012**, *54*, 1–40. e) M. Herberhold, G.-X. Jin. *Angew. Chem. Int. Ed.* **1994**, *33*, 964–966.

2. A. M. Chapman, S. R. Flynn, D. F. Wass. *Inorg. Chem.* **2016**, *55*, 1017–1021.

3. M. Devillard, R. Declercq, E. Nicolas, A. W. Ehlers, J. Backs, N. Saffon-Merceron, G. Bouhadir, J. C. Slootweg, W. Uhl, D. Bourissou. *J. Am. Chem. Soc.* **2016**, *138*, 4917–4926.

4. T. P. Brewster, T. H. Nguyen, Z. Li, W. T. Eckenhoff, N. D. Schley, N. J. DeYonker. *Inorg. Chem.* **2018**, *57*, 1148–1157.

5. R. M. Charles III, T. W. Yokley, N. D. Schley, N. J. DeYonker, T. P. Brewster. *Inorg. Chem.* **2019**, *58*, 12635–12645.

6. J. Campos. *J. Am. Chem. Soc.* **2017**, *139*, 2944–2947.

7. T. A. Rokob, A. Hamza, A. Stirling, I. Pápai. *J. Am. Chem. Soc*. **2009**, *131*, 2029−2036.

8. F.-G. Fontaine, D. W. Stephan. *Philos. Trans. R. Soc. A,* **2017**, *375*, 20170004.

9. a) T. Mahdi, D. W. Stephan. *J. Am. Chem. Soc*. **2014**, *136*, 15809−15812. b) D. J. Scott, M. J. Fuchter, A. E. Ashley. *J. Am. Chem. Soc.* **2014**, *136*, 15813–15816. c) M. A. Légaré, E. Rochette, J. Légaré Lavergne, N. Bouchard, F.-G. Fontaine. *Chem. Commun*. **2016**, *52*, 5387–5390.

10. J. Légaré Lavergne, A. Jayaraman, L. C. Misal Castro, E. Rochette, F.-G. Fontaine. *J. Am. Chem. Soc.* **2017**, *139*, 14714−14723.

11. M. V. Mane, K. Vanka. *ChemCatChem* **2017**, *9*, 3013−3022.

12. See for example: a) M. K. Karunananda, S. R. Parmelee, G. W. Waldhart, N. P. Mankad. *Organometallics* **2015**, *34*, 3857−3864. b) L.-J. Cheng, N. P. Mankad. *J. Am. Chem. Soc.* **2019**, *141*, 3710−3716. c) I. M. Riddlestone, N. A. Rajabi, J. P. Lowe, M. F. Mahon, S. A. Macgregor, M. K. Whittlesey. *J. Am. Chem. Soc*. **2016**, *138*, 11081−11084. d) K. M. Gramigna, D. A. Dickie, B. M. Foxman, C. M. Thomas. *ACS Catalysis*, **2019**, *9*, 3153−3164. e) A. M. Baranger, R. G. Bergman. *J. Am. Chem. Soc*. **1994**, *116*, 3822–3835. f) C. M. Thomas, J. W. Napoline, G. T. Rowe, B. M. Foxman. *Chem. Commun*. **2010**, *46*, 5790– 5792.

13. J. Bauer, H. Braunschweig, R. D. Dewhurst. *Chem. Rev.* **2012**, *112*, 4329−4346.

14. M. Marín, J. J. Moreno, M. M. Alcaide, E. Álvarez, J. López-Serrano, J. Campos, M. C. Nicasio, E. Carmona. *J. Organomet. Chem.* **2019**, *896*, 120−128.

15. M. F. Espada, J. Campos, J. López-Serrano, M. L. Poveda, E. Carmona. *Angew. Chem. Int. Ed.* **2015**, *54*, 15379−15384.

16. L. X. Dang, G. K. Schenter, T.-M. Chang, S. M. Kathmann, T. Autrey. *J. Phys. Chem. Lett.* **2012**, *3*, 3312−3319.

17. a) A. M. Chapman, M. F. Haddow, D. F. Wass. *Eur. J. Inorg. Chem.* **2012**, *9*, 1546–1554. b) O. J. Metters, S. J. K. Forrest, H. A. Sparkes, I. Manners, D. W. Wass. *J. Am. Chem. Soc.* **2016**, *138*, 1994–2003. c) A. M. Chapman, M. F. Haddow, D. F. Wass. *J. Am. Chem. Soc.* **2011**, *133*, 18463–18478. d) S. R. Flynn, O. J. Metters, I. Manners, D. F. Wass. *Organometallics* **2016**, *35*, 847–850. e) O. J. Metters, S. R. Flynn, C. K. Dowds, H. A. Sparkes, I. Manners, D. F. Wass. *ACS Catal.* **2016**, *6*, 6601–6611. f) H. B. Hamilton, A. M. King, H. A. Sparkes, N. E. Pridmore, D. F. Wass. *Inorg. Chem.* **2019**, *58*, 6399−6409.

18. J. Bauer, H. Braunschweig, A. Damme, K. Radacki. *Angew. Chem. Int. Ed*. **2012**, *51*, 10030–10033.

19. a) H. Braunschweig, K. Radacki, K. Schwab. *Chem. Commun*. **2010**, *46*, 913–915. b) J. Bauer, H. Braunschweig, P. Brenner, K. Kraft, K. Radacki, K. Schwab. *Chem. Eur. J.* **2010**, *16*, 11985−11992. c) M.

Ma, A. Sidiropoulos, L. Ralte, A. Stasch, C. Jones. *Chem. Commun.* **2013**, *49*, 48–50. d) H. Braunschweig, R. D. Dewhurst, F. Hupp, C. Schneider. *Chem. Commun*. **2014**, *50*, 15685–15688. e) B. R. Barnett, C. E. Moore, P. Chandrasekaran, S. Sproules, A. L. Rheingold, S. DeBeerde, J. S. Figueroa. *Chem. Sci*. **2015**, *6*, 7169−7178.

20. A. V. Marenich, C. J. Cramer, D. G. Truhlar. *J. Phys. Chem. B* **2009**, *113*, 6378−6396.

21. a) T. A. Rokob, I. Pápai. *Top. Curr. Chem.* **2013**, *332*, 157−211. b) J. Paradies. *Eur. J. Org. Chem*. **2019**, 283–294. c) L. Rocchigiani. *Isr. J. Chem*. **2015**, *55*, 134–149. d) L. Liu, B. Lukose, P. Jaque, B. Ensing. *Green Energy Environ.* **2019**, *4*, 20–28.

22. a) G. Skara, F. De Vleeschouwer, P. Geerlings, F. De Proft, B. Pinter. *Sci. Rep.* **2017**, *7*, 16024. b) J. Daru, I. Bakó, A. Stirling, I. Pápai. *ACS Catal.* **2019**, *9*, 6049−6057. c) S. Grimme, H. Kruse, L. Goerigk, G. Erker. *Angew. Chem. Int. Ed.* **2010**, *49*, 1402–1405. d) D. Yepes, P. Jaque, I. Fernández. *Chem. Eur. J.* **2016**, *22*, 18801–18809. e) L. Liu, L. L. Cao, Y. Shao, G. Ménard, D. W. Stephan. *Chem*, **2017**, *3*, 259–267. f) H. B. Hamilton, D. F. Wass. *Chem*, **2017**, *3*, 198–210. g) T. A. Rokob, I. Bakó, A. Stirling, A. Hamza, I. Pápai. *J. Am. Chem. Soc.* **2013**, *135*, 4425−4437. h) G. Bistoni, A. A. Auer, F. Neese. *Chem. Eur. J.* **2017**, *23*, 865–873.

23. S. R. Flynn, D. F. Wass. *ACS Catal.* **2013**, *3*, 2574–2581.

24. a) R. M. Bullock, G. M. Chambers. *Phil. Trans. R. Soc. A*, **2017**, *375*, 20170002. b) M. K. Karunanan, N. P. Mankad. *ACS Catal.* **2017**, *7*, 6110−6119. c) E. R. M. Habraken, A. R. Jupp, M. B. Brands, M. Nieger, A. W. Ehlers, C. J. Slootweg. *Eur. J. Inorg. Chem.* **2019**, 2436–2442.

25. a) N. P. Mankad. *Chem. Commun*. **2018**, *54*, 1291–1302. b) I. G. Powers, C. Uyeda. *ACS Catal.* **2017**, *7*, 936−958. c) R. C. Cammarota, L. J. Clouston, C. C. Lu. *Coord. Chem. Rev*. **2017**, *334*, 100–111. d) J. Berry, C. C. Lu. *Inorg. Chem.* **2017**, *56*, 7577−7581. e) N. P. Mankad. *Chem. Eur. J.* **2016**, *22*, 5822–5829.

26. R. G. Goel, R. C. Srivastava. *Can. J. Chem.* **1983**, *61*, 1352−1359.

27. R. G. Goel, W. O. Ogiri, R. C. Srivastava. *Organometallics* **1982**, *1*, 819–824.

28. a) C. González-Arellano, A. Corma, M. Iglesias, F. Sánchez. *Chem. Commun*. **2005**, 3451–3453. b) A. Comas-Vives, G. Ujaque. *J. Am. Chem. Soc.* **2013**, *135*, 1295−1305.

29. a) E. Y. Tsui, P. Muller, J. P. Sadighi. *Angew. Chem. Int. Ed.* **2008**, *47*, 8937–8940. b) A. Escalle, G. Mora, F. Gagosz, N. Mezailles, X. F. Le Goff, Y. Jean, P. Le Floch. *Inorg. Chem.* **2009**, *48*, 8415–8422. c) R. J. Harris, R. A. Widenhoefer. *Angew. Chem. Int. Ed*. **2014**, *53*, 9369–9371.

30. H. Schmidbaurab, A. Schiera. *Chem. Soc. Rev*. **2012**, *41*, 370–412.

31. N. Phillips, T. Dodson, R. Tirfoin, J. I. Bates, S. Aldridge. *Chem. Eur. J.* **2014**, *20*, 16721–16731.

32. S. Tussing, L. Greb, S. Tamke, B. Schirmer, C. Muhle-Goll, B. Luy, J. Paradies. *Chem. Eur. J.* **2015**, *21*, 8056–8059.

33. A. J. Esswein, A. S. Veige, P. M. B. Piccoli, A. J. Schultz, D. G. Nocera. *Organometallics* **2008**, *27*, 1073–1083.

34. Y. Zhang, M. K. Karunananda, H.-C. Yu, K. J. Clark, W. Williams, N. P. Mankad, D. H. Ess. *ACS Catal.* **2019**, *9*, 2657−2663.

35. Computational studies at the ωB97xD/6-31g(d,p)+SDD level carried out by Drs. Joaquín López Serrano and Juan José Moreno.

36. The calculations yield a geometry for **6b** with a different conformation of the terphenyl phosphine that is 9.9 kcal·mol^{-1} above than the most stable conformation used as the origin of energies. See M. Marín, J. J. Moreno, C. Navarro-Gilabert, E. Álvarez, C. Maya, R. Peloso, M. C. Nicasio, E. Carmona. *Chem. Eur. J.* **2019**, *25*, 260–272.

37. A recent study on H_2 activation by a N/Sn Lewis pair supports a related role for the couteranion (OTf^-) to the acidic $^iPr_3Sn^+$ fragment: S. Das, S. Mondal, S. K. Pati. *Chem. Eur. J.* **2018**, *24*, 2575–2579.

38. J. J. Cabrera-Trujillo, I. Fernández. *Inorg. Chem.* **2019**, *58*, 7828−7836.

39. a) T.-Y. Cheng, R. M. Bullock. *J. Am. Chem. Soc.* **1999**, *121*, 3150−3155. b) H. C. Lo, A. Haskel, M. Kapon, E. Keinan. *J. Am. Chem. Soc.* **2002**, *124*, 3226−3228.

40. J. Bigeleisen. *J. Pure. Appl. Chem.* **1964**, *8*, 217−223.

41. M. Gómez-Gallego, M. A. Sierra. *Chem. Rev.* **2011**, *111*, 4857–4963.

42. For some selected examples see: a) R. A. Periana, R. G. Bergman. *J. Am. Chem. Soc*. **1986**, *108*, 7332−7346 and reference 14 therein. b) D. G. Churchill, K. E. Janak, J. S. Wittenberg, G. Parkin. *J. Am. Chem. Soc.* **2003**, *125*, 1403−1420. c) O. T. Northcutt, D. D. Wick, A. J. Vetter, W. D. Jones. *J. Am. Chem. Soc.* **2001**, *123*, 7257−7270.

43. See for example: a) M. A. Dureen, D. W. Stephan. *J. Am. Chem. Soc.* **2009**, *131*, 8396–8397. b) S. J. Geier, M. A. Dureen, E. Y. Ouyang, D. W. Stephan. *Chem. Eur. J.* **2010**, *16*, 988–993.

44. Z. Lu, H. Y. He, H. Wang. *Top. Curr. Chem.* **2012**, *334*, 59–80.

45. L. Ortega-Moreno, M. Fernández-Espada, J. J. Moreno, C. Navarro, J. Campos, S. Conejero, J. López-Serrano, C. Maya, R. Peloso, E. Carmona. *Polyhedron*, **2016**, *116*, 170–181.

46. D. Steinborn, A. M. A. Aisa, F. W. Heinemann, S. Lehmann. *J. Organomet. Chem.* **1997**, *527*, 239–245.

47. T. J. Brown, R. A. Widenhoefer. *Organometallics* **2011**, *30*, 6003–6009.

48. C. F. Jiang, O. Blacque, H. Berke. *Organometallics* **2010**, *29*, 125−133.

49. Y. Guo, S. Li. *Eur. J. Inorg. Chem.* **2008**, 2501–2505.

50. a) W. Debrouwer, T. S. A. Heugebaert, B. I. Roman, C. V. Stevens. *Adv. Synth. Catal*. **2015**, *357*, 2975–3006. b) A. Couce-Rios, A. Lledós, I. Fernández, G. Ujaque. *ACS Catal.* **2019**, *9*, 848–858.

51. See for example: a) A. Gimeno, A. B. Cuenca, S. Suárez-Pantiga, C. R. De Arellano, M. Medio-Simýn, G. Asensio. *Chem. Eur. J.* **2014**, *20*, 683–688. b) M. M. Hansmann, F. Rominger, M. P. Boone, D. W. Stephan, A. S. K. Hashmi. *Organometallics* **2014**, *33*, 4461–4470. c) A. Grirrane, H. García, A. Corma, E. Álvarez. *Chem. Eur. J.* **2013**, *19*, 12239–12244. d) C. Obradors, A. M. Echavarren,. *Chem. Eur. J.* **2013**, *19*, 3547–3551. e) A. Grirrane, H. García, A. Corma, E. Álvarez. *ACS Catal.* **2011**, *1*, 1647–1653. f) A. Gómez-Suárez, S. Dupuy, A. M. Z. Slawin, S. P. Nolan. *Angew. Chem. Int. Ed.* **2013**, *52*, 938–942.

52. E. Rivard. *Dalton Trans.* **2014**, *43*, 8577−8586.

53. a) T. J. Marks. *J. Am. Chem. Soc*. **1971**, *93*, 7090−7091. b) T. J. Marks, A. R. Newman. *J. Am. Chem. Soc.* **1973**, *95*, 769−773. c) C. Eisenhut, T. Szilvasi, G. Dübek, N. C. Breit, S. Inoue. *Inorg. Chem*. **2017**, *56*, 10061−10069. d) S. K. Grumbine, D. A. Straus, T. D. Tilley, A. L. Rheingold. *Polyhedron* **1995**, *14*, 127−148.

54. a) M. Y. Abraham, Y. Wang, Y. Xie, P. Wei, H. F. Schaefer, P. V. R. Schleyer, G. H. Robinson. *J. Am. Chem. Soc.* **2011**, *133*, 8874−8876. b) K. C. Thimer, S. M. I. Al-Rafia, M. J. Ferguson, R. McDonald, E. Rivard. *Chem. Commun*. **2009**, 7119−7121. c) A. K. Swarnakar, S. M. McDonald, K. C. Deutsch, P. Choi, M. J. Ferguson, R. McDonald, E. Rivard. *Inorg. Chem*. **2014**, *53*, 8662−8671. d) S. M. I. Al-Rafia, A. C. Malcolm, S. K. Liew, M. J. Ferguson, E. Rivard. *J. Am. Chem. Soc*. **2011**, *133*, 777−779. e) S. M. I. Al-Rafia, O. Shynkaruk, S. M. McDonald, S. K. Liew, M. J. Ferguson, R. McDonald, R. H. Herber, E. Rivard. *Inorg. Chem*. **2013**, *52*, 5581−5589.

55. a) R. S. Ghadwal, H. W. Roesky, S. Merkel, D. Stalke. *Chem. Eur. J.* **2010**, *16*, 85−88. b) R. Azhakar, G. Tavcar, H. W. Roesky, J. Hey, D. Stalke. *Eur. J. Inorg. Chem*. **2011**, 475− 477. c) S. M. I. Al-Rafia, A. C. Malcolm, R. McDonald, M. J. Ferguson, E. Rivard. *Chem. Commun*. **2012**, *48*, 1308−1310. d) R. S. Ghadwal, R. Azhakar, K.

Pröpper, J. J. Holstein, B. Dittrich, H. W. Roesky. *Inorg. Chem*. **2011**, *50*, 8502−8508.

56. a) J. A. Cabeza, P. García-Álvarez, D. Polo. *Eur. J. Inorg. Chem.* **2016**, 10−22. b) M. F.Lappert, R. S. Rowe. *Coord. Chem. Rev*. **1990**, *100*, 267−292. c) W. Petz. *Chem. Rev*. **1986**, *86*, 1019−1047.

57. a) B. Michelet, C. Bour, V. Gandon. *Chem. Eur. J.* **2014**, *20*, 14488−14492. b) J. A. B. Abdalla, I. M. Riddlestone, R. Tirfoin, S. Aldridge. *Angew. Chem. Int. Ed.* **2015**, *54*, 5098−5102. c) J. Backs, M. Lange, J. Possart, A. Wollschlager, C. Muck-Lichtenfeld, W. Uhl. *Angew. Chem. Int. Ed.* **2017**, *56*, 3094−3097. d) Y. Yu, J. Li, W. Liu, O. Yeb, H. Zhu, *Dalton Trans.* **2016**, *45*, 6259−6268.

58. a) A. Jana, I. Objartel, H. W. Roesky, D. Stalke. *Inorg. Chem*. **2009**, *48*, 7645−7649. b) A. Jana, G. Tavčar, H. W. Roesky, C. Schulzke. *Dalton Trans.* **2010**, *39*, 6217−6220.

59. A. K. Swarnakar, M. J. Ferguson, R. McDonald, E. Rivard. *Dalton Trans*. **2016**, *45*, 6071−6078.

60. a) H. Yang, J. Zhao, M. Qiu, P. Sun, D. Han, L. Niu, G. Cui. *Biosens. Bioelectron*. **2019**, *124-125*, 191−198. b) L. Wang, E. Guan, J. Zhang, J. Yang, Y. Zhu, Y. Han, M. Yang, C. Cen, G. Fu, B. C. Gates, F.-S. Xiao. *Nature Comm.* **2018**, *9*, 1362.

61. a) A. Aouissi, S. S. Al-Deyab, H. Al-Shahri. *Molecules* **2010**, *15*, 1398−1407. b) B. Pan, F. P. Gabbaï. *J. Am. Chem. Soc.* **2014**, *136*, 9564−9567.

62. a) A. Bauer, A. Schier, H. Schmidbaur. *J. Chem. Soc. Dalton Trans.* **1995**, 2919−2920. b) A. Bauer, H. Schmidbaur. *J. Am. Chem. Soc.* **1996**, *118*, 5324–5325. c) J. A. Dilts, M. P. Johnson. *Inorg. Chem.* **1966**, *5*, 2079–2081.

63. a) R. V. Bojan, J. M. López-de-Luzuriaga, M. Monge, M. E. Olmos, R. Echeverría, O. Lehtonen, D. Sundholm. *ChemPlusChem* **2016**, *81*, 176–186. b) R. V. Bojan, J. M. López-de-Luzuriaga, M. Monge, M. E. Olmos, R. Echeverria, O. Lehtonen, D. Sundholm. *ChemPlusChem* **2014**, *79*, 67–76.

64. P. Pérez-Galán, N. Delpont, E. Herrero-Gómez, F. Maseras, A. M. Echavarren. *Chem. Eur. J.* **2010**, *16*, 5324–5332.

65. a) U. Anandhi, P. R. Sharp. *Inorg. Chim. Acta* **2006**, *359*, 3521–3526. b) J. A. Cabeza, J. M. Fernández-Colinas, P. García-Álvarez, D. Polo. *Inorg. Chem*. **2012**, *51*, 3896–3903. c) M. Walewska, J. Hlina, W. Gaderbauer, H. Wagner, J. Baumgartner, C. Marschner. *Z. Anorg. Allg. Chem*. **2016**, *642*, 1304–1313.

66. a) J. Hlina, H. Arp, M. Walewska, U. Florke, K. Zangger, C. Marschner, J. Baumgartner. *Organometallics* **2014**, *33*, 7069–7077. b) B. Findeis, M. Contel, L. H. Gade, M. Laguna, M. C. Gimeno, I. J. Scowen, M. McPartlin. *Inorg. Chem.* **1997**, *36*, 2386–2390. c) C. Marschner, J. Baumgartner, H. Arp, K. Rasmussen, N. Siraj, P. Zark, T. Muller. *J. Am. Chem. Soc.* **2013**, *135*, 7949–7959.

67. a) S. D. Bunge, O. Just, W. S. Rees. *Angew. Chem. Int. Ed.* **2000**, *39*, 3082–3084. b) K. Angermaier, H. Schmidbaur. *Chem. Ber.* **1995**, *128*, 817. c) A. Shiotani, H. Schmidbaur. *J. Am. Chem. Soc.* **1970**, *92*, 7003–7004. d) S. D. Bunge, J. L. Steele. *Inorg. Chem*. **2009**, *48*, 2701–2706.

68. a) F. Hupp, M. Ma, F. Kroll, J. O. C. Jimenez-Halla, R. D. Dewhurst, K. Radacki, A. Stasch, C. Jones, H. Braunschweig. *Chem. Eur. J.* **2014**, *20*, 16888–16898. b) H. Braunschweig, M. A. Celik, R. D. Dewhurst, M. Heid, F. Huppa, S. S. Sen. *Chem. Sci*. **2015**, *6*, 425–435.

69. a) H. Braunschweig, K. Gruss, K. Radacki. *Angew. Chem. Int. Ed.* **2007**, *46*, 7782–7784.

70. T. Yoshida, S. Otsuka. *J. Am. Chem. Soc*. **1977**, *99*, 2134–2140.

71. G. W. Bushnell, D. T. Eadie, A. Pidcock, A. R. Sam, R. D. Holmes-Smith, S. R. Stobart, E. T. Brennan, T. S. Cameron. *J. Am. Chem. Soc*. **1982**, *104*, 5837–5839.

72. Z. Béni, R. Scopelliti, R. Roulet. *Inorg. Chem. Commun.* **2005**, *8*, 99–101.

73. J. Pipek, P. G. Mezey. *J. Chem. Phys*. **1989**, *90*, 4916–4926.

74. a) S. Arndt, M. M. Hansmann, P. Motloch, M. Rudolph, F. Rominger, A. S. K. Hashmi, *Chem. Eur. J.* **2017**, *23*, 2542–2547. b) R. Uson, J. Gimeno, J. Fornies, F. Martinez, C. Fernandez. *Inorg. Chim. Act.* **1982**, *63*, 91–96. c) H. El-Amouri, A. A. Bahsoun, J. Fischer, J. A. Osborn, M.-T. Youinou. *Organometallics* **1991**, *10*, 3582–3588.

75. B. E. Cowie, F. A. Tsao, D. J. H. Emslie. *Angew. Chem. Int. Ed*. **2015**, *54*, 2165–2169.

76. a) J. Campos, R. Peloso, E. Carmona. *Angew. Chem. Int. Ed.* **2012**, *51*, 8255–8258. b) J. Campos, L. Ortega-Moreno, S. Conejero, R. Peloso, J. López-Serrano, C. Maya, E. Carmona. *Chem. Eur. J.* **2015**, *21*, 8883–8896. c) M. Marín, J. J. Moreno, C. Navarro-Gilabert, E. Álvarez, Celia Maya, R. Peloso, M. C. Nicasio, E. Carmona. *Chem. Eur. J.* **2019**, *25*, 260–272.

77. R. R. Sharp, J. W. Tolan. *J. Chem. Phys.* **1976**, *65*, 522–530.

78. J. Campos, M. F. Espada, J. López-Serrano, E. Carmona. *Inorg. Chem.* **2013**, *52*, 6694– 6704.

79. a) K. Wolinski, J. F. Hinton, P. Pulay. *J. Am. Chem. Soc.* **1990**, *112*, 8251–8260. b) M. Häser, R. Ahlrichs, H. P. Baron, P. Weiss, H. Horn. *Theor. Chim. Acta* **1992**, *83*, 455–470.

80. R. Uson, A. Laguna, M. Laguna, D. A. Briggs, H. H. Murray, J. P. Fackler. *Inorg. Synth.* **2007**, *26*, 85–91.

81. H. R. C. Jaw, W. R. Mason. *Inorg. Chem.* **1989**, *28*, 4370–4373.

82. X.-K. Wan, X.-L. Cheng, Q. Tang, Y.-Z. Han, G. Hu, D. Jiang, Q.-M. Wang. *J. Am. Chem. Soc.* **2017**, *139*, 9451–9554.

83. Gaussian 09, Revision B.01, M. J. Frisch, G. W. Trucks, H. B. Schlegel, G. E. Scuseria, M. A. Robb, J. R. Cheeseman, G. Scalmani, V. Barone, B. Mennucci, G. A. Petersson, H. Nakatsuji, M. Caricato, X. Li, H. P. Hratchian, A. F. Izmaylov, J. Bloino, G. Zheng, J. L. Sonnenberg, M. Hada, M. Ehara, K. Toyota, R. Fukuda, J. Hasegawa, M. Ishida, T. Nakajima, Y. Honda, O. Kitao, H. Nakai,

T. Vreven, J. A. Montgomery Jr., J. E. Peralta, F. Ogliaro, M. Bearpark, J. J. Heyd, E. Brothers, K. N. Kudin, V. N. Staroverov, T. Keith, R. Kobayashi, J. Normand, K. Raghavachari, A. Rendell, J. C. Burant, S. S. Iyengar, J. Tomasi, M. Cossi, N. Rega, J. M. Millam, M. Klene, J. E. Knox, J. B. Cross, V. Bakken, C. Adamo, J. Jaramillo, R. Gomperts, R. E. Stratmann, O. Yazyev, A. J. Austin, R. Cammi, C. Pomelli, J. W. Ochterski, R. L. Martin, K. Morokuma, V. G. Zakrzewski, G. A. Voth, P. Salvador, J. J. Dannenberg, S. Dapprich, A. D. Daniels, O. Farkas, J. B. Foresman, J. V. Ortiz, J. Cioslowski, and D. J. Fox, Gaussian, Inc., Wallingford CT, **2010**.

84. J.-D. Chai, M. Head-Gordon. *Phys. Chem. Chem. Phys*. **2008**, *10*, 6615–6620.

85. S. Grimme. *J. Comp. Chem.* **2006**, *27*, 1787–1799.

86. a) R. Ditchfield, W. J. Hehre, J. A. Pople. *J. Chem. Phys.* **1971**, *54*, 724–728. b) W. J. Hehre, R. Ditchfield, J. A. Pople. *J. Chem. Phys.* **1972**, *56*, 2257–2261. c) P. C. Hariharan, J. A. Pople. *Theor. Chim. Acta* **1973**, *28*, 213–222. d) M. M. Francl, W. J. Pietro, W. J. Hehre, J. S. Binkley, M. S. Gordon, D. J. DeFrees, J. A. Pople. *J. Chem. Phys.* **1982**, *77*, 3654–3665.

87. D. Andrae, U. Haeussermann, M. Dolg, H. Stoll, H. Preuss. *Theor. Chim. Acta* **1990**, *77*, 123–141.

88. R. F. Ribeiro, A. V. Marenich, C. J. Cramer, D. G. Truhlar. *J. Phys. Chem. B* **2011**, *115*, 14556–14562.

89. I. Funes-Ardoiz, R. S. Paton, (2016). Goodvibes: Goodvibes 2.0.2 http://doi.org/10.5281/zenodo.595246

90. NBO 6.0. E. D. Glendening, J. K. Badenhoop, A. E. Reed, J. E. Carpenter, J. A. Bohmann, C. M. Morales, C. R. Landis, and F. Weinhold (Theoretical Chemistry Institute, University of Wisconsin, Madison, WI, 2013); http://nbo6.chem.wisc.edu/

91. R. F. W. Bader, Atom in Molecules: A Quantum Theory; Oxford University Press: Oxford, UK, 1995.

92. a) Multiwfn: A multifunctional wavefunction analyser. T. Lu, F. Chen. *J. Comput. Chem.* ***2012***, *33*, 580–592. b) Multiwfn 3.6, http://sobereva.com/multiwfn/

93. CYLview, 1.0b; Legault, C. Y., Université de Sherbrooke, 2009 (http://www.cylview.org)

CHAPTER III.

Synthesis and Reactivity Studies of Platinum-Based Metal-Only Lewis pairs (MOLPs)

III.1. MOLPs Based on [Pt(P^tBu_3)$_2$] (1) and Ag(I) Compounds

III.1.1. Introduction to Pt(0)/Ag(I) Systems

As discussed in Chapter 1 (section I.2.3), metal-only Lewis pairs (MOLPs)[1] have attracted considerable attention in recent times as an interesting class of unsupported bimetallic compounds. Among the many metals that exhibit Lewis acidic character, the use of group 11 metals for the synthesis of MOLPs is well-documented.[2] For instance, our bimetallic Pt(0)/Au(I) adducts described in Chapter 2, as well as other previously reported related systems, may be categorized as MOLPs. Another interesting example based on the pair Pt(0)/Cu(I) was already discussed in Chapter 1 as an effective couple for the activation of O−H bonds in water, in a process highly relevant to the results discussed in the present Chapter.

In the case of silver, a wide range of MOLPs have been synthesized and characterized for a variety of purposes and applications. For instance, Krossing described a bare silver cation coordinated to two [Fe(CO)$_5$] as metalloligands. Donation from the iron centres to the silver cation results in a considerably diminished back-donation from the former metal to the carbonyl ligands.[2a] Nonetheless, the Fe−Ag bonding seems to be of primarily ionic/electrostatic nature.[2e] Interestingly, polydentate metalloligand versions are also capable of binding electrophilic silver

[1] J. Bauer, H. Braunschweig, R. D. Dewhurst. *Chem. Rev.* **2012**, *112*, 4329–4346.
[2] a) P. J. Malinowsky, I. Krossing. *Angew. Chem. Int. Ed.* **2014**, *53*, 13460–13462. b) D. E. Janzen, L. F. Mehne, D. G. VanDerveer, G. J. Grant. *Inorg. Chem.* **2005**, *44*, 8182–8184. c) Z. Xie, T. Jelínek, R. Bau, C. A. Reed. *J. Am. Chem. Soc.* **1994**, *116*, 1907–1913. d) T. Yamaguchi, F. Yamazaki, T. Ito. *J. Am. Chem. Soc.* **2001**, *123*, 743–744. e) G. Wang, Y. S. Ceylan, T. R. Cundari, H. V. R. Dias. *J. Am. Chem. Soc.* **2017**, *139*, 14292–14301. f) S. Takemoto, T. Tsujimoto, H. Matsuzaka. *Organometallics* **2018**, *37*, 1591–1597.

centres[2f] and even supramolecular chains based on dative bonds between silver and Lewis basic transition metals have been reported.[2f]

Moreover, accessing silver-based MOLPs acquires particular relevance in connection to the use of silver species as halide abstractors[3] or transmetallation reagents (Figure 1A).[4] In both processes the formation of metal-silver bonds is postulated to be key for the subsequent aimed transformation to take place. Besides, the photoluminescent properties of silver-containing heterometallic compounds are at least partly associated to the existence of these bimetallic dative interactions.[5] In addition, TM→Ag dative bonds have served as an experimental gauge to calibrate the basicity of transition metals.[6] For instance, when the $[Ru{\rightarrow}Ag{\leftarrow}Ru]^+$ MOLP depicted in Figure 1B was treated with $[Pt(PCy_3)_2]$ (Cy = cyclohexyl), rapid transfer of the silver cation occurred to yield the corresponding $[Pt{\rightarrow}Ag{\leftarrow}Pt]^+$ species. In fact, these experiments overcome the limitation of using $GaCl_3$ as a suitable Lewis acid for gauging transition metal basicity due to reduced stability. It is important to remark that this approach is one of the only experimental tools for determining Lewis basicity in transition metals, which is also not trivial in the computational realm.

[3] a) G. Weber, F. Rominger, B. F. Straub, *Eur. J. Inorg. Chem*. **2012**, 2863–2867. b) G. Sipos, P. Gao, D. Foster, B. W. Skelton, A. N. Sobolev, R. Dorta. *Organometallics* **2017**, *36*, 801–817 c) K. Sasakura, K. Okamoto, K. Ohe. *Organometallics* **2018**, *37*, 2319–2324.
[4] a) M. Baya, Ú. Belío, D. Campillo, I. Fernández, S. Fuertes, A. Martín. *Chem. Eur. J.* **2018**, *24*, 13879–13889. b) I. Meana, P. Espinet, A. C. Albéniz, *Organometallics* **2014**, *33*, 1–7. c) M. Asay, B. Donnadieu, W. W. Schoeller, G. Bertrand. *Angew. Chem. Int. Ed.* **2009**, *48*, 4796–4799.
[5] a) J. Moussa, L. M. Chamoreau, M. P. Gullo, A. Degli Esposti, A. Barbieri, H. Amouri. *Dalton Trans.* **2016**, *45*, 2906–2913. b) L. R. Falvello, J. Forniés, E. Lalinde, B. Menjón, M. A. García-Monforte, M. T. Moreno, M. Tomás. *Chem. Commun.* **2007**, 3838–3840. c) K. M.-C. Wong, C.-K., Hui, K.-L. Yu and V. W.-W. Yam. *Coord. Chem. Rev.* **2002**, *229*, 123–132.
[6] H. Braunschweig, C. Brunecker, R. D. Dewhurst, C. Schneider, B. Wennemann. *Chem. Eur. J.* **2015**, *21*, 19195–19201.

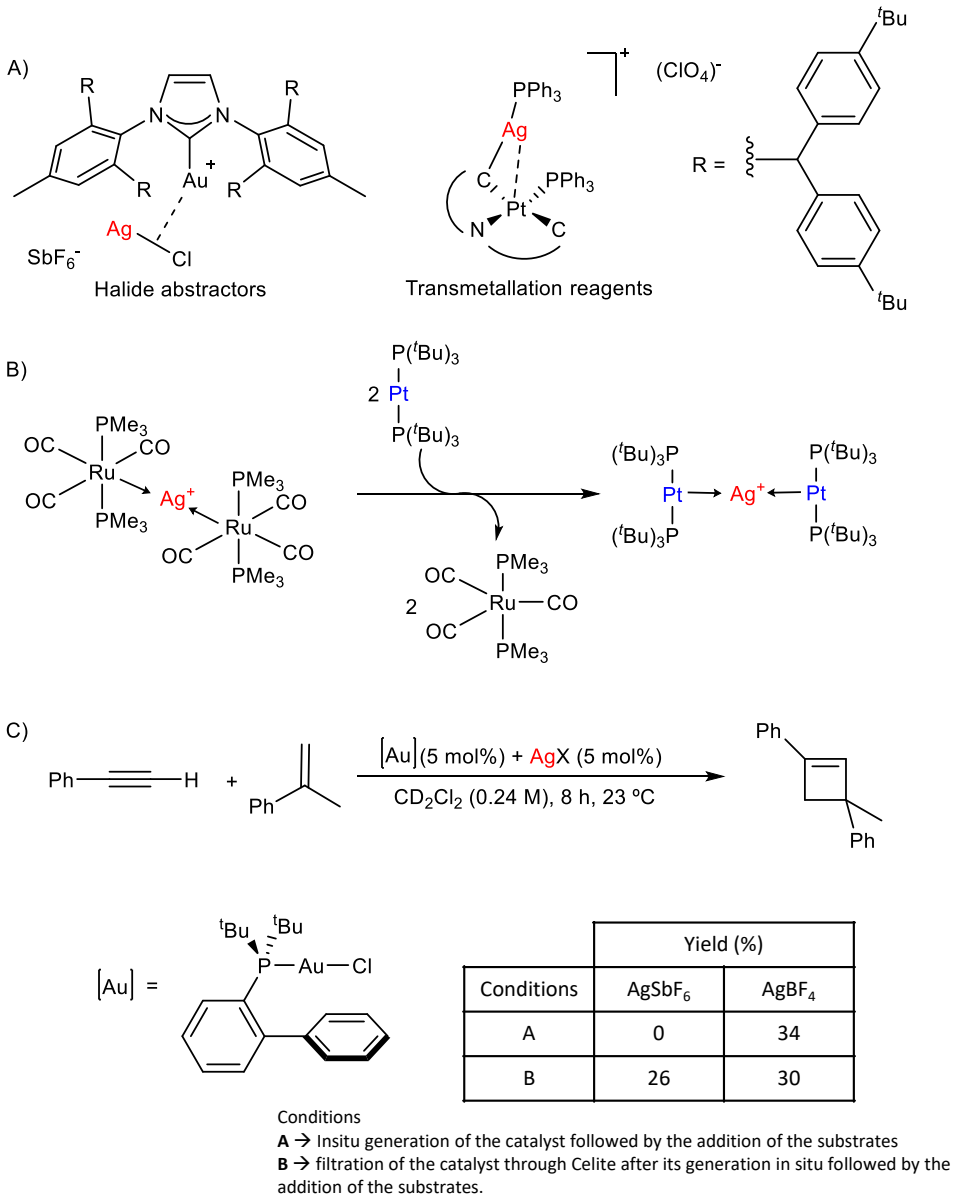

	Yield (%)	
Conditions	$AgSbF_6$	$AgBF_4$
A	0	34
B	26	30

Figure 1. A) Proposed key intermediates in halide abstraction reactions[3a] or transmetalation processes.[4a] B) Transfer of Ag^+ between Ru and Pt compounds as a tool to gauge Lewis basicity.[6] C) Selected example of silver effect in catalysis.[7a]

Metal-metal interactions involving silver centres are also key in catalysis, where the so-called silver effect has been regularly invoked in a variety of transition-metal catalysed transformations (Figure 1C).[7] Likewise, well-defined silver-based heterobimetallic catalysts can outperform their monometallic parent precursors and provide unusual selectivity in certain cases.[8]

On this basis, and following the results on bimetallic bond activation using the basic Pt(0) compound [Pt(P^tBu_3)$_2$] (**1**) described in Chapter II, we decided to investigate the reactivity of Pt(0)/Ag(I) MOLPs based on the same highly congested Pt(0) species. We embarked on this goal additionally motivated by the fact that there is sufficient precedent for the synthesis of Pt(0)/Ag(I) MOLPs in the recent literature (Figure 2) but, rather surprisingly, the cooperative reactivity of those pairs remains unexplored.[9]

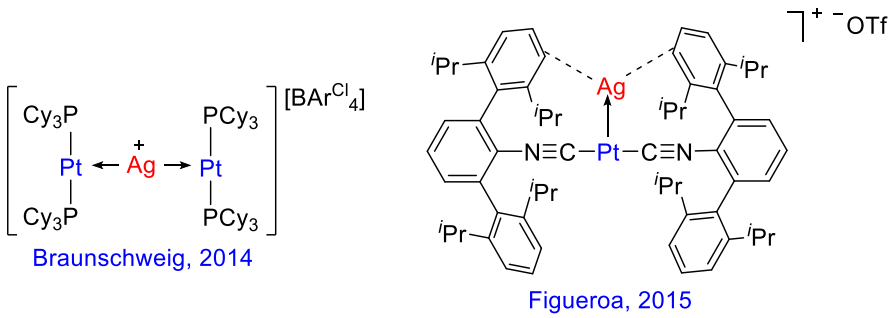

Figure 2. Previous recent examples of Pt(0)/Ag(I) MOLPs.

[7] a) A. Homs, I. Escofet, A. M. Echavarren. Org. Lett. **2013**, *15*, 5782–5785. b) D. Weber, M. R. Gagné. *Org. Lett.* **2009**, *11*, 4962–4965. c) C. Chen, C. Hou, Y. Wang, T. S. A. Hor, Z. Weng. Org. Lett. **2014**, *16*, 524–527.
[8] M. K. Karunananda, N. P. Mankad. *J. Am. Chem. Soc.* **2015**, *137*, 14598–14601.
[9] a) B. R. Barnett, C. E. Moore, P. Chandrasekaran, S. Sproules, A. L. Rheingold, S. DeBeerde, J. S. Figueroa. *Chem. Sci.* **2015**, *6*, 7169–7178. b) B. R. Barnett, J. S. Figueroa. *Chem. Commun.* **2016**, *52*, 13829–13839. c) H. Braunschweig, R. D. Dewhurst, F. Hupp, C. Schneider. *Chem. Commun.* **2014**, *50*, 15685–15688.

III.1.2 Results and Discussion

III.1.2.1. Synthesis of Pt(0)/Ag(I) MOLPs

The formation of Pt→Ag adducts **2** and **3** proceeds readily in benzene or dichloromethane upon mixing [Pt(P^tBu_3)$_2$] (**1**) and the corresponding silver salt in the absence of light (Scheme 1), resulting in the instant coloration of the solution from colourless to bright yellow.

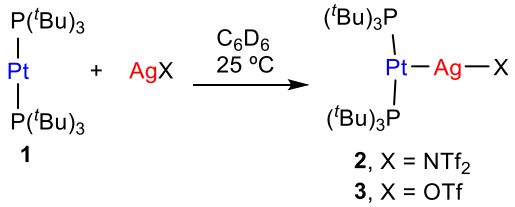

Scheme 1. Synthesis of Pt(0)/Ag(I) metal-only adducts (NTf_2^- = $[N(SO_2CF_3)_2]^-$; OTf^- = $[OSO_2CF_3]^-$).

A chemical shift towards slightly lower frequencies is recorded by $^{31}P\{^1H\}$ NMR monitoring, accompanied by a pronounced decrease in the $^1J_{PPt}$ coupling constant (**2**: δ = 99.6 ppm, $^1J_{PPt}$ = 3298 Hz; **3**: δ = 99.2 ppm, $^1J_{PPt}$ = 3244 Hz) with respect to precursor **1** (δ = 100.2 ppm, $^1J_{PPt}$ = 4410 Hz). The diminished $^1J_{PPt}$ values in **2** and **3** are expected considered the reduced *s* character of P−Pt bonds as a consequence of the new Pt−Ag interaction (Figure 3).

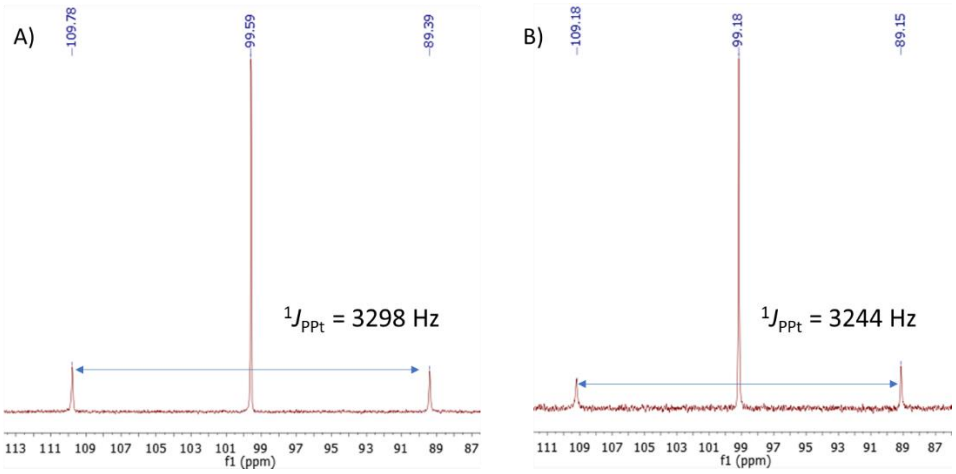

Figure 3. $^{31}P\{^1H\}$ NMR of compounds **2** (A) and **3** (B).

These data are similar to the NMR changes observed in the formation of the trimetallic compound of formula $[(PCy_3)_2Pt\rightarrow Ag^+\leftarrow Pt(PCy_3)_2]$ previously described by the group of Braunschweig and already discussed above.[9c] However, in our case the use of slightly coordinating anions such as triflimide (NTf_2^-, $[N(SO_2CF_3)_2]^-$) or triflate (OTf^-, $[OSO_2CF_3]^-$) seems to prevent the formation of the trimetallic compound in favour of the bimetallic MOLPs **2** and **3**. This was demonstrated by the reaction of **1** with 0.5 equivalents of silver salts $Ag(NTf_2)$ or Ag(OTf), which results in the formation of equimolar mixtures of unreacted **1** and compounds **2** and **3**, respectively. Interestingly, the use of silver reagents containing less coordinating counteranions (i.e. BF_4^- and PF_6^-) also led to related Pt/Ag MOLPs, as inferred from $^{31}P\{^1H\}$ NMR studies, that displayed limited stability (Scheme 2). More precisely, the resulting compounds evolved towards the cyclometalation of one of the *tert*-butyl fragments of a P^tBu_3 ligand to yield compounds $[Pt^{II}(\kappa^2P,C\text{-}P^tBu_2CMe_2CH_2)(P^tBu_3)]^+$ ($\delta(^{31}P\{^1H\})$ = 55.9, 23.2 ppm (d, $^2J_{PP}$ = 319 Hz)) and $[Pt^{II}(P^tBu_3)_2H]^+$

(δ(^{31}P{^{1}H}) = 86.3 ppm, $^{1}J_{PPt}$ = 2723 Hz; δ(^{1}H) = -33.0 ppm ($^{1}J_{HPt}$ = 2224 Hz)).

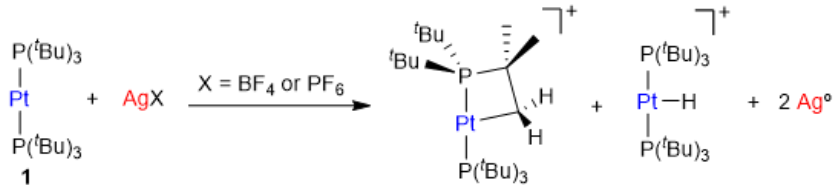

Scheme 2. Reactivity of complex **1** with silver salts with less coordinating counteranions (i.e. BF_4^- and PF_6^-). The counteranions have been excluded for clarity.

The same reactivity was noticed upon dissolving compounds **1** and silver salts in tetrahydrofuran. An identical transformation was latterly reported using a ferrocinium salt as the one-electron oxidant,[10] a role presumably played by the silver salt in the compounds reported herein (scheme 3).

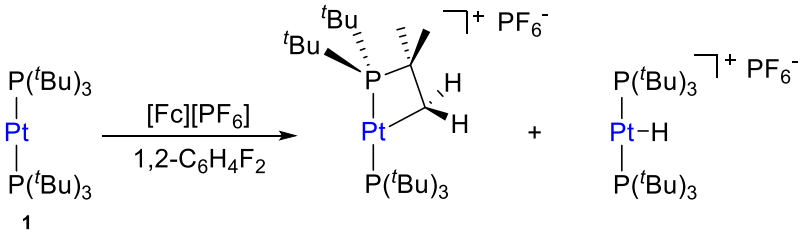

Scheme 3. Cyclometallation of **1** in the presence of ferricenium as a one-electron oxidant reported by Chaplin.

[10] T. Troadec, S.-Y. Tan, C. J. Wedge, J. P. Rourke, P. R. Unwin, A. B. Chaplin. *Angew. Chem. Int. Ed.* **2016**, *55*, 3754–3757.

The molecular structures of compounds **2** and **3** were authenticated by single-crystal X-ray diffraction studies, confirming the proposed bimetallic formulation of the metal-metal core. While compound **2** crystallized as a monomer in the solid state (Figure 4a), the structure of **3** reveals a dimeric configuration with two triflate anions as bridging fragments (Figure 4b). Nevertheless, diffusion NMR experiments ruled out a dimeric formulation as the main species in solution. The structures are otherwise comparable to previous Pt(0) Lewis adducts,[9c] exhibiting slightly distorted T-shaped configurations around the metal centre (P−Pt−P = 167.07(5) (**2**) and 174.69° (4) (**3**)). The Pt−P bond distances (2.30–2.32 Å) are elongated in comparison to precursor **1** (2.25 Å).[11] This may be attributed to the release of electrons from the platinum centre towards the silver atom, in analogy to the Pt−P bond lengthening observed upon one-electron oxidation of precursor **1**, whose origin is still a matter of debate.[12]

[11] S. Otsuka, T. Yoshida, M. Matsumoto, K. Nakatsu. *J. Am. Chem. Soc.* **1976**, *98*, 5850–5858.
[12] M. C. MacInnis, J. C. DeMott, E. M. Zolnhofer, J. Zhou, K. Meyer, R. P. Hughes, O. V. Ozerov. *Chem.* **2016**, *1*, 902–920.

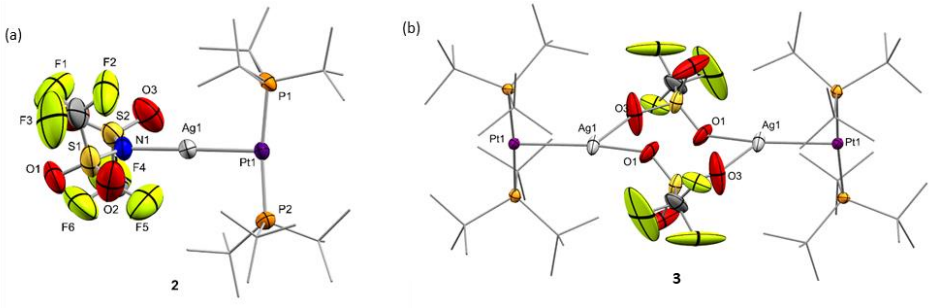

Figure 4. ORTEP diagram of compounds **2** and **3**; for the sake of clarity hydrogen atoms are excluded and some substituents have been represented in wireframe format, while thermal ellipsoids are set at 50% probability.

III.1.2.2. Reactivity Studies with Pt(0)/Ag(I) MOLPs

Given the superior stability of compound **2** over **3**, we chose the former to investigate its reactivity and compare the outcomes with its independent components, that is, compounds **1** and silver salts. We examined the reactivity of **2** towards the activation of hydrogen, alkynes and polar X-H bonds (X = O, N), including those in water and ammonia. Compound **2** cleanly evolves in the presence of H_2 under mild conditions (1 atm, 25 °C) to yield the heterobimetallic Pt(II)/Ag(I) dihydride **4** that contains a terminal and a bridging hydride (Scheme 4). Related Pt/Ag heterobimetallic hydrides have been previously prepared by mixing platinum(II) dihydrides with silver salts.[13]

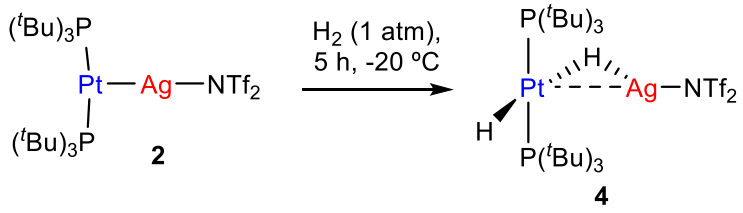

Scheme 4. Reactivity of **2** towards the activation of hydrogen.

Nevertheless, it is important to remark that neither precursor **1** nor $AgNTf_2$ exhibit any reactivity towards dihydrogen even under harsher conditions (4 atm, 60 °C). This demonstrates that both metals are required for the cleavage of the H-H bond to take place. The course of the reaction can be monitored by $^{31}P\{^1H\}$ NMR spectroscopy, following the appearance

[13] a) A. Alhinati, F. Demartin, L. M. Venanzi, M. K. Wolfer. *Angew. Chem. Int. Ed.* **1988**, *27*, 563. b) A. Albinati, H. Lehner, L. M. Venanzi, M. Wolfer. *Inorg. Chem.* **1987**, *26*, 3933–3939.

of a new resonance at 94.6 ppm ($^1J_{PPt}$ = 2663 Hz) due to the heterobimetallic dihydride **4**. This compound exhibits fluxional behavior in solution, as evinced by a single and distinctive low-frequency ^{1}H NMR resonance (-4.88 ppm) at 25 °C due to the two hydride ligands (Figure 5). This signal appears as an apparent double quartet due to coupling to ^{107,109}Ag ($^1J_{AgH}$ = 120 Hz) and ^{31}P ($^2J_{HP}$ = 10 Hz) flanked by ^{197}Pt satellites ($^1J_{HPt}$ = 778 Hz).

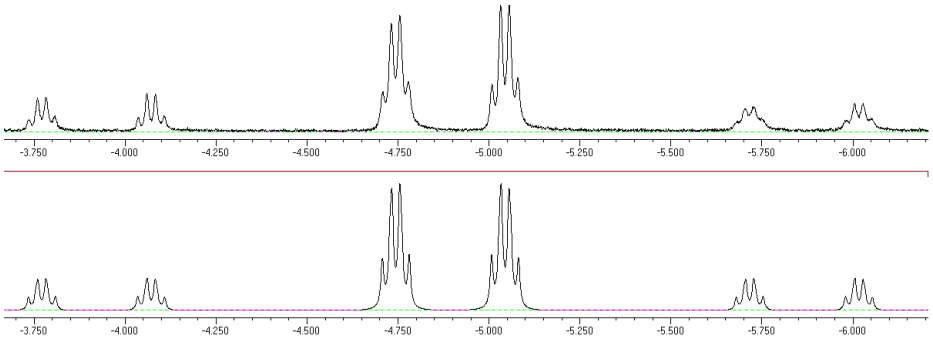

Figure 5. Hydride region of the ^{1}H NMR spectrum of compound **4** (above) and its simulated counterpart (below) by using the gNMR program (version 5.0.6, 2006 IvorySoft). Simulated parameters: δ (^{1}H) = -4.89 ppm; $^1J_{HPt}$= 778.2, $^1J_{HAg}$ = 111.8, $^2J_{HP}$ = 10.6 Hz.

The dynamic process is quenched at temperatures below -50 °C, at which the initial signal is split into two resonances at -3.98 ($^1J_{AgHt}$ = 182, $^1J_{HPt}$ = 750 Hz) and -5.21 ($^1J_{AgHt}$ = 44, $^1J_{HPt}$ = 984 Hz) ppm due to the bridging and terminal hydrides, respectively (Figure 6).

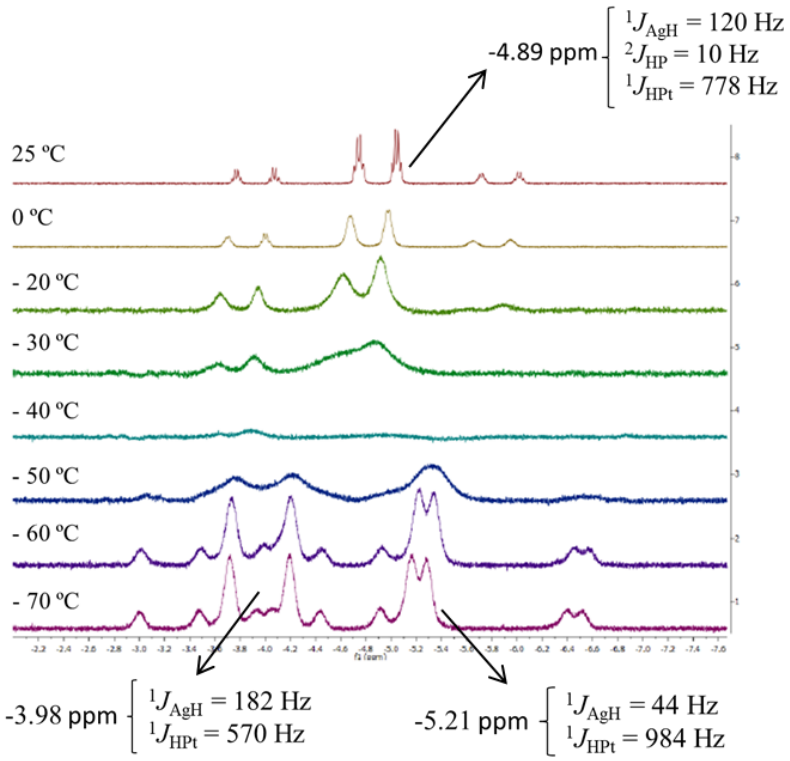

Figure 6. Variable temperature ^{1}H NMR experiment of complex **4**.

In fact, the lability of the Pt→Ag bond[14] is attested by the reaction of **1** with 0.5 equivalents of $AgNT_2$ under H_2 atmosphere, which forms an equimolar mixture of compound **4** and unreacted **1** after 5 hours and eventually evolves to a *ca.* 1:1 mixture of the former and $[Pt(P^tBu_3)_2(H)_2]$, along with variable amounts of $[Pt^{II}(P^tBu_3)_2H]^+$ as a recurrent side-product. Having in mind that precursor **1** does not react with H_2 under our experimental conditions, the formation of $Pt(H)_2(P^tBu_3)_2$ may imply transfer of silver from hydride **4** to unreacted **1** forming compound **2**, which could subsequently be hydrogenated by the synergistic action of silver.

We next investigated the reactivity of **2** towards acetylene and phenylacetylene (Scheme 5). As mentioned in Chapter 2, compound **1** act as a catalyst for the polymerization of C_2H_2, provoking the rapid precipitation of a dark purple solid upon exposure to the gas. The formation of the polymer is, however, visibly inhibited in the presence of the silver salt, in which case the trinuclear $[(P^tBu_3)_2(H)Pt(\mu\text{-}CCH)Ag(\mu\text{-}CCH)Pt(H)(P^tBu_3)_2]$ (**5**) is obtained in quantitative spectroscopic yield.

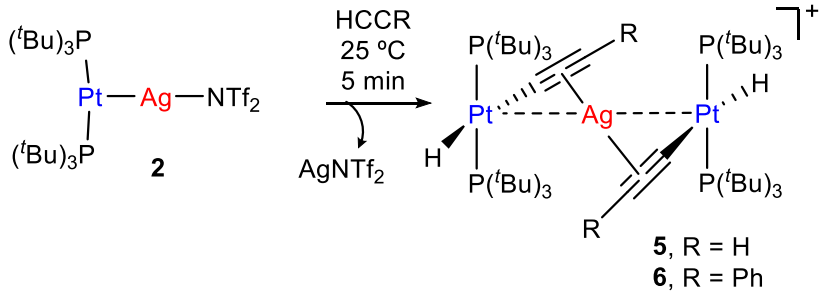

Scheme 5. Reactivity of **2** towards acetylene and phenylacetylene. The triflimide counteranion has been excluded for clarity.

Analogous reactivity is derived from the addition of phenylacetylene, resulting in the formation of the heterobimetallic dibridged bisacetylide **6**. Similarly to our studies with H_2, neither precursor **1** nor the silver salt exhibit any reactivity towards phenylacetylene as monometallic species. Compounds **5** and **6** are related to other Pt/Ag bridging acetylides that have been prepared by the addition of silver salts to pre-formed platinum(II) acetylides,[14] an approach that contrasts to the bimetallic cooperative alkyne activation described herein. The new heterobimetallic

[14] a) Q.-H. Wei, L.-J. Han, Y. Jiang, X.-X. Lin, Y.-N. Duan, G.-N. Chen. *Inorg. Chem.* **2012**, *51*, 11117–11125. b) Z. Dai, A. J. Metta-Magaña, J. E. Nuñez, *Inorg. Chem.* **2014**, *53*, 7188–7196. c) S. Yamazaki, A. J. Deeming, D. M. Speel, D. E. Hibbs, M. B. Hursthousec, K. M. A. Malik. *Chem. Commun.* **1997**, 177–178.

compounds are characterized by $^{31}P\{^{1}H\}$ NMR resonances at 83.5 (**5**) and 82.8 (**6**) ppm flanked by ^{195}Pt satellites ($^{1}J_{PPt}$ = 2796 and 2763 Hz, respectively), shifted to lower frequencies by *ca*. 16 ppm with respect to their precursor **2**. In ^{1}H NMR, complex **5** presents two characteristic signal at 3.28 and -10.37 ppm corresponding to the Pt−H and C≡CH, respectively (Figure 7).

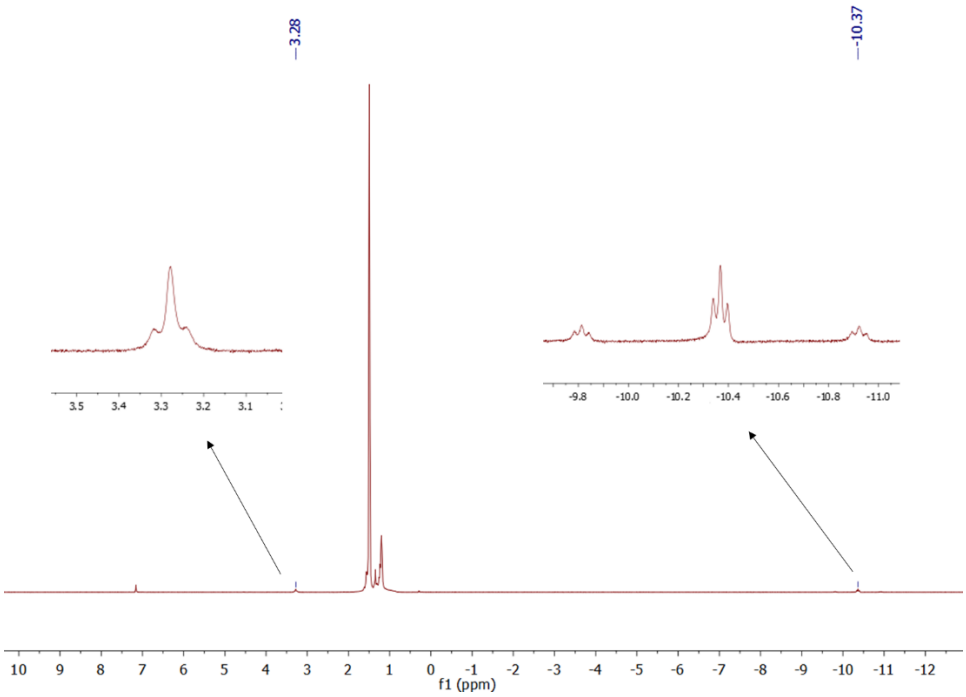

Figure 7. ^{1}H NMR (C_6D_6, 25 ºC, 400 MHz) of complex **5**.

These compounds are thermally unstable in solution, particularly complex **5**. However, we managed to grow single-crystals of the latter species. X-ray diffraction studies revealed the trimetallic formulation of the dibridged σ,π bisacetylide (Figure 8). The Pt···Ag distance is markedly elongated (3.634(9) Å) compared to the metallic Lewis pair **2** (2.658(1) Å), indicating that the dative Pt→Ag bond is no longer present. The σ,π-bridged acetylide fragments are characterized by short bond distances with the silver

nuclei ($d_{Ag\text{-}centroid}$ 2.216(6) Å), along with relatively lengthened Pt−C bond distances ($d_{Pt\text{-}C}$ 2.107(12) Å) compared to other compounds of formula [Pt(H)(CCR)(PR_3)$_2$(CCR)] (*ca.* 1.9-2.0 Å).[15]

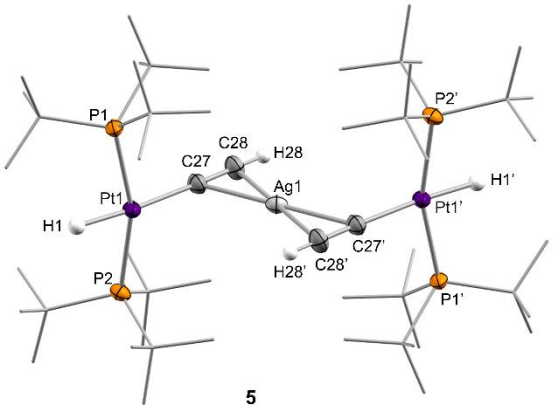

Figure 8. ORTEP diagram of compound **5**; for the sake of clarity most hydrogen atoms and the triflimide counteranion have been excluded and some substituents have been represented in wireframe format, while thermal ellipsoids are set at 50% probability.

The formulation of compounds **5** and **6** as trimetallic bisacetylides was corroborated in solution by the reactions of equimolar mixtures of **1** and **2** with the two investigated alkynes, leading to compounds **5** and **6**, respectively, accompanied by complete consumption of the two platinum precursors, that is, using only one equivalent of silver per two platinum nuclei.

[15] a) A. Furalani, S. Licoccia, M. V. Russo, A. C. Villa, C. Guastini. *J. Chem. Soc. Dalton Trans.* **1982**, 2449–2453. b) J. R. Berenguer, M. Bernechea, E. Lalinde, *Organometallics* **2007**, *26*, 1161–1172. c) I. Ara, J. R. Berenguer, E. Eguizabal, J. Forniés, J. Gómez, E. Lalinde, J. M. Saez-Rocher. *Organometallics* **2000**, *19*, 4385–4397.

We additionally tested the reactivity of **2** towards the activation of polar X−H (X = O, N) bonds. Before discussing these results, it is pertinent to highlight that none of the reagents tested for X−H bond cleavage exhibited any reactivity towards precursor **1**. However, addition of methanol (5 equiv.) to a C_6D_6 solution of **2** provides quantitative formation of the previously reported[16] cationic T-shaped platinum hydride **7** after around one hour at 25 °C (Scheme 6). This compound is characterized by a distinctive low-frequency ^{1}H NMR resonance at -33.0 ppm. Its molecular formulation was further confirmed by X-ray diffraction studies (Figure 9).

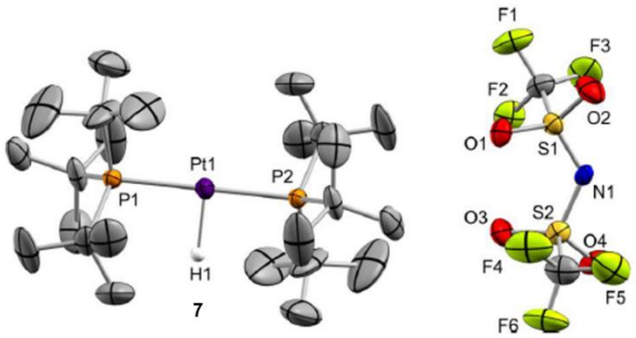

Figure 9. ORTEP diagram of compound **7**; hydrogen atoms, except platinum hydride have been excluded for clarity. Thermal ellipsoids are set at 50% probability.

More interestingly, analogous reactivity arises from the addition of water or ammonia, yielding the corresponding cationic Pt-hydride complexes further stabilized by coordination of a water (**8a**) or ammonia (**8b**) ligand, respectively (Scheme 6). While the activation of water (50 equiv) in benzene solution takes up to 12 hours to reach completion,

[16] R. G. Goel, R. C. Srivasta. *Can. J. Chem.* **1983**, *61*, 1352–1359.

likely due to water immiscibility, using wet acetonitrile yields $[PtH(CH_3CN)(P^tBu_3)_2]^+$ (**8c**) instantly. The reaction with ammonia (1 bar), requires heating at 60 ºC to form compound 8b in *ca.* 60% yield after 16 hours.

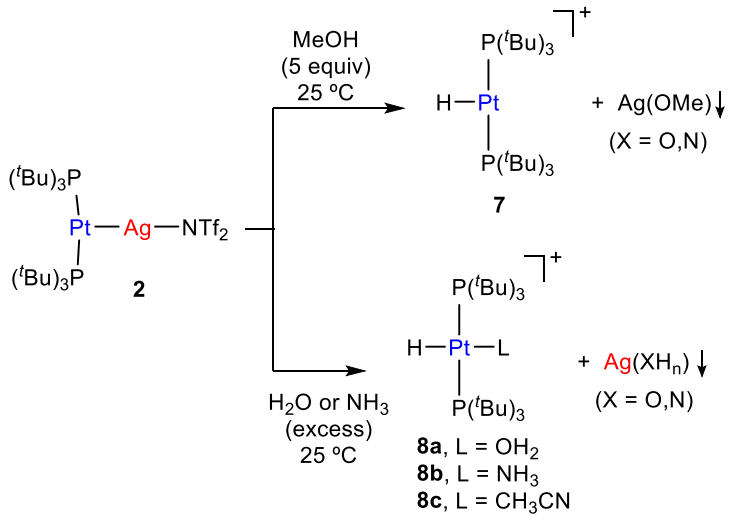

Scheme 6. Reactivity of compound **2** towards polar X−H (X = O, N) bonds.

The activation of X−H bonds in methanol, water and ammonia is accompanied by the appearance of greyish precipitates that we attribute to the corresponding silver alkoxide, hydroxide or amide salts, respectively. The formation of compounds **8a-c** was unequivocally confirmed by ^1H and $^{31}P\{^1H\}$ NMR spectroscopy.[16] The solid structure of the aquo/hydride complex **8a** was validate by X-ray diffraction studies (Figure 9).

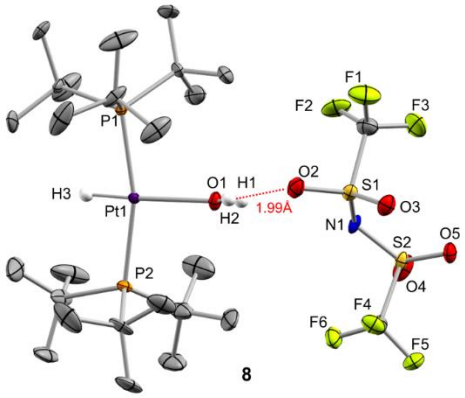

Figure 10. ORTEP diagram of compound **8a**; most hydrogen atoms have been excluded for clarity. The hydrogen bond between H1 and O2 of the triflimide anion is highlighted. Thermal ellipsoids are set at 50% probability.

The cooperative activation of water using a related bimetallic Pt(0)/Cu(I) pair has been recently described, as we commented in the general introduction of Chapter 1 (see Scheme 48).[17] However, the cleavage of N−H bonds in ammonia remains a challenge in transition metal chemistry, where formation of Werner-type adducts is typically preferred.[18] Thus, compound **2** adds to the limited list of transition metal systems capable of activating ammonia under mild conditions by virtue of the synergistic cooperation between the two metals.

[17] S. Jamali, S. Abedanzadeh, N. K. Khaledi, H. Samouei, Z. Hendi, S. Zacchini, R. Kiaa, H. R. Shahsavari. *Dalton Trans.* **2016**, *45*, 17644–17651.
[18] Selected examples of ammonia activation by transition metal complexes: a) J. Zhao, A. S. Goldman, J. F. Hartwig. *Science* **2005**, *307*, 1080–1082. b) C. M. Fafard, D. Adhikari, B. M. Foxman, J. Mindiola, O.V. Ozerov. *J. Am. Chem. Soc.* **2007**, *129*, 10318–10319. e) M. G. Scheibel, J. Abbenseth, M. Kinauer, F. W. Heinemann, C. Würtele, B. de Bruin, S. Schneider. *Inorg. Chem.* **2015**, *54*, 9290–9302.

III.2. MOLPs Based on [Pt(P^{t}Bu$_3$)$_2$] (1) and Zinc (I/II) Compounds

III.2.1. Introduction to Zn-Based MOLPs

MOLPs constructed around Lewis acidic zinc(II) fragments are particularly appealing due to their relevance to Negishi cross-coupling catalysis. In fact, intermediates containing dative Pd→Zn interactions are crucial to accessing low-energy transition states during transmetalation,[19] and play essential roles in *cis/trans* isomerization[20] and deleterious homocoupling processes.[21] Only on this basis and considering the widespread application of Negishi cross-coupling reactions, the interest on the study of bimetallic compounds between zinc and group 10 metals is obvious. Moreover, the coordination of zinc species to late transition metals have proved key to modify the reactivity at the latter acting as a sort of metallic Z-type ligand. In a notable example, Bergman and Tilley have shown that biaryl reductive elimination from Pt(II) compounds is accelerated upon Zn(C_6F_5)$_2$ coordination (Scheme 7A).[22] Thus, while (phen)PtAr$_2$ (phen = 1,10-phenantroline) is stable in solution even after heating at 200 ºC for two days, mild heating at 60 ºC in the presence of Zn(C_6F_5)$_2$ results in quantitative biaryl elimination after only 15 minutes.

[19] a) R. Álvarez, A. R. De Lera, J. M. Aurrecoechea, A. Durana. *Organometallics* **2007**, *26*, 2799–2802. b) B. Fuentes, M. García-Melchor, A. Lledós, F. Maseras, J. A. Casares, G. Ujaque, P. Espinet. *Chem. Eur. J.* **2010**, *16*, 8596–8599. c) R. J. Oeschger, P. A. Chen. *Organometallics* **2017**, *36*, 1465−1468. d) E. Paenurk, R. Gershoni-Poranne, P. Chen. *Organometallics* **2017**, *36*, 4854−4863.

[20] a) J. A. Casares, P. Espinet, B. Fuentes, G. Salas. *J. Am. Chem. Soc*. **2007**, *129*, 3508−3509. b) J. delPozo, E. Gioria, J. A. Casares, R. Álvarez, P. Espinet. *Organometallics* **2015**, *34*, 3120−3128.

[21] a) Q. Liu, Y. Lan, J. Liu, G. Li, Y.-D. Wu, A. Lei. *J. Am. Chem. Soc.* **2009**, *131*, 10201–10210. b) R. V. Asselt, C. J. Elsevier. *Organometallics* **1994**, *13*, 1972–1980.

[22] A. L. Liberman-Martin, D. S. Levine, M. S. Ziegler, R. G. Bergman, T. D. Tilley. *Chem. Commun.* **2016**, *52*, 7039−7042.

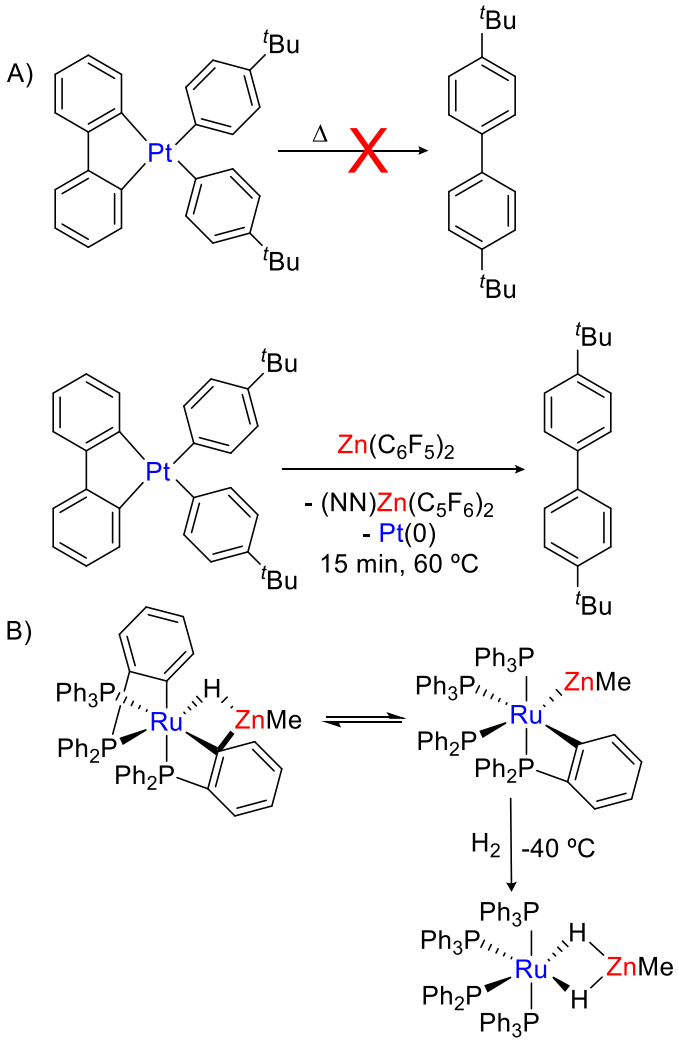

Scheme 7. A) Reductive biaryl elimination from (phen)$PtAr_2$ mediated by coordination of $Zn(C_6F_5)_2$. B) Reductive elimination and dihydrogen activation in a Ru/Zn heterobimetallic complex.

In a somewhat related work, Whittlesey and Macgregor have also concluded that the coordination of zinc as a Z-type fragment facilitates reductive elimination from electron-rich transition metals. In this case the

authors explored a heterobimetallic Ru/Zn compound and demonstrated that the unsaturated 'ZnMe' terminus promotes C−H reductive elimination and dihydrogen activation at the Ru(II) site (Scheme 7B).[23] The role of zinc in these studies is emphasized by the fact that related lithium and magnesium bimetallic species do not show this degree of reaction acceleration.

Despite all the above, Zn-based MOLPs remain rare.[24] Our group became recently interested in isolating the first unsupported MOLPs constructed around the Rh→Zn motif. As such, compounds $[(\eta^5\text{-}C_5Me_5)(PMe_3)_2Rh{\rightarrow}ZnR_2]$, where R stands for CH_3 or C_6F_5, were reported and fully characterized (Figure 11).[24a] These species are presumably relevant intermediates in rhodium-mediated Negishi coupling reactions.[25] The isolation of these and other related heterobimetallic compounds allowed our group to examine the dative bimetallic bond in detail, revealing a considerably covalent degree in the case of Rh−Zn bonds when compared to other more electropositive elements such as Li, Na or Mg. Nonetheless, as for Lewis basic fragments in the field of MOLPs, $[Pt(PCy_3)_2]$ is likely the most extensively investigated donor.[26] In fact, the

[23] F. M. Miloserdov, N. A. Rajabi, J. P. Lowe, M. F. Mahon, S. A. Macgregor. *J. Am. Chem. Soc.* **2020**, *142*, 6340−6349.

[24] a) S. Bajo, M. G. Alférez, M. M. Alcaide, J. López-Serrano, J. Campos. *Chem. Eur. J.* **2020**, *26*, 16833–16845. b) T. D. Lohrey, L. Maron, R. G. Bergman, J. Arnold. *J. Am. Chem. Soc.* **2019**, *141*, 800−804. c) J. J. Gair, Y. Qiu, R. L. Khade, N. H. Chan, A. S. Filatov, Y. Zhang, J. C. Lewis. *Organometallics* **2019**, *38*, 1407−1412. d) U. Jayarathne, T. J. Mazzacano, S. Bagherzadeh, N. P. Mankad. *Organometallics* **2013**, *32*, 3986−3992.

[25] a) C. J. Pell, W.-C. Shih, S. Gatard, O. V. Ozerov. *Chem. Commun.* **2017**, *53*, 6456–6459. b) H. Takahashi, S. Inagaki, N. Yoshii, F. Gao, Y. Nishihara, K. Takagi. *J. Org. Chem.* **2009**, *74*, 2794–2797. c)S. Ejiri, S. Odo, H. Takahashi, Y. Nishi-Mura, K. Gotoh, Y. Nishihara, K. Takagi. *Org. Lett.* **2010**, *12*, 1692–1695.

[26] See for example: a) H. Braunschweig, K. Gruss, K. Radacki. *Angew. Chem. Int. Ed*. **2009**, *48*, 4239–4241. b) H. Braunschweig, A. Damme, R. D. Dewhurst, F. Hupp, J. O. C. Jiménez-Halla, K. Radacki. *Chem. Commun.* **2012**, *48*, 10410–10412. c) H. Braunschweig, K. Gruss, K. Radacki. *Angew. Chem. Int. Ed*. **2007**, *46*, 7782–7784. d) J. Bauer, H. Braunschweig, A. Damme, K. Radacki. *Angew. Chem. Int. Ed*. **2012**, *51*, 10030–10033. e) J. K. Schuster, J. H. Muessig, R. D. Dewhurst, H. Braunschweig. *Chem. Eur. J.* **2018**, *24*,

recently reported [$(PCy_3)_2Pt\rightarrow ZnBr_2$] is the first well-defined unsupported M→Zn(II) adduct (Figure 11).[27]

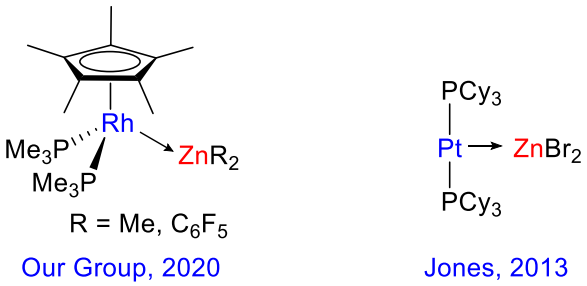

Figure 11. Examples of unsupported Zn-based MOLPs.

These examples provide evidence that this type of compounds, although yet rare, may be rationally prepared, in particular for Pt(0) bases as the one being discussed along this Thesis. Moreover, the aforesaid reactivity and its connection to cross-coupling processes highlight the opportunities that may emerge from combining zinc electrophiles with electron-rich transition metal compounds. On these grounds, we decided to inspect the formation and reactivity of zinc-containing MOLPs based on [$Pt(P^tBu_3)_2$] (**1**). In doing so, we have examined its reactivity with a range of zinc precursors, more precisely ZnX_2 (X = Cl, Br, I, OTf; OTf = trifluoromethanesulfonate), ZnR_2 (R = Me, Et, Ph, η^5-C_5Me_5, C_6F_5) and the more exotic Zn(I) dimer [$Zn_2(\eta^5$-$C_5Me_5)_2$] ($Zn_2Cp^*_2$).[28]

9692–9697. f) R. Bertermann, J. Böhnke, H. Braunschweig. R. D. Dewhurst, T. Kupfer, J. H. Muessig, L. Pentecost, K. Radacki, S. S. Sen, A. Vargas. *J. Am. Chem. Soc.* **2016**, *138*, 16140–16147.

[27] M. Ma, A. Sidiropoulos, L. Ralte, A. Stasch, C. Jones. *Chem. Commun.*, **2013**, *49*, 48–50.

[28] I. Resa, E. Carmona, E. Gutierrez-Puebla, A. Monge. *Science* **2004**, *305*, 1136–1138.

III.2.2 Results and Discussion

III.2.2.1. Synthesis of Pt(0)/Zn(I/II) MOLPs

Treatment of [Pt(P^tBu_3)$_2$] (**1**) with zinc (pseudo)halides in toluene did not offer any hint of adduct formation by NMR in the temperature range of −80 to +70 ºC, which contrasts with the readily accessible [(PCy_3)$_2$Pt→$ZnBr_2$].[27] Considering that the basicity of **1** may be superior to that of [Pt(PCy_3)$_2$], we ascribe the absence of MOLP formation from the former to steric reasons. Switching to dichloromethane, fluorobenzene and tetrahydrofuran to improve the solubility of the zinc salt did not alter these results. However, addition of one equivalent of the more acidic $Zn(C_6F_5)_2$ to a colorless C_6D_6 solution of **1** caused instant coloration to bright yellow. Multinuclear NMR spectroscopic analysis suggested formation of the bimetallic adduct [(P^tBu_3)$_2$Pt→$Zn(C_6F_5)_2$] (**9** in Scheme 8). The most distinctive feature is a pronounced decrease in the $^1J_{PPt}$ coupling constant to a value of 3328 Hz (δ = 93.1 ppm; *c.f* **1**: δ = 100.2 ppm, $^1J_{PPt}$ = 4410 Hz), a common symptom of MOLP formation in Pt(0) compounds due to the reduced *s* character of the Pt−P bonds in the bimetallic adduct.[26] Alongside this, a new set of $^{19}F\{^1H\}$ resonances at -115.7, -157.4 and -162.0 ppm (*c.f.* $Zn(C_6F_5)_2$: δ = -118.0, -152.5, -160.5 ppm) was recorded.

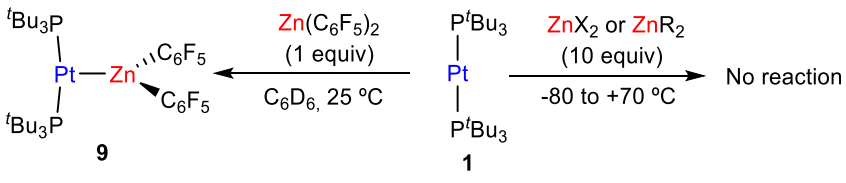

Scheme 8. Reaction of [Pt(P^tBu_3)$_2$] (**1**) with zinc (pseudo)halides and organozinc compounds. X = Cl, Br, I, OTf; R = Me, Et, Ph, C_5Me_5; Solvent = C_6D_6, CD_2Cl_2, THF or C_6H_5F.

The molecular structure of **9** was authenticated by single-crystal X-ray diffraction studies (Figure 12a) confirming the proposed bimetallic formulation. This represents the first example of a Pt(0)/organozinc MOLP. It exhibits a T-shaped geometry around the platinum center, slightly distorted due to the steric pressure exerted by the *tert*-butyl groups in close proximity to the perfluorinated aryl rings (P−Pt−P = 165.32(4)º). As in other bisphosphine Pt(0)-based MOLPs, the Pt−P bond distances (2.325 Å on average) are modestly elongated with respect to precursor **1** (2.25 Å).[11] The Pt−Zn bond length (2.4663(6) Å) is shorter than in the related [(phen)Ar_2Pt^{II}→$Zn(C_6F_5)_2$] (phen = phenanthroline) adduct, which contains a less basic Pt(II) donor (2.5526(5) Å),22 and just marginally longer than in [$(Cy_3P)_2$Pt→$ZnBr_2$] (2.4040(6) Å).[27] Steric constraints in **9** force the perfluorphenyl rings to bend away from the platinum center, with the C25−Zn−C31 angle of 117.73(18)º significantly reduced compared to $Zn(C_6F_5)_2$ (172.6º)[29] and even [(phen)Ar_2Pt^{II}→$Zn(C_6F_5)_2$] (134.8º).22

[29] Y. Sun, W. E. Piers, M. Parvez. *Can. J. Chem.* **1998**, *76*, 513–517.

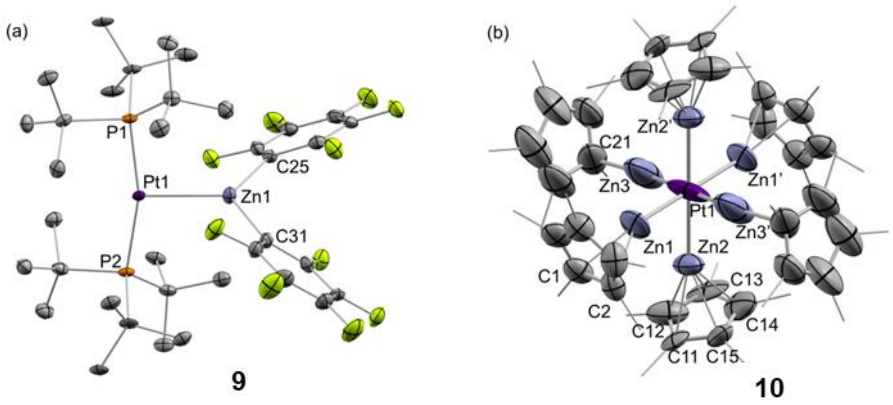

Figure 12. ORTEP diagram of compounds **9** and **10**. Hydrogen atoms have been excluded and methyl groups of Cp* ligands represented in wireframe format for clarity. Thermal ellipsoids are set at 50% probability.

At variance with its fluorinated analogue, the less acidic $ZnPh_2$ does not react with **1**, as monitored by variable temperature NMR and visually inferred by the colorless appearance of the reaction mixture even after prolonged periods of time. Similarly, no Pt→Zn interactions were detected upon addition of 10 equiv. of ZnR_2 (R = Me, Et, η^5-C_5Me_5) to C_6D_6 solutions of **1**, again pointing out the need for a highly electrophilic Zn center to overcome the distortion of the linear Pt(0) precursor to accommodate the bimetallic dative bond. Next, we examined the reactivity of **1** with the Zn(I) dimer [$Zn_2Cp^*_2$]28 in light of its capacity to form zinc-rich polymetallic complexes with transition metal precursors.[30] For instance, Fischer has investigated the reactivity between [$Zn_2Cp^*_2$] and low-valent M(0) precursors (M = Ni, Pd, Pt), recurrently identifying the homolytic cleavage

[30] T. Bollermann, C. Gemel, R. A. Fischer. *Coord. Chem. Rev.* **2012**, *256*, 537–555.

of the Zn−Zn bond by insertion of the transition metal.[31] Some of the most relevant examples are depicted in Figure 13.

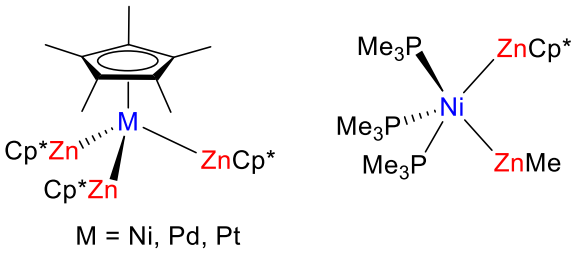

Figure **13**. Selected examples of Zn-rich polymetallic structures reported by Fischer.

$^{31}P\{^{1}H\}$ NMR monitoring of an equimolar mixture of **1** and $[Zn_2Cp^*_2]$ in C_6D_6 showed the release of free phosphine (δ = 63.0 ppm) without any other detectable intermediate. It soon became evident that a three-fold excess of the Zn(I) dimer was required to achieve complete consumption of **1**. Under these conditions the highly unstable compound $[Pt(ZnCp^*)_6]$ (**10**) forms as the major species (*ca*. 80% NMR yield) by insertion of the Pt center into the Zn−Zn bonds of three molecules of $[Zn_2Cp^*_2]$. (Scheme 9). Compound **10** slowly precipitates as bright orange crystals, which allowed us to ascertain its heptametallic structure by X-ray diffraction analysis (Figure 12b). It can be described as an unusual 16-electron octahedral complex in which each vertex is occupied by a

[31] a) T. Bollermann, K. Freitag, C. Gemel, R. D. Seidel, M. V. Hopffgarten, G. Frenking, R. A. Fischer. *Angew. Chem. Int. Ed.* **2011**, *50*, 772–776. b) T. Cadenbach, T. Bollermann, C. Gemel, M. Tombul, I. Fernández, M. V. Hopffgarten, G. Frenking, R. A. Fischer. *J. Am. Chem. Soc.* **2009**, *131*, 16063–16077. c) J. Hornung, J. Weßing, M. Molon, K. Dilchert, C. Gemel, R. A. Fischer. *J. of Organom. Chem.* **2018**, *860*, 78–84. d) T. Bollermann, K. Freitag, C. Gemel, R. W. Seidel, R. A. Fischer. *Organometallics* **2011**, *30*, 4123–4127. e) K. Freitag, M. Molon, P. Jerabek, K. Dilchert, C. Rösler, R. W. Seidel, C. Gemel, G. Frenking, R. A. Fischer. *Chem. Sci.* **2016**, *7*, 6413–6421.

neutral one-electron ZnCp* ligand. For this rationalization the same analysis proposed by Fischer after a thorough computational analysis carried out by the Frenking group has been followed. More precisely, each [Cp*Zn] fragment has been considered as a neutral one-electron ligand.

The fact that compound **10** can be regarded as a 16-electron platinum species is in stark contrast with all prior Zn-rich polymetallic compounds of late transition metals, which consistently fulfill the 18 VE rule.30 The steric shrouding provided by the six planar cyclopentadienyl ligands stabilizes the somewhat encapsulated electron-rich platinum center and may be responsible for this peculiarity.

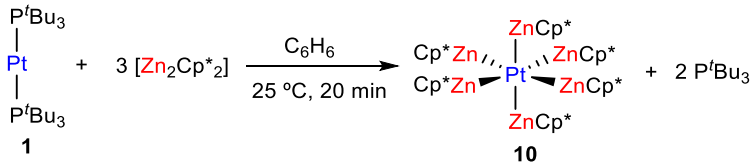

Scheme 9. Synthesis of compound **10** by the reaction between **1** and [$Zn_2Cp^*_2$].

The solid-state structure shows three pairs of ZnCp* ligands that differ slightly from each other in terms of Zn coordination. Two of these fragments present η^5-coordination ($d_{Zn\text{-}C} \approx 2.24 - 2.37$ Å), a second pair binds to the Cp* in a η^2-fashion, while the third pair exhibits η^1-binding (shortest $d_{Zn3\text{-}C21} = 2.06(3)$ Å; the rest > 2.6 Å). While the former two pairs present Pt–Zn bond distances (2.419(3) and 2.401(4) Å) comparable to prior examples,31 the η^1-bound ZnCp* fragment displays a Pt–Zn bond (2.238(7) Å) shortened by 0.34 Å with respect to the sum of the covalent radii

(2.58 Å).[32] In THF-d_8 solution, a single ^{1}H NMR resonance at 1.92 ppm indicates rapid dynamic exchange among the possible conformations of the ZnCp* ligands. In fact, low temperature NMR (up to −80 ºC) was insufficient to freeze the dynamic process.

Compound **10** strongly resembles the closed shell 18-electron [Pt(ZnCp*)$_4$(ZnR)$_4$] species (R = Me, Et) described by Fischer and co-workers.[17b] The latter compounds exhibit rather long Zn···Zn distances (ranging from 2.812 to 3.115 Å), which have been regarded as non- or only weakly interacting.[17e] Similar Zn···Zn distances were found in **10** (> 3.0 Å). To confirm the negligible interaction between the zinc centers in **10**, and in collaboration with Prof. Israel Fernández, the topology of the model system Pt(ZnH)$_6$, analogous to the model Pt(ZnH)$_8$ used by Fischer and Frenking to understand the bonding situation in [Pt(ZnCp*)$_4$(ZnR)$_4$],[17b,e] was computationally explored using the QTAIM (Quantum Theory of Atoms in Molecules) method. Figure 14 shows the Laplacian distribution of Pt(ZnH)$_6$ computed in the Zn−Pt−Zn plane. As expected, bond critical points (BCPs) together with their associated bond paths (BPs) are found between the zinc and platinum centers (computed Pt−Zn bond distances of ~2.47 Å). At variance, no BCPs or BPs were located between the zinc atoms (computed Zn···Zn bond distances ranging from 2.91 to 2.93 Å), which, similarly to Pt(ZnR)$_8$,[17b,e] supports the above-commented non-interacting nature of Zn···Zn in **10**.

[32] B. Cordero, V. Gómez, A. E. Platero-Prats, M. Revés, J. Echeverra, E. Cremades, F. Barragán, S. Alvarez. *Dalton Trans*. **2008**, 2832–2838.

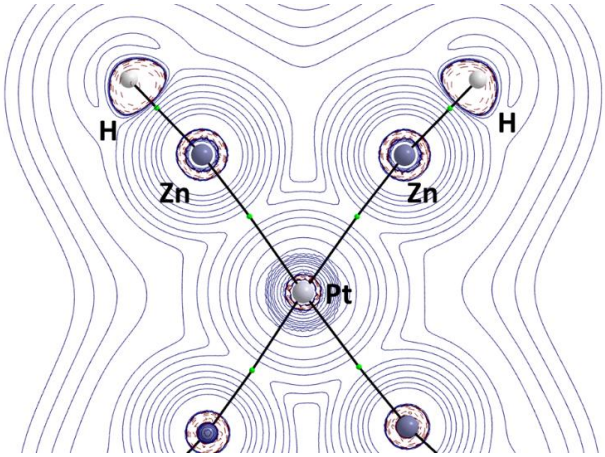

Figure 14. Contour line diagrams $\nabla^2\rho(r)$ for $Pt(ZnH)_6$ in the Zn−Pt−Zn plane. The solid lines connecting the atomic nuclei are the bond paths while the small green spheres indicate the corresponding bond critical points.

More quantitative insight into the bonding situation in **10** can be obtained by means of the Energy Decomposition Analysis (EDA) method, also used by Fischer, Frenking and co-workers to analyze the bonding in the analogous $Pt(ZnH)_8$ (D_{4d}).[17b] Thus, we compare the EDA data for $Pt(ZnH)_6$ and $Pt(ZnH)_8$ using the same partitioning scheme reported previously, namely Pt(0) and $(ZnH)_n$ (n = 6, 8) in their singlet states as fragments. Table 1 gathers the corresponding EDA values computed at the ZORA-BP86-D3/TZ2P//BP86-D3/def2-TZVPP level including the original data reported previously for $Pt(ZnH)_8$ (D_{4d}) computed at the rather similar ZORA-BP86/TZ2P//RI-BP86/def2-TZVPP level. From the data in Table 1, the resemblance between both Pt(0) compounds becomes evident. Although the computed interaction energy, ΔE_{int}, is higher in $Pt(ZnH)_8$ (which is not surprising as the Pt center interacts with two additional one-electron ZnH ligands), in both cases, the platinum atom bears a small negative charge,

which is consistent with the chosen neutral fragments. Despite that, the main contribution to the bonding comes from the electrostatic interactions, which represent ca. 76−77% of the total attractions. The contribution resulting from orbital interactions (mainly involving the *d* atomic orbitals of platinum) is significantly much lower, and almost negligible those coming from dispersion interactions. This therefore indicates that the bonding in the newly prepared compound **10** (and the analogous [Pt(ZnCp*)$_4$(ZnR)$_4$]) can be viewed mainly as a result of the electrostatic interactions between the platinum center and the surrounding ZnCp* ligands.

Table 1. EDA results at ZORA-BP86-D3/TZ2P for [Pt(ZnH)n] (n = 6,8) with the fragments $M(s^0d^{10})$ and $(ZnH)_n$ in the singlet state. Energy values in kcal/mol.

Compound	**$Pt(ZnH)_6$**	**$Pt(ZnH)_8$**	**$Pt(ZnH)_8$**[a]
ΔE_{int}	-234.1	-288.9	-279.0
ΔE_{Pauli}	434.7	468.8	486.0
ΔE_{elstat}[b]	-518.4 (77.5%)	-575.6 (76.0%)	-583.4 (76.3%)
ΔE_{orb}[b]	-145.5 (21.8%)	-175.2 (23.1%)	-181.6 (23.7%)
ΔE_{disp}[b]	-4.8 (0.7%)	-6.9 (0.9%)	□
q(Pt)[c]	-0.21	-0.21	□

[a] Values taken from reference 17b. [b] Percentage values in parentheses give the contributions to the total attractive energy $\Delta E_{elstat} + \Delta E_{orb} + \Delta E_{disp}$. [c] Computed Hirshfeld charges at the platinum center.

III.2.2.2. Reactivity Studies with Pt/Zn MOLPs

We next interrogated the ability of these Pt/Zn bimetallic pairs to activate both polar and non-polar bonds using water and dihydrogen as model substrates. We mainly directed our efforts towards pairs containing inorganic zinc salts, as organozinc compounds (**1**/ZnR_2, **9** and **10**) were rapidly hydrolyzed in the presence of water. Besides, those species remained inactive towards H_2 under all attempted conditions. In contrast, equimolar benzene suspensions of **1** and ZnX_2 (X = Cl, Br, I, OTf) readily react with H_2O (5 equiv.) by means of O−H bond activation (Scheme 10).[17] It is important to remark that **1** does not react with water on its own even under more forcing conditions (80 ºC, 24 hours). However, in the presence of zinc halides formation of *trans*-[PtHX(P^tBu_3)$_2$] (X = Cl, Br, I; **11**, Scheme 10) is evidenced by a distinctive low frequency ^{1}H NMR resonance due to the metal hydride (δ = -19.2 (**11a**, Cl), -18.4 (**11b**, Br), -16.4 (**11c**, I) ppm), exhibiting scalar coupling to both ^{31}P ($^2J_{HP} \approx 12$ Hz) and ^{195}Pt ($^1J_{HPt} \approx 1100$ Hz) nuclei. In the case of $Zn(OTf)_2$, the reduced coordinating capacity of the triflate moiety compared to halide anions led to the cationic hydride-aquo complex *trans*-[PtH(OH_2)(P^tBu_3)$_2$]$^+$ (**12**) as the only observable product. Formation of compounds **11** and **12** is accompanied by the appearance of a fine precipitate of zinc hydroxide salts.

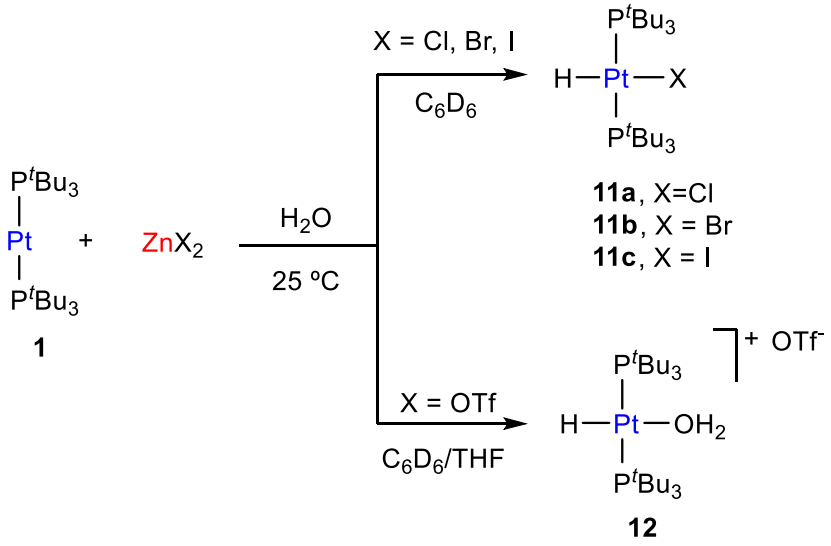

Scheme 10. Activation of polar O−H bond towards Pt(0)/Zn(II) FLPs.

As discussed in the previous section, water activation by combining **1** with the transition metal Lewis acid $[Cu(CH_3CN)_4]PF_6$[17] has been studied. More recently and as part of this Thesis the use of $AgNTf_2$ for similar purposes was demonstrated, with those studies constituting the core of Section III.1. Formation of an intermediate characterized by a Pt→M dative interaction is proposed as the initial step in both cases, after which the cooperative cleavage of the O−H bond takes place. Our experiments indicate that bimetallic adduct formation is not favored for zinc salts, and thus an FLP-type mechanism seems more likely. In fact, in Chapter 2 we have already demonstrated that compound **1** acts as a Lewis basic site in bimetallic FLPs by partnering it with sterically crowded Au(I) compounds. The mechanistic investigations discussed in section II.2.2 allowed us to conclude that those Pt(0)/Au(I) pairs mediate the cleavage of the H−H bond in dihydrogen by a genuine FLP mechanism (see Chapter II). We wondered

if the same would apply for the Pt/Zn pairs investigated herein. Once again, it is worth mentioning that neither **1** nor zinc (pseudo)halides react with H_2 on their own (Scheme 11a). Similarly, the combination of **1** and zinc halides in benzene or THF did not provide any reactivity upon exposure to H_2 (2 bar, 70 ºC). However, in the presence of the more acidic $Zn(OTf)_2$ dihydrogen activation proceeds smoothly to generate Pt(II) dihydride **13**[33] even under mild conditions (H_2 1 bar, 25 ºC, 5h; Scheme 11b). Compound **13** is produced in *ca*. 85% spectroscopic yield, exhibiting a characteristic ^{1}H NMR resonance at -2.91 ppm ($^2J_{HP}$ = 16.4 Hz, $^1J_{HPt}$ = 780.6 Hz).

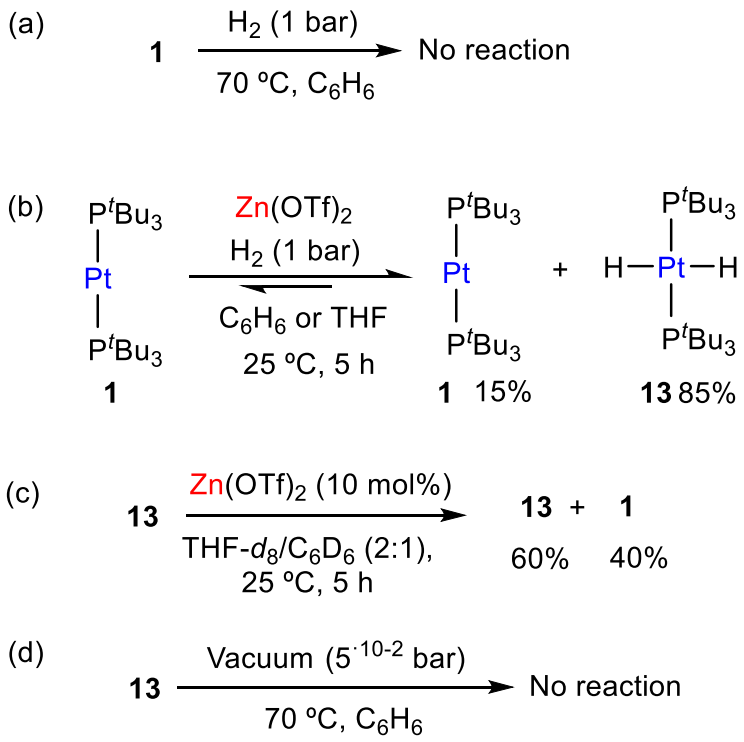

Scheme 11. Reactivity of bimetallic pair **1**/$Zn(OTf)_2$ with H_2.

[33] R. G. Goel, W. O. Ogiri, R. C. Srivastava. *Organometallics* **1982**, *1*, 819–824.

Formation of **13** suggests a catalytic role of $Zn(OTf)_2$ during the hydrogenation of **1**, which has previously been observed for the hydrogenation of imines catalyzed by the same zinc species.[34] In fact, decreasing the amount of $Zn(OTf)_2$ to only 5 mol% with respect to **1** under otherwise identical conditions led to the formation of **13** in comparable yields. In fact, the amount of zinc and the nature of the solvent did not have any apparent influence on the extent of dihydride produced, which was obtained in yields between 80 and 90% in all cases. Attempts to reach full hydrogenation of **1** were unsuccessful despite longer reaction times, higher temperatures and increasing loadings of zinc. These observations imply that hydrogenation of **1** is a reversible process. We confirmed this idea by adding $Zn(OTf)_2$ (10 mol%) to a THF-d_8/C_6D_6(2:1) solution of dihydride **13** in a sealed NMR tube (Scheme 11c). Reaction monitoring evidenced evolution to a mixture of both **1** and **13** in a *ca.* 2:3 ratio after 5 hours, as well a minute amount of free H_2 identified by a ^{1}H NMR peak at 4.42 ppm. Replacing the atmosphere by H_2 (1 bar) led to **13** in around 85% yield. The presence of zinc is also essential for dehydrogenation, since in its absence the release of H_2 could not be detected even by heating **13** under dynamic vacuum (70 ºC, 50 mbar, Scheme 11d). This process resembles both the dehydrogenation of $[PtH_2(PCy_3)_2]$ promoted by C_{60},[35] as well as the role played by $Zn(C_6F_5)_2$ in facilitating biaryl reductive elimination from Zn(II) complexes that has already been discussed and appears in Scheme 7.22

The mechanism of reversible heterolytic dihydrogen splitting holds great interest due to its connection to hydrogen production and the action of hydrogenase enzymes. As discussed in Chapter 1, it has also been largely

[34] S. Werkmeister, S. Fleischer, S. Zhou, K. Junge, M. Beller. *ChemSusChem* **2012**, *5*, 777–782.
[35] L. Pandolfo, M. Maggini. *J. Organom. Chem.* **1997**, *540*, 61–65.

studied as a benchmark transformation to gauge FLP behavior and, despite its apparent simplicity, remains a topic of intense research.[36] In this line, the absence of adduct formation from the pair **1**/$Zn(OTf)_2$ along with its cooperative bond activation could be understood in terms of FLP principles.[37] We performed several experiments to gain some preliminary mechanistic information. First, we determined the kinetic isotopic effect (KIE) for H_2 *vs* D_2 splitting, which has a strong inverse value of 0.59±0.1 (see section III.3.2. for details). This is an uncommon finding[38] that compares well with the values described for the Pt(0)/Au(I) bimetallic FLP (KIE = 0.46 ± 0.04) discussed in the previous Chapter, where a genuine frustrated mechanism was ascertained. As we analyzed earlier, we postulate that the origin for such a strong inverse KIE derives from an FLP product-like transition state whose bimetallic structure offered an assortment of H-containing bending modes that contribute to the zero-point energy (ZPE). We anticipate that a similar transition state in the present system (**B** in Scheme 12) would analogously derive in a strong inverse KIE, as observed experimentally.

[36] a) G. Skara, F. De Vleeschouwer, P. Geerlings, F. De Proft, B. Pinter. *Sci. Rep.* **2017**, *7*, 16024. b) J. Daru, I. Bakó, A. Stirling, I. Pápai. *ACS Catal.* **2019**, *9*, 6049–6057. c) D. Yepes, P. Jaque, I. Fernández. *Chem. Eur. J.* **2016**, *22*, 18801–18809. d) L. Liu, L. Cao, Y. Shao, G. Mnard, D. W. Stephan. *Chem* **2017**, *3*, 259–267. e) H. B. Hamilton, D. F. Wass. *Chem* **2017**, *3*, 198–210.

[37] a) R. Dobrovetsky, D. W. Stephan. *Isr. J. Chem.* **2015**, *55*, 206–209. b) P. Jochmann, D. W. Stephan. *Angew. Chem. Int. Ed.* **2013**, *52*, 9831–9835.

[38] Y. Zhang, M. K. Karunananda, H.-C. Yu, K. J. Clark, W. Williams, N. P. Mankad, D. H. Ess. *ACS Catal*. **2019**, *9*, 2657–2663.

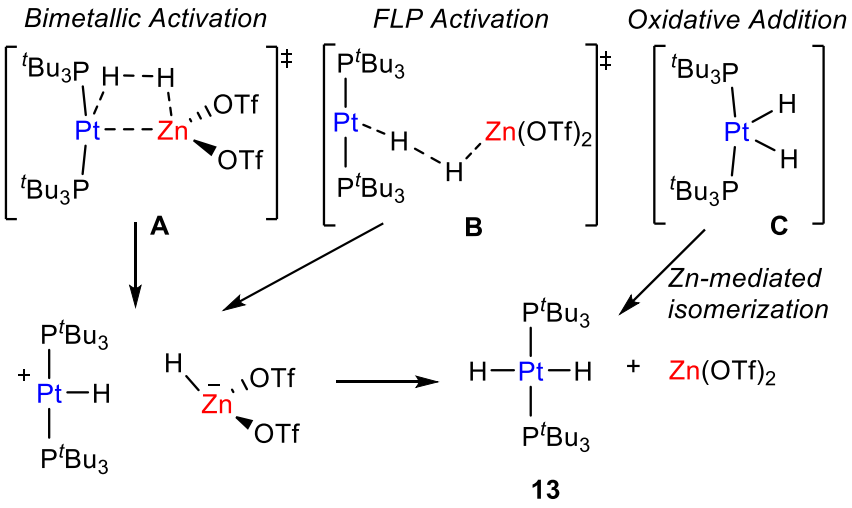

Scheme 12. Potential mechanisms for H_2 activation by **1**/$Zn(OTf)_2$.

Direct oxidative addition of dihydrogen over **1** to form *cis*-$[PtH_2(P^tBu_3)_2]$ followed by Zn-assisted isomerization20 could be considered as an alternative mechanism (**C** in Scheme 12). However, solutions of **1**:$Zn(OTf)_2$ catalyze rapid ($t_{1/2}$ < 15 min) exchange between H_2 and D_2 to produce HD (δ = 4.36 ppm, $^1J_{HD}$ = 42.6 Hz) in a statistical amount (Scheme 13A), which seems to disfavor a classical oxidative addition route. In fact, the individual monometallic species mediate the exchange at a considerable slower pace ($t_{1/2}$ > 2 days) (Scheme 12B). Interestingly, compound $[PtH(P^tBu_3)_2]^+$ (**14**), which would be an intermediate during FLP-type H_2 activation, promotes H/D scrambling at a rate comparable to the bimetallic pair (Scheme 13C). This agrees with its existence as a transient intermediate during the hydrogenation of **1**, thus supporting the idea of a bimetallic FLP mechanism (through **B** in Scheme 12). Nevertheless, these preliminary experiments cannot yet rule out a more traditional bimetallic H_2 activation

route implying a transient dative Pt→Zn bond (**A** in Scheme 12) or the active participation of triflate substituents.[39]

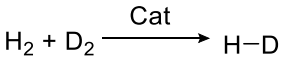

Entry	Cat	$t_{1/2}$
1	**1**:Zn(OTf)$_2$	< 15 min
2	1	$t_{1/2}$ > 2 days
3	14	< 15 min

Scheme 13. Preliminary mechanistic experiments regarding the heterolytic bimetallic activation of H_2 by **1**/Zn(OTf)$_2$

[39] R. U. Nisaa, K. Ayub. *New J. Chem.* **2017**, *41*, 5082–5090.

III.3. Experimental Section

III.3.1. Synthesis and Characterization of New Complexes

General consideration

All preparations and manipulations were carried out using standard Schlenk and glove-box techniques, under an atmosphere of argon and of high purity nitrogen, respectively. All solvents were dried, stored over 3 Å molecular sieves, and degassed prior to use. Toluene (C_7H_8) and n-pentane (C_5H_{12}) were distilled under nitrogen over sodium. Tetrahydrofuran (THF) and diethyl ether were distilled under nitrogen over sodium/benzophenone. [D_6]Benzene and [D_8]Toluene were dried over molecular sieves (3 Å), [D_8]THF was distilled under argon over sodium/benzophenone, and CD_2Cl_2 and fluorobenzene over CaH_2 distilled under argon. Compounds **1**,[40] $ZnPh_2$,[41] [$Zn_2Cp^*_2$][42] and [$PtHCl(PtBu_3)_2$][33] were prepared as described previously. Other chemicals were commercially available and used as received. Solution NMR spectra were recorded on Bruker AMX-300, DRX-400 and DRX-500 spectrometers. Spectra were referenced to external $SiMe_4$ (δ: 0 ppm) using the residual proton solvent peaks as internal standards (^{1}H NMR experiments), or the characteristic resonances of the solvent nuclei (^{13}C NMR experiments), while ^{31}P was referenced to H_3PO_4 and ^{19}F to $CFCl_3$. Spectral assignments were made by routine one- and two-dimensional NMR experiments where appropriate. For elemental analyses, a LECO TruSpec CHN elementary analyzer was utilized. Infrared spectra were recorded on a Bruker Vector 22 spectrometer and sampling

[40] H.-R. C. Jaw, W. R. Mason. *Inorg. Chem*. **1989**, *28*, 4370–4373.
[41] J. E. Fleckenstein, K. Koszinowski. *Organometallics* **2011**, *30*, 5018–5026.
[42] R. Peloso, I. Resa, A. Rodríguez, E. Carmona. *Inorg. Synth.* **2018**, *37*, 37.

preparation was made in Nujol. The supplementary crystallographic data has been deposited in the Cambridge Crystallographic Data Centre. CCDC: 1909269, 1909268, 1909266, 1909270, 1909267, 2062801 and 2062802.

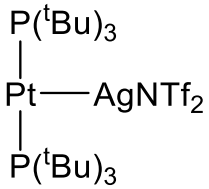

Compound 2. A solution of precursor **1** (50 mg, 0.083 mmol) in toluene (10 mL) was added over silver triflimide (32.4 mg, 0.083 mmol) under nitrogen atmosphere. The colourless solution became yellow after 5 min. Compound **2** was obtained as a yellow crystalline solid (33 mg, 40%) by slow diffusion of pentane at -20 ºC (2:1 by vol.).

Anal. Calcd. for $C_{26}H_{54}AgF_6NO_4P_2PtS_2$: C, 31.6; H, 5.5; N, 1.4; S, 6.5. **Found:** C, 31.5; H, 5.8; N, 1.5; S, 6.6.

^{1}H NMR (400 MHz, C_6D_6, 25 ºC) δ: 1.34 (vt, 54 H, $^{3}J_{HP}$ = 6.2 Hz, ^{t}Bu).

^{13}C{^{1}H} NMR (100 MHz, C_6D_6, 25 ºC) δ: 120.8 (q, $^{1}J_{CF}$ = 321 Hz, CF_3), 39.3 (vt, $^{1}J_{CP}$ = 8 Hz, $^{2}J_{CPt}$ = 35 Hz, Pt−P(*C*$(CH_3)_3$), 33.4 (Pt−P(C(*C*$H_3)_3$).

^{31}P{^{1}H} NMR (160 MHz, C_6D_6, 25 ºC) δ: 99.6 ($^{1}J_{PPt}$ = 3298 Hz, $^{2}J_{PAg}$ = 3 Hz).

^{19}F{^{1}H} NMR (376 MHz, C_6D_6, 25 ºC) δ: -75.2.

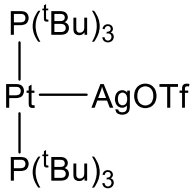

Compound 3. A solution of precursor **1** (50 mg, 0.083 mmol) in toluene (10 mL) was added over silver triflimide (21.4 mg, 0.083 mmol) under nitrogen atmosphere. The colourless solution became yellow after 5 min. Compound **3** was obtained as a yellow crystalline solid (28 mg, 39%) by slow diffusion of pentane at -20 ºC (2:1 by vol.).

Anal. Calcd. for $C_{25}H_{54}AgF_3O_3P_2PtS$: C, 35.1; H, 6.4; S, 3.7. **Found:** C, 35.2; H, 6.7; S, 3.9.

^{1}H NMR (400 MHz, C_6D_6, 25 ºC) δ: 1.33 (vt, 54 H, $^{3}J_{HP}$ = 6.2 Hz, ^{t}Bu).

^{13}C{^{1}H} NMR (100 MHz, C_6D_6, 25 ºC) δ: 121.8 (q, $^{1}J_{CF}$ = 319 Hz, CF_3), 39.4 (vt, $^{1}J_{CP}$ = 8 Hz, $^{2}J_{CPt}$ = 33 Hz, Pt−P(*C*$(CH_3)_3$), 33.4 (Pt−P(C(*C*$H_3)_3$).

^{31}P{^{1}H} NMR (160 MHz, C_6D_6, 25 ºC) δ: 99.2 ($^{1}J_{PPt}$ = 3244 Hz).

^{19}F{^{1}H} NMR (376 MHz, C_6D_6, 25 ºC) δ: -76.7.

X-H (X = H, C, O, N) bond activation studies using compound 2. All the reactions were carried out using the same experimental procedure. A solution of compound **1** (20 mg, 0.033 mmol) in either C_6D_6 or toluene-d_8 (0.5 mL) was added over silver triflimide (13 mg, 0.033 mml) in a *J. Young* NMR tube. The solution was shaken and then the corresponding liquid or gas reagent was added and the progress of the reaction monitored by ^{1}H and $^{31}P\{^{1}H\}$ NMR spectroscopy. More precise details are given below.

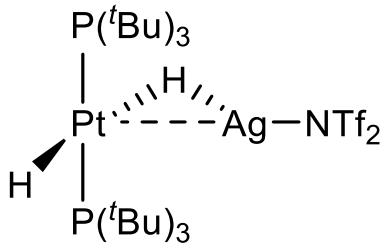

Compound 4. Compound **4** was formed in quantitative spectroscopic yield after 5 hours at -20 ºC under H_2 atmosphere (1 bar). The limited stability of this compound precluded its isolation in pure form.

^{1}H NMR (400 MHz, Tol-d_8, 25 ºC) δ: 1.34 (vt, 54 H, $^{3}J_{HP}$ = 6.4 Hz, ^{t}Bu), -4.89 (dq, 2 H, $^{1}J_{AgH}$ = 120, $^{2}J_{HP}$ = 10, $^{1}J_{HPt}$ = 778 Hz).

^{13}C{^{1}H} NMR (100 MHz, Tol-d_8, 25 ºC) δ: 120.5 (q, $^{1}J_{CF}$ = 322 Hz, CF_3), 40.3 (vt, $^{1}J_{CP}$ = 9 Hz), 32.1 (Pt−P(C(*C*H$_3$)$_3$).

^{31}P{^{1}H} NMR (160 MHz, Tol-d_8, 25 ºC) δ: 94.6 ($^{1}J_{PPt}$ = 2660 Hz).

^{19}F{^{1}H} NMR (376 MHz, C_6D_6, 25 ºC) δ: -76.7.

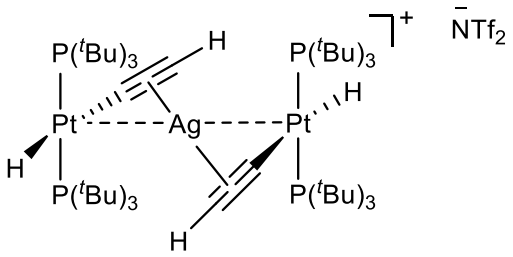

Compound 5. A toluene solution of **1** (50 mg, 0.083 mmol) and $AgNTf_2$ (16 mg, 0.042 mmol) was placed under acetylene atmosphere (0.5 bar) and vigorously stirred at -20 ºC for 20 min. Compound **5** was obtained as a brownish solid after precipitation with pentane (22 mg, 31%). Alternatively, compound **5** was formed in quantitative spectroscopic yield after 5 min at 25 ºC under C_2H_2 atmosphere (0.5 bar) and working under the NMR tube conditions stated above.

^{1}H NMR (500 MHz, C_6D_6, 25 ºC) δ: 3.28 (t, 2 H, J, C≡CH), 1.50 (vt, 108 H, $^{3}J_{HP}$ = 6.2 Hz, ^{t}Bu), -10.37 (t, 2 H, $^{2}J_{HP}$ = 14.3, $^{1}J_{HPt}$ = 277.5 Hz, Pt−H).

^{13}C{^{1}H} NMR (100 MHz, C_6D_6, 25 ºC) δ: 40.8 (vt, $^{1}J_{CP}$ = 8 Hz, $^{2}J_{CPt}$ = 32 Hz, Pt−P(*C*$(CH_3)_3$), 33.3 Pt−P(C(*C*$H_3)_3$). Signal due to the acetylide carbon centres could not be located neither in the ^{13}C{^{1}H} NMR spectrum nor by 2D NMR correlations.

^{31}P{^{1}H} NMR (200 MHz, C_6D_6, 25 ºC) δ: 83.4 ($^{1}J_{PPt}$ = 2782 Hz).

^{19}F{^{1}H} NMR (376 MHz, C_6D_6, 25 ºC) δ: -78.2.

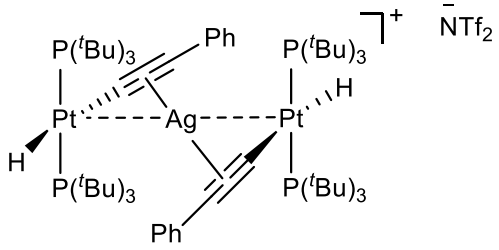

Compound 6. A toluene solution of **1** (50 mg, 0.083 mmol) and $AgNTf_2$ (16 mg, 0.042 mmol) was treated with phenylacetylene (9µL, 0.083 mmol) and stirred at -20 ºC for 20 min. Compound **6** was obtained as a brownish solid after precipitation with pentane (25 mg, 32%). Alternatively, compound **6** was formed in quantitative spectroscopic yield after 5 min at 25 ºC.

^{1}H NMR (400 MHz, C_6D_6, 25 ºC) δ: 7.63 (m, 4 H, *o*-C_6H_5), 7.18 (m, 4 H, *m*-C_6H_5), 7.02 (t, 4 H, $^{3}J_{HH}$ = 7.5 Hz, *p*-C_6H_5), 1.49 (vt, 108 H, $^{3}J_{HP}$ = 6.7 Hz, ^{t}Bu), -9.60 (t, 2 H, $^{2}J_{HP}$ = 13.4, $^{1}J_{HPt}$ = 619.4 Hz, Pt−H).

^{13}C{^{1}H} NMR (100 MHz, C_6D_6, 25 ºC) δ: 132.4 (*o*-C_6H_5), 131.2 (*ipso*-C_6H_5), 128.9 (*m*-C_6H_5), 128.6 (*p*-C_6H_5), 121.0 (q, $^{1}J_{CF}$ = 323 Hz, CF_3), 40.6 (vt, $^{1}J_{CP}$ = 8 Hz, $^{2}J_{CPt}$ = 33 Hz, Pt−P(*C*$(CH_3)_3$), 33.1 (Pt−P(C(*C*$H_3)_3$). Signal due to the acetylide carbon centres could not be located neither in the ^{13}C{^{1}H} NMR spectrum nor by 2D NMR correlations.

^{31}P{^{1}H} NMR (160 MHz, C_6D_6, 25 ºC) δ: 82.8 ($^{1}J_{PPt}$ = 2759 Hz).

^{19}F{^{1}H} NMR (376 MHz, C_6D_6, 25 ºC) δ: -76.3.

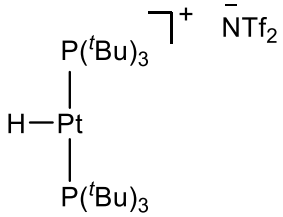

Compound 7. Compound **7** was formed in around 80% yield after one hour at 25 ºC in the presence of methanol (7 µL, 0.165 mmol). ^{1}H and $^{31}P\{^{1}H\}$ NMR spectroscopic details match perfectly with those previously reported.[16]

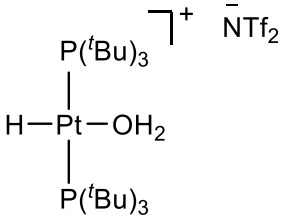

Compound 8a. Compound **8a** was formed in around 90% spectroscopic yield after one day at 25 ºC in the presence of water (100 µL, 5.55 mmol). ^{1}H and $^{31}P\{^{1}H\}$ NMR spectroscopic details match perfectly with those previously reported.[16]

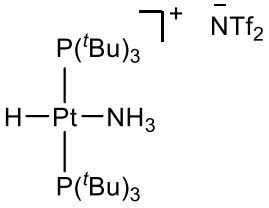

Compound 8b. Compound **8b** was formed in 60% spectroscopic yield after 16 hours at 60 ºC in the presence of ammonia (0.5 bar). ^{1}H and $^{31}P\{^{1}H\}$ NMR spectroscopic details match perfectly with those previously reported.[16]

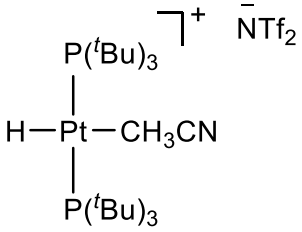

Compound 8c. Compound **8c** was formed in around 90% spectroscopic yield after 5 min at 25 ºC when using a 1:1 mixture of C_6D_6 and wet acetonitrile (0.5 mL) as solvent. ^{1}H and $^{31}P\{^{1}H\}$ NMR spectroscopic details match perfectly with those previously reported.[17]

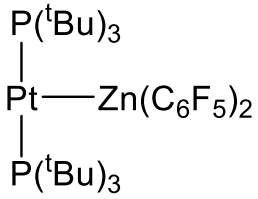

Compound 9. To a mixture of [Pt(P^{t}Bu$_3$)$_2$] (**1**) (50 mg, 0.083 mmol) and Zn(C$_6$F$_5$)$_2$ (33 mg, 0.083 mmol) was added 5 mL of toluene and the solution was stirred for 30 minutes, then kept at -30 ºC. Orange crystals of **9** were collected and washed with cold pentane (43 mg, 52%).

Anal. Calcd. for $C_{36}H_{54}F_{10}P_2PtZn$: C, 43.3; H, 5.5. **Found:** C, 43.0; H, 5.7.

^{1}H NMR (400 MHz, C_6D_6, 25 ºC) δ: 1.28 (vt, 54 H, $^3J_{HP}$ = 6.3 Hz, ^{t}Bu).

^{13}C{^{1}H} NMR (100 MHz, CD_2Cl_2, 25 ºC) δ: 148.6 (br d, $^1J_{CF}$ = 227 Hz, *o*-C_6F_5), 139.8 (br d, $^1J_{CF}$ = 232 Hz, *p*-C_6F_5), 136.6 (br d, $^1J_{CF}$ = 254 Hz, *m*-C_6F_5), 128.2 (br, *ipso*-C_6F_5), 40.2 (vt, $^1J_{CP}$ = 8 Hz, Pt−P(*C*(CH$_3$)$_3$), 33.0 (Pt−P(C(*C*H$_3$)$_3$).

^{31}P{^{1}H} NMR (160 MHz, C_6D_6, 25 ºC) δ: 93.1 ($^1J_{PPt}$ = 3328 Hz).

^{19}F{^{1}H} NMR (376 MHz, C_6D_6, 25 ºC) δ: -115.7, -157.4, -162.0.

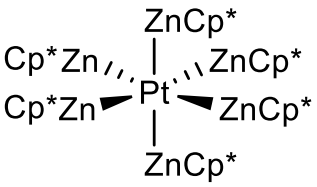

Compound 10. To a mixture of complex [Pt(P^tBu_3)$_2$] (**1**) (50 mg, 0.083 mmol) and [$Zn_2Cp^*_2$] (99 mg, 0.249 mmol) was added 3 mL of benzene. The solution was stirred for 20 minutes at room temperature. Complex **10** crystallized from the crude reaction after 12 hours (34 mg, 30%).

Anal. Calcd. for $C_{60}H_{90}PtZn_6$: C, 51.5; H, 6.5. **Found:** C, 51.5; H, 6.8.

^{1}H NMR (400 MHz, C_6D_6, 25 ºC) δ: 1.45 (Me).

^{13}C{^{1}H} NMR (100 MHz, THF-d_8, 25 ºC) δ: 112.0 (C_5Me_5), 12.0 (C_5Me_5).

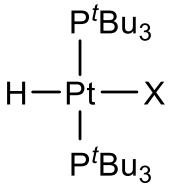

11a, X=Cl; **11b**, X = Br; **11c**, X = I

Compounds 11. The synthesis of compounds **11** were carried out using the same experimental procedure. A solution of compound **1** (20 mg, 0.033 mmol) in C_6D_6 (0.5 mL) was added over 1 eq. of the corresponding zinc halide, ZnX_2 (X = Cl, Br, I) in a *J. Young* NMR tube. The suspension was shaken and then water (3 µL, 0.165 mmol) was added and the progress of the reaction monitored by ^1H and $^{31}P\{^1H\}$ NMR spectroscopy. Compounds **11a-c** were formed in >90% spectroscopic yield after one hour at 25 ºC. ^1H and $^{31}P\{^1H\}$ NMR spectroscopic details match perfectly with those previously reported.[33]

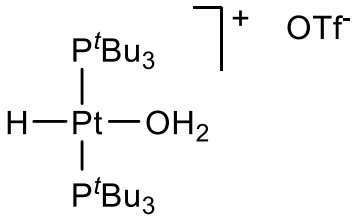

Compound 12. A solution of $[Pt(P^tBu_3)_2]$ (**1**) (20 mg, 0.033 mmol) in C_6D_6/THF (0.2/0.4 mL) was added over $Zn(OTf)_2$ (12 mg, 0.033 mmol) in a *J. Young* NMR tube. The solution was shaken and then water (3 µL, 0.165 mmol) was added. Compound **12** was formed in around 85% spectroscopic yield after 10 minutes at 25 ºC. ^1H and $^{31}P\{^1H\}$ NMR spectroscopic details match perfectly with those previously reported.[16]

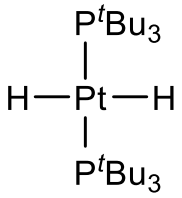

Compound 13. A solution of compound **1** (20 mg, 0.033 mmol) in THF/C_6D_6 (0.4/0.2 mL) was added over $Zn(OTf)_2$ (12 mg, 0.033 mmol) in a *J. Young* NMR tube. The solution was shaken and the nitrogen atmosphere replaced by hydrogen (1 atm). Compound **13** was formed in around 85% spectroscopic yield after 5 hours at 25 ºC. ^1H and $^{31}P\{^1H\}$ NMR spectroscopic details match perfectly with those previously reported.[33]

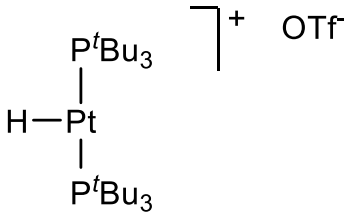

$[PtH(PtBu_3)_2]^+$. To a mixture of $[PtHCl(PtBu_3)_2]$ (50 mg, 0.079 mmol) and AgOTf (20 mg, 0.079 mmol) was added toluene (8 mL) under N_2 atmosphere. The reaction was covered with aluminum foil and stirred at room temperature for 1 hour. The solution was filtered and the volatiles were removed in vacuo to yield the compound as a white powder (42 mg, 71%). ^1H and $^{31}P\{^1H\}$ NMR spectroscopic details match perfectly with those previously reported.[16]

III.3.2. Kinetic Studies

Kinetic studies were carried out to determine the kinetic isotopic effect (KIE) of dihydrogen activation by compound **1** and $Zn(OTf)_2$. In a *J. Young* NMR tube, a mixture of compounds **1** (5 mg, 0.008 mmol) and $Zn(OTf)_2$ (3 mg, 0.008 mmol) was dissolved in THF-d_8/C_6D_6 (0.4/0.2 mL) at room temperature. The nitrogen atmosphere was replaced by either H_2 or D_2 (1 bar) and the solution was shaken. The progress of the reaction was monitored by $^{31}P\{^1H\}$ NMR spectroscopy at 25 ºC by means of the disappearance of compound **1** and using triphenylphosphine oxide as internal standard.

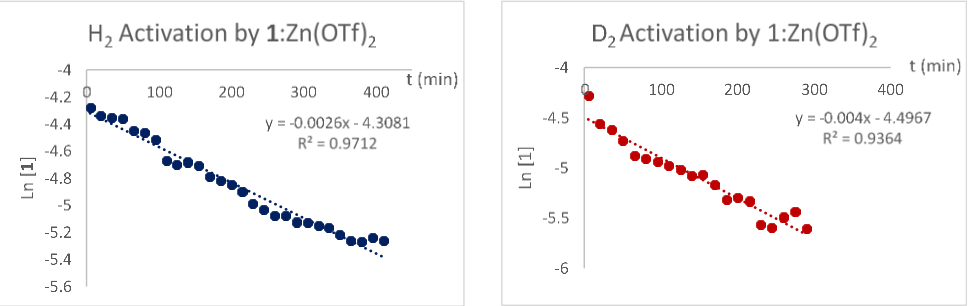

Figure 15. Representative examples of the kinetic profiles for the activation of H_2 or D_2 by the **1**:$Zn(OTf)_2$ system.

III.3.3. Isotopic Exchange Experiments

A solution of [Pt(P^tBu_3)$_2$] (**1**) (5 mg, 0.008 mmol) and Zn(OTf)$_2$ (3 mg, 0.008 mmol) was dissolved in THF-d_8/C_6D_6 (0.4/0.2 mL) and a H_2/D_2 mixture (1:1, 1 bar) was added in a *J. Young* NMR tube. The reaction was monitored by ^{1}H NMR NMR spectroscopy at 25 ºC to track the progress of HD evolution. To complete these studies, the same procedure was performed with [Pt(^{t}Bu$_3$)$_2$], Zn(OTf)$_2$ and [PtH(PtBu$_3$)$_2$]$^+$, separately.

III.3.4. Computational Details

Geometry optimization of compounds $Pt(ZnH)_6$ and $Pt(ZnH)_8$ (D_{4d}) were performed by Prof. Israel Fernández using the Gaussian16[43] suite of programs at the BP86[44]/def2-TZVPP[45] level of theory using the D3 dispersion correction suggested by Grimme et al.[46] This level is denoted BP86-D3/def2-TZVPP. All AIM results described in this work correspond to calculations performed at the BP86-D3/def2-TZVPP/WTBS(for Pt) level on the optimized geometry obtained at the BP86-D3/def2-TZVPP level. The WTBS (well-tempered basis sets)[47] have been recommended for AIM calculations involving transition metals.[48] The topology of the electron density was conducted using the AIMAll program package.[49]

The interaction between Pt(0) and $(ZnH)_n$ (n=6,8) has been investigated with the Energy Decomposition Analysis (EDA)[50] method.

[43] Gaussian 16, Revision B.01, M. J. Frisch, G. W. Trucks, H. B. Schlegel, G. E. Scuseria, M. A. Robb, J. R. Cheeseman, G. Scalmani, V. Barone, B. Mennucci, G. A. Petersson, H. Nakatsuji, M. Caricato, X. Li, H. P. Hratchian, A. F. Izmaylov, J. Bloino, G. Zheng, J. L. Sonnenberg, M. Hada, M. Ehara, K. Toyota, R. Fukuda, J. Hasegawa, M. Ishida, T. Nakajima, Y. Honda, O. Kitao, H. Nakai, T. Vreven, J. A. Montgomery, Jr., J. E. Peralta, F. Ogliaro, M. Bearpark, J. J. Heyd, E. Brothers, K. N. Kudin, V. N. Staroverov, T. Keith, R. Kobayashi, J. Normand, K. Raghavachari, A. Rendell, J. C. Burant, S. S. Iyengar, J. Tomasi, M. Cossi, N. Rega, J. M. Millam, M. Klene, J. E. Knox, J. B. Cross, V. Bakken, C. Adamo, J. Jaramillo, R. Gomperts, R. E. Stratmann, O. Yazyev, A. J. Austin, R. Cammi, C. Pomelli, J. W. Ochterski, R. L. Martin, K. Morokuma, V. G. Zakrzewski, G. A. Voth, P. Salvador, J. J. Dannenberg, S. Dapprich, A. D. Daniels, O. Farkas, J. B. Foresman, J. V. Ortiz, J. Cioslowski, and D. J. Fox, Gaussian, Inc., Wallingford CT, **2016**.
[44] a) A. D. Becke. *Phys. Rev. A* **1988**, *38*, 3098–3100. b) J. P. Perdew. *Phys. Rev. B* **1986**, *33*, 8822–8824.
[45] F. Weigend, R. Ahlrichs. *Phys. Chem. Chem. Phys*. **2005**, *7*, 3297–3305.
[46] S. Grimme, J. Antony, S. Ehrlich, H. A. Krieg. *J. Chem. Phys*. **2010**, *132*, 154104.
[47] a) S. Huzinaga, B. A. Miguel. *Chem. Phys. Lett*. **1990**, *175*, 289–291. b) S. Huzinaga, M. Klobukowski. *Chem. Phys. Lett*. **1993**, *212*, 260–264.
[48] J. A. Cabeza, J. F. van der Maelen, S. García-Granda. *Organometallics* **2009**, *28*, 3666–3672 and references therein.
[49] Keith, T. A. AIMAll, **2010**, http://tkgristmill.com.
[50] For a recent review, see: M. von Hopffgarten, G. Frenking. *WIREs Comput. Mol. Sci*. **2012**, *2*, 43–62.

Within this approach, the interaction energy can be decomposed into the following physically meaningful terms:

$$\Delta E_{\text{int}} = \Delta E_{\text{elstat}} + \Delta E_{\text{Pauli}} + \Delta E_{\text{orb}} + \Delta E_{\text{disp}}$$

The term ΔE_{elstat} corresponds to the classical electrostatic interaction between the unperturbed charge distributions of the deformed reactants and is usually attractive. The Pauli repulsion ΔE_{Pauli} comprises the destabilizing interactions between occupied orbitals and is responsible for any steric repulsion. The orbital interaction ΔE_{orb} accounts for charge transfer (interaction between occupied orbitals on one moiety with unoccupied orbitals on the other, including HOMO–LUMO interactions) and polarization (empty-occupied orbital mixing on one fragment due to the presence of another fragment). Finally, the ΔE_{disp} term takes into account the interactions which are due to dispersion forces.

The EDA-NOCV calculations were carried out using the BP86-D3/def2-TZVPP optimized geometries with the program package ADF 2019.01[51] using the same functional (BP86-D3) in conjunction with a triple-ζ-quality basis set using uncontracted Slater-type orbitals (STOs) augmented by two sets of polarization function with a frozen-core approximation for the core electrons.[52] An auxiliary set of s, p, d, f, and g STOs were used to fit the molecular densities and to represent the Coulomb and exchange potentials accurately in each SCF cycle.[53] Scalar relativistic effects were

[51] ADF program: www.scm.com.
[52] J. G. Snijders, P. Vernooijs, E. J. Baerends. *At. Data. Nucl. Data Tables* **1982**, *26*, 483–509.
[53] A. Krijn, E. J. Baerends. Fit Functions in the HFS-Method, Internal Report (in Dutch), Vrije Universiteit Amsterdam, The Netherlands, **1984**.

incorporated by applying the zeroth-order regular approximation (ZORA).[54] This level of theory is denoted ZORA-BP86-D3/TZ2P//BP86-D3/def2-TZVPP.

[54] a) E. van Lenthe, E. J. Baerends, J. G. Snijders. *J. Chem. Phys.* **1993**, *99*, 4597–4610. b) E. van Lenthe, E. J. Baerends, J. G. Snijders. *J. Chem. Phys.* **1994**, *101*, 9783–9792. c) E. van Lenthe, A. Ehlers, E. J. Baerends. *J. Chem. Phys.* **1999**, *110*, 8943–8953.

III.4. References

1. J. Bauer, H. Braunschweig, R. D. Dewhurst. *Chem. Rev.* **2012**, *112*, 4329–4346.

2. a) P. J. Malinowsky, I. Krossing. *Angew. Chem. Int. Ed.* **2014**, *53*, 13460–13462. b) D. E. Janzen, L. F. Mehne, D. G. VanDerveer, G. J. Grant. *Inorg. Chem.* **2005**, *44*, 8182–8184. c) Z. Xie, T. Jelínek, R. Bau, C. A. Reed. *J. Am. Chem. Soc.* **1994**, *116*, 1907–1913. d) T. Yamaguchi, F. Yamazaki, T. Ito. *J. Am. Chem. Soc.* **2001**, *123*, 743–744. e) G. Wang, Y. S. Ceylan, T. R. Cundari, H. V. R. Dias. *J. Am. Chem. Soc.* **2017**, *139*, 14292–14301. f) S. Takemoto, T. Tsujimoto, H. Matsuzaka. *Organometallics* **2018**, *37*, 1591–1597.

3. a) G. Weber, F. Rominger, B. F. Straub, *Eur. J. Inorg. Chem*. **2012**, 2863–2867. b) G. Sipos, P. Gao, D. Foster, B. W. Skelton, A. N. Sobolev, R. Dorta. *Organometallics* **2017**, *36*, 801–817 c) K. Sasakura, K. Okamoto, K. Ohe. *Organometallics* **2018**, *37*, 2319–2324.

4. a) M. Baya, Ú. Belío, D. Campillo, I. Fernández, S. Fuertes, A. Martín. *Chem. Eur. J.* **2018**, *24*, 13879–13889. b) I. Meana, P. Espinet, A. C. Albéniz, *Organometallics* **2014**, *33*, 1–7. c) M. Asay, B. Donnadieu, W. W. Schoeller, G. Bertrand. *Angew. Chem. Int. Ed.* **2009**, *48*, 4796–4799.

5. a) J. Moussa, L. M. Chamoreau, M. P. Gullo, A. Degli Esposti, A. Barbieri, H. Amouri. *Dalton Trans.* **2016**, *45*, 2906–2913. b) L. R. Falvello, J. Forniés, E. Lalinde, B. Menjón, M. A. García-Monforte, M. T. Moreno, M. Tomás. *Chem. Commun.* **2007**, 3838–3840. c) K. M.-C. Wong, C.-K., Hui, K.-L. Yu and V. W.-W. Yam. *Coord. Chem. Rev.* **2002**, *229*, 123–132.

6. H. Braunschweig, C. Brunecker, R. D. Dewhurst, C. Schneider, B. Wennemann. *Chem. Eur. J.* **2015**, *21*, 19195–19201.

7. a) A. Homs, I. Escofet, A. M. Echavarren. Org. Lett. **2013**, *15*, 5782–5785. b) D. Weber, M. R. Gagné. *Org. Lett.* **2009**, *11*, 4962–4965. c) C. Chen, C. Hou, Y. Wang, T. S. A. Hor, Z. Weng. Org. Lett. **2014**, *16*, 524–527.

8. M. K. Karunananda, N. P. Mankad. *J. Am. Chem. Soc.* **2015**, *137*, 14598–14601.

9. a) B. R. Barnett, C. E. Moore, P. Chandrasekaran, S. Sproules, A. L. Rheingold, S. DeBeerde, J. S. Figueroa. *Chem. Sci.* **2015**, *6*, 7169–7178. b) B. R. Barnett, J. S. Figueroa. *Chem. Commun.* **2016**, *52*, 13829–13839. c) H. Braunschweig, R. D. Dewhurst, F. Hupp, C. Schneider. *Chem. Commun.* **2014**, *50*, 15685–15688.

10. T. Troadec, S.-Y. Tan, C. J. Wedge, J. P. Rourke, P. R. Unwin, A. B. Chaplin. *Angew. Chem. Int. Ed.* **2016**, *55*, 3754–3757.

11. S. Otsuka, T. Yoshida, M. Matsumoto, K. Nakatsu. *J. Am. Chem. Soc.* **1976**, *98*, 5850–5858.

12. M. C. MacInnis, J. C. DeMott, E. M. Zolnhofer, J. Zhou, K. Meyer, R. P. Hughes, O. V. Ozerov. *Chem.* **2016**, *1*, 902–920.

13. a) A. Alhinati, F. Demartin, L. M. Venanzi, M. K. Wolfer. *Angew. Chem. Int. Ed.* **1988**, *27*, 563. b) A. Albinati, H. Lehner, L. M. Venanzi, M. Wolfer. *Inorg. Chem.* **1987**, *26*, 3933–3939.

14. a) Q.-H. Wei, L.-J. Han, Y. Jiang, X.-X. Lin, Y.-N. Duan, G.-N. Chen. *Inorg. Chem.* **2012**, *51*, 11117–11125. b) Z. Dai, A. J. Metta-Magaña, J. E. Nuñez, *Inorg. Chem.* **2014**, *53*, 7188–7196. c) S. Yamazaki, A. J. Deeming, D. M. Speel, D. E. Hibbs, M. B. Hursthousec, K. M. A. Malik. *Chem. Commun.* **1997**, 177–178.

15. a) A. Furalani, S. Licoccia, M. V. Russo, A. C. Villa, C. Guastini. *J. Chem. Soc. Dalton Trans.* **1982**, 2449–2453. b) J. R. Berenguer, M. Bernechea, E. Lalinde, *Organometallics* **2007**, *26*, 1161–1172. c) I. Ara, J. R. Berenguer, E. Eguizabal, J. Forniés, J. Gómez, E. Lalinde, J. M. Saez-Rocher. *Organometallics* **2000**, *19*, 4385– 4397.

16. R. G. Goel, R. C. Srivasta. *Can. J. Chem.* **1983**, *61*, 1352–1359.

17. S. Jamali, S. Abedanzadeh, N. K. Khaledi, H. Samouei, Z. Hendi, S. Zacchini, R. Kiaa, H. R. Shahsavari. *Dalton Trans.* **2016**, *45*, 17644–17651.

18. Selected examples of ammonia activation by transition metal complexes: a) J. Zhao, A. S. Goldman, J. F. Hartwig. *Science* **2005**, *307*, 1080–1082. b) C. M. Fafard, D. Adhikari, B. M. Foxman, J. Mindiola, O.V. Ozerov. *J. Am. Chem. Soc.* **2007**, *129*, 10318–10319. e) M. G. Scheibel, J. Abbenseth, M. Kinauer, F. W. Heinemann, C. Würtele, B. de Bruin, S. Schneider. *Inorg. Chem.* **2015**, *54*, 9290–9302.

19. a) R. Álvarez, A. R. De Lera, J. M. Aurrecoechea, A. Durana. *Organometallics* **2007**, *26*, 2799–2802. b) B. Fuentes, M. García-Melchor, A. Lledós, F. Maseras, J. A. Casares, G. Ujaque, P. Espinet. *Chem. Eur. J.* **2010**, *16*, 8596–8599. c) R. J. Oeschger, P. A. Chen. *Organometallics* **2017**, *36*, 1465−1468. d) E. Paenurk, R. Gershoni-Poranne, P. Chen. *Organometallics* **2017**, *36*, 4854−4863.

20. a) J. A. Casares, P. Espinet, B. Fuentes, G. Salas. *J. Am. Chem. Soc*. **2007**, *129*, 3508−3509. b) J. delPozo, E. Gioria, J. A. Casares, R. Álvarez, P. Espinet. *Organometallics* **2015**, *34*, 3120−3128.

21. a) Q. Liu, Y. Lan, J. Liu, G. Li, Y.-D. Wu, A. Lei. *J. Am. Chem. Soc.* **2009**, *131*, 10201–10210. b) R. V. Asselt, C. J. Elsevier. *Organometallics* **1994**, *13*, 1972–1980.

22. A. L. Liberman-Martin, D. S. Levine, M. S. Ziegler, R. G. Bergman, T. D. Tilley. *Chem. Commun.* **2016**, *52*, 7039−7042.

23. F. M. Miloserdov, N. A. Rajabi, J. P. Lowe, M. F. Mahon, S. A. Macgregor. *J. Am. Chem. Soc.* **2020**, *142*, 6340−6349.

24. a) S. Bajo, M. G. Alférez, M. M. Alcaide, J. López-Serrano, J. Campos. *Chem. Eur. J.* **2020**, *26*, 16833–16845. b) T. D. Lohrey, L. Maron, R. G. Bergman, J. Arnold. *J. Am. Chem. Soc.* **2019**, *141*, 800−804. c) J. J. Gair, Y. Qiu, R. L. Khade, N. H. Chan, A. S. Filatov, Y. Zhang, J. C. Lewis. *Organometallics* **2019**, *38*, 1407−1412. d) U. Jayarathne, T. J. Mazzacano, S. Bagherzadeh, N. P. Mankad. *Organometallics* **2013**, *32*, 3986−3992.

25. a) C. J. Pell, W.-C. Shih, S. Gatard, O. V. Ozerov. *Chem. Commun.* **2017**, *53*, 6456–6459. b) H. Takahashi, S. Inagaki, N. Yoshii, F. Gao, Y. Nishihara, K. Takagi. *J. Org. Chem.* **2009**, *74*, 2794–2797. c)S. Ejiri, S. Odo, H. Takahashi, Y. Nishi-Mura, K. Gotoh, Y. Nishihara, K. Takagi. *Org. Lett.* **2010**, *12*, 1692–1695.

26. See for example: a) H. Braunschweig, K. Gruss, K. Radacki. *Angew. Chem. Int. Ed*. **2009**, *48*, 4239–4241. b) H. Braunschweig, A. Damme, R. D. Dewhurst, F. Hupp, J. O. C. Jiménez-Halla, K. Radacki. *Chem. Commun.* **2012**, *48*, 10410–10412. c) H. Braunschweig, K. Gruss, K. Radacki. *Angew. Chem. Int. Ed*. **2007**, *46*, 7782–7784. d) J. Bauer, H. Braunschweig, A. Damme, K. Radacki. *Angew. Chem. Int. Ed*. **2012**, *51*, 10030–10033. e) J. K. Schuster, J. H. Muessig, R. D. Dewhurst, H. Braunschweig. *Chem. Eur. J.* **2018**, *24*, 9692–9697. f) R. Bertermann, J. Böhnke, H. Braunschweig. R. D. Dewhurst, T. Kupfer, J. H. Muessig, L. Pentecost, K. Radacki, S. S. Sen, A. Vargas. *J. Am. Chem. Soc.* **2016**, *138*, 16140–16147.

27. M. Ma, A. Sidiropoulos, L. Ralte, A. Stasch, C. Jones. *Chem. Commun.*, **2013**, *49*, 48–50.

28. I. Resa, E. Carmona, E. Gutierrez-Puebla, A. Monge. *Science* **2004**, *305*, 1136–1138.

29. Y. Sun, W. E. Piers, M. Parvez. *Can. J. Chem.* **1998**, *76*, 513–517.

30. T. Bollermann, C. Gemel, R. A. Fischer. *Coord. Chem. Rev.* **2012**, *256*, 537–555.

31. a) T. Bollermann, K. Freitag, C. Gemel, R. D. Seidel, M. V. Hopffgarten, G. Frenking, R. A. Fischer. *Angew. Chem. Int. Ed.* **2011**, *50*, 772–776. b) T. Cadenbach, T. Bollermann, C. Gemel, M. Tombul, I. Fernández, M. V. Hopffgarten, G. Frenking, R. A. Fischer. *J. Am. Chem. Soc.* **2009**, *131*, 16063–16077. c) J. Hornung, J. Weßing, M. Molon, K. Dilchert, C. Gemel, R. A. Fischer. *J. of Organom. Chem.* **2018**, *860*, 78–84. d) T. Bollermann, K. Freitag, C. Gemel, R. W. Seidel, R. A. Fischer. *Organometallics* **2011**, *30*, 4123–4127. e) K. Freitag, M. Molon,

P. Jerabek, K. Dilchert, C. Rösler, R. W. Seidel, C. Gemel, G. Frenking, R. A. Fischer. *Chem. Sci.* **2016**, *7*, 6413–6421.

32. B. Cordero, V. Gómez, A. E. Platero-Prats, M. Revés, J. Echeverra, E. Cremades, F. Barragán, S. Alvarez. *Dalton Trans*. **2008**, 2832–2838.

33. R. G. Goel, W. O. Ogiri, R. C. Srivastava. *Organometallics* **1982**, *1*, 819–824.

34. S. Werkmeister, S. Fleischer, S. Zhou, K. Junge, M. Beller. *ChemSusChem* **2012**, *5*, 777–782.

35. L. Pandolfo, M. Maggini. *J. Organom. Chem.* **1997**, *540*, 61–65.

36. a) G. Skara, F. De Vleeschouwer, P. Geerlings, F. De Proft, B. Pinter. *Sci. Rep.* **2017**, *7*, 16024. b) J. Daru, I. Bakó, A. Stirling, I. Pápai. *ACS Catal.* **2019**, *9*, 6049–6057. c) D. Yepes, P. Jaque, I. Fernández. *Chem. Eur. J.* **2016**, *22*, 18801–18809. d) L. Liu, L. Cao, Y. Shao, G. Mnard, D. W. Stephan. *Chem* **2017**, *3*, 259–267. e) H. B. Hamilton, D. F. Wass. *Chem* **2017**, *3*, 198–210.

37. a) R. Dobrovetsky, D. W. Stephan. *Isr. J. Chem.* **2015**, *55*, 206–209. b) P. Jochmann, D. W. Stephan. *Angew. Chem. Int. Ed.* **2013**, *52*, 9831–9835.

38. Y. Zhang, M. K. Karunananda, H.-C. Yu, K. J. Clark, W. Williams, N. P. Mankad, D. H. Ess. *ACS Catal*. **2019**, *9*, 2657–2663.

39. R. U. Nisaa, K. Ayub. *New J. Chem.* **2017**, *41*, 5082–5090.

40. H.-R. C. Jaw, W. R. Mason. *Inorg. Chem*. **1989**, *28*, 4370–4373.

41. J. E. Fleckenstein, K. Koszinowski. *Organometallics* **2011**, *30*, 5018–5026.

42. R. Peloso, I. Resa, A. Rodríguez, E. Carmona. *Inorg. Synth*. **2018**, *37*, 37.

43. Gaussian 16, Revision B.01, M. J. Frisch, G. W. Trucks, H. B. Schlegel, G. E. Scuseria, M. A. Robb, J. R. Cheeseman, G. Scalmani, V. Barone, B. Mennucci, G. A. Petersson, H. Nakatsuji, M. Caricato, X. Li, H. P. Hratchian, A. F. Izmaylov, J. Bloino, G. Zheng, J. L. Sonnenberg, M. Hada, M. Ehara, K. Toyota, R. Fukuda, J. Hasegawa, M. Ishida, T. Nakajima, Y. Honda, O. Kitao, H. Nakai, T. Vreven, J. A. Montgomery, Jr., J. E. Peralta, F. Ogliaro, M. Bearpark, J. J. Heyd, E. Brothers, K. N. Kudin, V. N. Staroverov, T. Keith, R. Kobayashi, J. Normand, K. Raghavachari, A. Rendell, J. C. Burant, S. S. Iyengar, J. Tomasi, M. Cossi, N. Rega, J. M. Millam, M. Klene, J. E. Knox, J. B. Cross, V. Bakken, C. Adamo, J. Jaramillo, R. Gomperts, R. E. Stratmann, O. Yazyev, A. J. Austin, R. Cammi, C. Pomelli, J. W. Ochterski, R. L. Martin, K. Morokuma, V. G. Zakrzewski, G. A. Voth, P. Salvador, J. J. Dannenberg, S. Dapprich, A. D. Daniels, O. Farkas, J. B. Foresman, J. V. Ortiz, J. Cioslowski, and D. J. Fox, Gaussian, Inc., Wallingford CT, **2016**.

44. a) A. D. Becke. *Phys. Rev. A* **1988**, *38*, 3098–3100. b) J. P. Perdew. *Phys. Rev. B* **1986**, *33*, 8822–8824.

45. F. Weigend, R. Ahlrichs. *Phys. Chem. Chem. Phys*. **2005**, *7*, 3297–3305.

46. S. Grimme, J. Antony, S. Ehrlich, H. A. Krieg. *J. Chem. Phys*. **2010**, *132*, 154104.

47. a) S. Huzinaga, B. A. Miguel. *Chem. Phys. Lett*. **1990**, *175*, 289–291. b) S. Huzinaga, M. Klobukowski. *Chem. Phys. Lett*. **1993**, *212*, 260–264.

48. J. A. Cabeza, J. F. van der Maelen, S. García-Granda. *Organometallics* **2009**, *28*, 3666–3672 and references therein.

49. Keith, T. A. AIMAll, **2010**, http://tkgristmill.com.

50. For a recent review, see: M. von Hopffgarten, G. Frenking. *WIREs Comput. Mol. Sci*. **2012**, *2*, 43–62.

51. ADF program: www.scm.com.

52. J. G. Snijders, P. Vernooijs, E. J. Baerends. *At. Data. Nucl. Data Tables* **1982**, *26*, 483–509.

53. A. Krijn, E. J. Baerends. Fit Functions in the HFS-Method, Internal Report (in Dutch), Vrije Universiteit Amsterdam, The Netherlands, **1984**.

54. a) E. van Lenthe, E. J. Baerends, J. G. Snijders. *J. Chem. Phys.* **1993**, *99*, 4597–4610. b) E. van Lenthe, E. J. Baerends, J. G. Snijders. *J. Chem. Phys.* **1994**, *101*, 9783–9792. c) E. van Lenthe, A. Ehlers, E. J. Baerends. *J. Chem. Phys.* **1999**, *110*, 8943–8953.

Conclusions

1. We have demonstrated that combining a pair of sterically hindered Au(I)/Pt(0) complexes that present Lewis acidic and basic character, respectively, permits the design of bimetallic frustrated Lewis pairs. Our combined experimental and computational approach strongly supports, for the first time, a genuine bimetallic FLP mechanism for the heterolytic cleavage of H_2 and different alkynes.

2. We have confirmed that subtle modifications of the phosphine ligands bound to gold allows tuning of the equilibrium between monometallic components and bimetallic adduct formation. This equilibrium is also dependent on solvent polarity and has an important impact on the capacity of the bimetallic pair to activate small molecules.

3. We have analyzed that the aforesaid ligand modification has a strong effect on the regioselectivity of small molecule activation. As a representative example, the activation of acetylene leads to two Au/Pt bimetallic isomers, a σ,π-bridging acetylide and a vinylene, being the formation of one or the other isomer highly dependent on the sterics of the phosphine bound to gold. In the case of hydrogen activation a dissimilar product distribution was found for the three investigated terphenyl phosphines. Besides, these studies revealed an uncommon strong inverse kinetic isotopic effect (KIE) whose origin opposes the traditional view based on an inverse equilibrium isotopic effect (EIE) prior to an irreversible rate-determining step, while

rather suggesting a single rate-determining step featuring a strong inverse KIE.

4. The reactivity of tin and germanium dihalides with one of our transition metal-only frustrated Lewis pairs based on Pt(0) and Au(I) fragments was studied. Our results reveal a dissimilar reactivity of the tetrylenes in the presence of the two metals compared to the reactions displayed with the individual Au(I) and Pt(0) monometallic species. While the insertion chemistry of :$GeCl_2$ and :$SnCl_2$ into Au−X bonds is analogous to prior studies, their reactivity with [Pt(P^tBu_3)$_2$] contrasts with previous work based on less hindered phosphines. As such, we have demonstrated that :$SnCl_2$ promotes phosphine exchange reactions at Pt(0) centres to access uncommon heteroleptic diphosphine platinum(0) compounds. In addition, an unusual highly-reduced heteropolymetallic aggregate containing a Pt_2Sn_3 has been prepared and fully characterized. The different reactivity exhibited by :$GeCl_2$ compared to :$SnCl_2$ is also apparent by their addition to the Au(I)/Pt(0) pair. In the former case a metal-only Pt→Au Lewis adduct is readily produced, while in the latter experiment a cationic heteroleptic diphosphine gold compound is the major species.

5. We have demonstrated that the transition metal Lewis base [Pt(P^tBu_3)$_2$] is a suitable precursor for the formation of metal-only Lewis pairs, which have been isolated for both silver and zinc electrophiles. The reactivity of the Pt(0)/Ag(I) MOLP markedly

differs from that of its independent metal components. Thus, while [Pt(P^tBu_3)$_2$] does not react with H_2, phenylacetylene, methanol, water or ammonia, the presence of a silver salt readily facilitates the activation of these molecules by X–H (X = H, C, O, N) bond cleavage. These results demonstrate the usefulness of MOLP systems for small molecule activation and, as an immediate consequence, for catalytic applications, a research avenue for which this Thesis has established the ground foundations.

6. We have isolated and fully characterized two new Pt/Zn polymetallic complexes. While the metal-only Lewis adduct [(P^tBu_3)$_2$Pt→Zn(C_6F_5)$_2$] represents the first Pt(0)/organozinc MOLP, the reaction between [Pt(P^tBu_3)$_2$] and [$Zn_2Cp^*_2$] yields the exotic hexametallic, homoleptic compound [Pt($ZnCp^*$)$_6$]. At variance with previous Zn-rich polymetallic compounds, the latter does not fulfill the 18 VE rule, being considered an octahedral 16-electron species. While these complexes remain inactive towards dihydrogen, pairing [Pt($Pt Bu_3$)$_2$] with Zn(OTf)$_2$ results in cooperative dihydrogen cleavage. Preliminary kinetic and isotopic exchange experiments support a bimetallic FLP-type mechanism. Similarly, the activation of O−H bonds in water proceeds readily in the presence of Pt/Zn pairs, while the individual components reveal no activity.

Conclusiones

1. Hemos demostrado que la combinación de un par de complejos de Au(I)/Pt(0) estéricamente impedidos que presentan carácter ácido y básico de Lewis, respectivamente, permite el diseño de pares de Lewis frustrados bimetálicos. Nuestro enfoque combinando estudios experimentales y computacionales apoya firmemente, por primera vez, un mecanismo FLP bimetálico para la ruptura heterolítica de H_2 y diferentes alquinos.

2. Hemos confirmado que las modificaciones sutiles de los ligandos de fosfina unidos al oro permiten ajustar el equilibrio entre los componentes monometálicos y la formación de aductos bimetálicos. Este equilibrio también depende de la polaridad del disolvente y tiene un impacto importante en la capacidad del par bimetálico para activar moléculas pequeñas.

3. Hemos analizado que la modificación del ligando antes mencionada tiene un fuerte efecto sobre la regioselectividad de la activación de moléculas pequeñas. Como ejemplo representativo, la activación del acetileno conduce a dos isómeros bimetálicos de Au/Pt, con un acetiluro puente de tipo σ,π y un vinileno, siendo la formación de uno u otro isómero altamente dependiente de impedimento estérico de la fosfina unida al oro. En el caso de la activación con hidrógeno, se encontró una distribución de productos diferente para las tres terfenilfosfinas investigadas. Además, estos estudios revelaron un fuerte efecto isotópico cinético inverso (KIE) poco común, cuyo

origen se opone a la visión tradicional basada en un efecto isotópico de equilibrio inverso (EIE) antes de un paso irreversible determinante de la velocidad. En este caso, sin embargo, nuestros estudios sugieren un paso único que determina la velocidad con un fuerte KIE inverso.

4. Hemos estudiado la reactividad de los dihaluros de estaño y germanio con uno de nuestros pares de Lewis frustrados de tipo Au(I)/Pt(0). Nuestros resultados revelan una reactividad diferente de los tetrilenos en presencia de los dos metales en comparación con las reacciones mostradas con las especies monometálicas de Au(I) y Pt(0) individuales. Si bien la química de inserción de :$GeCl_2$ y :$SnCl_2$ en enlaces Au−X es análoga a estudios anteriores, su reactividad con [$Pt(P^tBu_3)_2$] contrasta con trabajos previos basados en fosfinas menos impedidas. Así pues, hemos demostrado que la molécula de :$SnCl_2$ promueve reacciones de intercambio de fosfina en los centros de Pt(0) para acceder a compuestos heterolépticos de platino(0) poco comunes. Además, se ha preparado y caracterizado completamente un agregado heteropolimetálico inusual que contiene una agrupación Pt_2Sn_3. La diferente reactividad exhibida por :$GeCl_2$ en comparación con :$SnCl_2$ también es evidente por su adición al par Au(I)/Pt(0). En el primer caso, se produce fácilmente un aducto de Pt→Au, mientras que en el último experimento la especie principal es un compuesto catiónico heteroléptico de oro con dos fosfinas.

5. Hemos demostrado que la base de Lewis metálica [Pt(P^tBu_3)$_2$] es un precursor adecuado para la formación de pares de Lewis bimetálicos (MOLPs, por sus siglas en inglés). Se han aislado especies de este tipo empleando electrófilos de plata y zinc. La reactividad del MOLP Pt(0)/Ag(I) difiere notablemente de la de sus componentes metálicos independientes. Así, mientras que [Pt(P^tBu_3)$_2$] no reacciona con H_2, fenilacetileno, metanol, agua o amoníaco, la presencia de una sal de plata facilita la activación de estas moléculas por la ruptura de los enlaces X–H (X = H, C , O, N). Estos resultados demuestran la utilidad de los sistemas de tipo MOLP para la activación de moléculas pequeñas y, como consecuencia inmediata, para aplicaciones catalíticas, una vía de investigación para la que esta Tesis ha sentado las bases fundamentales.

6. Hemos aislado y caracterizado completamente dos nuevos complejos polimetálicos de Pt/Zn. Mientras que el aducto de Lewis [(P^tBu_3)$_2$Pt→Zn(C_6F_5)$_2$] representa el primer MOLP de Pt(0)/organozinc, la reacción entre [Pt(P^tBu_3)$_2$] y [$Zn_2Cp^*_2$] produce el compuesto homoléptico hexametálico [Pt($ZnCp^*$)$_6$]. A diferencia de los compuestos polimetálicos ricos en Zn descritos anteriormente, este último no cumple la regla de 18 VE, siendo considerado una especie octaédrica de 16 electrones. Si bien estos complejos permanecen inactivos frente al dihidrógeno, la combinación de [Pt($Pt Bu_3$)$_2$] con Zn(OTf)$_2$ da como resultado una escisión cooperativa de dihidrógeno. Los experimentos preliminares de intercambio cinético e isotópico apoyan un mecanismo bimetálico de tipo FLP para esta transformación. De manera similar, la activación

de los enlaces O−H en el agua se produce fácilmente en presencia de pares Pt/Zn, mientras que los componentes individuales no revelan actividad.